



THE UNIVERSITY OF
WAIKATO
Te Whare Wānanga o Waikato

Research Commons

<http://waikato.researchgateway.ac.nz/>

Research Commons at the University of Waikato

Copyright Statement:

The digital copy of this thesis is protected by the Copyright Act 1994 (New Zealand).

The thesis may be consulted by you, provided you comply with the provisions of the Act and the following conditions of use:

- Any use you make of these documents or images must be for research or private study purposes only, and you may not make them available to any other person.
- Authors control the copyright of their thesis. You will recognise the author's right to be identified as the author of the thesis, and due acknowledgement will be made to the author where appropriate.
- You will obtain the author's permission before publishing any material from the thesis.

SEQUESTRATION OF METAL AND METALLOID IONS BY THERMOPHILIC BACTERIA

A thesis submitted in fulfillment of the requirements for the degree of

Doctor of Philosophy in Biological Sciences at the University of Waikato by

ADRIAN HETZER



University of Waikato, Department of Biological Sciences, Hamilton, New Zealand

2007

Für meine ertraute,

meine reundin,

meine eliebte ...

Gewidmet meiner Ehefrau Mauritia, die all dies für mich verkörpert.

Abstract

This Ph. D. thesis presents results and conclusions from studies 1) investigating the interaction between metal and metalloid ions and thermophilic bacteria, and 2) characterizing microbial populations in a geothermally active habitat with relatively high concentrations of metalloid ions and compounds.

In initial cadmium ion toxicity assays, the minimal inhibition concentration for 46 thermophilic bacteria of the genera *Aneurinibacillus*, *Anoxybacillus*, *Bacillus*, *Brevibacillus*, *Geobacillus*, and *Thermus* were determined. The highest tolerances to cadmium ions (Cd^{2+}) in the range of 400 to 3200 μM were observed for species belonging to the genus *Geobacillus*.

The thermophilic Gram-positive bacteria *Geobacillus stearothermophilus* and *G. thermocatenulatus* were selected to describe further biosorption reactions between cadmium ions and chemically reactive functional groups (potential ligands) within and onto the bacterial cell walls. Data obtained from electrophoretic mobility, potentiometric titration and cadmium ion adsorption experiments were used to quantify the number and concentrations of ligands and to determine the thermodynamic stability constants for the ligand-cation complexes. The first reported surface complexation models (SCMs) quantifying metal ion adsorption by thermophilic microorganisms predicted cadmium adsorption and desorption by both studied *Geobacillus* strains over a range of pH values and for different biomasses. The results indicated the functional group, with a deprotonation constant $\text{p}K$ value of approximately 3.8, to be more dominant in cation biosorption accounting for 66 and 80% of all titrable groups for *G. thermocatenulatus* and *G. stearothermophilus*, respectively. The generated SCMs are different from model parameters obtained from mesophilic species that have been studied to date and might indicate a different biosorption behavior for both studied *Geobacillus* strains.

Another objective of this thesis was to characterize microbial populations in the hot spring Champagne Pool, located in Waiotapu, New Zealand. The thermal

spring is approximately 65 m in diameter and discharges water at 75° C and pH 5.5, which is oversaturated with arsenic and antimony compounds that precipitate and form orange deposits. Recovered nucleic acids and adenosine 5'-triphosphate (ATP) concentrations obtained for Champagne Pool water samples indicated low microbial density and were in good agreement with relatively low cell numbers of $5.6 \pm 0.5 \times 10^6$ cells per ml. Denaturing gradient gel electrophoresis (DGGE) and 16S rRNA gene clone library analyses revealed the abundance of *Sulfurihydrogenibium*, *Sulfolobus* and *Thermofilum*-like populations in Champagne Pool.

Two novel bacteria and one novel archaeon were successfully isolated with a distant phylogenetic relationship to *Sulfurihydrogenibium*, *Thermoanaerobacter*, and *Thermococcus*, respectively. Genotypic and metabolic characteristics differentiated isolate CP.B2^T from described species of the genus *Sulfurihydrogenibium*. CP.B2^T represents a novel genus within the *Aquificales* order, for which the name *Venenivibrio stagnispumantis* gen. nov., sp. nov. is proposed. *V. stagnispumantis* is a thermophilic, chemolithotrophic bacterium, that utilizes molecular hydrogen as electron donor and oxygen as electron acceptor and displayed growth in the presence of up to 8 mM NaAsO₂ (As³⁺) and more than 20 mM Na₂HAsO₄·7H₂O (As⁵⁺). However, growth was not observed when Na₂HAsO₄·7H₂O and NaAsO₂ were provided as the sole electron acceptor and donor pair. Arsenic resistance was conferred by the genes *arsA* and *arsB*.

Abstract (German)

Die vorliegende Doktorarbeit stellt Ergebnisse und Schlussfolgerungen von Studien vor, welche die Wechselwirkung zwischen Metall- bzw. Metalloidionen und thermophilen Bakterien untersuchen, und die mikrobielle Zusammensetzung in einem geothermalen Habitat mit relativ hohen Konzentrationen an Metalloidionen und -verbindungen beschreiben.

In Kadmiumtoxizitätstests wurde die minimale Wachstumshemmkonzentration für 46 thermophile Bakterien der Gattung *Aneurinibacillus*, *Anoxybacillus*, *Bacillus*, *Brevibacillus*, *Geobacillus* und *Thermus* bestimmt. Die höchsten Toleranzen gegenüber Kadmiumionen (Cd^{2+}), in der Größenordnung von 400 μM bis 3200 μM , wurden für Bakterien der Gattung *Geobacillus* beobachtet.

Die thermophilen, Grampositiven Bakterien *Geobacillus stearothermophilus* und *G. thermocatenulatus* wurden ausgewählt, um deren Biosorptionsverhalten näher zu untersuchen, d.h. die chemischen Reaktionen zwischen Kadmiumionen und reaktionsfähigen funktionellen Gruppen (mögliche Liganden) innerhalb und an den Bakterienzellwände zu beschreiben. Daten aus potentiometrischen Titrations- und Kadmiumionadsorption-Experimenten, die die elektrophoretische Mobilität der Zellen berücksichtigten, wurden verwendet, um die Anzahl und die Konzentrationen der Liganden zu quantifizieren und die thermodynamischen Stabilitätskonstanten für die Ligand-Kation Komplexe festzustellen. Das erste bekannte Oberflächen-Komplexbildungs-Modell, das Biosorption von Metallionen durch thermophile Mikroorganismen quantifiziert, konnte Kadmiumadsorption und -desorption durch die beiden untersuchten *Geobacillus*-Arten in Abhängigkeit von verschiedenen pH-Werten und für unterschiedliche Biomassen vorhersagen. Die Ergebnisse zeigten, dass die funktionelle Gruppe mit einer Deprotonierungskonstanten pK von circa 3.8 dominant in der Biosorption von Kationen zu sein scheint, und für 66% bzw. 80% aller titrierbaren Gruppen von *G. stearothermophilus* und *G. thermocatenulatus* verantwortlich war. Die erstellten Oberflächen-Komplexbildungs-Modelle unterschieden sich von den Modelldaten der bis heute untersuchten mesophilen Arten, und weisen auf ein

anderes Adsorptionsverhalten für die beiden untersuchten *Geobacillus*-Arten hin.

Ein weiteres Ziel dieser Doktorarbeit war, die mikrobielle Population in der heißen Quelle „Champagne Pool“ in Waiotapu, Neuseeland zu charakterisieren. Die Thermalquelle, ungefähr 65 m im Durchmesser, setzt 75° C warmes Wasser mit pH 5.5 frei, welches mit Arsen- und Antimonverbindungen übersättigt ist, die als orangefarbene Niederschlag ausfallen. Nukleinsäure- und Adenosin-5'-triphosphat (ATP)-Konzentrationen, gewonnen aus Wasserproben von „Champagne Pool“, deuteten auf niedrige Zelldichten hin, und bestätigten die ermittelten relativ niedrigen Zellzahlen von $5.6 \pm 0.5 \times 10^6$ Zellen pro ml. Denaturierende Gradienten-Gelelektrophorese (DGGE) und 16S rRNA Gen-Klonbibliotheken zeigten das Vorkommen von *Sulfurihydrogenibium*-, *Sulfolobus*- und *Thermofilum*-ähnlichen Arten in „Champagne Pool“ an.

Zwei unbekannte Bakterienarten und eine unbekannte Archaeonart konnten erfolgreich isoliert werden, die phylogenetisch entfernt mit *Sulfurihydrogenibium*, *Thermoanaerobacter* und *Thermococcus* verwandt waren. Genotypische und metabolische Eigenschaften unterschieden Isolat CP.B2^T von beschriebenen Arten der Gattung *Sulfurihydrogenibium*. CP.B2^T stellt eine neue Gattung innerhalb der Ordnung *Aquificales* dar, für die der Name *Venenivibrio stagnispumantis* gen. nov., sp. nov. vorgeschlagen wird. *V. stagnispumantis*, ein thermophiles, chemolithothrophes Bakterium, das molekularen Wasserstoff als Elektronendonator und Sauerstoff als Elektronenakzeptor benutzte, konnte in der Anwesenheit von bis zu 8 mM NaAsO₂ (As³⁺) und mehr als 20 mM Na₂HAsO₄·7H₂O (As⁵⁺) wachsen. Wachstum wurde jedoch nicht beobachtet, wenn Na₂HAsO₄·7H₂O und NaAsO₂ als das alleinige Elektronenakzeptor- und Elektronendonatorpaar zur Verfügung gestellt wurde. Arsenresistenz wurde durch die Gene *arsA* und *arsB* vermittelt.

Acknowledgements

The present thesis is a product of interactions not merely with microorganisms but also with other life forms. It is a pleasure to acknowledge those people who contributed to this research work.

Firstly, and most importantly, I love to thank Mauritia Hetzer, who finally became my wife during our stay in New Zealand. Our harmonic relationship was always an endless source of support and encouragement for me. To Mauritia I dedicate this thesis.

I am grateful to Doctor Chris Daughney for giving me the opportunity to be part of the project “Extremophilic microorganisms for metal sequestration from aqueous solutions” and for sponsoring my scholarship. It was very informative and enjoyable to do research work together with you in Wairakei and on the NZAPLUME III cruise.

To Pat and Hugh Morgan I remain indebted for the hearty welcome to New Zealand. I wish to thank my supervisors Professor Hugh Morgan, Professor Ian McDonald, and Doctor Ron Ronimus for their kind help and competent guidance throughout my studies and for giving me so much freedom in my research.

I acknowledge all the colleagues at the University of Waikato in Hamilton and at the Institute of Geological and Nuclear Sciences in Wairakei who contributed to this work.

Last but not least, very special thanks to Stephen Harte, who is the International Student Advisor at the University of Waikato, for his great effort to help my wife and me in dealing with New Zealand Immigration.



Table of content

Abstract	III
Abstract (German)	V
Acknowledgements	VII
Table of content	VIII
List of tables	XII
List of figures	XIV
List of abbreviations	XVIII
Chapter 1: Introduction	1
1.1 Thermophilic bacteria: life on the edge	1
1.2 Metals and metalloids: a double-edged sword for life	3
1.3 Sequestration	8
1.4 Objectives	10
Chapter 2: Cadmium ion toxicity experiments	16
2.1 Introduction	16
2.2 Materials and Methods	17
2.2.1 Bacteria and culture conditions	17
2.2.2 Toxicity experiments	19
2.2.3 Small-scale plasmid isolation	19
2.3 Results	20
2.3.1 Cadmium ion susceptibility tests	20
2.3.2 Plasmid isolation	26
2.4. Discussion	26
2.5 Acknowledgements	28
	VIII

Chapter 3: Cadmium ion biosorption	29
3.1 Abstract	29
3.2 Introduction	29
3.3 Materials and Methods	31
3.3.1 Culture conditions	31
3.3.2 Acid-base titrations	33
3.3.3 Metal ion adsorption	34
3.3.4 Electrophoretic mobility measurements	34
3.3.5 Surface complexation model (SCM)	35
3.4 Results	36
3.4.1 Potentiometric titration experiments	36
3.4.2 Cadmium ion biosorption	43
3.5 Discussion	45
3.6 Acknowledgements	51
Chapter 4: Champagne Pool	53
4.1 Abstract	53
4.2 Introduction	53
4.3 Materials and Methods	56
4.3.1 Sampling and ATP measurements	56
4.3.2 DNA extraction	58
4.3.3 PCR amplification of 16S rRNA gene and gene cloning experiments	58
4.3.4 DGGE analysis of 16S rRNA gene fragments	64
4.3.5 Enrichment experiments	64
4.3.6 Light and electron microscopy	66
4.3.7 Phylogenetic analyses	67
4.3.8 Nucleotide sequence accession numbers	67
4.3.9 Eh-pH diagram	68
4.4 Results	69
4.4.1 Physico- and biochemical properties	69
4.4.2 Microscopy	71

4.4.3 Molecular analysis	72
4.4.4 Enrichment	78
4.4.5 Growth experiments using Champagne Pool water	80
4.4.6 Stability of arsenic compounds	80
4.5 Discussion	81
4.6 Acknowledgements	84
Chapter 5: <i>Venenivibrio stagnispumantis</i>	86
5.1 Abstract	86
5.2 Introduction	86
5.3 Materials and Methods	88
5.3.1 Collection of samples	88
5.3.2 Enrichment and isolation	88
5.3.3 Culture conditions	89
5.3.4 Light and electron microscopy	90
5.3.5 DNA isolation and base composition	91
5.3.6 PCR amplification and sequencing	92
5.3.7 Phylogenetic analyses	94
5.4 Results	94
5.4.1 Isolation	94
5.4.2 Morphology	94
5.4.3 Physiological characteristics	95
5.4.4 Metabolic characteristics	96
5.4.5 Arsenic and antimony ion susceptibility tests	97
5.4.6 Genotypic characteristics	98
5.5 Discussion and proposal of a novel genus	101
5.5.1 Description of the genus <i>Venenivibrio</i> gen. nov.	104
5.5.2 Description of the species <i>Venenivibrio stagnispumantis</i> sp. nov.	104
5.6 Acknowledgements	105
Chapter 6: General discussion	106
References	111

Appendix A: Growth curves	135
Appendix B: One-site and two-site models	140
Appendix C: Surface complexation model data	148
Appendix D: Clone library analyses	164
Appendix E: Nucleotide sequences and alignments	169
Appendix F: Culture experiments	195
Appendix G: NZAPLUME III research cruise	200
Appendix H: Publications	210

List of tables

Table 01. Some representative metalloproteins and their metabolic functions	6
Table 02. Minimum inhibitory concentration (MIC) of Cd^{2+} for the microorganisms studied.	21
Table 03. Minimum inhibitory concentration (MIC) of Cd^{2+} for the investigated <i>Thermus</i> isolates.....	22
Table 04. Minimum inhibitory concentration (MIC) of Cd^{2+} [μM] for nine selected bacteria when cultivated in the complex media TSB and in the minimal medium CMD	24
Table 05. Selected biophysical parameters for <i>G. thermocatenulatus</i> (DSM 730) and <i>G. stearothermophilus</i> (DSM 6790).....	36
Table 06. Average model parameters for <i>G. thermocatenulatus</i> and <i>G.</i> <i>stearothermophilus</i> in comparison to other bacterial species	49
Table 07. Target, position, specificity, sequences, and annealing temperature of oligonucleotide primers used for PCR studies.	62
Table 08. Chemical composition of water samples collected from Champagne Pool ($T = 75.2^\circ \text{C}$, $\text{pH} = 5.17$).....	68
Table 09. Date, time, temperature, and pH values of water samples collected from 30 cm below water surface level of Champagne Pool in 2004, 2005, and 2006	69
Table 10. Summary of ATP content determined for Champagne Pool samples ..	70
Table 11. Summary of 16S rRNA gene sequences identified by culture and culture-independent approaches in samples obtained from Champagne Pool	75
Table 12. Growth temperature and pH ranges for microbial strains isolated from Champagne Pool	80
Table 13. Target and sequences of oligonucleotide primers used in PCR studies	93
Table 14. Comparison of properties of <i>Venenivibrio stagnispumantis</i> gen. nov., sp. nov. CP.B2 ^T with the related species.....	103
Table 15. One-site SCMs calculated for each individual dataset obtained from Cd^{2+} adsorption experiments using <i>G. thermocatenulatus</i> cells (DSM 730)	140

Table 16. One-site SCMs calculated for each individual dataset obtained from Cd ²⁺ adsorption experiments using <i>G. stearothermophilus</i> cells (DSM 6790)	142
Table 17. Two-site SCMs generated for each individual dataset obtained from Cd ²⁺ adsorption experiments using <i>G. thermocatenulatus</i> cells (DSM 730)	144
Table 18. Two-site SCMs generated for each individual dataset obtained from Cd ²⁺ adsorption experiments using <i>G. stearothermophilus</i> cells (DSM 6790)	146
Table 19. Dataset 1 obtained from titration experiments using <i>G. thermocatenulatus</i> cells (24.70 g wet cells).....	148
Table 20. Dataset 2 obtained from titration experiments using <i>G. thermocatenulatus</i> cells (24.70 g wet cells).....	150
Table 21. Dataset 3 obtained from titration experiments using <i>G. thermocatenulatus</i> cells (24.70 g wet cells).....	152
Table 22. Dataset 1 obtained from titration experiments using <i>G. stearothermophilus</i> cells (12.96 g wet cells).....	154
Table 23. Dataset 2 obtained from titration experiments using <i>G. stearothermophilus</i> cells (12.96 g wet cells).....	156
Table 24. Data obtained from Cd ²⁺ adsorption experiments using <i>G. thermocatenulatus</i> cells (19.71 g wet cells).....	158
Table 25. Data obtained from Cd ²⁺ adsorption experiments using <i>G. stearothermophilus</i> cells (10.56 g wet cells).....	161
Table 26. Effect of potential electron donors, electron acceptors, and carbon sources on growth of strain CP.B2 ^T	195
Table 27. Electron donors and acceptors pairs used in cultivation experiments (NZAPLUME III cruise).....	202
Table 28. Processing of water samples (NZAPLUME III cruise) for further analyses	203
Table 29. Location of sample sites (NZAPLUME III cruise) specified in geographic coordinates and water depths	208

List of figures

Figure 01. Rooted universal phylogenetic tree displaying the domains <i>Eukarya</i> , <i>Bacteria</i> and <i>Archaea</i> and some groups within the domains based on sequence similarities of 16S rRNA genes.....	2
Figure 02. Periodic table displaying elements based on their electron configuration	4
Figure 03. Scheme of surface complexation modeling to predict divalent cadmium cation adsorption by bacteria at the medium-bacterial cell surface interface.....	12
Figure 04. Water samples collected from Champagne Pool at Waiotapu in New Zealand.....	13
Figure 05. Chronological sequence of a DGGE profile of an environmental DNA sample obtained from a mud pool at Orakei Korako, New Zealand showing migration and separation process of two different archaeal 16S rRNA gene fragments	14
Figure 06. Microbial studies of Champagne Pool consisted of culture-independent and culture-dependent methods.....	15
Figure 07. Microbial growth monitored spectrophotometrically at 405 nm as a function of concentration of Cd^{2+} for <i>G. thermoleovorans</i> (DSM 5366) and for <i>G. stearothermophilus</i> (DSM 6790).....	23
Figure 08. Microbial growth monitored spectrophotometrically at 405 nm as a function of concentration of Cd^{2+} for <i>G. stearothermophilus</i> (DSM 6790) previously cultured without Cd^{+2} and in the presence of 200 μM Cd^{+2}	25
Figure 09. Image of an ethidium bromide-stained 0.7% agarose gel showing samples after plasmid extraction.....	26
Figure 10. Transmission electron micrographs of <i>G. thermocatenulatus</i> and <i>G. stearothermophilus</i>	38
Figure 11. Acid-base titration data normalized to dry mass and wet mass obtained for <i>G. stearothermophilus</i> (DSM 6790) and <i>G. thermocatenulatus</i> (DSM 730)	40
Figure 12. Zetapotentials obtained for <i>G. thermocatenulatus</i> and <i>G.</i>	

<i>stearothermophilus</i>	42
Figure 13. Cadmium ion adsorption experiment using 10 mM NaNO ₃ solution without bacterial cells	44
Figure 14. Percentage of cadmium ions adsorbed onto <i>G. thermocatenulatus</i> and <i>G. stearothermophilus</i> as a function of pH and dry biomass.....	46
Figure 15. Map of New Zealand North Island and enlargement of the central part. Dotted lines within the enlargement outline the Taupo Volcanic Zone, which exhibit many geothermally active features such as the hot spring Champagne Pool	56
Figure 16. Champagne Pool hot spring surrounded by a grey-white rim of silica	57
Figure 17. Scheme of ligation of a PCR product into a vector	63
Figure 18. Calibration curve for ATP concentration	71
Figure 19. Inverse image of DAPI-stained Champagne Pool water samples	72
Figure 20. Image of an ethidium bromide-stained 1.0% agarose gel showing different Champagne Pool samples after PCR amplification of nanoarchaeal 16S rRNA genes	73
Figure 21. DGGE profiles of archaeal and bacterial 16S rRNA gene fragments amplified by PCR from Champagne Pool water samples.....	74
Figure 22. The position of the partial 16S rRNA gene sequences of OTU Bac04 and Bac12 in relation to the 16 rRNA gene of <i>S. azorensis</i>	75
Figure 23. Phylogenetic tree demonstrating relationships of archaeal 16S rRNA gene sequences obtained from Champagne Pool spring samples	76
Figure 24. Phylogenetic tree demonstrating relationships of bacterial 16S rRNA gene sequences obtained from Champagne Pool spring samples	77
Figure 25. Scanning electron micrographs of isolate CP.B1 and CP.B2.....	79
Figure 26. Eh-pH diagram displays predominance fields of arsenic species in spring water of Champagne Pool at a temperature of 75.2° C and a pressure of 101.3 kPa	81
Figure 27. Structures of microbial membrane lipids found in samples obtained from Champagne Pool.....	83
Figure 28. Macroscopic, phase-contrast, and scanning electron micrographs of isolate CP.B2 ^T	95
Figure 29. Growth curve observed for CP.B2 ^T cells.....	96
Figure 30. Effect of temperature on the growth of CP.B2 ^T cells	97

Figure 31. Image of ethidium bromide-stained 1.75% agarose gels displaying <i>ars</i> gene fragments from CP.B1, CP.B2 ^T and CP.B3	98
Figure 32. Phylogenetic tree based on analysis of the 16S rRNA gene sequences of strain CP.B2 ^T , and closely related species of the <i>Aquificales</i> showing the position of the novel isolate	99
Figure 33. Image of ethidium bromide-stained 1.5% agarose gels. (A) displays the 500 bp gene fragment of <i>polA</i> amplified from CP.B2 ^T and <i>S. azorensis</i>	100
Figure 34. Microbial growth monitored spectrophotometrically at 405 nm as a function of concentration of Cd ²⁺ for <i>B. mycoides</i> (DSM 299) and for <i>G. thermocatenulatus</i> (DSM 730).....	135
Figure 35. Microbial growth monitored spectrophotometrically at 405 nm as a function of concentration of Cd ²⁺ for <i>G. thermoglucosidasius</i> (DSM 2543) and for TOK13.A4	136
Figure 36. Microbial growth monitored spectrophotometrically at 405 nm as a function of concentration of As ⁵⁺ for <i>G. thermoleovorans</i> (DSM 5366) and for <i>G. stearothermophilus</i> (DSM 6790).....	137
Figure 37. Microbial growth monitored spectrophotometrically at 405 nm as a function of concentration of As ⁵⁺ for <i>B. mycoides</i> (DSM 299) and for <i>G. thermocatenulatus</i> (DSM 730).....	138
Figure 38. Microbial growth monitored spectrophotometrically at 405 nm as a function of concentration of As ⁵⁺ for <i>G. thermoglucosidasius</i> (DSM 2543) and for TOK13.A4	139
Figure 39. RFLP profiles of bacterial 16S rRNA genes	164
Figure 40. RFPL profiles of archaeal 16S rRNA genes.....	167
Figure 41. Stainless steel stand accommodating 19 Niskin bottles	201
Figure 42. Relative position of the sample sites Monowai and Brothers Volcanoes to the New Zealand mainland	204
Figure 43. X-ray diffraction pattern obtained from the filtrate of the Brothers Volcano plume	205
Figure 44. X-ray diffraction pattern for the sample 17 obtained from Monowai Volcano plume	206
Figure 45. Scanning electron micrographs of plume samples showing a diatom skeleton, and a spherical structure (possibly a coccoid bacterium), both	

in close association with cubic crystals of halite	207
--	-----

List of abbreviations

° C	Degree Celsius
Å	Ångström(s), 0.1 nm
A	Adenosine, ampere
ATCC	American Type Culture Collection
ATP	Adenosine 5'-triphosphate
BLAST	Basic local alignment search tool
bp	Base pair(s)
BSA	Bovine serum albumin
C	Cytidine
CMD	Castenholz medium D
CTAB	Cetyltrimethylammoniumbromide
DAPI	4',6-diamidino-2-phenylindole
DGGE	Denaturing gradient gel electrophoresis
DMSO	Dimethyl sulfoxide
DNA	Deoxyribonucleic acid
dATP	2'-deoxyadenosine 5'-triphosphate
dCTP	2'-deoxycytidine 5'-triphosphate
dGTP	2'-deoxyguanosine 5'-triphosphate
dNTP	2'-deoxynucleotide 5'-triphosphate (dATP, dCTP, dGTP, dTTP)
DSM(Z)	Deutsche Sammlung von Mikroorganismen (und Zellkulturen)
DTT	Dithiothreitol
dTTP	2'-deoxythymidine 5'-triphosphate
EDS	Energy dispersive X-ray spectroscopy
EDTA	Ethylene diamine tetra-acetic acid
Eh	Oxidation-reduction potential
<i>et al.</i>	Latin: et alii, and others
FISH	Fluorescent <i>in situ</i> hybridization
g	Gram(s)
<i>g</i>	Gravitational force

G	Guanosine
h	Hour(s)
H	Adenosine, cytidine or thymidine
HEPES	2-hydroxyethyl-1-piperazinyethanesulfonic acid
http	Hypertext transfer protocol
IEP	Isoelectric point
IPTG	Isopropyl β -D-thiogalactoside
JCM	Japan Collection of Microorganisms
l	Liter(s)
LB	Luria-Bertani broth
μ	Micro, 10^{-6}
m	Milli, 10^{-3} or meter(s)
M	Mega, 10^6 or mol
min	Minute(s)
MES	2-N-morpholinoethanesulfonic acid
MIC	Minimal inhibition concentration
MOPS	3-N-morpholinopropanesulfonic acid
n	Nano, 10^{-9}
N	Adenosine, cytidine, guanosine or thymidine
N. A.	Not applicable
NCBI	National Centre of Biotechnology Information
N. C.	Does not converge
N. D.	Not determined
NTU	Nephelometric turbidity units
NZ	New Zealand
NZAPLUME	New Zealand and American plume mapping expedition
OD	Optical density
OTU	Operational taxonomic unit
Pa	Pascal (pressure unit)
PCR	Polymerase chain reaction
pH	Negative logarithm of the hydrogen ion concentration
PIPES	Piperazine-1,4-bis-2-ethanesulfonic acid
ppm	Part per million, e.g. 1 mg per 1 kg

ppb	Part per billion, e.g. 1 µg per 1 kg
PVP	Polyvinylpyrrolidone
qPCR	Quantitative polymerase chain reaction
r	Ribosomal
R	Adenosine or guanosine
RAPD	Randomly amplified polymorphic DNA
RFLP	Restriction fragment length polymorphism
RLU	Relative light units
RNA	Ribonucleic acid
rpm	Revolutions per minute
s	Second(s)
S	Svedberg, sedimentation coefficient; or cytidine or guanosine
SDS	Sodium dodecyl sulfate
SEM	Scanning electron microscopy
T	Thymidine
TAE	Tris-acetic acid EDTA buffer
TBE	Tris-borate EDTA buffer
TE	Tris EDTA buffer
TEM	Transmission electron microscopy
Tris	Tris hydroxymethyl aminoethane
tRNA	Transfer ribonucleic acid
TSB	Tryptic soy broth
UV	Ultra violet
V	Volt(s); or adenosine, cytidine or guanosine
v/v	Volume per volume, 10% (v/v) is equivalent to 10 ml per 100 ml
w/v	Weight per volume, 10% (w/v) is equivalent to 10 g per 100 ml
W	Watt; or adenosine or thymidine
www	World wide web
x	Time(s)
X-gal	5-bromo-4-chloro-3-indolyl-β-D-galactoside
Y	Cytidine or thymidine

Chapter 1: Introduction

The title “Sequestration of metal and metalloids ions by thermophilic bacteria” has been carefully chosen for the present Ph. D. thesis. Misunderstandings and misrepresentations often result when the same term, in various contexts, has a different meaning. As meanings might vary between scientific and everyday language, even between terminologies of different scientific fields and through time, the basic terms of the title, “thermophilic bacteria”, “metal and metalloid ion” and “sequestration”, will be first introduced in detail.

1.1 Thermophilic bacteria: life on the edge

The philosopher Aristotle (384-322 BC) introduced in his work ‘*Categoriae*’ a new concept to science by grouping ideas and objects according to their properties. These classification systems help to determine how various ideas or objects are similar and related to each other. The concept is still present in fields of modern-day biology, such as in taxonomy and in phylogeny. Aristotle classified living things as either plants or animals. However, the development of the microscope in the 17th century and new insights in molecular biology at the end of the 20th century (Woese *et al.*, 1990) showed furthermore the presence of bacteria and archaea, respectively. Currently, the most widely applied classification system for organisms in biology consists of three separate domains, the top-level taxa *Eukarya* (containing the kingdoms *Plantae* and *Animalia*), *Bacteria*, and *Archaea*, which is often visualized as the universal phylogenetic tree of life (Figure 1).

Although the term “bacteria” was traditionally used to describe unicellular organisms of microscopic size, it is not accurate as all three domains of life contain members that can fall under this definition: fungi of the domain *Eukarya*, and the entire domains *Bacteria* (except *Thiomargarita* species) and *Archaea*. Nowadays, the traditional meaning of the term “bacteria” is replaced by the terms “microorganism” and “microbes”, whereas the modern term “bacteria” refers exclusively to organisms of the domain *Bacteria*. Although bacteria share

phenotypic properties with fungi and archaea, lateral gene transfer occurred between the groups, and integration of bacterial and archaeal endosymbionts in eukaryotic cells (Martin, 1999); the domains can be genotypically clearly distinguished from each other and be identified by molecular distinctions of biomarkers such as the small-subunit ribosomal nucleic acid molecule (16S rRNA) essential for protein biosynthesis.

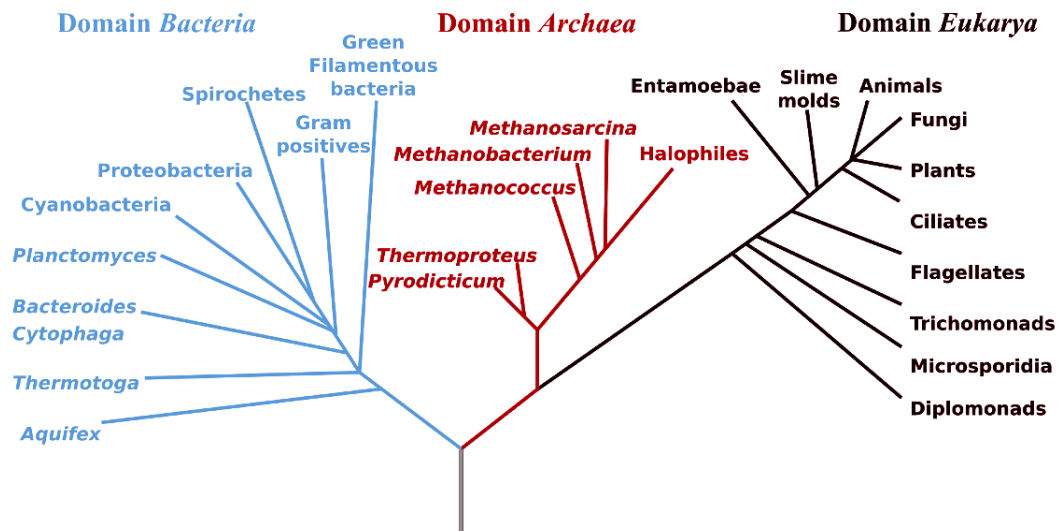


Figure 1. Rooted universal phylogenetic tree displaying the domains *Eukarya*, *Bacteria* and *Archaea* and some groups within the domains based on sequence similarities of 16S rRNA genes (modified from Woese *et al.*, 1990).

Besides phylogenetic groups, there are numerous potential categories by which microorganisms can be classified or grouped. The optimum growth temperature of an organism determines its classification as psychrophilic (Greek: psychros, cold; philos, love), mesophilic (Greek: mesos, middle; philos, love), thermophilic (Greek: thermos, heat; philos, love), or hyperthermophilic (Greek: hyper, beyond; thermos, heat; philos, love):

- under 15° C: psychrophilic (Morita, 1975),
- between 15° C and 45° C: mesophilic,
- between 45° C and 80° C: thermophilic (Madigan *et al.*, 2000),
- above 80° C: hyperthermophilic (Kelly & Adams, 1994).

The current observed maximum growth temperatures of eukaryotic (some fungal species), bacterial (*Aquifex* species), and archaeal monotypic cultures (Strain 121) are 62° C, 95° C, and 121° C, respectively (Deckert *et al.*, 1998; Kashefi & Lovley, 2003; Tansey & Brock, 1972). Thermophilic organisms are able to survive under mild or cold temperatures. Although the first isolated thermophilic bacterium was obtained from the River Seine in France at the end of the 19th century by Miquel (Skinner, 1968), they are generally limited for growth to anthropogenic and natural geologic thermal sources such as compost piles, haystacks, hot water heaters and pipes, terrestrial hot springs and marine hydrothermal vents. As a wide range of geological thermal environments exhibit relatively high concentrations of dissolved metal and metalloid ions (Hirner *et al.*, 1998), organisms within these habitats might have novel adaptive properties to metal and metalloid species. Which leads to the questions: What actually are metals and metalloids?

1.2 Metals and metalloids: a double-edged sword for life

Metals and metalloids, also termed semi-metals, can be distinguished from non-metals by different physical and chemical properties. Usually metals are characterized by good electrical and thermal conduction, malleability (the ability of a material to be deformed under compression without cracking, e.g. when stamped or rolled), ductility (the extent to which a material can be deformed without fracturing when being subject to tensile forces, e.g. when drawn into a thin wire), capacity to form cations (positive ions) and metal bonding. Although metalloids share some of these characteristics with metals, such as formation of cations and metal bonding, metalloids both insulate (like non-metals) and conduct electricity (like metals) as a function of temperature. The metalloids silicon (Si), tellurium (Te), arsenic (As), antimony (Sb), polonium (Po) and astatine (At) occur in negative and positive oxidations states, thus able to form cations and anions (negative ions). Metals, metalloids, and non-metals can be organized by their unique electron configurations and are relatively easily distinguished from each other (Figure 2). So far, 111 chemical elements have been fully characterized: 86 (77%) are metals and eight (7%) are metalloids, which underlies the variety of metal elements.

[illegible]

Figure 2. Periodic table displaying elements based on their electron configuration. The white fields refer to discovered elements, but yet not formally named. The subscripted numbers within the fields represent atomic numbers; the one- and two-letter codes the abbreviations used for the elements. Numbers on top of the periodic table indicate group numbers separating metals further in alkali metals (group 1 without hydrogen H), earth alkali metals (group 2), and transition metals (group 3 to 12). The block separated from the main table is the group of rare earth metals.

The terms “metal” and “metalloids” are widely used for elements and the corresponding chemical compounds and species. However, the chemical, physical, and physiological properties of an elemental metal can differ greatly from its chemical species, e.g. the trivalent species of elemental arsenic (As), arsenite (As^{3+}), is several times more toxic for biological systems than its pentavalent form arsenate (As^{5+}) (Bissen & Frimmel, 2003). In this study, the terms “metal” and “metalloid” refer to the corresponding elements, whereas the terms “metal ion” and “metalloid ion” is used for the corresponding chemical species. The common term “heavy metal” has no sound definition. Duffus (2002) summarized a multitude of suggested interpretations for the term used in scientific publications defined by inconsistent values for specific gravity (ranging from above 3.5 g per cm^3 to above 7.0 g per cm^3), atomic number or atomic weight. As the terminology of “heavy metal” is not consistent, the term will be completely avoided in the present thesis.

Why are metal ions biologically important? Cations are essential for a variety of physiological processes fulfilling catalytic and structural functions. Enzymes, a subclass of proteins, make biochemical reactions either possible in the first place or accelerate the rate of reactions significantly by lowering the activation energy for specific chemical reactions. The catalytic centres of many enzymes contain metal ions (Table 1). Cations are important structural elements of biomolecules, e.g. magnesium ions stabilize ribosomes and membranes (Smith & Maguire, 1998). The capacity of cells to maintain physiological conditions (homeostasis) includes the ability to regulate the intracellular concentration of hydrogen ions (H^+). The pH value, defined as the negative logarithm of the hydrogen ion concentration, can be adjusted by influx or efflux of hydrogen ions in or out the cell, thereby lowering or raising the intracellular pH, respectively. The transport process depends on monovalent metal cations (Kroll & Booth, 1983; Matin, 1990). Metalloid ions have been found to be involved for groups of microorganisms in cell-to-cell communication termed quorum sensing (boron ions); incorporated into the 21st described amino acid selenocysteine (selenium ions); and even antimony and cadmium ions, usually toxic for organisms in low concentration, have been found in marine diatoms incorporated into organic molecules such as lipids and one type of enzyme, respectively (Benson & Cooney,

1988; Chen *et al.*, 2002; Lane & Morel, 2000; Zinoni *et al.*, 1986).

Table 1. Some representative metalloproteins and their metabolic functions. Not all of the listed biomolecules are found in a single organism as some are involved in highly specific reactions. There are enzymes containing heterometallic centers, such as Ni-Fe hydrogenase consisting of nickel and iron ions. (Crowley *et al.*, 2000; Kisker *et al.*, 1997; Kobayashi & Shimizu, 1999; Köhler & Völsgen, 1997; Watt & Ludden, 1999)

Ions of	Biomolecule	Biological relevance
Iron (Fe)	Ferredoxin	Electron carrier
	Cytochrome oxidase	Electron carrier
	Hydrogenase	Activates molecular hydrogen (H_2)
Cobalt (Co)	Vitamin B_{12}	Methyl (CH_3^-) group transfer
Nickel (Ni)	Urease	Hydrolyses urea ($(\text{NH}_2)_2\text{CO}$)
	Hydrogenase	Activates molecular hydrogen (H_2)
	Cis-trans isomerase	Changes structure within a single molecule
Magnesium (Mg)	Phosphatase	Hydrolyses phosphoric acid monoesters (PO_4^{3-})
	Bacteriochlorophylls	Photosynthetic pigments
Molybdenum (Mo)	Nitrogenase	Fixes atmospheric nitrogen gas (N_2)
	Nitrate reductase	Reduces nitrate (NO_3^-) to nitrite (NO_2^-)
Manganese (Mn)	Superoxide dismutase	Disproportionates superoxide (O_2^-) into hydrogen peroxide (H_2O_2) and molecular oxygen (O_2)
Zinc (Zn)	RNA and DNA polymerases	Synthesize nucleic acids
	Alcohol dehydrogenase	Oxidizes ethanol ($\text{CH}_3\text{CH}_2\text{OH}$) to acetaldehyde (CH_3CHO)

Reduction-oxidation (redox) reactions serve as metabolic energy sources. For redox reactions, it is mandatory that reactants take part either in oxidation reactions by accepting electrons (oxidizing agents) or in reduction reactions by providing electrons (reducing agents). Therefore, the involved reactants must be able to occur in different oxidation states. Some metal and metalloid ions fulfill this requirement and are consequently used by many bacterial and archaeal strains as final electron acceptors during dissimilatory metal and metalloid reduction or as electron donor for chemolithotrophic growth (Greek: chemo, chemical; lithos, stone; trophy, nourishment: production of biomass by using oxidation of inorganic compounds as energy source). Redox transformations of various metal and metalloids by organisms have been described including compounds of iron, manganese, chromium, arsenic, mercury, and uranium (Croal *et al.*, 2004; Gihring & Banfield, 2001; Lovley, 1993; Stolz *et al.*, 2006; Stolz & Oremland, 1999; Straub *et al.*, 2001).

Besides the potential beneficial aspects described above, metal and metalloid ions can threaten living cells and even cause their death. Non-essential metal and metalloid species can displace for an organism essential metal and metalloid ions, thereby interfering with cellular functions. Metal and metalloid oxyanions can “mimic” structurally related non-metal species. In cell reactions arsenate (AsO_4^{3-}) and vanadate (VO_4^{3-}) compete with phosphate (PO_4^{2-}), and similarly, chromate (CrO_4^{2-}) and molybdate (MoO_4^{3-}) are analogues of sulfate (SO_4^{2-}) (Ballatori, 2002; Bissen & Frimmel, 2003). Disruptions of phosphate metabolism affect protein biosynthesis, cell integrity, and energy conservation, as phosphates are integral components of nucleic acids (DNA and RNA), lipid membranes, and adenosine 5'-triphosphate (ATP), respectively. Furthermore, the reduction of metal and metalloid oxyanions can result in the formation of radical species possessing an unpaired electron (Nies, 1999). These unpaired electrons are highly reactive and threaten the integrity of nucleic acids (mutations), proteins and lipids and can lead to cell death (Cheeseman & Slater, 1993). Some metal and metalloid ions tend to bind with great affinity to functional groups of proteins, particularly to thiol groups (SH^-), and might modifying the conformation and alter the activity of physiologically-relevant biomolecules (Nies, 1999).

1.3 Sequestration

As discussed earlier, metal and metalloid ions are potentially life-threatening, particularly at elevated concentrations. To guarantee their survival, cells have developed several homeostasis, protection, and detoxification strategies when interacting with metal and metalloids ions. Frequently described responses are:

- Active efflux system

Efflux systems are energy-dependent processes (consuming ATP) mediated by a specific carrier. The major families of enzymes involved in the export of cations are: 1) P-type ATPase family pumps cadmium (Cd^{2+}), copper (Cu^{2+}), potassium (K^+), sodium (Na^+), magnesium (Mg^{2+}), and calcium ions (Ca^{2+}) out of the cell; 2) ATP-binding cassette (ABC) family exports nickel (Ni^{2+}), manganese (Mn^{2+}), iron (Fe^{2+}), and molybdenum ions (Mo^{2+}); 3) Resistance-nodulation-cell division family (RND) effluxes Ni^{2+} , cobalt (Co^{2+}), Cd^{2+} , and zinc ions (Zn^{2+}); and 4) Cation diffusion facilitator family (CDF) transports Zn^{2+} , Cd^{2+} , and Co^{2+} (Nies, 2003; Paulsen & Saier, 1997; Saier, 2000; Silver & Phung, 1996; Spada *et al.*, 2002).

- Biotransformation

The possible enzymatic transformations of metal and metalloid compounds to less toxic forms consist of oxidation, reduction, methylation, and demethylation reactions. Arsenic resistance conferred by the *ars* operon is a model example. Intracellular arsenate is reduced to arsenite by the arsenate reductase (ArsC). This step seems to be irrational at first sight, as arsenite is more toxic than arsenate. However, as mentioned above, arsenate is a structural analogue of the physiologically important phosphate, and by reducing it, it is distinguishable from phosphate. Arsenite is then expelled from the cytoplasm through a specific efflux pump encoded by the *arsB* gene, either alone or together with an ATPase (ArsA). Another prominent example is the mercury resistance operon. (Bruins *et al.*, 2000; Nies, 1999; Stolz *et al.*, 2006)

- Intracellular complexation

Metal and metalloids ion are bound to cellular ligands (complexes one cation) and chelators (complexes more than one cation) such as polyphosphates,

glutathiones (Mendoza-Cozatl *et al.*, 2005), metallothioneins (Palmiter, 1998; Robinson *et al.*, 2001) and in plant cells to phytochelatinases (Knauer *et al.*, 1998) to prevent toxic cations interacting with essential biochemical reactions or structures. Intracellular complexation of mercury, cadmium, lead and silver ions have been reported (Singh *et al.*, 2001).

- Compartmentation

This strategy occurs nearly exclusively in eukaryotic cells as usually bacteria and archaea lack subcellular compartments. Compartmentation in the vacuole has been reported for plants, fungi, algae and yeasts (Hall, 2002; Mendoza-Cozatl *et al.*, 2005).

- Changes in ion permeability

The permeability of the outer membrane of Gram-negative bacteria might be decreased by altering the conformation of transmembrane transport proteins such as porins and thus reducing the import of the metal and metalloid ions (Li *et al.*, 1997; Zheng *et al.*, 2005).

- Extracellular complexation

Extracellular complexation includes two separate approaches: 1) The release of biopolymers with anionic character such as exopolysaccharides in the surrounding medium which complex or precipitate metal and metalloid cations (McSwain *et al.*, 2005); and 2) the adsorption of metal and metalloid ions onto and into the cell wall. The latter case is called biosorption and potential ligands, which form complex compounds with cations, are reactive functional groups such as deprotonated hydroxyl (R-OH, R represents the cell to which the functional group is attached), carboxyl (R-COOH), sulfhydryl (R-SH), sulfo (R-SO₃H), phosphono (R-PO(OH)₂), amino (R-NH₂), imino (R=NH), and amido (R-CONH₂) of peptidoglycans, teichoic and teichuronic acids, polysaccharides, and proteins exposed on, or incorporated in, the cell wall (Gadd, 1990; Vecchio *et al.*, 1998).

These strategies have been categorized, whether metal and metalloid species are sequestered or not. The general definition of the term “sequestration” is the act of forming a compound with an ion, atom, or molecule so that the ion, atom, or molecule is no longer available for chemical reactions. Of all the described strategies, only complexation and compartmentation fulfill this definition.

However, in this study, sequestration particularly refers to the interaction between thermophilic bacteria and aqueous metal or metalloid ions, in which the effective concentration of the metal or metalloid ions in a solution is lowered due to complexation. As noted above, compartmentation of metal and metalloid compounds in bacteria might be excluded.

1.4 Objectives

The ability of microorganisms to interact with cationic metal and metalloid species in various ways such as biotransformation, bioaccumulation, and biosorption greatly affects the geochemical cycles of metal and metalloid species. Microbial mediated mobilization and demobilizing of cations influences the distribution and availability of metal and metalloid ions in the environment (Gadd, 2000; Gadd, 2004; Unz & Shuttleworth, 1996). A recent example is the high arsenic concentration of groundwater above the limit recommended by the World Health Organization (10 µg per liter) (WHO, 2004) in parts of Bangladesh, India, Vietnam, Cambodia, Taiwan, Mexico, Argentina, Chile, Hungary, Romania, Canada, and the United States of America (USA) affecting the drinking water supply and the health of many millions of people (Bissen & Frimmel, 2003; Croal *et al.*, 2004). Arsenic compounds are human carcinogens associated with hyperpigmentation and hyperkeratosis of the skin, cardiovascular and cerebrovascular diseases, and reproductive effects including higher rates of spontaneous abortions and stillbirths (Ahmad *et al.*, 2001; Bissen & Frimmel, 2003). Although naturally-occurring arsenic species are immobilized in aquifer sediments, either adsorbed to iron oxyhydroxides (FeOOH; both arsenate and arsenite) or incorporated into arsenopyrite (FeAsS; arsenite), microbial reduction of iron oxyhydroxides or oxidation of arsenopyrite leads to the release of arsenate or arsenite from the sediment to the drinking water (Islam *et al.*, 2005; Zobrist *et al.*, 2000). Microorganisms play a fundamental role in geological processes such as transformation and degradation of minerals containing arsenic (As), antimony (Sb), mercury (Hg), iron (Fe), manganese (Mn), chromium (Cr), molybdenum (Mo), vanadium (V), and uranium (U) (Ehrlich, 1995).

The further understanding of the interactions between microbial cells and metal and metalloid species would support novel, or improve existing, biotechnical applications. Mesophilic microorganisms are commercially employed in bioleaching of copper, uranium, and gold-bearing ores by acidophilic ferrous- and sulfur-oxidizing bacteria involving *Acidithiobacillus ferrooxidans* and *Acidithiobacillus thiooxidans* (formerly *Thiobacillus*) (Rawlings, 2002) and are potential bioremediation agents for recovering metal and metalloid species from waste waters and soils (Gadd, 2000). However, little is known about the interaction between thermophilic microorganisms and metal and metalloid species. This study is part of the biotechnology program “Extremophilic microorganisms for metal sequestration from aqueous solutions”. The aim of the program is to describe and predict metal ion biosorption behavior by thermophilic microorganisms to permit future biotechnology applications.

The objectives of the thesis are as follow: 1) to screen the culture collection of the Thermophile Research Unit located at the University of Waikato consisting of approximately 900 archaeal and bacterial strains for metal-tolerant bacteria; 2) based on the initial toxicity experiments to select model organisms and to investigate the interaction of the bacteria and the dissolved metal ion; and 3) try to enrich thermophilic microorganisms from geothermal environments rich in metal or metalloid compounds, and if monotypic organisms could be successfully isolated, to identify and characterize novel isolates.

It has been proposed that thermophilic bacteria, in comparison to psychrophilic and mesophilic microorganisms, have adapted to elevated temperatures by faster metabolic turnover due to replacement of thermal denaturated biomolecules and the ability to stabilize essential molecules and structures such as proteins, nucleic acids and cell membranes (Mulks *et al.*, 1980). Thermophilic bacteria incorporate a higher degree of saturated and iso- and anteiso-branched fatty acids, of elongated fatty acyl chains, and of carbohydrate-enriched lipids into their cell membranes than mesophiles (Edwards, 1990; Konings *et al.*, 2002; Langworthy & Pond, 1986; Sundaram, 1986). Although the current knowledge of metal ion tolerance is almost completely based on mesophilic organisms, thermophiles, which are physiologically and structurally different from mesophiles, might have

elaborated unique strategies to interact with dissolved metal ions. In an initial susceptibility assay of 46 thermophilic bacterial strains with three mesophilic as an out-group, minimal inhibition concentration (MIC) for divalent cadmium cations have been determined (Chapter 2). Bacteria were differentiated into cadmium ion-sensitive and cadmium ion-tolerant organisms with *Geobacillus stearothermophilus* and *G. thermocatenulatus* displaying tolerance to high concentration of cadmium ions and were selected for further investigation into the mode of metal ion-bacteria interaction.

Surface complexation modeling is based upon a set of molecular-scale thermodynamic reactions, which specify electrostatic and chemical interactions occurring at the solution-surface interface. It can be applied in biosorption reactions describing adsorption and desorption of dissolved metal species to potential ligands onto and into bacterial cell walls. Computer analysis of data obtained from acid-base titration and metal ion adsorption experiments on bacterial cell suspensions provide information on number and concentration of ligands and on the stability of the ligand-cation complexes as a function of pH (Figure 3). In Chapter 3 are the first reported surface complexation models (SCMs) quantifying metal ion adsorption by thermophilic microorganisms. SCMs were developed to describe cadmium ion biosorption by *G. stearothermophilus* and *G. thermocatenulatus* cells.

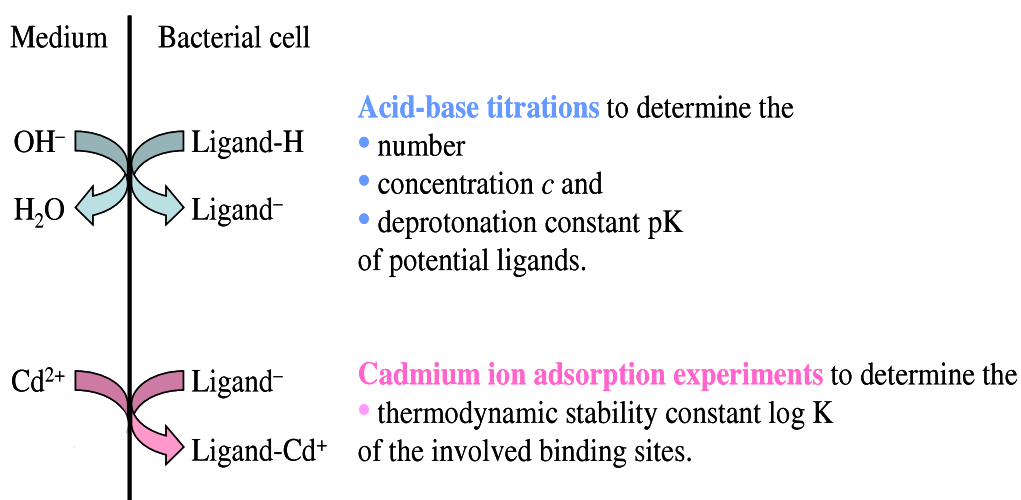


Figure 3. Scheme of surface complexation modeling to predict divalent cadmium cation adsorption by bacteria at the medium-bacterial cell surface interface.

Another aim of this thesis was to study metal ion-tolerant microorganisms obtained from high-temperature environments. New Zealand is famous for its many geothermal features. The North and South Islands of New Zealand lies on the boundary where the Australian and Pacific tectonic plates of the Earth's crust collide. Underneath the North Island, the Pacific plate is subducted below the Indio-Australian plate. When the subducted lithosphere reaches a certain depth, pressure, and heat from the isotopic decay of radioactive elements melts the rock and less dense magma ascends (Price *et al.*, 2005). The thermal energy is transferred to geothermally active areas as magma heats solid surface rock (conduction), or groundwater, which then rises to the surface (convection). Terrestrial thermal activity is noticeable at the surface and associated with volcanoes (magma expelled as lava), fumaroles (local vents that release steam and gases), steaming grounds (areas with diffuse discharge of steam and gases), mud pools (super-heated steam condenses and dissolves surface rock into clay), hot springs (springs that discharge hot water) and geysers (hot springs that erupt periodically).



Figure 4. Water samples collected from Champagne Pool at Waiotapu in New Zealand.

The Waiotapu area located at the center of the North Island is one of the largest geothermal areas in New Zealand. The most prominent feature within the area is the hot spring Champagne Pool (Figure 4) which is around 65 m in diameter and has an estimated volume of 50,000 m³. The spring water is oversaturated with arsenic and antimony compounds, which precipitate and form the orange deposits at the shelf around Champagne Pool. Although Champagne pool is geochemically well characterized, hardly anything is known about its role as a possible habitat for microbial life. In Chapter 4 microbial density and diversity in Champagne Pool is discussed using first culture-independent and then culture-dependent methods.

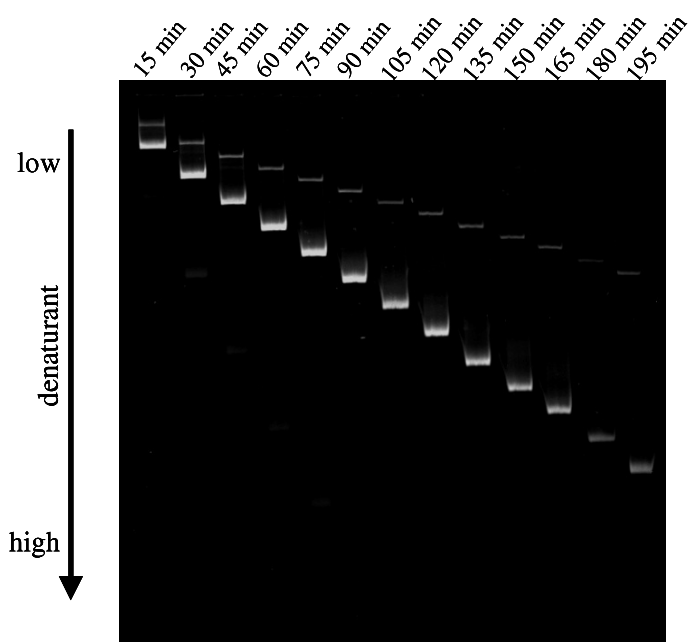


Figure 5. Chronological sequence of a DGGE profile of an environmental DNA sample obtained from a mud pool at Orakei Korako, New Zealand showing migration and separation process of two different archaeal 16S rRNA gene fragments.

Polymerase chain reactions (PCRs) of environmental DNA samples generate fragments of differing sequences (depending on the microbial composition within the samples) but of similar size. In comparison to conventional separation of PCR products by agarose gel electrophoresis, Denaturing Gradient Gel Electrophoresis (DGGE) separates a mix of various DNA species not by nucleotide number but according to the melting behavior based on the nucleotide sequence. PCR

products are electrophoresed through a linear gradient of increasing chemical denaturing concentrations until each DNA species reaches the denaturant concentration equivalent to their individual melting temperature. At that point the two strands of the DNA fragment start separating (“melting”) and due the conformation change the molecule slows down its migration and is immobilized at an unique gel position (Figure 5). The DNA fragment can then be excised and analyzed. Based on results obtained from DGGE and 16S rRNA (small-subunit ribosomal nucleic acid) gene clone libraries, a culture medium was designed (Figure 6). This approach has allowed isolation of the novel hydrogen-oxidizing bacterium *Venenivibrio stagnispumantis* (Chapter 5).

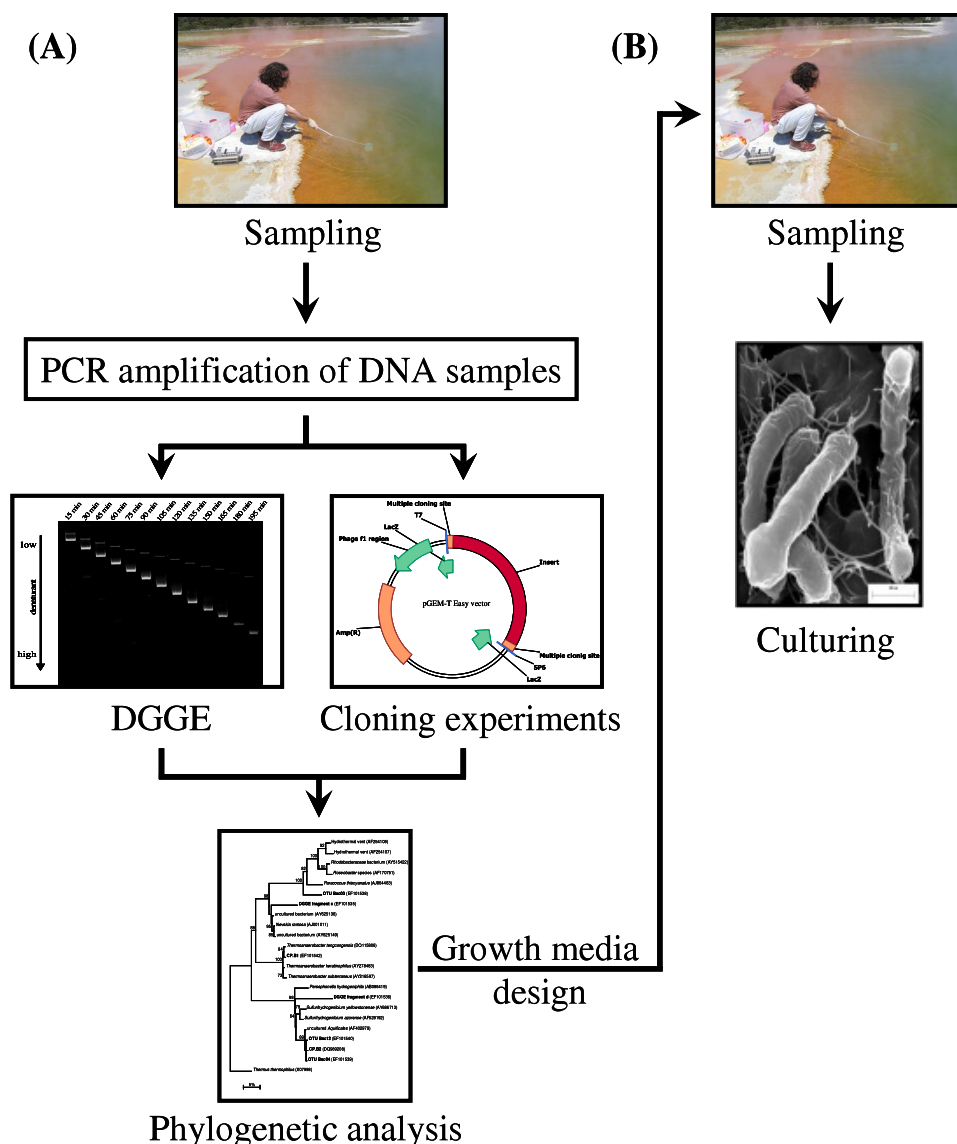


Figure 6. Microbial studies of Champagne Pool consisted of culture-independent (A) and culture-dependent methods (B)

Chapter 2: Cadmium ion toxicity experiments

2.1 Introduction

Cadmium is considered to be a toxic heavy metal, despite the lack of a chemically sound definition for the term heavy metal (Duffus, 2002) and an observed biological benefit of cadmium for zinc-limited marine diatoms (Lane & Morel, 2000). However, cadmium ions and compounds are important environmental pollutants affecting most eukaryotic, bacterial and archaeal cells. Although cadmium is a relatively rare element with an average content of 0.2 mg per kg in the geosphere (Lindsay, 1979), anthropogenic activities have led to local accumulation of cadmium compounds (Vig *et al.*, 2003). Cadmium is a common impurity of zinc ores, and it is most often obtained as a by-product of the smelting of zinc. It is a widely used constituent of nickel-cadmium batteries, of solar cells (cadmium telluride), of cadmium-based solder, of corrosion protective coatings for iron and steel surfaces, of the plastic, polyvinyl chloride (PVC) as stabilizer, and of pigments for coloring plastics, glass, ceramics, and paintings (cadmium sulfide and selenide in cadmium yellow, cadmium orange, and cadmium red). Besides industrial applications, cadmium-contaminated zinc sulfate in fertilizers is another important source of environmental pollution of cadmium compounds.

In this study, 46 thermophilic and 3 mesophilic strains of the genera *Thermus* and *Bacillus* (Table 2 and Table 3) available in the culture collection of the Thermophile Research Unit (University of Waikato, Hamilton, NZ) were tested in susceptibility assays to determine their tolerance to cadmium ions (Cd^{2+}). Thermophilic bacteria of both these genera are aerobic and have overlapping ranges of growth temperatures and pH values, but differ significantly in cell wall composition. Aerobic bacteria were selected as the relatively simple cultivation technique allows a quick determination of cadmium ion-tolerant model organisms for further investigations (Chapter 3).

Gram-staining is a standard method to differentiate bacteria based on differences in the structure of their cell walls into two large groups, either Gram-negative or

Gram-positive (Hucker & Conn, 1927), and into a small group of Gram-variable (Beveridge, 1990). Gram-positive cells contain multilayers of peptidoglycan, whereas Gram-negative cells have a single peptidoglycan layer surrounded by a lipopolysaccharide bilayer (outer membrane). *Thermus* cells stain Gram-negative and *Bacillus* cells react Gram-positive. However, in the peptidoglycan of *Thermus*-like organisms the dibasic amino acid ornithine is present in place of the more typical Gram-negative constituent, diaminopimelic acid (Pask-Hughes & Williams, 1978). Potential differences of the cadmium ion toxicity between bacteria of both genera may reflect the different types of cell wall structures.

The first *Thermus* isolate, *Thermus aquaticus*, was described in 1969. The isolation of its thermostable DNA polymerase (*Taq* polymerase) and use in polymerase chain reactions (PCRs) to amplify *in vitro* nucleic acids has greatly influenced molecular biology (Chien *et al.*, 1976). Since then several species have been obtained from thermal environments. Hudson (1986) grouped *Thermus* isolates obtained from New Zealand, Iceland and USA in 14 clusters (A to N) by numerical classification. In the cadmium ion toxicity assays, at least one representative from each cluster was selected except for the smallest clusters C and N (Table 3). All strains listed in Table 2 were assigned to the genus *Bacillus* until the last decade. However, as more and more information about DNA base compositions became available, a major reorganization for the genus *Bacillus* began (Zeigler, 2001). Due to the changes in nomenclature, the bacteria listed in Table 2 now belong to the genera *Aneurinibacillus*, *Anoxybacillus*, *Bacillus*, *Brevibacillus*, and *Geobacillus*.

2.2 Materials and Methods

2.2.1 Bacteria and culture conditions

The following thermophilic bacteria were tested in toxicity experiments for cadmium ion tolerance (Table 2 and Table 3): *Aneurinibacillus thermoaerophilus* (DSM 10154); *Anoxybacillus flavithermus* (milk powder isolate); *Bacillus sp.* (DSM 2349), *B. caldolyticus* (DSM 405), *B. caldotenax* (DSM 406), *B. caldovelox* (DSM 411), *B. coagulans* (DSM 1, as mesophilic out-group for

comparison), *B. licheniformis* (milk powder isolate), *B. mycoides* (DSM strain 299, as mesophilic out-group), *B. smithii* (DSM 460, 4216), *B. sphaericus* (DSM 462, 463); *Brevibacillus brevis* (DSM 5507), *B. borstelensis* (DSM 6453, as mesophilic out-group); *Geobacillus thermocatenulatus* (DSM 730), *G. thermodenitrificans* (DSM 13147, 13148, 13149), *G. thermoglucosidasius* (DSM 2543), *G. thermoleovorans* (DSM 5366), *G. stearothermophilus* (DSM 458, 6790, 13240); *Thermus aquaticus* (DSM 625, ATCC 27737), *Thermus sp.* T351 (ATCC 31674), *T. thermophilus* (DSM 579), *T. rubber* (DSM 1279); fifteen environmental strains isolated from various hot springs in New Zealand: HS.8A1 (Hanmer Springs); KP.A3, RT.4A1, RT.8A1, RT26.A1, RT.41A, RT.355A1 (all from Rotorua); OH.A2 (Ohaki); TOK10.A3, TOK13.A4, TOK.20A1 (all from Tokaanu); TP.10A2 (Taupo); WAI21.A2, WAI.33A2, WAI.33A3 (all from Waimangu); and five isolates obtained from overseas: NMX.2A1 and YSP.2AA1 (both from the USA); and ZHGI.A1, ZHGIC.A1 and ZVIE.A3 (all from Iceland).

Prior to the experiments, all bacterial strains were successively sub-cultured at least twice in fresh medium. Castenholz medium D (CMD) was used to cultivate the *Thermus* species (Table 3) and contained (per liter): 0.10 g of nitrilotriacetic acid, 0.10 g of $\text{MgSO}_4 \cdot 7\text{H}_2\text{O}$, 0.06 g of $\text{CaSO}_4 \cdot 2\text{H}_2\text{O}$, 8.00 mg of NaCl, 0.10 g of KNO_3 , 0.69 g of NaNO_3 , 0.11 g of Na_2HPO_4 , 0.47 mg of $\text{FeCl}_3 \cdot 6\text{H}_2\text{O}$, 1.00 g of trypticase peptone, 1.00 g of yeast extract, and Nitsch's trace elements (per liter medium: 2.20 mg of $\text{MnSO}_4 \cdot 4\text{H}_2\text{O}$, 0.50 mg of $\text{ZnSO}_4 \cdot 7\text{H}_2\text{O}$, 0.50 mg of H_3BO_3 , 0.016 mg of CuSO_4 , 0.025 mg of $\text{Na}_2\text{MoO}_4 \cdot 2\text{H}_2\text{O}$, and 0.046 mg $\text{CoCl}_2 \cdot 6\text{H}_2\text{O}$). The pH value of the medium was 7. The basal medium to grow RT26.A1 and WAI21.A2 contained (per liter): 0.25 g of $\text{CaCl}_2 \cdot 2\text{H}_2\text{O}$, 0.50 g of $\text{MgSO}_4 \cdot 7\text{H}_2\text{O}$, 0.20 g of $(\text{NH}_4)_2\text{SO}_4$, 2.00 g of yeast extract, 5.00 g of glucose, 3.00 g of KH_2PO_4 , and trace element solution SL-6 (per liter medium: 0.10 mg of $\text{ZnSO}_4 \cdot 7\text{H}_2\text{O}$, 0.03 mg of $\text{MnCl}_2 \cdot 4\text{H}_2\text{O}$, 0.30 mg of H_3BO_3 , 0.20 mg of $\text{CoCl}_2 \cdot 6\text{H}_2\text{O}$, 0.01 mg of $\text{CuCl}_2 \cdot 2\text{H}_2\text{O}$, 0.02 mg of $\text{NiCl}_2 \cdot 6\text{H}_2\text{O}$, and 0.03 mg of $\text{Na}_2\text{MoO}_4 \cdot 2\text{H}_2\text{O}$). The final pH value of the medium was adjusted to 4. The culture medium for the other bacterial strains (Table 2) except RT26.A1 and WAI21.A2 was 30 g per liter tryptic soy broth (TSB, Difco) adjusted to a pH value of 7.

2.2.2 Toxicity experiments

All bacterial strains mentioned above were tested for tolerance to elevated cadmium ion levels ($\text{CdCl}_2 \cdot 2.5\text{H}_2\text{O}$). Growth curves for strains displaying tolerance to cadmium ion concentration above $500 \mu\text{M}$ were also obtained in the presence of different arsenate concentrations ($\text{Na}_2\text{HAsO}_4 \cdot 7\text{H}_2\text{O}$). $160 \mu\text{l}$ medium per well in microtiter plates and 5 ml medium in test tubes supplemented with different defined concentrations of $\text{CdCl}_2 \cdot 2.5\text{H}_2\text{O}$ were inoculated using 5% inocula of freshly grown cultures. The growth was monitored in microtiter plates at a wavelength of 405 nm (FLUOstar Optima, BMG Labtechnologies) and in test tubes at 600 nm (Ultrospec 3000, Pharmacia Biotech). The minimum inhibitory concentration (MIC) was defined as absence of growth of the species after 16 h (microtiter plates) and 2 d (test tubes) at the lowest tested cadmium ion concentration. Additionally, samples were subsequently observed under a phase-contrast microscope (Olympus BH-2).

2.2.3 Small-scale plasmid isolation

Small-scale plasmid isolation according to Ronimus (1993), a derivation of the alkaline lysis method of Birnboim and Doly (1979), was performed to detect the presence of extrachromosomal DNA. Plasmid-encoded genes for cadmium resistance are commonly found in bacteria. *G. stearrowthermophilus* (DSM 6790) and *G. thermocatenulatus* (DSM 730) cells were grown in the presence of $200 \mu\text{M}$ Cd^{2+} and without Cd^{2+} prior to the plasmid isolation. *Escherichia coli* cells (strain JM109) were used as a control. A 3 ml aliquot of cell suspension was centrifuged at $12,000 \times g$ (Eppendorf Centrifuge 5415D) for 30 s and the resulting pellet was resuspended in the “Solution A” (50 mM glucose, 23 mM Tris, 10 mM EDTA; pH 8.0). The suspension was centrifuged at $12,000 \times g$ for 15 s and cells were resuspended in $20 \mu\text{l}$ lysozyme (10 mg per ml) and incubated for 15 min at 37°C . Then $200 \mu\text{l}$ “Solution A” and $400 \mu\text{l}$ “Solution B” (1% SDS, 0.2 M NaOH) were added and the cells were incubated in the lysis buffer on ice for 3 min. $300 \mu\text{l}$ of “Solution C” (3.0 M potassium acetate, 5.0 M glacial acetic acid; pH 4.8) was added, mixed for 10 min and then incubated on ice for 10 min. The suspension

was centrifuged at 12,000×g for 10 min to pellet chromosomal DNA and high molecular weight RNA. A 750 µl aliquot of the supernatant was transferred into 750 µl isopropanol. After 10 min incubation at room temperature, the sample was centrifuged at 12,000 g for 7 min. The pellet (extrachromosomal DNA and low molecular weight RNA) was then washed twice in 70% ethanol, air-dried and resuspended in 100 µl TE buffer (10 mM Tris-HCl, pH 8; 1 mM EDTA) containing 1 µl of 10 mg per ml RNase. The sample was incubated at 37° C for 20 min to digest any co-isolated RNA. The presence of plasmids was determined by electrophoresis in 0.7% agarose gel and TAE buffer (40 mM Tris, 20 mM acetic acid, 1 mM EDTA; pH 8.0) at 86 V for 1 h.

2.3 Results

2.3.1 Cadmium ion susceptibility tests

The values of the minimum inhibitory concentration (MIC) of Cd^{2+} for the bacterial species tested are displayed in Table 2 and Table 3. It is noteworthy that the thermophilic species displaying the highest cadmium ion tolerance in the experiments belong to a phylogenetic group proposed in 1991 as “group 5” (Ash *et al.*, 1991) that were later defined as the genus *Geobacillus* (Nazina *et al.*, 2001). In comparison to the mesophilic out-group *B. mycoides*, the thermophilic species were more sensitive to Cd^{2+} , while *G. thermoleovorans* tolerated similar Cd^{2+} concentration as *B. mycoides* as high as 3.2 mM. The highest MIC value for *Thermus* strains was 400 µM of Cd^{2+} and was determined for *T. aquaticus* and *T. thermophilus*. The lower values obtained for *Thermus* isolates indicate the cells to be more sensitive to cadmium ions. However, the use of different growth media, CMD for *Thermus* species and TSB for *Bacillus*-like organisms, might have influenced the tolerance to Cd^{2+} . Therefore, the cadmium ion toxicity experiments were repeated for those bacteria displaying a high tolerance to Cd^{2+} . Selected *Bacillus* species were used in the minimal medium CMD, and selected *Thermus* strains were grown in the complex medium TSB, respectively. This approach enables the comparison of the cadmium toxicity between bacteria of both genera in the same medium and the effects of the alternated media composition on the cadmium ion toxicity within a genus. The results clearly demonstrated that the

medium composition affected the ability of the tested bacteria to tolerate Cd^{2+} . All selected mesophilic and thermophilic bacteria exhibited a lower tolerance to Cd^{2+} in the other medium (Table 4).

Table 2. Minimum inhibitory concentration (MIC) of Cd^{2+} for the microorganisms studied and the temperature at which the toxicity experiments were conducted. Strains marked in bold displayed the highest tolerance and growth curves in the presence of different Cd^{2+} concentrations were obtained for these bacteria.

Microorganism	Strain ^a	T [° C]	MIC [Cd^{2+} μM]
<i>Bacillus mycoides</i>	299	25	>3200
<i>B. coagulans</i>	1	40	80
<i>Brevibacillus borstelensis</i>	6453	40	600
<i>Aneurinibacillus</i>	10154	55	80
<i>Bacillus sp.</i>	2349	55	80
<i>B. licheniformis</i>	Milk powder	55	80
<i>B. smithii</i>	460	55	80
<i>B. smithii</i>	4216	55	80
<i>B. sphaericus</i>	462	55	200
<i>Brevibacillus brevis</i>	5507	55	80
<i>Geobacillus stearothermophilus</i>	458	55	400
<i>G. stearothermophilus</i>	6790	55	600
<i>G. thermocatenulatus</i>	730	55	600
<i>G. thermodenitrificans</i>	13147	55	400
<i>G. thermodenitrificans</i>	13148	55	80
<i>G. thermodenitrificans</i>	13149	55	80
<i>G. thermoglucosidasius</i>	2543	55	600
<i>G. thermoleovorans</i>	5366	55	>3200
KP.A3	Rotorua	55	80
<i>Anoxybacillus flavithermus</i>	Milk powder	60	200
<i>Bacillus caldolyticus</i>	405	60	400
<i>B. caldotenax</i>	406	60	400
<i>B. caldovelox</i>	411	60	200
<i>B. sphaericus</i>	463	60	200
<i>Geobacillus stearothermophilus</i>	13240	60	200
Tok10.A3	Tokaanu	60	80
Tok13.A4	Tokaanu	60	600
Rt26.A1	Rotorua	65	80
Wai21.A2	Waimangu	65	80

^a Numbers refer to the corresponding DSM strain (Deutsche Sammlung von Mikroorganismen, the German Collection of Microorganisms).

Table 3. Minimum inhibitory concentration (MIC) of Cd^{2+} for the investigated *Thermus* isolates and the temperature at which the experiments were conducted. Hudson (1986) grouped the studied strains in different clusters. The corresponding cluster names are displayed.

<i>Thermus</i> species	Cluster	Strain ^a	T [° C]	MIC [Cd^{2+} μM]
<i>Thermus ruber</i>	-	DSM 1279	55	80
<i>Thermus</i> sp. T351	H	ATCC 31674	70	200
<i>T. aquaticus</i>	I	DSM 625	70	200
<i>T. aquaticus</i>	I	ATCC 27737	70	400
<i>T. thermophilus</i>	J	DSM 579	70	400
HS.8A1	A	Maruia Springs	70	80
OH.A2	L	Ohaki	70	200
RT.4A1	F	Rotorua	70	80
RT.8A1	M	Rotorua	70	200
RT.41A	H	Rotorua	70	200
RT.355A1	N	Rotorua	70	200
TOK.20A1	G	Tokaanu	70	200
TP.10A2	E	Taupo	70	80
WAI.33A2	E	Waimangu	70	80
WAI.33A3	K	Waimangu	70	80
NMX.2A1	A	Jemez	70	200
YSP.2AA1	I	Yellowstone NP	70	80
ZHGI.A1	L	Iceland	70	80
ZHGIC.A1	D	Iceland	70	200
ZVIE.A3	B	Iceland	70	200

^a Numbers refer to the corresponding DSM (Deutsche Sammlung von Mikroorganismen, the German Collection of Microorganisms) or ATCC strain (American Type Culture Collection).

Subsequent studies of the species showing MIC values of more than 500 μM Cd^{2+} revealed two different patterns of growth response. An increasing concentration of Cd^{2+} resulted either in a decrease of the maximum optical density with no change in the onset of growth and was observed for *B. mycoides*, *G. thermocatenulatus*, and *G. thermoleovorans* (Figure 7 A, Appendix A: Figure 34) or, alternatively a delay of the onset of growth but no significant effect on maximum optical density and was observed for *G. stearothermophilus*, *G. thermoglucosidasius*, and Tok13.A4 (Figure 7 B, Appendix A, Figure 35), respectively. These results may indicate two different strategies to interact with elevated concentrations of Cd^{2+} .

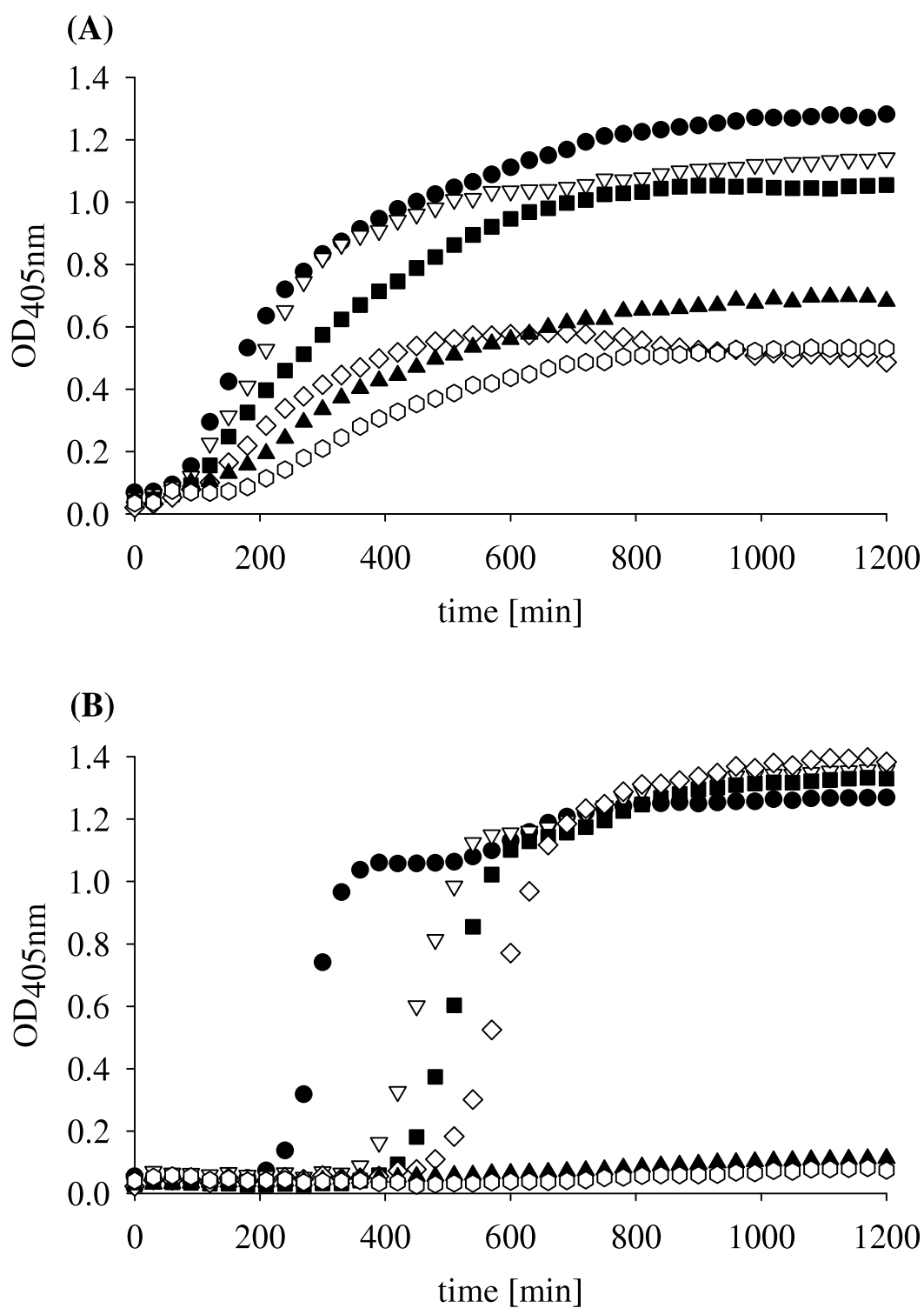


Figure 7. Microbial growth monitored spectrophotometrically at 405 nm as a function of concentration of Cd²⁺ (black circles: 0 μM, white triangles: 100 μM, black squares: 200 μM, white diamonds: 400 μM, black triangles: 600 μM, white hexagons: 800 μM). (A) Growth curves for *G. thermoleovorans* (DSM 5366) and (B) growth curves for *G. stearothermophilus* (DSM 6790). For clarity, only every second data point is shown.

Similar types of growth responses due to Cd^{2+} exposure could be monitored for *G. thermoleovorans* and *G. stearothermophilus* (DSM 6790) when the cells were cultivated in the presence of As^{5+} (Appendix A: Figure 36). However, the growth curves of the other bacteria studied could not be assigned to one of the described types, as the As^{5+} concentrations were too low to inhibit effectively their growth (Appendix A: Figure 37, Figure 38) and no general conclusion can be drawn.

Table 4. Minimum inhibitory concentration (MIC) of Cd^{2+} [μM] for nine selected bacteria when cultivated in the complex media TSB and in the minimal medium CMD.

Species	Strain ^a	T [° C]	MIC (TSB)	MIC (CMD)
<i>B. mycoides</i>	DSM 299	25	>3200	80
<i>G. stearothermophilus</i>	DSM 6790	55	600	80
<i>G. thermocatenulatus</i>	DSM 730	55	600	80
<i>G. thermoglucosidasius</i>	DSM 2543	55	600	80
<i>G. thermoleovorans</i>	DSM 5366	55	>3200	80
TOK.13A4	Tokaanu	65	600	80
Thermus sp.T351	ATCC 31674	70	no growth	200
<i>T. aquaticus</i>	ATCC 27737	70	80	400
TOK.20A1	Tokaanu	70	no growth	200

^a Numbers refer to the corresponding DSM (Deutsche Sammlung von Mikroorganismen, the German Collection of Microorganisms) or ATCC strain (American Type Culture Collection).

Although *G. stearothermophilus* (DSM 6790) cells showed the same growth pattern when pre-cultured in the presence of 200 μM Cd^{2+} prior to the cadmium ion susceptibility tests the cells displayed higher MIC values and the delay of the onset of growth was reduced in comparison to untreated *G. stearothermophilus* cells (Figure 8). It was assumed that the last described pattern might be the effect of inducible gene expression of a cadmium-resistance factor-carrying plasmid. Therefore, experiments were conducted to isolate plasmids that might be present.

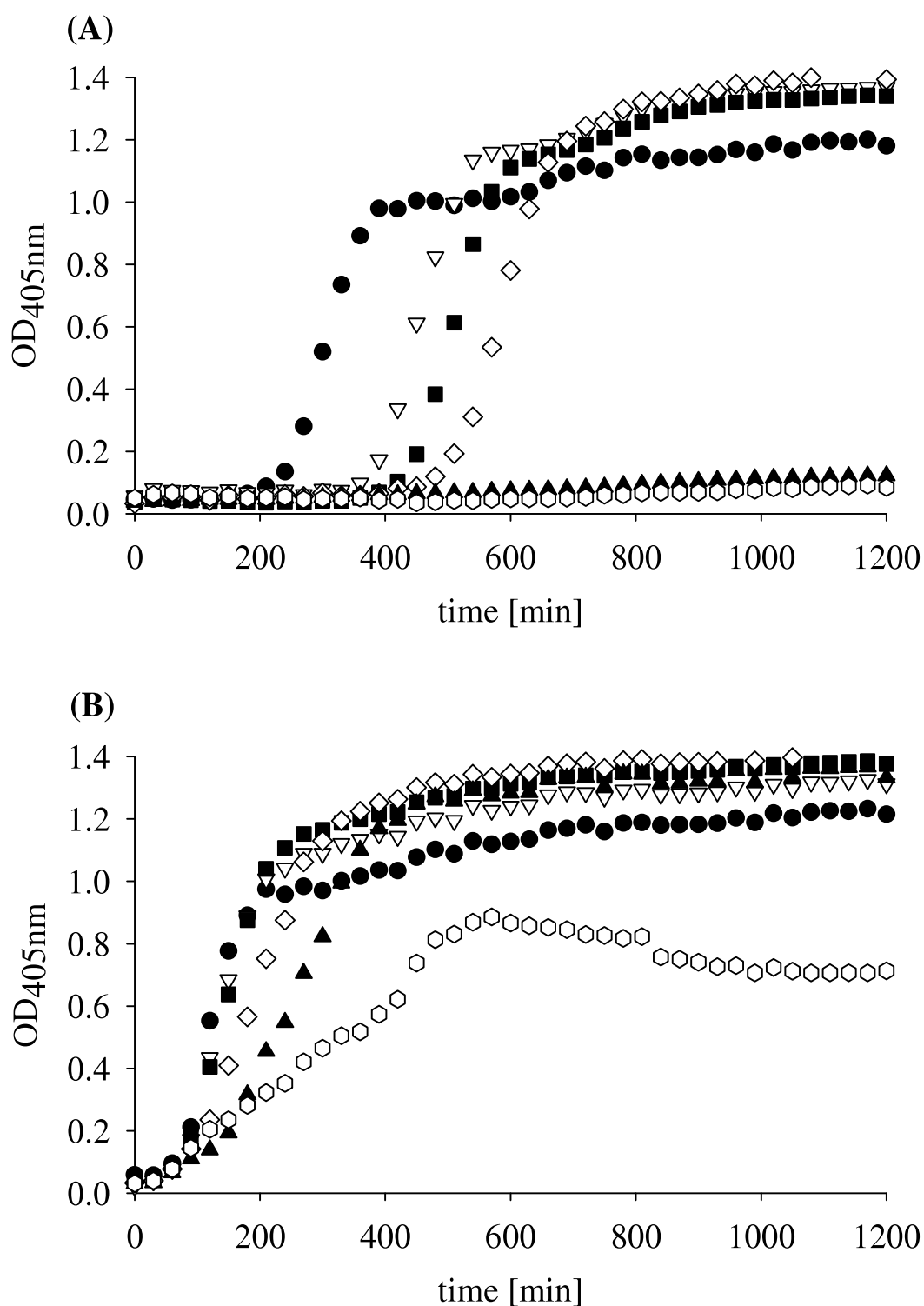


Figure 8. Microbial growth monitored spectrophotometrically at 405 nm as a function of concentration of Cd²⁺ (black circles: 0 µM, white triangles: 100 µM, black squares: 200 µM, white diamonds: 400 µM, black triangles: 600 µM, white hexagons: 800 µM). Growth curves for *G. stearothermophilus* (DSM 6790) previously cultured (A) without Cd²⁺ and (B) in the presence of 200 µM Cd²⁺. For clarity, only every second data point is shown.

2.3.2 Plasmid isolation

Although plasmid-encoded genes for cadmium ion resistance are widely distributed within the bacterial domain, plasmid isolations from *G. stearothersophilus* (DSM 6790) or *G. thermoleovorans* cells were negative. No extrachromosomal DNA was obtained (Figure 9).

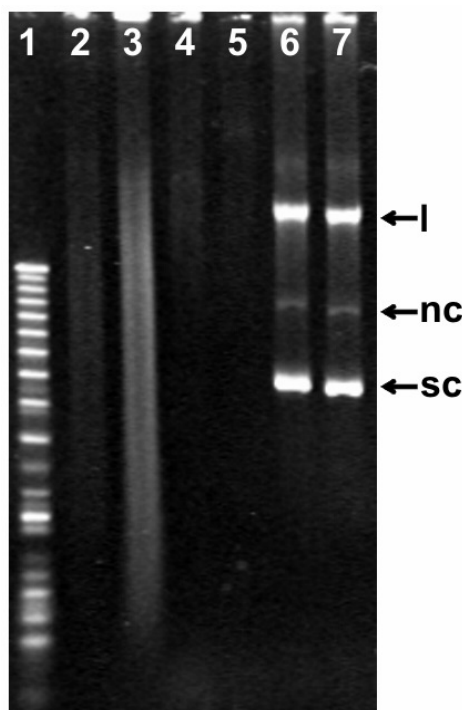


Figure 9. Image of an ethidium bromide-stained 0.7% agarose gel showing samples after plasmid extraction. Lanes: 1, 1 Kb Plus DNA ladder (Invitrogen); 2, *G. stearothersophilus* (DSM 6790); 3, *G. stearothersophilus* (DSM 6790) cultured in the presence of 200 μm Cd^{2+} ; 4, *G. thermoleovorans* (DSM 5366); 5, *G. thermoleovorans* (DSM 5366) cultured in the presence of 200 μm Cd^{2+} ; 6 and 7, *E. coli* JM109 as control. Abbreviations: l, linear plasmid DNA; nc, nicked circular plasmid DNA; sc, supercoiled circular plasmid DNA.

2.4. Discussion

The physiochemical composition of microbial cell walls can vary considerably within a species with organic and inorganic composition of the growth medium (Malouin *et al.*, 1991; Schär-Zammaretti *et al.*, 2005). The cadmium ion susceptibility assays revealed that the determined MIC values for Cd^{2+} for the studied bacteria depend on the growth medium used (Table 4). The results suggest

either that the *Thermus* cells in the complex media TSB and the *Bacillus*-like cells in the minimal medium CMD were already in a stressed situation and unable to tolerate additionally toxic cations or, that the alternate growth medium might have lead to changes of the bacterial cell surface properties and modified the interaction with cations.

Members of the genus *Geobacillus* displayed the highest Cd^{2+} tolerance with MIC values ranging from 80 to more than 3200 μM (Table 2). Although the diversity of growth media and conditions complicate a meaningful comparison with published studies, some of the results were higher than previously reported MIC values ranging from 10 to 500 μM of Cd^{2+} for thermophilic *Bacilli* (Llanos *et al.*, 2000). No correlation could be established in general for growth temperature and MIC values, and particularly for the studied *Thermus* strains between their cluster affiliation and their tolerance to Cd^{2+} .

Further studies on the strains displaying MIC values of more than 500 μM Cd^{2+} showed two different types of growth curves when exposed to elevated Cd^{2+} concentrations (Figure 7). An elongation of lag growth phase has been previously described for *Bacillus circulans* (Cd^{2+}), *Desulfovibrio vulgaris* (Cu^{2+} , Hg^{2+}) and *Flavobacterium sp.* (Sb^{3+}) when cells were exposed to increasing concentration of metal ions (Chang *et al.*, 2004; Jenkins *et al.*, 2002; Yilmaz, 2003). It is postulated that the response might be due to induced DNA repair mechanism (Bruins *et al.*, 2003). *G. stearothermophilus* (DSM 6790) and *G. thermoleovorans* cells were selected as representatives for each observed pattern. Although plasmid-encoded genes for metal ion tolerance are widely distributed through the domain *Bacteria* (Silver & Phung, 1996) and plasmid-mediated cadmium ion tolerance has been described for *Pseudomonas* (Bruins *et al.*, 2003; Malik & Jaiswal, 2000), *Staphylococcus* (Oger *et al.*, 2003; Udo *et al.*, 2000), plasmids could not be detected for *G. stearothermophilus* (DSM 6790) and *G. thermoleovorans* cells. The successful isolation of plasmids and following sequencing identification of the genetic carrier, may have given deeper insights in the tolerance mechanism and the transfer of plasmids into other bacteria could have been used as biotechnological application to generate multi-metal ion tolerances.

Regarding the known detoxification strategies summarized in Chapter 1, biotransformation and compartmentation can be excluded: Cadmium only occurs in one oxidation state and compartments could not be observed for *Geobacillus* strains. Biosorption reactions might play an important role in microbial tolerance to cadmium ions either solely or in combination with the remaining possibilities, efflux system, and regulation of the ion permeability, which are mediated by chromosomal genes. *G. stearothermophilus* (DSM 6790) and *G. thermocatenulatus* (DSM 730) displayed the same MIC value and had identical optimal growth temperature, but different growth responses in the presence of Cd^{2+} were observed. These two species were selected as model organisms for further experiments (Chapter 3).

2.5 Acknowledgements

The help of Ryan Todorovich in initial cadmium susceptibility tests on *Thermus* isolates is appreciated.

Chapter 3: Cadmium ion biosorption

Cadmium ion biosorption onto the thermophilic bacteria *Geobacillus stearothermophilus* and *G. thermocatenulatus*

(A condensed version of this chapter has been published in
Applied and Environmental Microbiology, June 2006)

3.1 Abstract

This study reports surface complexation models (SCMs) quantifying metal ion adsorption by thermophilic microorganisms. In initial cadmium ion toxicity tests, members of the genus *Geobacillus* displayed the highest tolerance to $\text{CdCl}_2 \cdot 2.5\text{H}_2\text{O}$ (as high as 400 to 3200 μM). The thermophilic, Gram-positive bacteria *Geobacillus stearothermophilus* and *G. thermocatenulatus* were selected for further electrophoretic mobility, potentiometric titration, and Cd^{2+} adsorption experiments to characterize Cd^{2+} complexation by functional groups within and on the cell wall. Distinct one-site SCMs described the extent of cadmium ion adsorption by both studied *Geobacillus* strains over a range of pH values and metal ion-to-bacteria concentration ratios. The results indicate that a functional group with a deprotonation constant $\text{p}K$ value of approximately 3.8 accounts for 66% and 80% of all titratable sites for *G. thermocatenulatus* and *G. stearothermophilus*, respectively, and is dominant in Cd^{2+} adsorption reactions. The results suggest a different type of functional group may be involved in cadmium biosorption for both thermophilic strains investigated here, compared to previous reports for mesophilic bacteria.

3.2 Introduction

As described in Chapter 1, various metal and metalloid compounds can be either essential or toxic for living organisms, depending on form and concentration. Therefore, organisms have developed several detoxification strategies including active efflux system, biotransformation, changes in ion permeability,

compartmentation and intra- and extracellular complexation (Bruins *et al.*, 2000; Gadd & Griffiths, 1978; Mendoza-Cozatl *et al.*, 2005; Rosen, 1996; Silver & Phung, 1996). Extracellular complexation of metal species by cell wall components is one of the more important interaction mechanisms, and it has been the subject of many previous studies (for reviews see Beveridge, 1989; Daughney & Fortin, 2001; Gadd, 1988; Schultze-Lam *et al.*, 1993; Shumate & Strandberg, 1985; Volesky & Holan, 1995). Previous investigations indicate that adsorption of metal ions by bacterial cells is affected by 1) the characteristics of the sorbate; 2) the characteristics of the bacteria such as the cell wall composition, growth phase and metabolic state; 3) the system composition (e.g. pH, ionic strength, metal ion-to-bacteria concentration ratio, presence of competing sorbates, sorbents or ligands); 4) the temperature; and 5) the reaction time. Many of these variables are known to affect metal ion adsorption by a variety of electrically charged colloid-sized particles, but some are specifically relevant to biological sorbents, for example the type and concentration of reactive binding sites found within the cell wall.

Several recent investigations have used surface complexation models (SCMs) to describe the extent of metal ion adsorption by bacteria as important physical, chemical, and biological parameters are independently varied (Borrok *et al.*, 2004a; Borrok & Fein, 2005; Daughney & Fein, 1998; Daughney *et al.*, 2001; Fein *et al.*, 1997; Haas, 2004; Yee & Fein, 2001). These SCMs are based upon a set of molecular-scale thermodynamic reactions, each describing adsorption of a particular dissolved chemical species to a particular type of cell wall functional group using a single stability constant (K). SCMs specifically account for the speciation of the sorbate and the bacterial surface. Some previous investigations indicate that different bacterial species display similar types of reactive surface functional groups (e.g. carboxyl, phosphono, hydroxyl, amino) and exhibit broadly similar reactivity toward certain metal ions (Borrok *et al.*, 2004a; Yee & Fein, 2001). However, in other cases, the absolute and relative concentrations of cell wall functional groups and their reactivities towards metal ions have been observed to vary substantially between species, and even for a single species as a function of population growth phase, growth conditions, or cell metabolic state (Claessens *et al.*, 2004; Daughney *et al.*, 2001; Haas, 2004).

The implication is that cell wall structure, while generally similar for the bacteria that have been studied to date, can still influence the nature and extent of metal ion interaction with the cell wall. Note that all previous SCMs have been developed for mesophilic bacteria; no single investigation has been ever published addressing metal ion adsorption onto thermophilic microorganisms. Metal ion adsorption reactions onto thermophilic microorganisms may therefore differ quantitatively and qualitatively from the mesophilic species that have been studied to date. A wide range of geological and anthropogenic thermal environments exhibit high concentrations of dissolved metals. In response to these conditions, microorganisms isolated from these habitats may have unique cell wall structures. Thus, studies of thermophilic microorganisms can supplement our present knowledge of metal biosorption that is completely based on mesophilic organisms.

In initial cadmium ion toxicity experiments (Chapter 2), 46 thermophilic bacteria of the genera *Aneurinibacillus*, *Anoxybacillus*, *Bacillus*, *Brevibacillus*, *Geobacillus*, and *Thermus* were tested. The highest tolerance to cadmium ($\text{CdCl}_2 \cdot 2.5\text{H}_2\text{O}$), 400 to 3200 μM , was observed for species belonging to the genus *Geobacillus*. *G. thermocatenulatus* (Golovacheva *et al.*, 1975) and *G. stearothermophilus* (Donk, 1920) were selected for further investigation based on their tolerance to Cd^{2+} . The aim of this investigation was to develop a SCM for cadmium ion adsorption onto the two thermophilic bacteria. Cadmium was also selected in the present investigation because SCMs describing the adsorption of cadmium ions by various mesophilic bacteria are available for comparison (Borrok *et al.*, 2004a; Borrok & Fein, 2005; Daughney & Fein, 1998; Daughney *et al.*, 2001; Fein *et al.*, 1997; Yee & Fein, 2001).

3.3 Materials and Methods

3.3.1 Culture conditions

Prior to the titration and cadmium ion adsorption experiments, *G. stearothermophilus* (DSM 6790) and *G. thermocatenulatus* (DSM 730) cells were

successively sub-cultured at least twice in new TSB medium adjusted to a final pH value of 7. For acid base titration and cadmium ion adsorption experiments cells were grown in 1 liter of TSB at 60° C in an orbital mixer incubator at 100 rpm. After 24 h, bacteria were harvested in the exponential growth phase by centrifugation at 8230×g (Beckmann Coulter Avanti J-E Centrifuge with fixed-angle rotor JLA-9.100) and washed five times in 250 ml 10 mM NaNO₃ to ensure complete removal of the growth medium and adsorbed cations from the bacterial surface. Between each wash step, the bacterial suspension was centrifuged for 10 min at 8230×g to form a pellet and the supernatant was discarded. After the final wash, the bacterial pellet was resuspended in a known weight of 10 mM NaNO₃ solution and the optical density at 600 nm (Hach DR2010) relative to the electrolyte was determined.

Prior to the experiments, to determine electrophoretic mobility, *G. stearothermophilus* (DSM 6790) and *G. thermocatenulatus* (DSM 730) were incubated in 200 ml TSB at 57° C at 100 rpm for 24 h. The optical density at 600 nm was measured and cells were harvested by centrifugation (8 min, 9820×g, 4° C). The pellet was resuspended in 1 mM NaNO₃ solution, divided into 3 aliquots and washed three times in 150 ml 1 mM, 10 mM, or 100 mM NaNO₃, respectively. The final pellets were resuspended in 1 ml of the respective electrolyte concentration and kept on ice.

The ratio of bacterial biomass to optical density at 600 nm was determined using two different methods. First, a bacterial suspension of known optical density was filtered through a pre-weighed filter membrane (pore size 0.45 µm, Millipore) and flushed with distilled water several times. The filter was dried at 80° C to constant weight. Second, aliquots of a bacterial suspension with known optical density and weight were centrifuged at 1850×g (Jouan CR 4.11) for 1 h, stopping three times to decant the supernatant. After 1 h, the wet weight of the bacterial pellet was determined. The dry mass of the pellet was recorded after drying at 80° C to constant weight. The cell number in relation to optical density was determined with a Thoma counting chamber (depth 0.02 mm).

Cell dimensions were recorded by evaluating images obtained from electron microscope. For transmission electron microscopy (TEM), cells were harvested by centrifugation (8 min, 9820×g) and three times washed in 10 mM NaNO₃. Specimens were fixed first in 3% glutaraldehyde in 0.1 M sodium cacodylate buffer with 0.3% ruthenium red and then postfixed in 2% osmium tetroxide in 0.1 M sodium cacodylate buffer with 0.3% ruthenium red according to Handley *et al.* (1988). The cells were embedded in agarose, following stepwise dehydration with ethanol and infiltration with Quetol 651 epoxy resin (ProSciTech) using a Lynx el Tissue Processor (Australian Biomedical Corporation). Thin sections of 80 to 90 nm were cut on a Reichert-Jung Ultracut E ultramicrotome and placed onto formvar coated slot grids. The grids were stained with uranyl acetate and lead citrate using an LKB Ultrastainer and examined using a Philips CM100 transmission electron microscope.

3.3.2 Acid-base titrations

Acid-base titrations were conducted using an automated potentiometric titrator (Metrohm titrator 736 GP Titrino) with a glass electrode (Metrohm 6.0130.100) and a separate Ag/AgCl reference electrode (Metrohm 6.07.26.110). The CO₂-free NaOH and the HNO₃ titrants were calibrated against potassium hydrogen phthalate and standardized NaOH, respectively. A known weight (c. 50 g) of homogenized bacterial suspension was placed in an air-tight polystyrene vessel, and the pH was adjusted to approximately 4 by addition of an aliquot of standardized HNO₃. The suspension was purged with humid N₂ gas for 30 min in order to remove dissolved CO₂. Then the suspension of bacteria cells was titrated in an up-pH direction while continuously stirred and under a positive-pressure N₂-atmosphere. Following the first titration, the suspension was again adjusted to pH 4, and a second up-pH titration was performed to evaluate reproducibility and the reversibility of the bacterial surface protonation reactions. For each titration, a stability of 5 mV per min was obtained prior to the addition of the next aliquot of titrant. All titrations were performed in a temperature-controlled room at 20 ± 2° C. At the end of each titration, the dry mass of the titrated bacteria was determined by drying the cells at 80° C, after accounting the dry weight of the electrolyte solution (NaNO₃), the added acid and base.

3.3.3 Metal ion adsorption

Batch cadmium ion adsorption experiments were conducted for each bacterial species as a function of pH and bacteria-to-metal ion concentration ratio. A weighed aliquot from a bacterial parent solution was dried to constant weight at 80° C, as described above, to determine the dry weight of bacteria. The remainder was used to prepare three suspensions (c. 150 g each), having 100%, 50% and 25% of the bacterial concentration as the parent suspension. These three suspensions were supplemented with 1000 ppm cadmium atomic absorption standard solution (Merck, $\text{Cd}(\text{NO}_3)_2$ in 0.5% HNO_3) to a final concentration of 5 ppm. After the addition of the metal, the optical density at 600 nm for each sample was recorded and each suspension was divided into 12 individual reaction vessels. The pH value in each reaction vessel was adjusted by adding small volumes of 100 mM NaOH solution to cover a pH range of 3.5 to 10.0 for each suspension. After a sufficient equilibration time of 2 h (Borrok *et al.*, 2004b) in an orbital mixer incubator (Ratek) set at 100 rpm and 20° C, the samples were centrifuged at 6870×g (Beckmann Coulter Avanti J-E Centrifuge with swinging-bucket rotor JLA-5.3) for 15 min. A portion of the supernatant was decanted and acidified with concentrated HNO_3 solution (ARISTAR grade) for subsequent metal analysis by flame atomic adsorption spectroscopy (Perkin Elmer Atomic Adsorption Spectrometer Analyst 800). The remaining supernatant was used for measurement of final equilibrium pH. The concentration of metal ions adsorbed to bacteria in each sample was calculated by subtracting the cadmium ion concentration remaining in the supernatant from the original concentration of 5 ppm.

3.3.4 Electrophoretic mobility measurements

Electrophoretic mobility measurements were carried out using a Malvern Zetasizer Nano ZS at 25° C. 10 ml volumes of 1 mM, 10 mM, and 100 mM NaNO_3 were prepared and adjusted to pH values between 1.8 and 9.5 by addition of HNO_3 and NaOH respectively. Additionally, 10 ml volumes of 30 μM , 300 μM , and 3 mM $\text{Cd}(\text{NO}_3)_2$ solution with final pH values of 4.5 to 5.5 were prepared. The ionic strength of all cadmium solutions was maintained at 10 mM

NaNO₃. 3 to 100 µl of the bacterial suspension was added to the 10 ml electrolyte solutions and the pH was measured. The samples were incubated for 2.5 to 5.0 h prior to measurement. The “auto” measurement duration was selected, which reports the electrophoretic mobility as an average of 10 to 30 runs. The isoelectric point values were located by determining the pH value where the electrophoretic mobility of the bacteria was zero.

3.3.5 Surface complexation model (SCM)

Surface complexation models (SCMs) were developed using the computer program FITMOD, a modified version of FITEQL (Westall, 1982). From the experimental acid-base titration data, FITMOD determines the concentrations and deprotonation constants of binding sites on the bacteria. As an example, for the following deprotonation reaction of carboxylic groups



where R represents the cell to which the functional group is attached, the stability constant K can be determined using the corresponding mass action equation

$$K_{\text{carboxyl}} = \frac{[\text{R-COO}^-] \times a_{\text{H}^+}}{[\text{R-COOH}]} \quad (2)$$

where a refers to the activity of the proton and square brackets represent surface site concentrations in moles per kg solution. The adsorption of cadmium cations onto carboxylic surface binding sites can be expressed by



FITMOD calculates the thermodynamic stability constants K for the metal complexes using the corresponding mass action equation (4).

$$K_{\text{Cd}^{2+}\text{-carboxyl}} = \frac{[\text{R-COOCd}^+]}{[\text{R-COO}^-] \times a_{\text{Cd}^{2+}}} \quad (4)$$

All SCMs incorporated the Donnan electrostatic model (Yee *et al.*, 2004).

SCM development required information about biophysical parameters such as the cell wall thickness, the dry-to-wet mass ratio, and specific surface area (Table 5). Methods to determine the first two parameters have been described above. The bacterial surface area A , was calculated assuming that the cells were cylindrical shaped with a radius r , a length l , a density p equal to 1 kg per liter by following equation

$$A = \frac{2}{p} \times \frac{r+l}{r \times l} \quad (5)$$

where r and l are expressed in μm , and A in m^2 per g wet bacteria (Chatellier & Fortin, 2004). Cell radius r and cell length l were determined by examining TEM micrographs (Figure 10).

Table 5. Selected biophysical parameters for *G. thermocatenulatus* (DSM 730) and *G. stearothermophilus* (DSM 6790).

Parameter	<i>G. thermocatenulatus</i>	<i>G. stearothermophilus</i>
Dry-to-wet mass ratio	1 to 15	1 to 8
Isoelectric point [pH]	3.25	3.95
Cell wall thickness [nm]	49.5 ± 3.5	35.0 ± 1.6
Cell length [μm]	4.3 ± 1.9	3.1 ± 0.3
Cell width [μm]	0.4 ± 0.04	0.7 ± 0.02
Surface area [m^2/g wet cells]	8.96	6.38

3.4 Results

3.4.1 Potentiometric titration experiments

Acid-base titration curves for *G. stearothermophilus* and *G. thermocatenulatus* cells in 10 mM NaNO₃ are displayed in Figure 11. These figures depict the concentration of protons adsorbed onto the bacterial surface as a function of pH. Titration experiments were conducted in triplicate for *G. thermocatenulatus* and in duplicate for *G. stearothermophilus* (Appendix C: Table 19, Table 20, Table 21, Table 22, and Table 23). Individual titration curves consisting of two titrations from low to high pH values are in excellent agreement with each other after taking dilution into account, indicating reproducibility of the data and complete reversibility of the adsorption reactions during the experiments. The curves are normalized to the dry (Figure 11 A) and wet cell mass of bacteria (Figure 11 B) to allow direct visual comparison between the two species. In comparison to titrated electrolyte solution without bacteria, *G. stearothermophilus* and *G. thermocatenulatus* cells significantly buffer pH over the entire range studied in this investigation, which is in agreement with published data for mesophilic microorganisms (Claessens *et al.*, 2004; Daughney & Fein, 1998; Fein *et al.*, 1997) and one thermophilic bacterium (Wightman *et al.*, 2001).

G. thermocatenulatus compared to *G. stearothermophilus* shows a slightly higher buffering capacity against addition of the base when titration data are normalized to dry cell mass (Figure 11 A). In contrast, when data are normalized to wet cell mass, *G. stearothermophilus* displays a stronger buffering capacity than *G. thermocatenulatus* (Figure 11 B). The difference is due to the different bacterial dry-to-wet mass ratio, 1 to 15 and 1 to 8, for *G. thermocatenulatus* and *G. stearothermophilus*, respectively (Figure 11). This result is unexpected as the data show a smaller surface area and thinner cell wall for *G. stearothermophilus*, hence indicating a smaller volume that may adsorb cations. Bacterial concentrations during titration were approximately $3.8 \pm 0.06 \times 10^8$ cells per ml for *G. thermocatenulatus*, and ranged from $4.8 \pm 0.06 \times 10^8$ to $5.3 \pm 0.07 \times 10^8$ cells per ml for *G. stearothermophilus*, representing a total bacterial dry mass of 1.59 ± 0.07 g. The bacterial surface areas calculated from biophysical parameters were 8.96 and 6.38 m² per g wet cells for *G. thermocatenulatus* and *G. stearothermophilus* cells, respectively. The values are much lower than values reported in other SCM studies (Yee *et al.*, 2004) where surface areas as high as 290 m² per g wet mass

for *B. subtilis* have been reported (Wightman *et al.*, 2001).

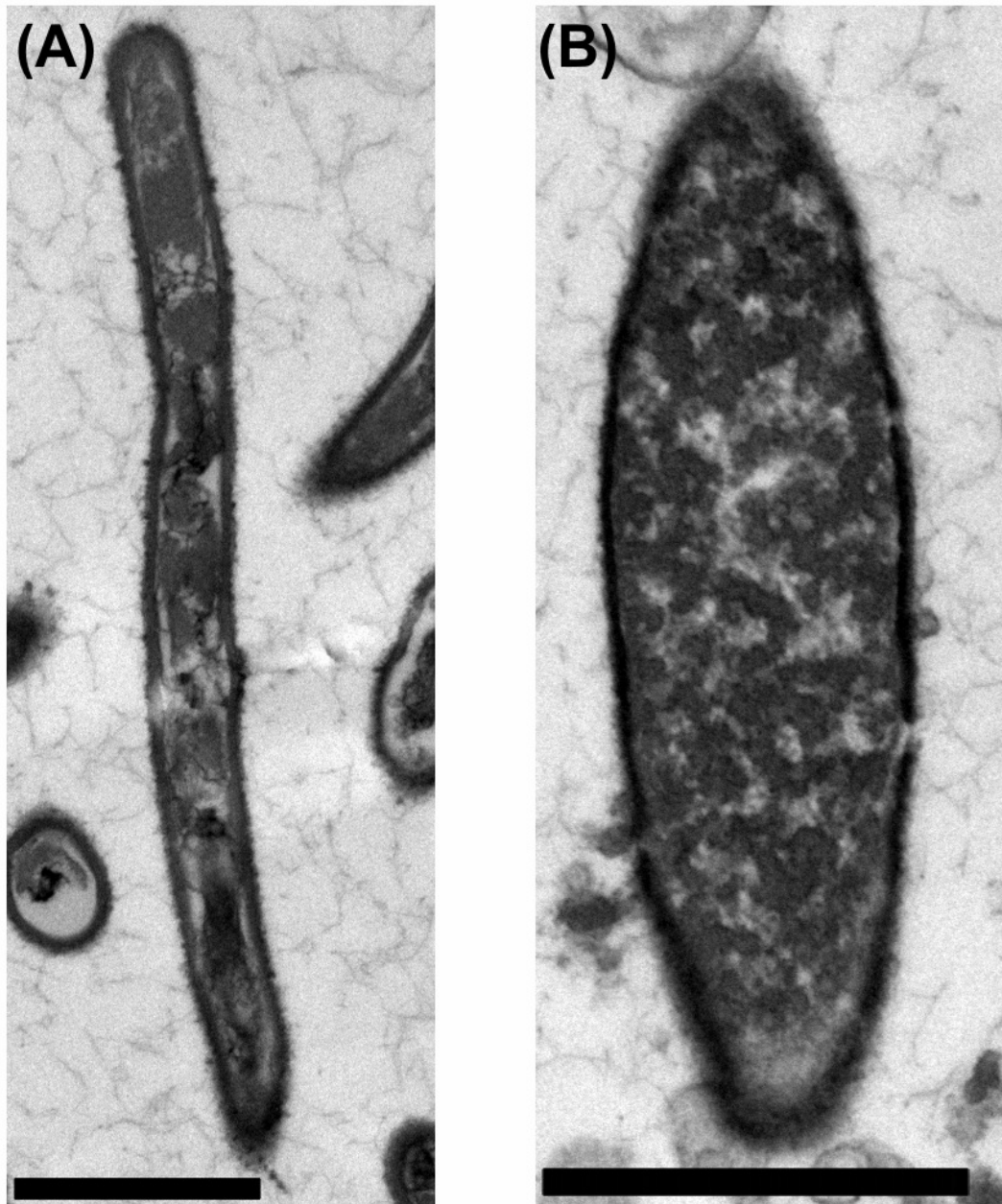


Figure 10. Transmission electron micrographs of *G. thermocatenulatus* (A) and *G. stearothermophilus* (B). Bars 1 µm.

To develop SCMs for the titration data, the electrophoretic mobility of the bacterial cells were taken into consideration. In theory, the net concentration of supplied protons can be quantified by

$$[\text{H}^+]_{\text{net added}} = [\text{H}^+]_{\text{added}} - [\text{OH}^-]_{\text{added}} + [\text{H}^+]_{\text{adsorbed}} - [\text{H}^+]_{\text{desorbed}} \quad (6)$$

where $[\text{H}^+]_{\text{added}}$ and $[\text{OH}^-]_{\text{added}}$ refer to the known concentrations of the added HNO_3 and the NaOH titrants, and where $[\text{H}^+]_{\text{adsorbed}}$ and $[\text{H}^+]_{\text{desorbed}}$ are the concentrations of protons consumed and released by the bacteria, respectively. The isoelectric point (IEP), when positive and negative charges of the chemical functional groups onto and within the microbial surface are in balance, can be described with the following relationship:

$$[\text{H}^+]_{\text{adsorbed}} = [\text{H}^+]_{\text{desorbed}} \quad (7)$$

The net concentration of added protons at the IEP results out of equations (6) and (7) and can be determined by

$$[\text{H}^+]_{\text{net added}} = [\text{H}^+]_{\text{added}} - [\text{OH}^-]_{\text{added}} \quad (8)$$

which as well represent the titration of a pure electrolyte solution. It is assumed that titration data obtained without and with cells at the corresponding IEP to be identical. Therefore, titration curves for both studied strains were normalized to intersect the titration curve of a pure electrolyte solution at the measured IEP at pH values of 3.25 for *G. thermocatenulatus* and 3.95 for *G. stearothermophilus* cells (Figure 12). IEP values commonly found for bacterial cells range from 2 to 4 depending on the species (Harden & Harris, 1953; van der Wal *et al.*, 1997). Although titrations at pH values below 4 or above 10 were avoided to minimize cell damage (Claessens *et al.*, 2004; Haas, 2004), the titration data were constrained by the electrophoretic mobility of the cells by iteration (Burnett *et al.*, 2006).

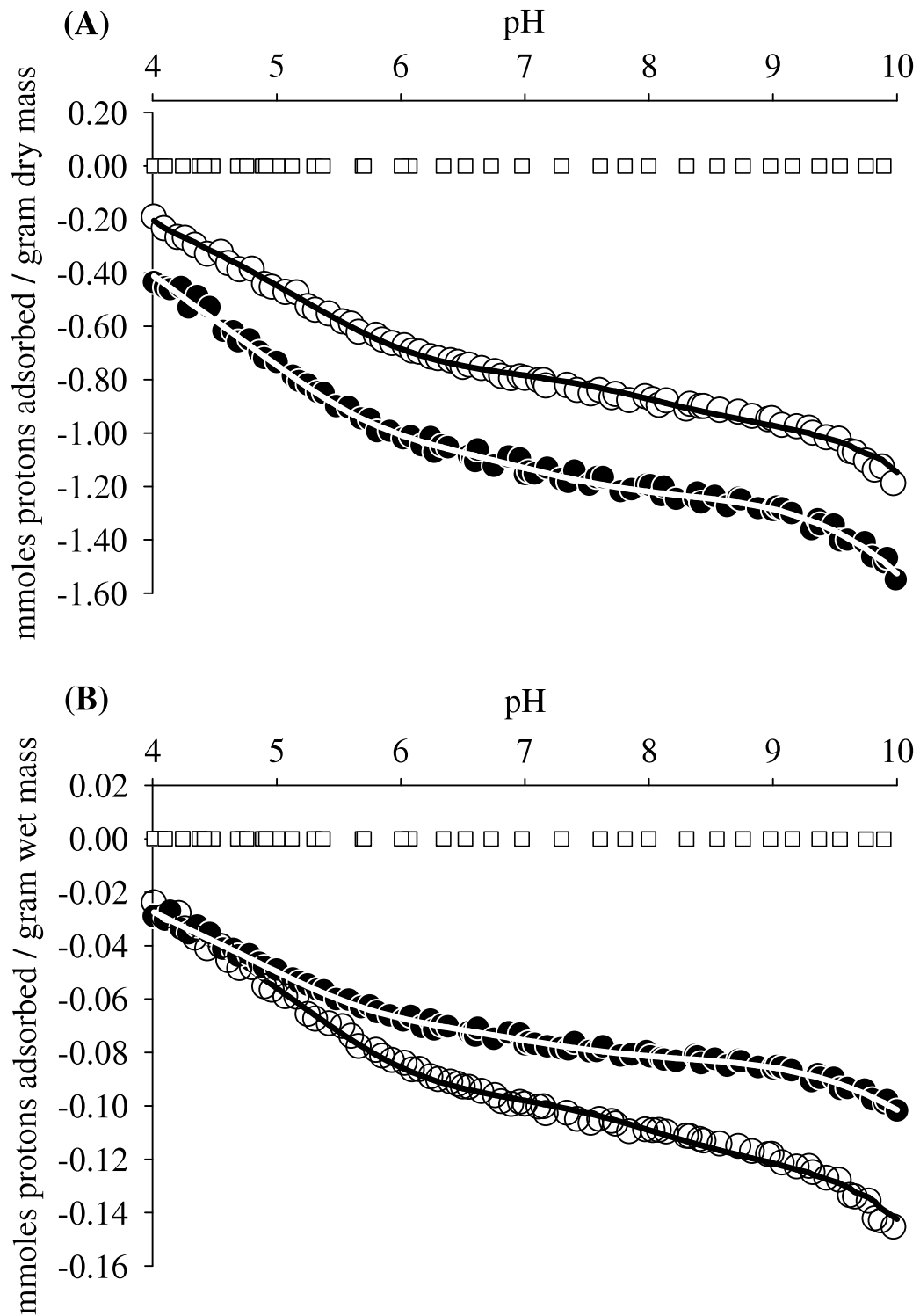


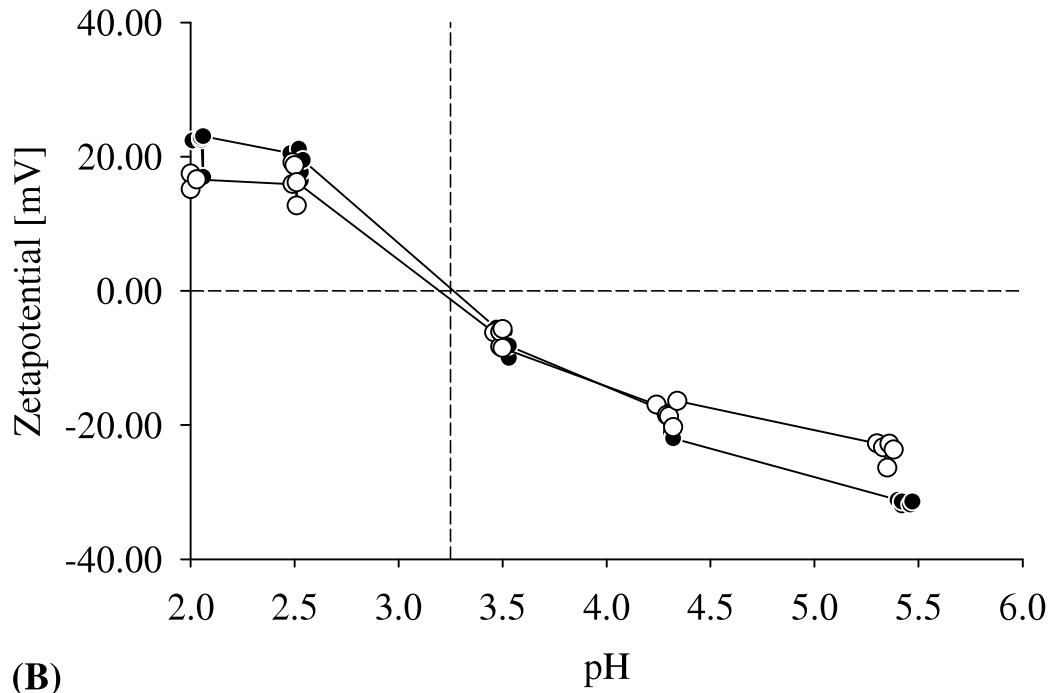
Figure 11. Acid-base titration data normalized to dry mass (A) and wet mass (B) obtained for *G. stearothermophilus* DSM 6790 (white circles) and *G. thermocatenulatus* DSM 730 (black circles) cells. Solid lines represent the best-fitting discrete multi-site model calculated by FITMOD. White squares represent titrated electrolyte solution without bacteria. For clarity, only every third data point is displayed.

A discrete multiple-site SCM can account for the buffering capacity of the bacterial species observed over the entire range studied between pH 4.0 and 10.0 (Figure 11). Best-fit approximations of the titration data resulted in a three-site model for *G. thermocatenulatus*, whereas only two individual binding sites were necessary to fully interpret the titration data of *G. stearothermophilus*. Besides the excellent visual agreement of measured experimental data and calculated SCM, the quality of fit was quantified using the overall variance $V(Y)$, which is the mean of weighted sum of squares of errors Y in the stoichiometric equation. The program FITMOD computes the variance as an output parameter. Low $V(Y)$ numbers indicate a better model fit to the data. For adsorption data, values of $V(Y)$ between 1 and 20 indicate a reasonable fit (Westall, 1982). The $V(Y)$ values for each SCM and corresponding pK values (negative log equilibrium constants for deprotonation reactions) and concentration c of proton-reactive surface sites are compiled in Table 6. The low variance values indicate a good fit to the experimental data. Values of pK are similar for both bacterial strains. The most abundant proton binding site has a pK value of approximately 3.8 and accounts for 66% and 80% of the total concentration of binding sites for *G. thermocatenulatus* and *G. stearothermophilus*, respectively.

Despite the present knowledge of the cell wall composition and structure of Gram-positive bacteria (Scheffers & Pinho, 2005; Schleifer & Kandler, 1972), such as *Geobacillus* species, the clear identification of a proton-reactive binding site solely based on its pK value remains complicated. Stability constants of individual functional groups can vary significantly depending on various parameters such as temperature, ionic strength (Borrok & Fein, 2005) and relative position of the functional group in the biomolecule. Due to this interpretation problem, the pK values will not be assigned to possible functional groups and the detected reactive binding sites will be referred as sites 1, 2, and 3. The best-fitting SCMs included deprotonation reactions onto the bacterial surface may be characterized for site 1 and 2 by



(A)



(B)

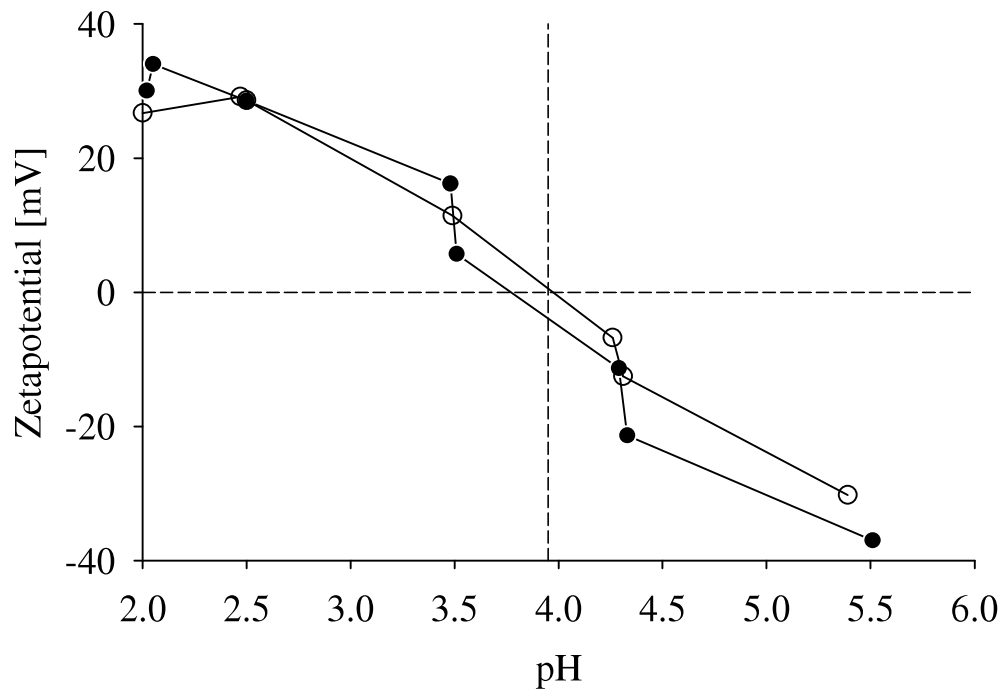


Figure 12. Zetapotentials obtained for *G. thermocatenulatus* (A) and *G. stearotheophilus* cells (B) at ionic strengths of 1 mM (black circles) and 10 mM NaNO₃ (white circles).

and for site 3



where L represents the functional group acting as a ligand. These formulations are consistent with the electrophoretic mobility data, which indicate that both bacteria maintain a positive cell surface charge at pH values below their IEP and negative surface charge at pH above their IEP. Although site 3 is required for both *Geobacillus* strains to explain the positive charge under acidic conditions, it does not play an active role in proton adsorption for *G. stearothermophilus* under the conditions covered in the experiments.

The cell wall thickness, the bacterial surface area and the concentration of the dominant site 1 indicate a density of 232.6 and 322.0 sites per nm³ for *G. thermocatenulatus* and *G. stearothermophilus*, respectively. Theoretically, an ionic radius for cadmium of 0.1 nm results in a maximum density of 238.7 Cd²⁺ per nm³ that may be complexed by functional groups in or on the bacterial cell wall. Therefore, it is assumed that all reactive groups of site 1 that are accessible by protons are also accessible by the larger cadmium ion.

3.4.2 Cadmium ion biosorption

Cadmium ion adsorption experiments performed as a function of pH and biomass revealed that both parameters strongly influenced the adsorption onto the microbial surfaces (Figure 14). Experiments were performed in 10 mM NaNO₃ in the presence of 5 ppm CdCl₂·2.5H₂O (44.5 μM) with bacteria-to-metal ion concentration ratios of 1:1, 1:2, and 1:4 resulting in total bacterial dry mass of 1.15 ± 0.20 g, 0.57 ± 0.09 g, and 0.30 ± 0.05 g, respectively. At a given pH, an increasing concentration of organic mass resulted in an increase in Cd²⁺ adsorption. *G. thermocatenulatus* cells (1.31 g dry mass) were able to adsorb up to 95% Cd²⁺ (Figure 14 A), whereas *G. stearothermophilus* cells (1.32 g dry mass) absorbed up to 85% (Figure 14 B). At a given biomass concentration, increasing pH results in increasing Cd²⁺ adsorption. Depending on the biomass concentration, most adsorption occurred in the pH range of 3.5 to 5.5,

demonstrating the importance of site 1 ($pK = 3.8$). This pH dependence is due to the deprotonation of cell wall functional groups that occurs with increasing pH, progressively resulting in increasing Cd^{2+} biosorption until saturation of binding sites occurs. Negative control experiments (no bacterial cells) indicated that there was a significant loss of Cd^{2+} at pH values above 8 within 2 hours (Figure 13). Thermodynamic calculations using the computer program MINTQA2 (Allison *et al.*, 1991) suggest that for a solution containing 5 ppm Cd^{2+} in equilibrium with the atmosphere, otavite ($CdCO_3$) should precipitate at pH values above 7.

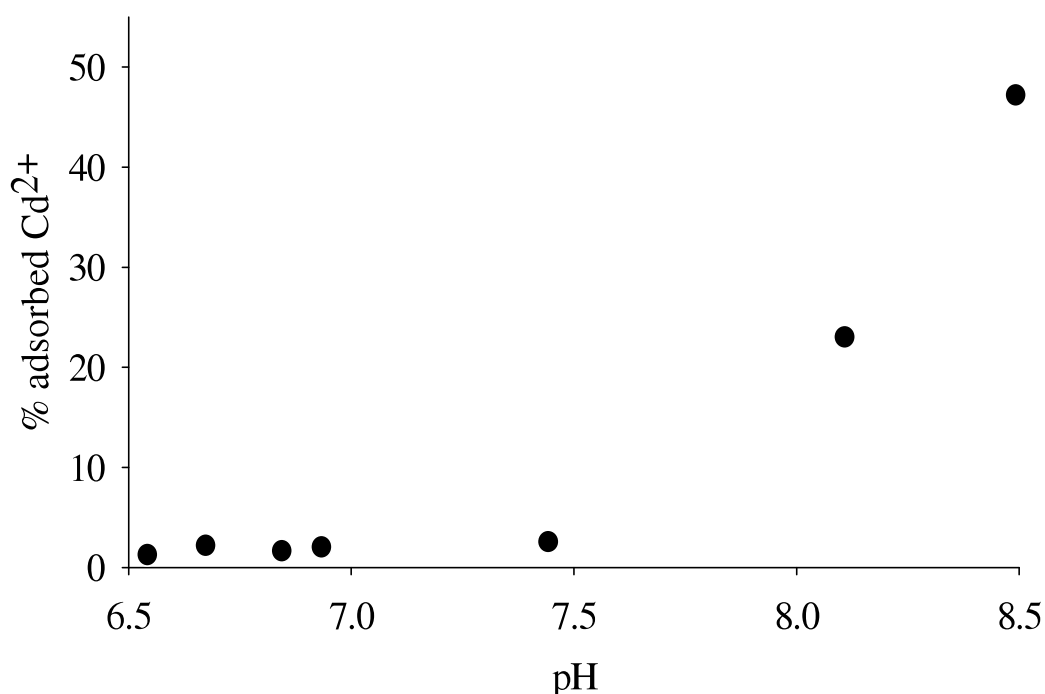


Figure 13. Cadmium ion adsorption experiment using 10 mM $NaNO_3$ solution without bacterial cells. Thermodynamic calculations indicate that Cd^{2+} precipitates at higher pH values.

The computer code FITMOD, incorporating the Donnan electrostatic model, was used to develop SCMs to describe the Cd^{2+} adsorption data. The SCMs used the concentrations and deprotonation constants of cell wall surface functional groups obtained from the potentiometric titration experiments (Table 6). SCMs did not consider data obtained at pH values above 8, due to the possibility of biasing caused by loss of Cd^{2+} by precipitation. For both bacteria, three individual

cultures each with three different biomass-metal ion ratios were investigated resulting in a total of nine data subsets per bacterium.

Initially, SCMs with unique thermodynamic stability constants K for the metal complexes were calculated for each individual subset (Appendix B: Table 15, Table 16, Table 17, and Table 18). A discrete one-site SCM fitted all data subsets. Additionally, for the two datasets displaying the lowest biomass-metal ion ratio for *G. stearothersophilus* (0.26 and 0.34 g dry mass), a two-site SCM could be applied (Appendix B: Table 18). The multi-site model for both datasets just slightly improves the fit in terms of lower $V(Y)$ value. However, it indicates that at lower cell concentrations site 1 may be saturated, hence Cd^{2+} complexation reaction significantly occurs at site 2 (Daughney & Fein, 1998).

Subsequently, a single one-site SCM was developed to fit all of the data for each bacterium. These one-site SCMs account for variation in pH and metal ion-to-bacteria concentration ratio. Good agreement with the analytical data was obtained, yielding an overall $V(Y)$ value of 1.8 and 5.9 for *G. thermocatenulatus* and *G. stearothersophilus*, respectively (Table 6). The higher log K value of 2.20 ± 0.16 obtained for *G. stearothersophilus* indicates a stronger interaction between Cd^{2+} and site 1, compared to *G. thermocatenulatus* ($\log K = 1.30 \pm 0.22$). The fit of the single best-fitting SCM to the experimental data is displayed in Figure 14.

3.5 Discussion

This study uses a combined approach of metal ion susceptibility tests and complexation modeling analysis. Initial cadmium ion toxicity experiments revealed a high MIC value of Cd^{2+} for *G. stearothersophilus* (DSM 6790) and *G. thermocatenulatus* (DSM 730) in comparison to 44 other studied thermophilic bacteria.

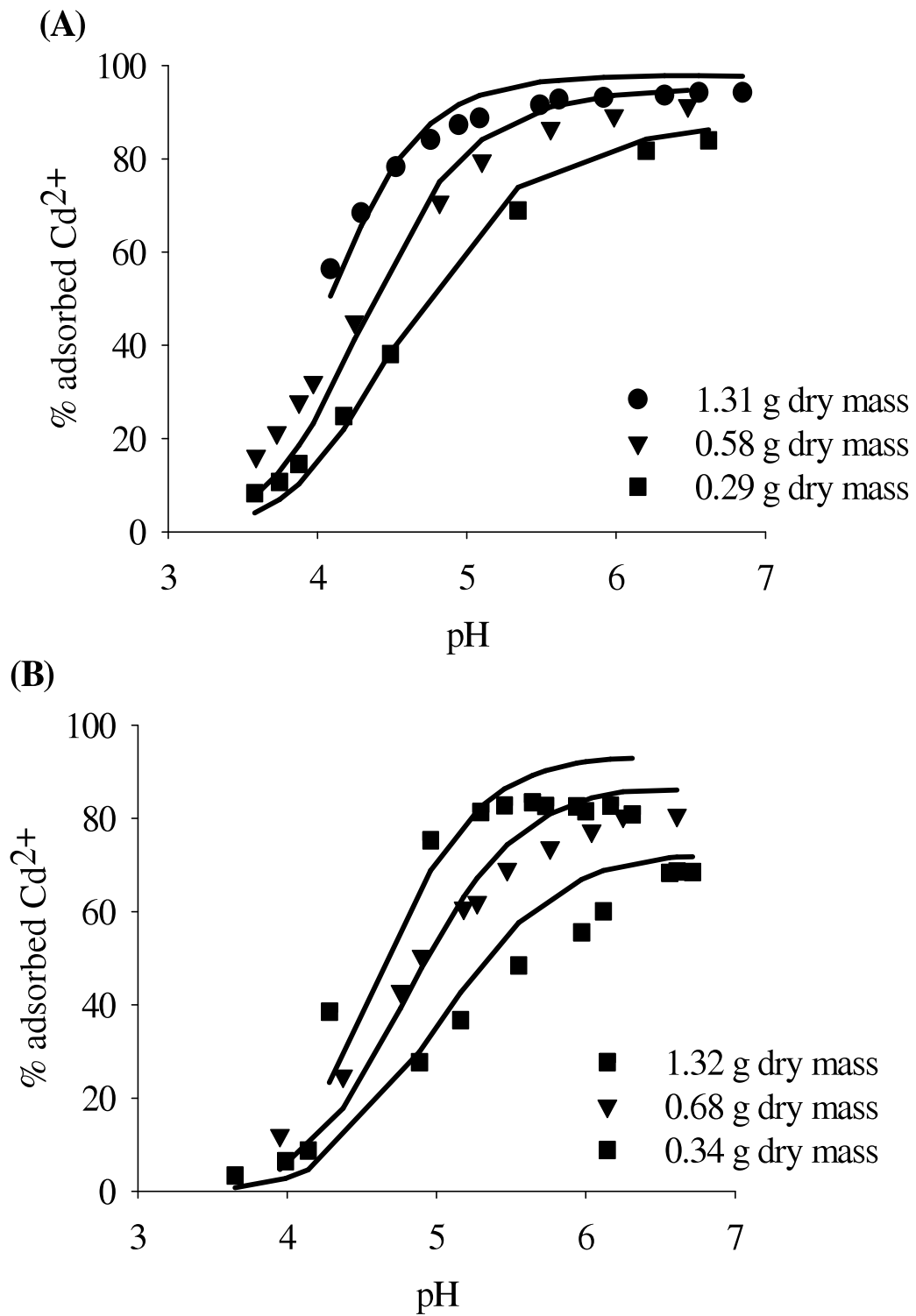


Figure 14. Percentage of cadmium ions adsorbed onto *G. thermocatenulatus* (A) and *G. stearothermophilus* (B) as a function of pH and dry biomass (black circles: 1.3 g, white triangles: 0.6 g, black squares: 0.3 g). Solid lines represent the best-fitting discrete one-site model developed by FITMOD. For clarity, for each species only data from one of three individual cultures are shown.

Calculations of SCMs for both microorganisms were performed using the Donnan model. In theory, the advantage of the Donnan model over other electrostatic models is that it considers the cell wall as a volume that is ion-penetrable, whereas other electrostatic models (e.g. Constant capacitance and Stern models) only account for ion-impenetrable planar surfaces (Yee *et al.*, 2004). Although the Donnan model assumes the surface binding sites to be uniformly distributed over the cell wall volume, some previous research on *Bacilli* suggests that binding sites may be concentrated on the cell poles (Sonnenfeld *et al.*, 1985a; Sonnenfeld *et al.*, 1985b). It is acknowledged that additional research is warranted to better define the most appropriate format for SCMs for bacterial surfaces, in particular with regard to the modeling of the effects of cell wall electric charge. However, in the absence of contradictory data, the Donnan model is employed under the assumption of uniform site distribution to quantify electrostatic interactions between aqueous metal ions and chemically functional groups within and on the cell walls.

Some of the model parameters are similar to previously published results (Table 6), although the diversity of biosorbants and modeling approaches described in the literature somewhat limit the comparisons that can be made. The deprotonation constant pK values determined for site 2 and site 3 for both *Geobacillus* strains are in good agreement with recent results reported for the thermophilic species TOR-39 (Wightman *et al.*, 2001) and *Anoxybacillus flavithermus* (Burnett *et al.*, 2006), the mesophilic bacterium *Bacillus subtilis* (Daughney *et al.*, 2001) and five natural bacterial consortia (Borrok *et al.*, 2004a). The pK values of site 1 for *G. stearothermophilus* and *G. thermocatenulatus* are considerably lower than those reported for the other bacteria, and may indicate that a different type of functional group is involved in complexation reactions for species of the genus *Geobacillus*.

Interestingly, the average of the pK values of site 1 and site 2 of the four-site model for the bacterial consortia (Borrok *et al.*, 2004a) is almost equivalent to the deprotonation constant for site 1 for the *Geobacillus* strains. Yee and Fein (Yee & Fein, 2001) proposed that metal-bacteria adsorption is independent of the bacterial species involved and therefore a generalized adsorption model may be applied. It is acknowledged that the differences between the SCMs developed in this

investigation and the generalized model of Yee and Fein (Yee & Fein, 2001) may relate to the different experimental methods or modeling approaches employed, but it is also possible that the generalized model is simply inappropriate for the two studied *Geobacillus* strains and therefore not universally applicable.

Although in all of the above-mentioned previous investigations site 1 is proportionally the most abundant binding site, only for the thermophiles *A. flavithermus*, *G. thermocatenulatus*, and *G. stearothermophilus* does it account for more than 62% of the total concentration of binding sites. The significantly lower proportions of site 1 observed for the other bacteria (below 44%) may indicate that *A. flavithermus*, *G. thermocatenulatus*, and *G. stearothermophilus* as thermophiles differ in cell wall composition from the other mesophilic bacteria and therefore expose different chemically reactive functional groups on and within their cell walls.

As mentioned above, site 1 ($pK = 3.8$) was not assigned to a particular identity or functional group structure. Many studies assume binding sites with low pK values to be carboxylic because short carboxylic acids have pK values below 4.5 and carboxylic acids are present in the cell wall. However, it must be borne in mind that functional groups can only be reliably identified by other methods such as X-ray spectroscopy analysis. X-ray adsorption spectroscopy experiments conducted by Boyanov and colleagues (2003) suggest that Cd^{2+} adsorption onto *Bacillus subtilis* at a pH value of 3.4 is predominated by phosphono ligands, whereas carboxylic ligands are the dominant binding sites in the range of pH 5.0 to 7.8.

The thermodynamic stability constants K for the cadmium ion-binding are not as high for the *Geobacillus* strains as for the bacteria described in the literature (Borrok *et al.*, 2004a; Burnett *et al.*, 2006; Daughney *et al.*, 2001; Wightman *et al.*, 2001; Yee & Fein, 2001). It is acknowledged that differences may be due to different modeling approaches employed. Alternatively, this may indicate a weaker interaction between the cadmium ions and the reactive surface sites of the *Geobacillus* strains compared to other species investigated to date.

Table 6. Average model parameters for *G. thermocatenulatus* and *G. stearothermophilus* in comparison to other bacterial species

Species	Model	Parameter	Site 1	Site 2	Site 3	Site 4	$V(Y)^d$
<i>G. thermocatenulatus</i> (this study)	Donnan	pK^a	3.84 ± 0.03	5.97 ± 0.08	8.70 ± 0.30		3.4
<i>G. thermocatenulatus</i> (this study)	Donnan	c^b	7.03 ± 0.14	1.20 ± 0.10	2.50 ± 0.52		
<i>G. thermocatenulatus</i> (this study)	Donnan	$\log K^c$	1.30 ± 0.22				1.8
<i>G. stearothermophilus</i> (this study)	Donnan	pK^a	3.73 ± 0.04	6.46 ± 0.07			4.9
<i>G. stearothermophilus</i> (this study)	Donnan	c^b	9.74 ± 0.03	2.40 ± 0.04			
<i>G. stearothermophilus</i> (this study)	Donnan	$\log K^c$	2.20 ± 0.16				5.9
TOR-39 (Wightman <i>et al.</i> , 2001)	Constant capacitance	$pK^{a, f}$	4.5 ± 0.2	5.8 ± 0.1	8.2 ± 0.1		0.9
TOR-39 (Wightman <i>et al.</i> , 2001)	Constant capacitance	c^b	6 ± 2	5 ± 1	3 ± 1		
<i>A. flavithermus</i> (Burnett <i>et al.</i> , 2006)	Donnan	pK^a	4.94 ± 0.35	6.85 ± 0.57	7.85 ± 0.27		15.5
<i>A. flavithermus</i> (Burnett <i>et al.</i> , 2006)	Donnan	$c^{b, e}$	3.57 ± 0.58	1.20 ± 0.56	0.95 ± 0.20		
<i>B. subtilis</i> (Daughney <i>et al.</i> , 2001)	Constant capacitance	pK^a	4.80 ± 0.1	6.49 ± 0.3	8.52 ± 0.6		8.5-13.5
<i>B. subtilis</i> (Daughney <i>et al.</i> , 2001)	Constant capacitance	c^b	6.78 ± 3.9	4.35 ± 2.6	6.17 ± 2.2		
<i>B. subtilis</i> (Daughney <i>et al.</i> , 2001)	Constant capacitance	$\log K^c$	3.62 ± 0.5	4.11			11

Table 6. Continued.

Species	Model	Parameter	Site 1	Site 2	Site 3	Site 4	$V(Y)^d$
Average model on nine individual bacterial species (Yee & Fein, 2001)	Constant capacitance	pK^a	5.0 ± 0.2	7.2	9.7		N. A. ^g
Average model on nine individual bacterial species (Yee & Fein, 2001)	Constant capacitance	$c^{b, e}$	20 ± 8	8	17		
Average model on nine individual bacterial species (Yee & Fein, 2001)	Constant capacitance	$\log K^c$	4.0 ± 0.3	N. A.	N. A.		3.3-34.6
Average model on five natural bacterial consortia (Borrok <i>et al.</i> , 2004a)	Non-electrostatic	pK^a	3.12 ± 0.13	4.70 ± 0.11	6.57 ± 0.17	8.99 ± 0.21	N. A.
Average model on five natural bacterial consortia (Borrok <i>et al.</i> , 2004a)	Non-electrostatic	c^b	6.65 ± 1.96	6.78 ± 2.65	3.68 ± 1.71	4.47 ± 2.19	
Average model on five natural bacterial consortia (Borrok <i>et al.</i> , 2004a)	Non-electrostatic	$\log K^c$	2.83 ± 0.30	2.70 ± 0.47	3.95 ± 0.22	5.22 ± 0.40	N. A.

^a Negative logarithm of deprotonation constant for subscripted surface functional groups with 1 σ errors.

^b Concentration of subscripted surface sites with 1 σ errors in $\times 10^{-5}$ mol/g of wet cells.

^c Logarithm of stability constant for Cd^{2+} complexation reaction with 1 σ errors.

^d Variance computed by FITMOD. A lower value indicates a better model fit.

^e Concentration of surface sites were published in mol/g of dry bacteria. The dry-to-wet mass ratio for *A. flavithermus* is 1 to 6.7 and for the nine bacterial species 1 to 9.9.

^f Wightman *et al.* determinate deprotonation constant at 50° C.

^g N. A., not applicable.

The variation between the SCM parameters of the two *Geobacillus* strains investigated here are too small to permit identification of any relationship between biosorption and growth responses to elevated concentrations of Cd^{2+} . *G. thermocatenulatus* and *G. stearothermophilus* may have evolved several metal ion detoxification strategies that account for the observed types of growth curves. The genome of *G. stearothermophilus* (DSM 13240) is being sequenced at the present time. A search of the genome data currently available shows evidence that *G. stearothermophilus* (DSM 13240) contains sequence information required for cadmium ion efflux, such as cadmium-transporting ATPases (<http://www.genome.ou.edu/bstearo.html>). When completely sequenced the genome may reveal even more cadmium ion detoxification systems.

This study demonstrates that the extent of cadmium ion adsorption by *G. thermocatenulatus* and *G. stearothermophilus* can be predicted for a range of pH values and metal ion-to-bacteria concentration ratios. SCMs can be applied to describe cation-bacteria interaction under a given set of conditions and may be valuable for development and optimization of bioremediation schemes. As for both studied bacterial strains Cd^{2+} is predominantly complexed at one binding site their use in bioremediation might be more cost-effective than organisms binding Cd^{2+} to two or more binding sites. The more binding sites involved, the more acid and base would be necessary to adsorb and to desorb the metal ions efficiently.

Investigations of microbial biosorption can deepen the insight of metal mobilization in the environment (such as contamination of drinking water) and can be used to improve waste treatment of metal-polluted water and soil. Further studies should evaluate the adsorption of other metals by the species studied here and by other thermophiles, for example to determine if systematic metal affinity series exist as have been observed for mesophiles (Borrok *et al.*, 2005; Yee & Fein, 2001).

3.6 Acknowledgements

Research funding was provided by the New Zealand Foundation of Research, Science & Technology (Contract Number C05X0303: Extremophilic

Microorganisms for Metal Sequestration from Aqueous Solutions). Special thanks are due to Hannah Heinrich for the TEM micrographs and the electrophoretic mobility measurements at the University of Otago, Dunedin, and Marshall Muller and Moya Appleby for their assistance at the Institute of Geological and Nuclear Sciences in Wairakei. The editor and the two anonymous reviewers offered comments and suggestions that greatly improved this manuscript.

Chapter 4: Champagne Pool

Microbial life in Champagne Pool, a geothermal spring in Waiotapu, New Zealand

(A condensed version of this chapter has been published in
Extremophiles, July 2007)

4.1 Abstract

Surveys of Champagne Pool, one of New Zealand's largest terrestrial hot springs and rich in arsenic ions and compounds, have been restricted to geological and geochemical descriptions, and a few microbiological studies applying culture-independent methods. In the current investigation, a combination of culture and culture-independent approaches were chosen to determine microbial density and diversity in Champagne Pool. Recovered total DNA and adenosine 5'-triphosphate (ATP) content of spring water revealed relatively low values compare to other geothermal springs within New Zealand and are in good agreement with low cell numbers of $5.6 \pm 0.5 \times 10^6$ cells per ml obtained for Champagne Pool water samples by 4',6-diamidino-2-phenylindole (DAPI) staining. Denaturing Gradient Gel Electrophoresis (DGGE) and 16S rRNA (small-subunit ribosomal nucleic acid) gene clone library analyses of environmental DNA indicated the abundance of *Sulfurihydrogenibium*, *Sulfolobus* and *Thermofilum*-like populations in Champagne Pool. From these results, media were selected to target the enrichment of hydrogen-oxidizing and sulfur-dependent microorganisms. Three isolates were successfully obtained having 16S rRNA gene sequences with similarities of approximately 98% to *Thermoanaerobacter tengcongensis*, 94% to *Sulfurihydrogenibium azorense*, and 99% to *Thermococcus waiotapuensis*, respectively.

4.2 Introduction

The Waiotapu geothermal region covers a surface area of around 18 km² in the

North Island of New Zealand. It is one of the largest areas of terrestrial thermal activity in New Zealand with a predicted surface heat flow of approximately 540 MW (Hedenquist, 1986b). The largest geothermal feature within the Waiotapu region is Champagne Pool. The hot spring is approximately 65 m in diameter (Figure 16 A), has an estimated volume of 50,000 m³ (Hedenquist & Henley, 1985) and was formed over 900 years ago by hydrothermal eruption (Lloyd, 1959). Many terrestrial thermal springs often exhibit sulfur- and iron-rich systems with pH values of approximately 1.8 to 2.2 or carbonate-bicarbonate systems with pH values of around pH 7.5 to 9.0 (Brock, 1986), reflecting the capacity of the main buffers in natural geothermal habitat: sulfuric acid (pK=1.8), carbonate (pK=6.3), and bicarbonate (pK=10.2). However, Champagne Pool does not follow any of the described bimodal distribution schemas. The alkali chloride spring water (pH 5.5 at around 75° C) consists of high concentrations of silica and metalloid ion-sulfide complexes (Jones *et al.*, 2001) which form the white terrestrial silica sinter rim that rises 50 cm above the pool surface and the orange subaqueous sediments around the margin of Champagne Pool (Figure 16 B). Champagne Pool fluid is oversaturated with orpiment (As₂S₃), stibnite (Sb₂S₃) and carlinite (Tl₂S) leading to precipitation of those sulfide minerals (Pope *et al.*, 2005). The hot spring discharges about 10 liter per s of undiluted geothermal water and around 7 liter per s of vapor (Hedenquist & Henley, 1985) providing a mean residence time of the order of 34 days. The pool name derives from its effervescence due to the copious amounts of gas evolved, mainly 73.0% (v/v) CO₂, 16.2% (v/v) N₂, 6.4% (v/v) CH₄, 2.3% H₂, 1.7% (v/v) H₂S, and traces of O₂ (Jones *et al.*, 2001), which simultaneously serves to mix the water and maintain an even temperature of around 75° C by convection and pH values of approximately 5.5 by buffering due CO₂.

The Waiotapu geothermal region has been subject to many geological and geochemical investigations (Giggenbach *et al.*, 1994; Hedenquist & Henley, 1985; Hedenquist, 1986a; Lloyd, 1959; Pope *et al.*, 2005). Only a few studies have recently described microbial activity in Champagne Pool restricted to electron microscopy examinations (Jones *et al.*, 2001; Mountain *et al.*, 2003; Phoenix *et al.*, 2005) and PCR studies (Ellis *et al.*, 2005). Micrographs have shown filamentous, rod- and coccoid structures to be similar to morphologies of

Chloroflexus, *Thermothrix*, *Thermus*, *Thermoproteus*, *Pyrobaculum* or *Thermofilum* species (Jones *et al.*, 2001) and S-layer patterns to be similar to *Clostridium thermohydrosulfuricum* or *Desulfotomaculum nigrifacans* (Phoenix *et al.*, 2005). Ellis *et al.* (2005) identified a 16S rRNA gene sequence closely related to *Thermofilum pendens*. However, successful attempts to culture microorganisms from Champagne Pool have not been reported.

Previous studies showed that the standing biomass and microbial diversity in the pool is low (Ellis *et al.*, 2005; Jones *et al.*, 2001) with reasons suggested being: 1) Lack of substrate due to long residence time of spring water; 2) Toxic levels of arsenic or other pool components; 3) Silica deposition precludes bacterial growth due to nucleation. Niederberger (2005) reported a dissolved organic carbon concentration for Champagne Pool water of 700 mg per m³, which was at least on a par with many other thermal pools, which contained greater biomass. Additionally, there would appear to be ample CO₂ and H₂ for methanogenesis and other reduced inorganics to support autotrophy. Champagne Pool is supersaturated in silica and evaporative cooling (or bacterial nucleation) enhances precipitation. Exposed glass slides build up a silica sinter at a rate of 0.023 mm per day to form mini-stromatolites in 2 to 3 months due to wave action. The sinter contains fossilized bacteria and has a complex chemistry (Mountain *et al.*, 2003). However, sinter does not form as readily in anaerobic zones and is unlikely to explain the low biomass throughout the pool.

In this investigation, culture-dependent and culture-independent approaches are applied to describe microbial density and diversity in Champagne Pool. Microbial density assessed by microscopy, DNA extraction and determination of the adenosine 5'-triphosphate (ATP) content of spring water and colonized slides revealed relatively low values compared to other hot springs in New Zealand (Niederberger, 2005). The culture-independent studies involved Denaturing Gradient Gel Electrophoresis (DGGE) analysis and construction of 16S rRNA (small-subunit ribosomal nucleic acid) gene clone libraries of environmental DNA obtained from Champagne Pool. On account of the results culture medium was selected and designed. Isolates phylogenetically related to strains of the genera *Sulfurihydrogenibium*, *Thermoanaerobacter* and *Thermococcus* were successfully

obtained.

4.3 Materials and Methods

4.3.1 Sampling and ATP measurements

Water and sediment samples were taken in 2004, 2005 and 2006 from the north-east side of the terrestrial hot spring Champagne Pool in Waiotapu, New Zealand (Figure 15, Figure 16 A). Samples were obtained from 10 cm, 30 cm, and 100 cm below water surface level (Figure 16 B) immediately transferred into sterile 2-liter glass flasks (Schott) and hermetically closed. By two hours at the latest, the samples were processed in the laboratory.

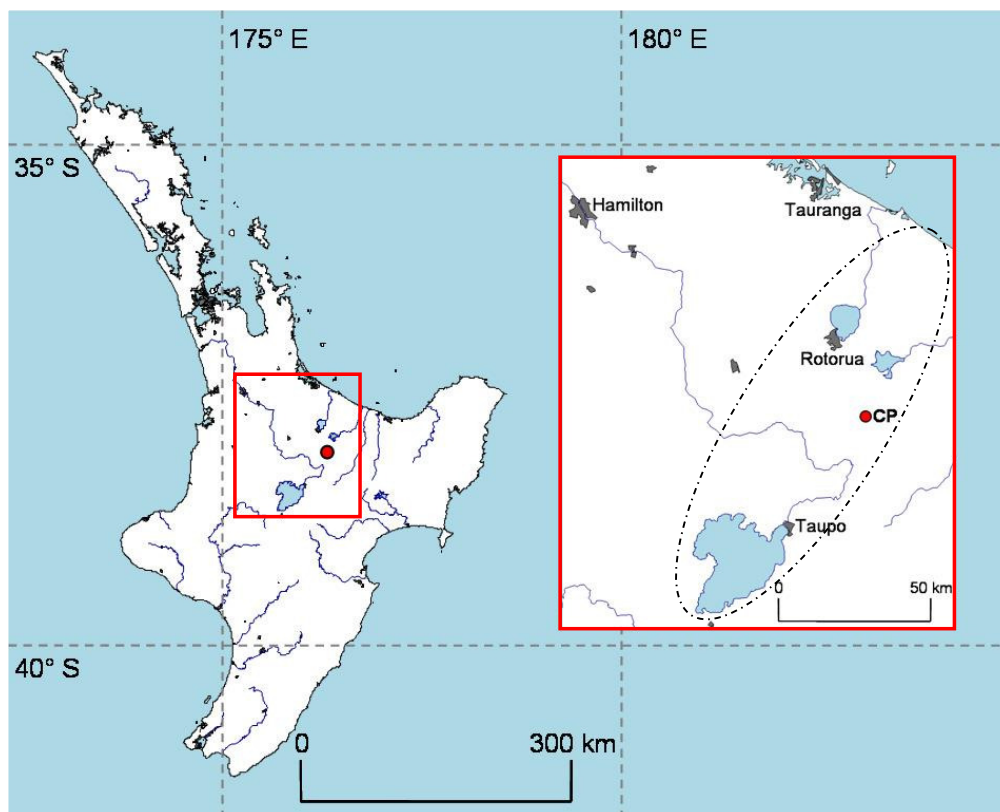


Figure 15. Map of New Zealand North Island and enlargement of the central part. Dotted lines within the enlargement outline the Taupo Volcanic Zone, which exhibit many geothermally active features such as the hot spring Champagne Pool (CP, red circle). Mapping was performed using the New Zealand Freshwater Fish Database Assistant software developed by I. G. Jowett (National Institute of Water & Atmospheric Research).

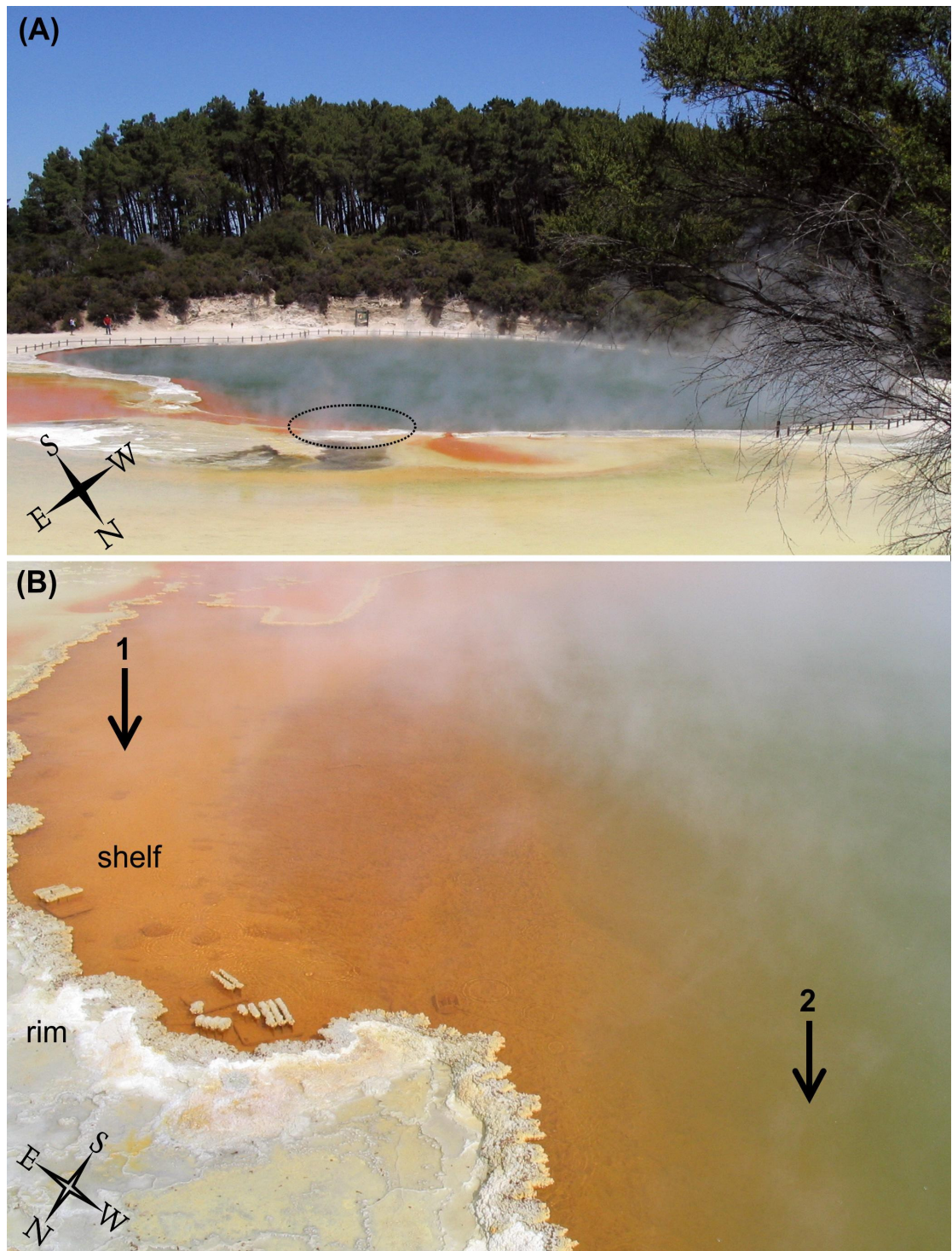


Figure 16. Champagne Pool hot spring surrounded by a grey-white rim of silica. (A) Sampling area is indicated by a dotted ellipse. (B) Sampling site 1 was located within the shallow water area (approximately 10 cm below surface water level) on the subaqueous shelf covered by orange-colored sediment. Site 2 was off the shelf within the deep-water area (maximum depth approximately 150 m) and samples were obtained from 30 to 100 cm below surface water level.

To estimate biomass in Champagne Pool the content of ATP was determined. Intracellular ATP is closely related to metabolic activity. Therefore, glass slides were immersed in Champagne Pool and incubated for several days. The glass slides provided a surface for potential microbial colonization (Niederberger, 2005). ATP measurements were carried out by wiping defined areas of the glass slides using a commercially available Clean Trace swab device (Biotrace). The swab system extracts ATP from microbial cells, and released ATP reacts with luciferin and luciferase reflected by light emission. Light production was measured using a portable ATP meter (Uni-Lite, Biotrace) and recorded as Relative Light Units (RLU). Fresh spring water samples were measured by dispensing a standard volume of sample directly onto a swab device and RLU were determined as described.

4.3.2 DNA extraction

Nucleic acids were extracted by enzymatic digestion (Marmur, 1961) and by a fast method based on physical disruption and cationic detergents modified from the protocol of Dempster *et al.* (1999). Approximately 500 ml spring water was filtered through a cellulose acetate filter (pore size 0.22 μm , diameter 47 mm). The filter was then placed in CTAB extraction buffer (100 mM Tris-HCl, 1.4 M NaCl, 20 mM EDTA, 2% (w/v) cetyltrimethylammoniumbromide (CTAB), 1% (w/v) polyvinylpyrrolidone (PVP) (360,000, pH 8.0) and freshly made 0.4% (w/v) 2-mercaptoethanol and incubated at 100° C for 20 min. Next, nucleic acids were extracted with an equal volume of phenol, followed by extraction with chloroform-isoamyl alcohol (24:1 (v/v)). To the aqueous phase, an equal volume of isopropanol and 0.1 volume of 3 M sodium acetate (pH 5.5) were added. After overnight incubation at -20° C, the solution was centrifuged. The pellets were then washed twice in 70% ethanol, air-dried and resuspended in TE buffer (10 mM Tris-HCl, pH 8; 1 mM EDTA).

4.3.3 PCR amplification of 16S rRNA gene and gene cloning experiments

Microbial 16S rRNA genes were amplified in PCR mixtures consisting of PCR buffer (10 mM Tris-HCl, 50 mM KCl; pH 8.3), 1.5 mM MgCl_2 , 0.2 mM dNTP

(dATP, dCTP, dGTP, and dTTP), 1.0 μ M of each primer, 5.0% (w/v) dimethyl sulfoxide (DMSO) and 1.0 unit of *Taq* polymerase (Roche). For DGGE-PCR reaction buffer (10 mM Tris-HCl, 50 mM KCl; pH 8.3), 1.25 mM $MgCl_2$, 0.2 mM dNTP (dATP, dCTP, dGTP, and dTTP), 0.2 μ M of each primer, and 1.25 units of *Taq* polymerase (Roche) were used. Sequences of PCR primers are shown in Table 7. For amplification 20 to 100 ng of DNA template was used. The *Taq* polymerase was added to the reaction mixtures after the initial denaturation step to minimize the possibility of nonspecific DNA amplification. PCR conditions using archaeal and bacterial primers were an initial denaturation step at 94° C for 210 s, 33 cycles annealing for 30 s, extension at 72° C for 120 s and denaturation at 94° C for 30 s, followed by a final extension step for 360 s. For DGGE-PCRs the initial denaturation was extended to 300 s, annealing and extension steps were applied for 60 s and the total cycle number was 36. The annealing temperatures for each primer set are enlisted in Table 7. Archaea-specific primers often lack specificity for Nanoarchaea. Therefore an additional primer set was used which was specific for Nanoarchaea. PCRs amplifying the nanoarchaeal 16S rRNA gene (primer 9bF and 511mcR) were performed according to Huber *et al.* (2002b).

Amplified 16 rRNA genes were purified by agarose gel electrophoresis and used in cloning experiments with pGEM-T Easy vector (Promega). After electrophoresis of PCR products in 1% agarose gel and TAE buffer, the gel was stained in ethidium bromide (0.5 mg per liter) for 10 min and observed under UV light with a wavelength of 302 nm. A slice of the agarose gel containing the DNA fragment of interest was excised and transferred into a sterile tube. An equal volume of phenol was added. Then the mix was snap-frozen in liquid N_2 and centrifuged at 12000 $\times g$ (Eppendorf Centrifuge 5415D) for 15 min. DNA from the aqueous phase was extracted with an equal volume chloroform-isoamyl alcohol (24:1 (v/v)). To the aqueous phase 2.5 volume of 100% ethanol and 0.1 volume of 4 M LiCl were added. After overnight incubation at -20° C, the solution was centrifuged at 12000 $\times g$ for 5 min. The pellets were then washed twice in 70% ethanol, air-dried and resuspended in TE buffer.

The appropriate amount of purified PCR product (insert) to be added in the ligation reactions was calculated by

$$\frac{\text{ng of vector} \times \text{kb size of insert}}{\text{kb size of vector}} \times \text{insert-to-vector ratio} = \text{ng of insert} \quad (11)$$

in which assuming an equal insert-to-vector ratio and a PCR product size of the 16S rRNA gene of 1.5 kb the following result was obtained

$$\frac{50 \text{ ng vector} \times 1.5 \text{ kb insert}}{3.0 \text{ kb vector}} \times \frac{1}{1} = 25 \text{ ng insert} \quad (12)$$

Ligation reactions consisting of rapid ligation buffer (60 mM Tris-HCl, 20 mM MgCl₂·6H₂O, 20 mM DTT, 2 mM ATP; pH 7.8), 10% polyethylene glycol, 50 ng of pGEM-T easy vector, 25 ng of purified PCR product, and 3 Weiss units of T4 DNA ligase were incubated overnight at 4° C.

For transformation, competent cells were prepared by growing *E. coli* JM 109 cells in 1 liter LB medium (10 g of trypticase peptone, 5 g of yeast extract, 5 g of NaCl; pH 7.5) at 37° C and 200 rpm until optical density at 600 nm reached around 0.600. Cells were harvested by centrifugation at 4000×g and 4° C (Sorvall RC 26 Plus) for 15 min. Pellets were washed in 1000 ml, 500 ml, and then 100 ml ice-cold, sterile 10% glycerol. The final cell pellet was resuspended in 10% glycerol to a final concentration of approximately 1×10¹⁰ cells per ml. Aliquots of 400 µl were frozen in liquid N₂ and stored at -70° C until further use.

The insert was transformed into competent cells by electroporation. A 2.0 µl aliquot of the overnight ligation reaction containing the vector was gently mixed with 80 µl thawed competent cell suspension and transferred to a chilled 0.1 cm gap Gene Pulser cuvette (Bio-Rad) on ice. Electroporation settings were 200 Ω (Ohm) resistance, 25 µF (Faraday) capacitance, and 1.8 kV voltage using a Gene Pulser (Bio-Rad). Immediately following transformation, cells were transferred to 920 µl 37° C-prewarmed SOC medium (containing per liter: 20.0 g of trypticase, 5.0 g of yeast extract, 10 mM NaCl, 10 mM KCl, 10 mM MgCl₂·6H₂O, 10 mM MgSO₄·7H₂O, 20 mM glucose; pH 7.0). After incubation at 37° C and 150 rpm for 2 h cell suspension was harvested by centrifugation at 800×g (Eppendorf Centrifuge 5415D) for 2.5 min and cell pellets were resuspended in 200 µl SOC

medium. 100 μ l aliquots of the transformed cells were then spread onto LB medium (which has been solidified by using 8 g of agarose per liter) supplemented with 100 mg of sodium ampicillin, 120 mg of IPTG, and 80 mg of X-gal per liter, respectively.

E. coli cells containing the plasmid and the insert were selected by blue-white screening of bacterial colonies. The vector used contains a *lacZ* gene with an internal multi-cloning site (Figure 17). The *lacZ* gene codes for the subunit of the enzyme β -galactosidase and gene expression is induced by IPTG. The enzyme β -galactosidase catalyzes the conversion of X-gal to a hardly soluble indigo dye. Cells containing a plasmid without an insert form blue-colored colonies due the activity of the β -galactosidase. In contrast, a successful ligation of a DNA fragment (PCR product) into the multi-cloning site inactivates the enzyme β -galactosidase due to the location of the insert within the *lacZ* gene (Figure 17). Colorless bacterial colonies indicate disrupted enzyme activity. However, cells without a plasmid might also form colorless colonies. To exclude this option, the vector used contains furthermore an *amp(R)* gene conferring ampicillin resistance (Figure 17). Ampicillin, a beta-lactam antibiotic, inhibits bacterial cell wall synthesis causing cell lysis. Only *E. coli* cells containing the plasmid are able to grow in the presence of ampicillin.

Plasmids were isolated as previously described in Chapter 2 (2.2.3 Small-scale plasmid isolation) and then categorized by restriction fragment length polymorphism (RFLP). The enzymatic digestions of the plasmids with *EcoR* I (cut site: G \uparrow AATTCC), *Rsa* I (cut site: GT \uparrow AC), and *BamH* I (cut site: G \uparrow GATCC) (Roche) followed electrophoresis in 3% agarose gel and TBE buffer (89 mM Tris borate and 2 mM EDTA, pH 8.3). Restriction reactions contained SuRE/ cut buffer A (Roche; 33 mM Tris acetate, 10 mM Mg-acetate, 66 mM K-acetate, 0.5 mM DDT; pH 7.9 at 37° C), 1% BSA, and 10 units of all three restriction enzymes used were incubated overnight at 37° C following 20 min at 80° C. Representatives of each distinct restriction enzyme fingerprint were selected for further sequence analyses.

Table 7. Target, position, specificity, sequences, and annealing temperature of oligonucleotide primers used for PCR studies.

Target	Position ^a	Oligonucleotide primer sequence (5' → 3')	T [° C]
Bacterial 16S rRNA gene (Johnson, 1994)	27F 1522R	AGAGTTTGATCCTGGCTCAG AAGGAGGTGATCCA(A/G)CCGCA	50 ^d
Bacterial 16S rRNA gene (DGGE) (Lane, 1991)	338F 519R	GC^b -CTCCTACGGGAGGCAGCAG ATTACCGCGGCTGCTGG	65 ^e
Archaeal 16S rRNA gene (Niederberger <i>et al.</i> , 2006)	347F 1335R	CCAGGCCCTACGGGGCGCA GTGTGCAAGGAGCAGGGAC	60
Archaeal 16S rRNA gene (DGGE) (Niederberger <i>et al.</i> , 2006)	915F 1335R	GC^c -AGGAATTGGCGGGGGAGCAC TGTGCAAGGAGCAGGGACG	60
Nanoarchaeal 16S rRNA gene (Huber <i>et al.</i> , 2002b)	9F 511R	G(A/G)GTTTGATCCTGGCTCAG CTTGCCCACCGCTT	65 ^e

^a Corresponding 16S rRNA gene sequence position in *Escherichia coli*.

^b GC-clamp: **CGCCCGCCGCGCCCCGCGCCCGTCCCGCCGCCCCCGCC**.

^c GC-clamp: **CGCCCGCCGCGCCCCGCGCCCGGCCCGCCGCCCCCGCCCC** (Ferris *et al.*, 1996).

^d Annealing temperature was 50° C for two cycles and 48° C for 31 cycles.

^e Annealing temperature was decreased from 65° C to 54° C in intervals of 0.5° C per cycle.

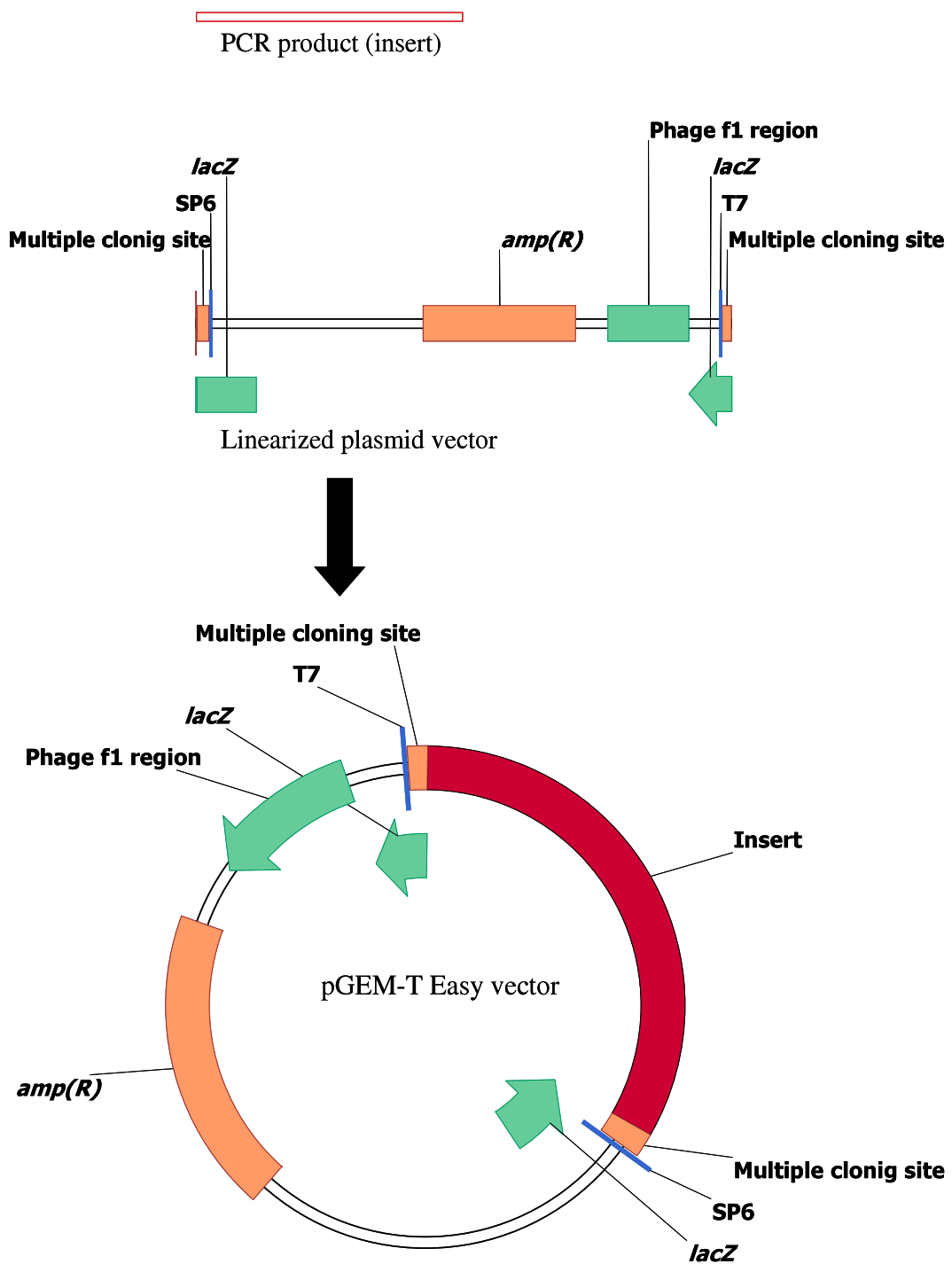


Figure 17. Scheme of ligation of a PCR product into a vector.

DNA sequencing of clone inserts were carried out by the Waikato DNA Sequencing Facility at the University of Waikato, Hamilton, New Zealand based on MegaBACE DNA analysis system (Amersham Biosciences). In sequencing

reactions the oligonucleotide primers M13pUC forward (5'- CCC AGT CAC GAC GTT GTA AAA CG -3'), M13pUC reverse (5'- AGC GGA TAA CAA TTT CAC ACA GG -3') and T7 (5'-TAA TAC GAC TCA CTA TAG GG -3') were used.

4.3.4 DGGE analysis of 16S rRNA gene fragments

DGGE profiles were obtained by separation of the DGGE-PCR products obtained from environmental DNA in polyacrylamide gels with denaturing gradients (Muyzer *et al.*, 1993) ranging from 40% to 80% and 45% to 65% for bacterial and archaeal samples, respectively (100% denaturant is defined as 7 M urea and 40% (v/v) deionized formamide). Electrophoresis was conducted in TAE buffer (40 mM Tris, 20 mM acetic acid, 1 mM EDTA; pH 8.0) at constant voltage of 140 V for 5 hours using a DCode system (Bio-Rad). After electrophoresis, gels were stained with ethidium bromide (0.5 mg per liter) for 10 min, washed in distilled water for 5 min and then photographed (AlphaImager System, AlphaInnotech) under UV light with a wavelength of 302 nm. DNA fragments were excised from polyacrylamide gels, reamplified in DGGE-PCRs, and verified by a second DGGE analysis to ensure purity. Representative DNA fragments were sequenced.

4.3.5 Enrichment experiments

Based on the results of DGGE analysis and gene cloning experiments media for hydrogen-oxidizing (modified MSH medium), sulfur-oxidizing (*Sulfolobus* medium) and sulfur-reducing (V24N medium) microorganisms were used in enrichment experiments. Medium V24N (Stetter, 1986) and *Sulfolobus* medium (Brock *et al.*, 1972) were prepared as previously described, except that the final pH was adjusted to a value of 5.5.

The V24N medium contained per liter: 1.30 g of (NH₄)₂SO₄, 0.28 g of K₂HPO₄, 0.25 g of MgSO₄·7H₂O, 0.07 g of CaCl₂·2H₂O, 0.02 g of FeCl₃·6H₂O, 1.80 mg of MnCl₂·4H₂O, 4.50 mg of Na₂B₄O₇·10H₂O, 0.22 mg of ZnSO₄·7H₂O, 0.05 mg of CuCl₂·2H₂O, 0.03 mg of Na₂MoO₄·2H₂O, 0.03 mg of VOSO₄·2H₂O, 0.01 mg of

CoSO₄, 1.00 g of powdered sulfur, 0.20 g of yeast extract, 2.0 g of starch, and 0.2 mg of resazurin. Medium was prepared and distributed under 100% N₂ atmosphere and sterilized by heating 2 h at 90° C on three consecutive days.

Sulfolobus medium for lithotrophic growth consisted of the V24N medium without the starch and only 0.10 g of yeast extract per liter. The medium was prepared anaerobically. After autoclaving the initial CO₂ gas phase was replaced with 80% H₂/ 20% CO₂. *Sulfolobus* medium composition for heterotrophic growth was the V24N medium without sulfur, starch, resazurin, and with 1.00 g of yeast extract per liter. Medium was autoclaved and cultivation was carried out under aerobic conditions.

MSH medium (Aguiar *et al.*, 2004) was modified and contained the following components (per liter of anaerobic water): 0.15 g of NaOH, 0.50 g of KCl, 1.36 g of MgCl₂.6H₂O, 7.00 g of MgSO₄.7H₂O, 2.00 g of Na₂S₂O₃.5H₂O, 0.40 g of CaCl₂.2H₂O, 0.20 g of NH₄Cl, 0.25 g of K₂HPO₄, 1.95 g of MES and trace minerals containing final concentrations per liter medium: 5.00 mg of Na-EDTA.2H₂O, 1.50 mg of CoCl₂.6H₂O, 1.00 mg of MnCl₂.4H₂O, 1.00 mg of FeSO₄.7H₂O, 1.00 mg of ZnCl₂, 0.40 mg of AlCl₃.6H₂O, 0.30 mg of Na₂WO₄.2H₂O, 0.20 mg of CuCl, 0.20 mg of Ni₂SO₄.6H₂O, 0.10 mg of NaSeO₃, 0.10 mg of H₃BO, 0.10 mg of Na₂MoO₄.2H₂O. The pH value of the medium was adjusted to 5.5. Aliquots of 40 ml and 8 ml were autoclaved under CO₂ atmosphere in 160 ml serum bottles and 30 ml test tubes, respectively. After inoculation using 5% inocula, the initial gas phase was exchanged with 79% H₂/ 16% CO₂/ 5% O₂ at 170 kPa.

In addition, growth medium to enrich carbon monoxide-utilizing microorganisms (Svetlichny *et al.*, 1991) was made (per liter): 0.33 g of KCl, 0.50 g of MgCl₂.6H₂O, 0.33 g of CaCl₂.2H₂O, 0.33 g of NH₄Cl, 0.33 g of KH₂PO₄, 1.95 g of MES, 0.05 g of yeast extract, 0.5 mg of resazurin, and trace minerals containing final concentrations per liter medium: 15.00 mg of nitrilotriacetic acid, 30.00 mg of MgSO₄.7H₂O, 6.00 mg of MnSO₄.4H₂O, 10.00 mg of NaCl, 1.00 mg of FeSO₄.7H₂O, 1.80 mg of CoSO₄.7H₂O, 1.00 mg of CaCl₂.2H₂O, 1.80 mg of ZnSO₄.7H₂O, 0.70 mg of CuSO₄, 0.20 mg of KAl(SO₄)₂.12H₂O, 0.10 mg of

H₃BO₃, 0.10 mg of Na₂MoO₄·2H₂O, 0.25 mg of Ni₂SO₄·6H₂O, and 0.30 mg of Na₂SeO₃·5H₂O. The pH was adjusted to a value of 5.4. Aliquots of 40 ml were autoclaved under N₂ atmosphere in 160 ml serum bottles. After autoclaving the following heat-labile components were added from sterile stock solutions (per liter of medium): 1.00 g of NaHCO₃, 0.35 g of Na₂S·9H₂O, and vitamin solution containing 2.00 mg of biotin (vitamin B₇), 5.00 mg of nicotinic acid (vitamin B₃), 5.00 mg of thiamine-HCl·2H₂O (vitamin B₁), 5.00 mg of p-aminobenzoic acid (vitamin B₁₀), 5.00 mg of D-Ca-pantothenate (vitamin B₅), 10.00 mg of pyridoxine-HCl (vitamin B₆), 1.00 mg of cyanocobalamine (vitamin B₁₂), 2.00 mg of folic acid (vitamin B₉), 5.00 mg of riboflavin (vitamin B₂), and 5.00 mg of lipoic acid. The initial gas phase of inoculated vessels was exchanged with CO and 80% CO/ 20% H₂ at 170 kPa.

Pure cultures were obtained by dilution series continued over eight 10-fold steps. Cells from the highest dilution step were inoculated in medium solidified by 0.6% (w/v) gel rite gellan gum and 0.06% (w/v) MgSO₄·7H₂O. Individual colonies were picked from the solidified medium for new dilution series. This process was repeated at least twice. The first pure cultures were designated as strains CP.B1, CP.B2, and CP.B3.

Culture experiments were performed with *Bacillus caldotenax* cultures using untreated, N₂ or CO₂ sparged, sterile-filtered (filter pore size of 0.22 µm), and autoclaved (20 min at 121° C and 104 kPa) Champagne Pool water supplemented with tryptic soy broth (TSB; Difco) to final 1x and 0.1x concentrations. Lower TSB concentrations were used as higher concentrations might alter spring water compounds in the culture medium (e.g. precipitation) due to the autoclaving process. *Bacillus caldotenax* was selected due to its simple culture requirements and its ability to grow under thermophilic and slightly acidic conditions as found in Champagne Pool. Incubations were performed at 70° C at pH 6.0.

4.3.6 Light and electron microscopy

Microbial cells were subsequently observed under a phase-contrast microscope (Olympus BH-2). Microbial enumeration was performed by staining DNA with

4',6-diamidino-2-phenylindole (DAPI). Formalin-fixed water samples obtained from Champagne Pool were filtered through black polycarbonate nucleopore filters (Osmonics Inc., pore size 0.22 μm). Filter-bound cells were stained with DAPI using standard procedures (Porter & Feig, 1980; Wetzel & Likens, 2000) and observed under a Leica DMR research microscope (excitation filter BP 340-380 nm, dichromic mirror RKP 400 nm, suppression filter LP 425 nm) at 100x objective magnification. Images were taken with an Olympus DP70 digital camera.

For scanning electron microscopy (SEM), cells were captured onto a 0.22 μm filter by filtration and fixed using 2.5% glutaraldehyde. The filter was exposed to four changes of 0.1 M sodium cacodylate buffer, rinsed in water and dehydrated in an increasing concentration series of ethanol, 50%, 75% and 90%, respectively, then four changes of absolute ethanol. The filter was critical point dried, sputtered with platinum, and viewed using a Hitachi S-4100 field emission SEM.

4.3.7 Phylogenetic analyses

The partial 16S rRNA gene sequences were analyzed using the Basic Local Alignment Search Tool (BLAST) (Altschul *et al.*, 1997) and the sequences were aligned using the ARB software package (Ludwig *et al.*, 2004). The phylogenetic position of the 16S rRNA gene sequences were determined using the PHYLIP package within ARB with analysis of sequences undertaken using DNADIST, DNAML, DNAPARS, FITCH, NEIGHBOR, and SEQBOOT programs (Felsenstein, 1993).

4.3.8 Nucleotide sequence accession numbers

16S rRNA gene sequences (Appendix E) have been deposited in the GenBank database under accession numbers as follows: EF101533 (DGGE fragment a), EF101534 (DGGE fragment b), EF101535 (DGGE fragment c), EF101536 (DGGE fragment d), EF101537 (OTU Arc03), EF101538 (OTU Bac03), EF101539 (OTU Bac04), EF101540 (OTU Bac12), EF101541 (CP.B3), EF101542 (CP.B1), and DQ989208 (CP.B2).

4.3.9 Eh-pH diagram

The stability of arsenic compounds in Champagne Pool spring water as a function of the activity of hydrogen ions (pH) and the activity of electrons (Eh) were calculated from chemical species and concentrations listed in Table 8. Eh-pH diagram was generated using the Act2 module of the Geochemist's Workbench software package (RockWare).

Table 8. Chemical composition of water samples collected from Champagne Pool (T = 75.2° C, pH = 5.17) according to Jones *et al.* (2001).

Compound		Concentration
Chlorine	Cl	1915.0 ppm
Sodium	Na	1150.0 ppm
Silica	SiO ₂	472.0 ppm
Sulfate	SO ₄ ²⁻	255.0 ppm
Carbonate	CO ₃ ²⁻	195.0 ppm
Calcium	Ca	34.5 ppm
Lithium	Li	8.5 ppm
Arsenic	As	5.2 ppm
Fluorine	F	3.8 ppm
Aluminum	Al	375.0 ppb
Strontium	Sr	295.0 ppb
Tungsten	W	130.0 ppb
Manganese	Mn	84.0 ppb
Iron	Fe	50.0 ppb
Magnesium	Mg	40.0 ppb
Barium	Ba	10.0 ppb
Titanium	Ti	6.6 ppb
Zinc	Zn	1.7 ppb
Lead	Pb	0.2 ppb
Potassium	K	0.2 ppb
Silver	Ag	0.1 ppb
Gold	Au	0.1 ppb
Vanadium	V	0.1 ppb

4.4 Results

4.4.1 Physico- and biochemical properties

No seasonal variability is expected for the geothermal site and during sampling from 2004 to 2006 spring water from Champagne Pool displayed only slight fluctuations in temperature ($74.2 \pm 0.8^\circ \text{C}$) and pH (5.5 ± 0.1) values (Table 9). Although some hot springs in the Rotorua area (ca. 30 km away from Champagne Pool) showed significant changes in water levels in the past 3 years, the water level of Champagne Pool remained stable.

Table 9. Date, time, temperature, and pH values of water samples collected from 30 cm below water surface level of Champagne Pool in 2004, 2005, and 2006. The pH values were measured at the corresponding pool temperature.

Date	Time	T [$^\circ \text{C}$]	pH	Weather
02.06.2004	12.00	74.0	5.6	cloudy
12.02.2005	14.00	74.5	5.5	sunny
24.02.2005	12.00	75.5	5.5	sunny, windy
16.05.2005	13.00	73.5	5.5	cloudy
18.05.2005	10.45	74.0	5.5	cloudy
30.05.2005	12.00	74.0	5.5	cloudy, windy
22.06.2005	12.00	74.0	5.5	rainy
05.09.2005	11.30	75.0	5.5	cloudy
29.09.2005	13.30	75.0	5.5	sunny
05.05.2006	11.30	75.5	5.6	rainy
23.06.2006	12.00	73.0	5.4	cloudy, windy
11.07.2006	12.30	73.0	5.5	cloudy
24.10.2006	15.30	74.0	5.5	cloudy, windy
13.12.2006	11.30	74.0	5.5	sunny

Sediment and water samples collected from different depths revealed low concentrations of ATP (Table 10, Figure 18). Inhibitory effects of Champagne Pool water on the ATP assay can be excluded as measurements of ATP standards

of defined concentrations in sterile water and in spring water samples showed similar values. The highest ATP levels in Champagne Pool were detected in the orange-colored sediment indicating a higher biomass in the sediments than in the water column. Similar results were obtained by measurements on the surface of glass slides that had been immersed in Champagne Pool for 24 days and had been colonized by microorganisms.

Table 10. Summary of ATP content determined for Champagne Pool samples. ATP values for the hot springs KP1 (75° C, pH 7.5) and AQ1 (95° C, pH 7.5) are listed as reference. Values are given as Relative Light Units (RLU) and ATP concentrations.

Sample	Depth [m]	RLU	ATP [ng per ml]
25 µl of water sample	0.00	677	1.8
25 µl of sediment suspension	0.10	4800	12.4
25 µl of water sample	0.10	740	1.9
25 µl of water sample	1.00	875	2.3
Glass slides (1976 mm ²) immersed in sediment	0.10	8900	^a
Glass slides (1976 mm ²) immersed in water	0.30	2300	^a
25 µl of 1:1 mix of sediment suspension and 100 ng/ml ATP	0.10	17051	44.0
25 µl of 1:1 mix of sterile water and 100 ng/ml ATP	-	18389	47.4
Glass slides immersed in KP1 (Kuirau Park, Rotorua, NZ) ^b		57,826	^a
Glass slides immersed in AQ1 (Kuirau Park, Rotorua, NZ) ^b		>180,000	^a

^a Data were obtained from slide surfaces and cannot be expressed per volume.

^b Niederberger *et al.*, 2005.

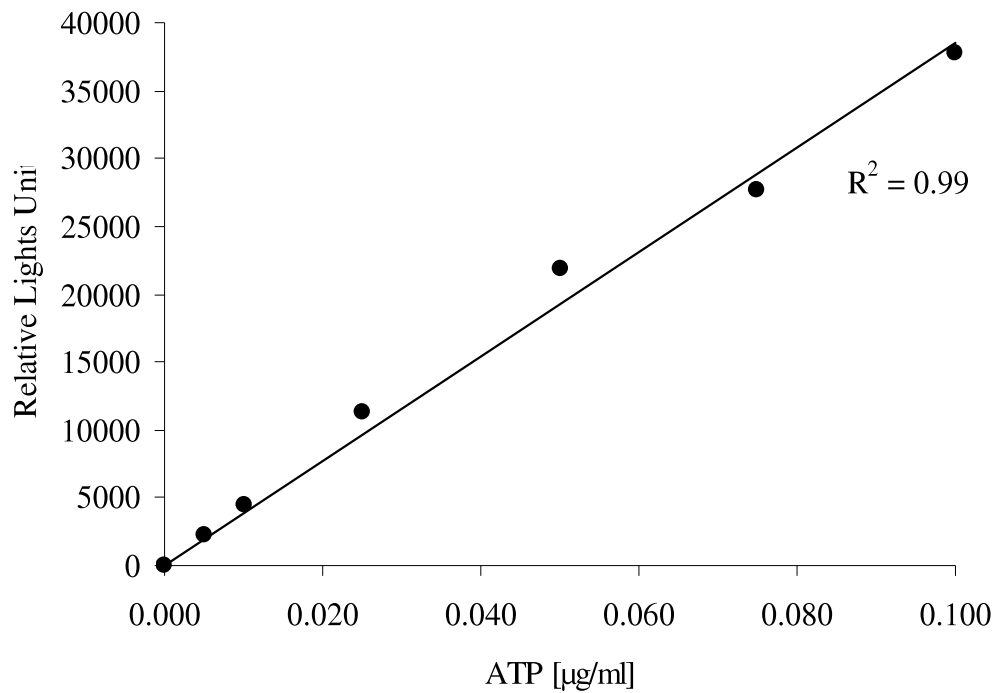


Figure 18. Calibration curve for ATP concentration. The coefficient of determination (R^2) value is 99%.

Nucleic acid concentrations of up to 6.4 μg per l could be extracted from mixed spring water and sediment samples. Values were significantly lower than for DNA concentrations obtained from enrichment cultures isolated from Champagne Pool (3.9 mg per l). To exclude possible inhibition of the applied DNA isolation method by Champagne Pool compounds, DNA from *Escherichia coli* cells was extracted with and without pool sample water. No inhibition of the assay could be detected.

4.4.2 Microscopy

Microscopic observation of water and sediment samples and glass slides incubated in Champagne Pool revealed coccoid, various rod-shaped and predominately filamentous cell structures (Figure 19). SEM micrographs of the isolates CP.B1 and CP.B2 showed different morphologies to each other (Figure 25).

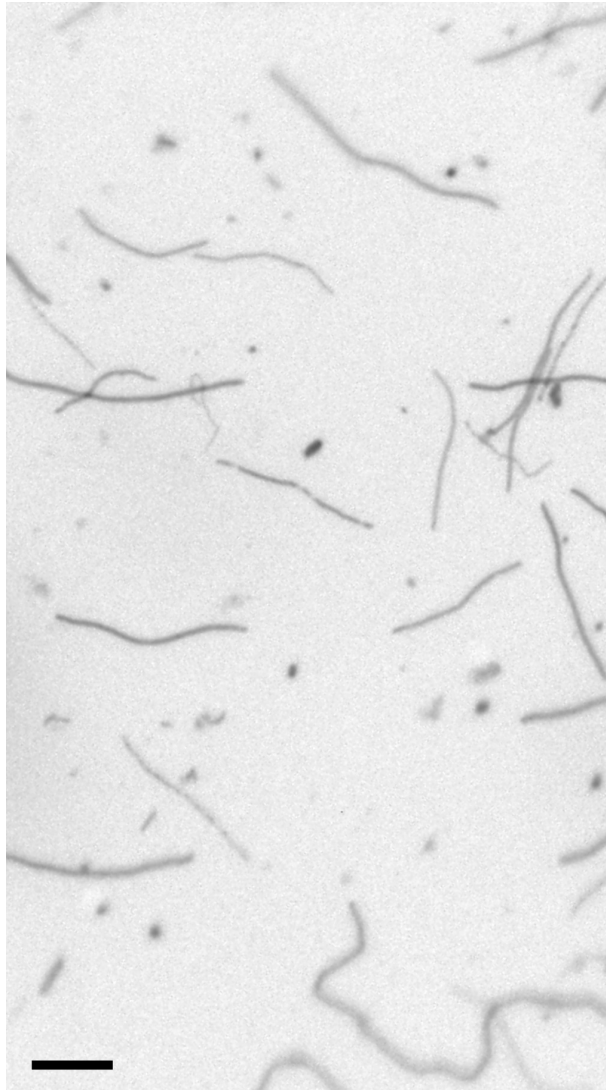


Figure 19. Inverse image of DAPI-stained Champagne Pool water samples. Bar 5 μm .

Total cell numbers by direct counting of DAPI-stained cells using epifluorescence microscopy were $5.6 \pm 0.5 \times 10^6$ cells per ml of mixed Champagne Pool sediment and water samples.

4.4.3 Molecular analysis

Archaeal and bacterial 16S rRNA genes were successfully amplified by PCR, whereas amplification of nanoarchaeal 16S rRNA genes remained negative (Figure 20). DGGE profiles derived from the archaeal and bacterial PCR products, displayed two (Figure 21 A) and five distinct bands (Figure 21 B), respectively. Sequences were obtained for four of the excised DNA fragments. Phylogenetic

analysis of both the archaeal DNA sequences and two of the bacterial DNA sequences revealed relationships to species of the genera *Sulfolobus*, *Thermofilum*, *Nevskia*, and *Sulfurihydrogenibium* (Table 11, Figure 23, and Figure 24).

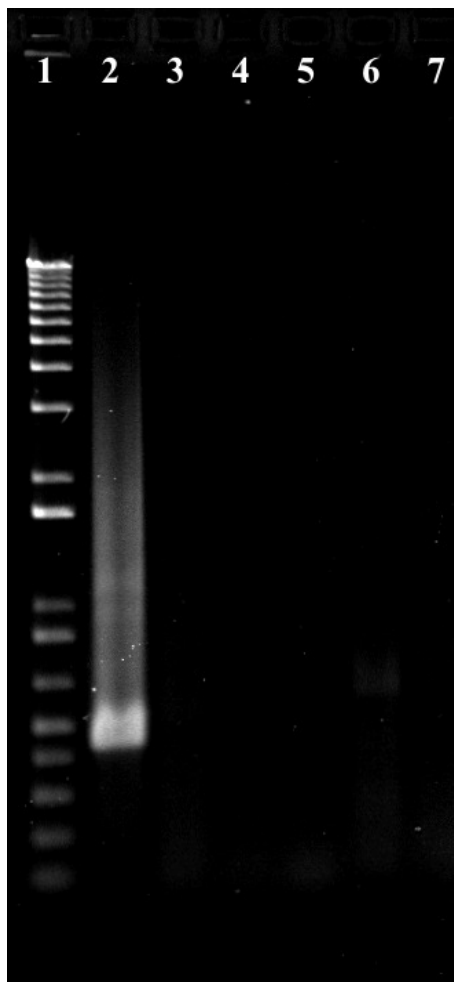


Figure 20. Image of an ethidium bromide-stained 1.0% agarose gel showing different Champagne Pool samples after PCR amplification of nanoarchaeal 16S rRNA genes. Lanes: 1, 1 Kb Plus DNA ladder (Invitrogen); 2, positive control; 3, glass slide immersed in the spring; 4, sediment suspension; 5, sediment suspension, diluted 1 to 20; 6, enrichment cultures growing in V24N medium; 7, negative control.

Clone libraries consisting of 40 archaeal and 90 bacterial 16S rRNA genes amplified by PCR were generated. Analysis of the clone libraries (Appendix D: Figure 39, Figure 40) indicated species of the genera *Sulfolobus*, *Sulfurihydrogenibium* and *Paracoccus* (Table 11, Figure 23, Figure 24) to be present in Champagne Pool partially confirming the results of the DGGE analysis.

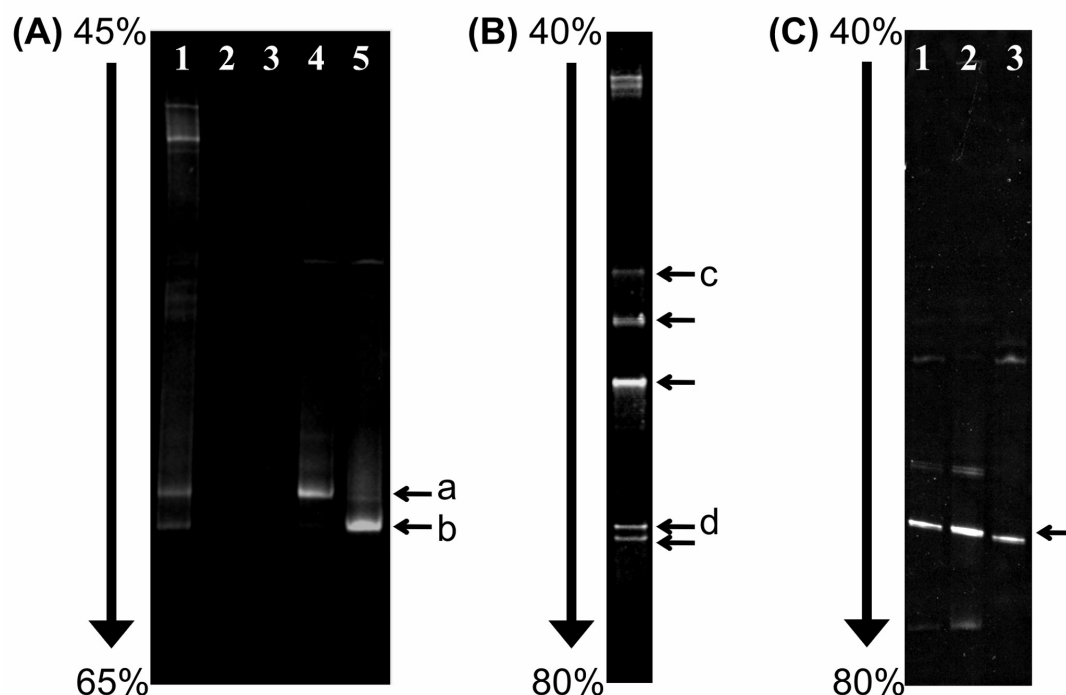


Figure 21. DGGE profiles of archaeal and bacterial 16S rRNA gene fragments amplified by PCR from Champagne Pool water samples in polyacrylamide gels with corresponding denaturing gradients. (A) Archaeal DGGE profile. Lanes: 1, Champagne Pool; 2, no sample; 3, negative control; 4, reamplified DNA fragment a from lane 1; 5, reamplified DNA fragment b from lane 1. DNA fragments revealed phylogenetic relationship to species of the genera *Thermofilum* (a) and *Sulfolobus* (b). (B) Bacterial DGGE profile obtained in April 2004. Lane: 1, Champagne Pool. DNA fragments showed phylogenetic relationship to species of the genera *Nevskia* (c) and *Sulfurihydrogenibium* (d). (C) Bacterial DGGE profile obtained in October 2004. Lanes: 1 and 2, Champagne Pool; 3, Isolate CP.B2. The arrow indicates the position of DNA fragment obtained for isolate CP.B2.

Operational Taxonomic Units (OTUs) were defined as groups of 16S rRNA gene sequences in which nucleotide sequences differed by not more than 1%. Alignment of the 16S rRNA gene sequences of the most abundant bacterial OTUs Bac12 and Bac04 with *Sulfurihydrogenibium azorense* revealed a gap of 258 base pairs between both OTUs indicating that OTUs Bac12 and Bac04 were the same inserts but with different orientation within the cloning vector (Figure 22). Although OTU Bac03 had close database matches to species of *Paracoccus*, the highest sequence similarities were for several uncultured bacteria and a thiosulfate-oxidizing bacterium from a hydrothermal vent. For OTU Bac86 no sequence similarity to known 16S rRNA gene sequences could be established.

Table 11. Summary of 16S rRNA gene sequences identified by culture and culture-independent approaches in samples obtained from Champagne Pool. The lengths of the DNA fragments and the sequence identities to the closest relatives are displayed.

Sample	Species	[bp]	[%]
DGGE			
Fragment a	<i>Thermofilum pendens</i>	330	92
Fragment b	<i>Sulfolobus acidocaldarius</i>	411	95
Fragment c	<i>Nevskia ramosa</i>	146	91
Fragment d	Uncultured <i>Sulfurihydrogenibium</i> sp.	64	92
Clone libraries			
OTU Arc03 (100% ^a)	<i>Sulfolobus tokodaii</i>	699	94
OTU Bac03 (17% ^b)	<i>Paracoccus thiocyanatus</i>	1,426	90
OTU Bac04 (61% ^b)	<i>Sulfurihydrogenibium azureense</i>	715	95
OTU Bac12 (20% ^b)	<i>Sulfurihydrogenibium azureense</i>	536	95
OTU Bac86 (2% ^b)	Non-specific amplicon	600	
Cultures			
CP.B3	<i>Thermococcus waiotapuensis</i>	962	99
CP.B1	<i>Thermoanaerobacter tengcongensis</i>	1,310	98
CP.B2	<i>Sulfurihydrogenibium azureense</i>	1,506	94

^a Percentage of clones containing archaeal inserts.

^b Percentages of clones containing bacterial inserts.

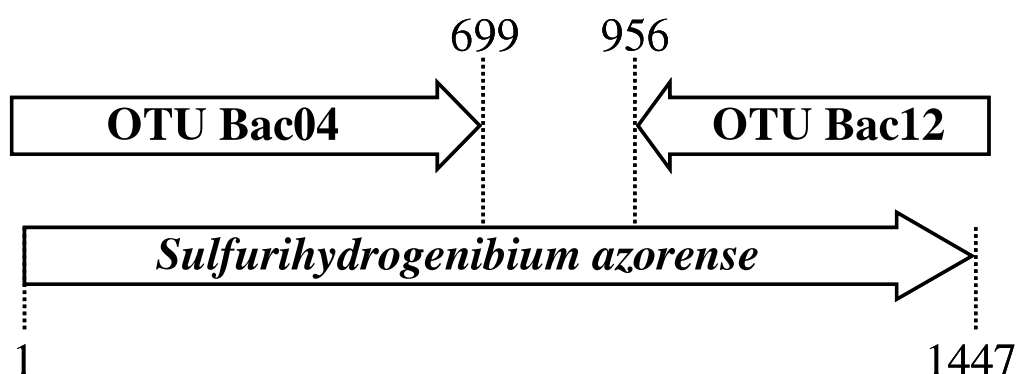


Figure 22. The position of the partial 16S rRNA gene sequences of OTU Bac04 and Bac12 in relation to the 16S rRNA gene of *S. azureense*. Numbers indicate the nucleotide position within the *S. azureense* sequence.

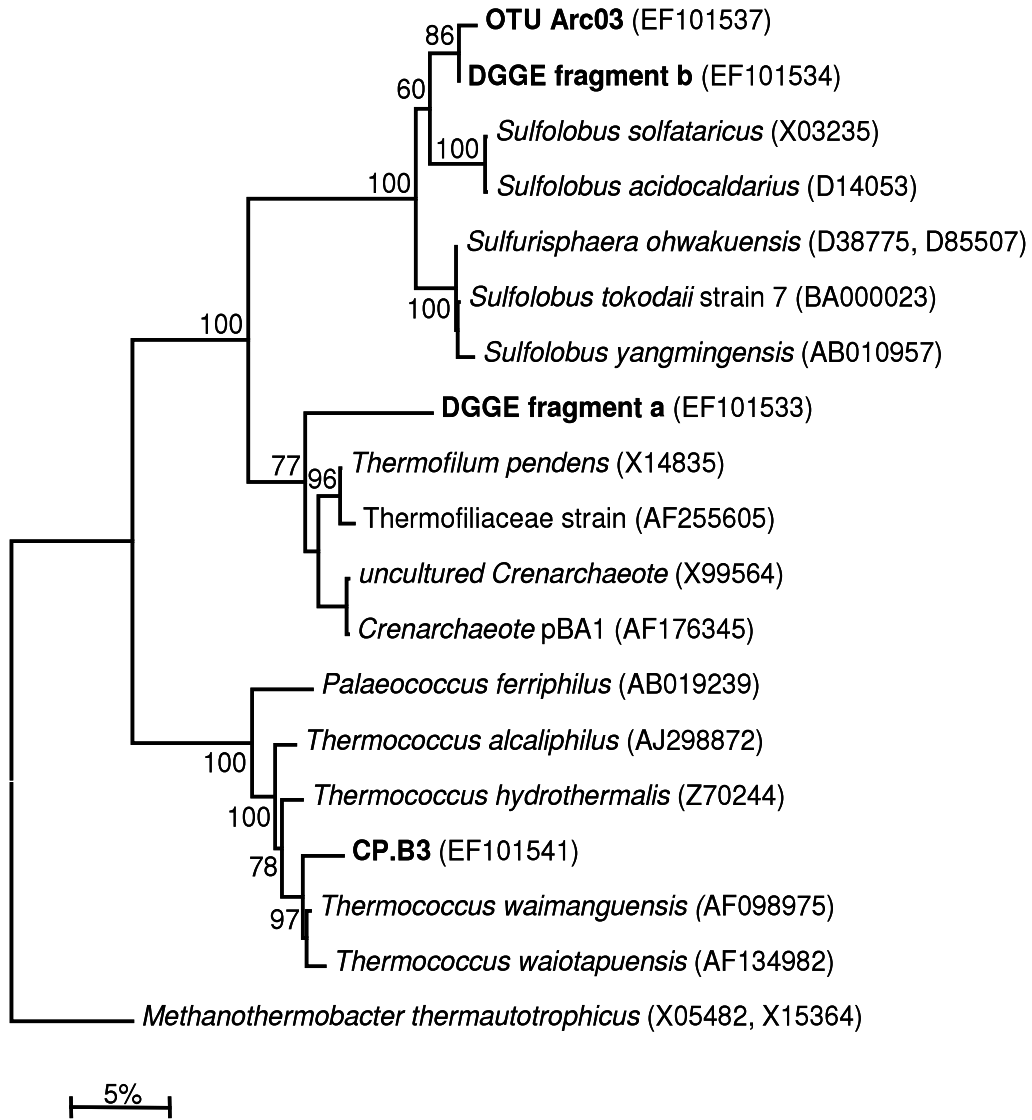


Figure 23. Phylogenetic tree demonstrating relationships of archaeal 16S rRNA gene sequences obtained from Champagne Pool spring samples. The dendrogram was produced with ARB (Neighbor joining) and bootstrap values were determined using PHYLIP. Bootstrap values at the nodes are from 1,000 iterations (only bootstrap values >60% are indicated). The numbers in parentheses are accession numbers. Sequences obtained in this study are indicated in bold. The scale bars represents an estimated sequence divergence of 5%.

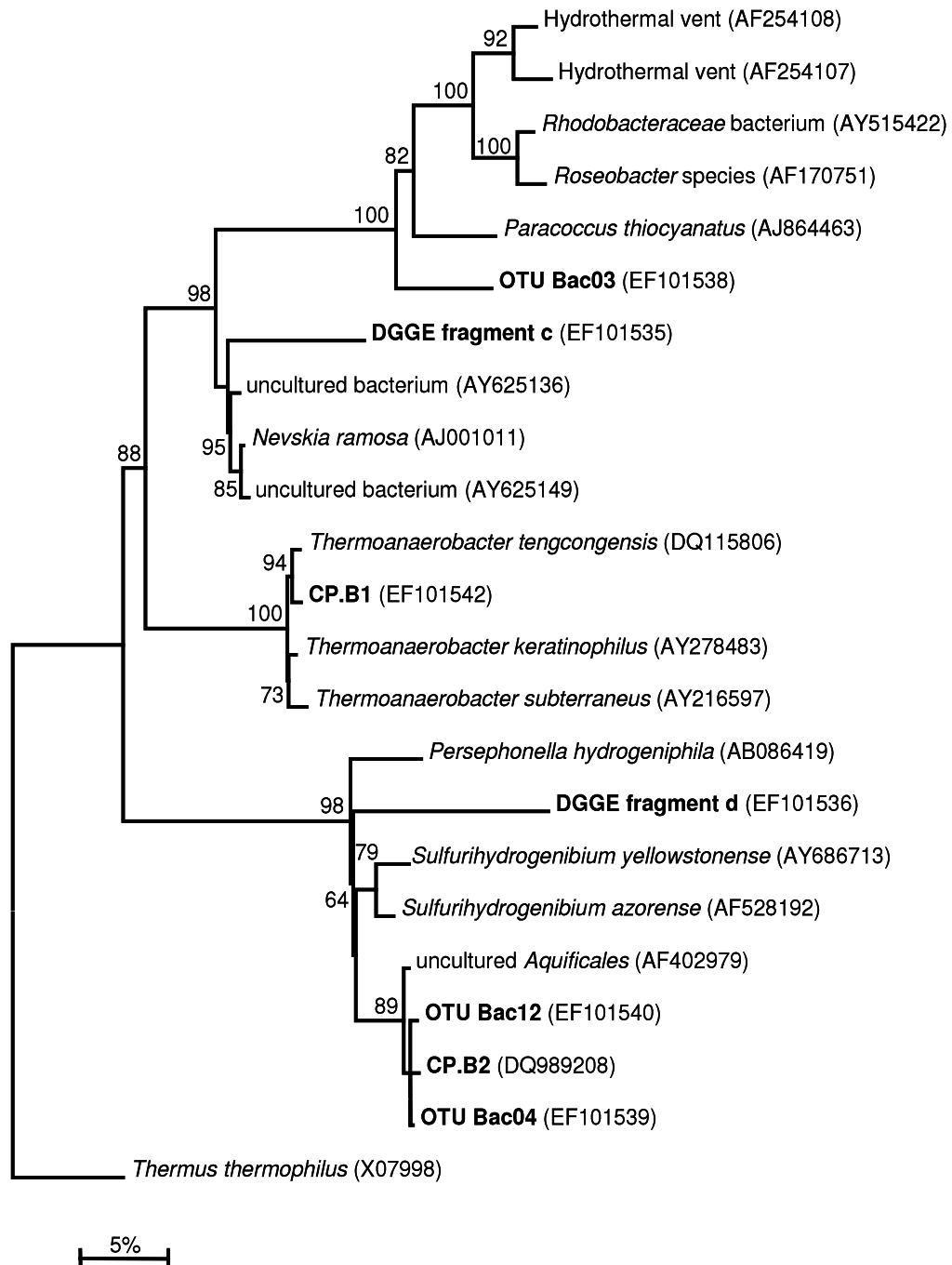


Figure 24. Phylogenetic tree demonstrating relationships of bacterial 16S rRNA gene sequences obtained from Champagne Pool spring samples. The dendrogram was produced with ARB (Neighbor joining) and bootstrap values were determined using PHYLIP. Bootstrap values at the nodes are from 1,000 iterations (only bootstrap values >60% are indicated). The numbers in parentheses are accession numbers. Sequences obtained in this study are indicated in bold. The scale bars represents an estimated sequence divergence of 5%.

Differences between DGGE and clone library results might be due to possible DNA extraction and PCR biases (Suzuki & Giovannoni, 1996; von Wintzingerode *et al.*, 1997) and/ or changes in the microbial community. DGGE and clone library analyses have been conducted separately using DGGE samples obtained from different sampling periods. Bacterial DGGE profiles (Figure 21 B and C) varied over time showing fewer bands and changes in band intensities. While DNA fragment d (Figure 21 B) assigned to *Sulfurihydrogenibium*, showed only a relatively weak band intensity in April 2004; in October 2006 a DNA fragment of the isolate CP.B2 (closest related to *Sulfurihydrogenibium*) was the most intense band (Figure 21 C). Although band intensities might not reflect the degree of abundance of species in an environment due to PCR biases, the latter DGGE profile is in good agreement with the clone library results, in which *Sulfurihydrogenibium*-like cells are the most abundant bacterial species.

According to the results obtained from DGGE analysis and the gene cloning experiments growth media were designed to isolate species closely related to members of the genera *Sulfolobus*, *Thermophilum*, and *Sulfurihydrogenibium*. As *Nevskia* and *Paracoccus* strains are both mesophilic bacteria and the 16S rRNA gene sequences obtained shared low sequence similarities of approximately 91% to *Nevskia ramosa* and 90% to *Paracoccus thiocyanatus*, medium was not selected to enrich those species.

4.4.4 Enrichment

To enrich hydrogen-oxidizing microorganisms modified MSH medium as described was used. After inoculation with Champagne Pool spring water (inoculum size 5%) microbial growth was observed by changes in turbidity within two days. Cells appeared to have a slightly curved rod-shaped morphology (Figure 25 B). The first pure culture was designated as strain CP.B2.

In V24N growth medium (Stetter, 1986) selected to enrich sulfur-reducing microorganisms different morphologies could be distinguished. A rod-shaped bacterium (isolate CP.B1, Figure 25 A) and a coccoid archaeon (strain CP.B3 was isolated by Hugh Morgan) were successfully obtained.

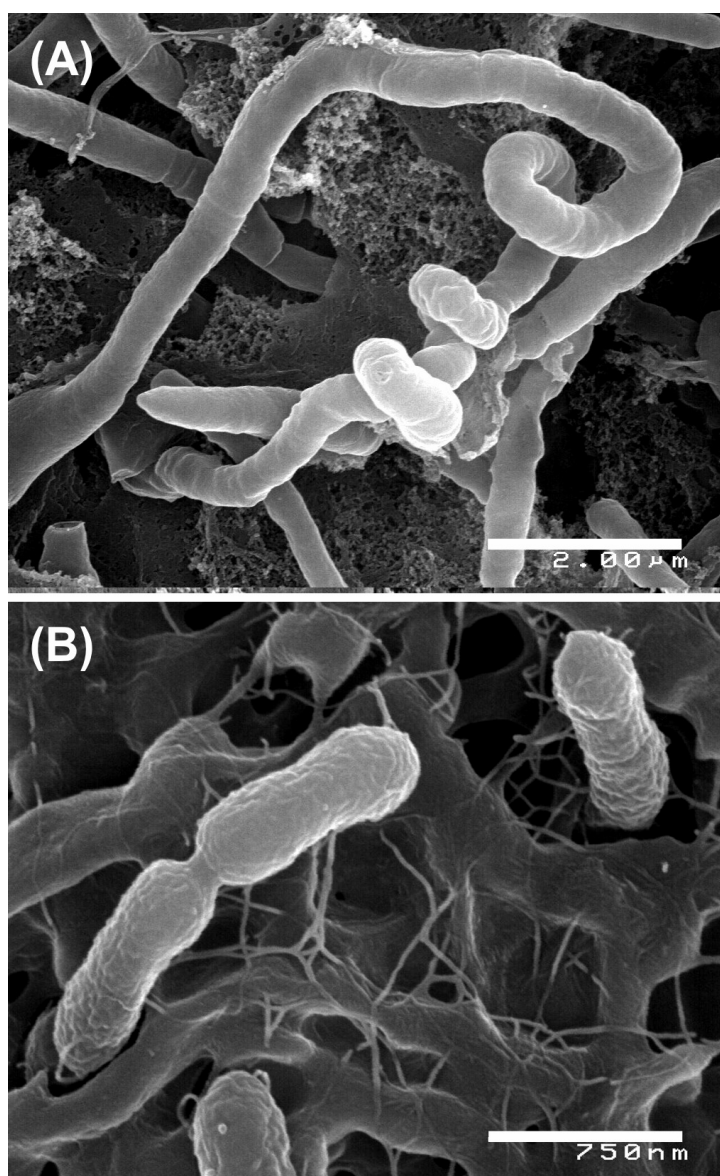


Figure 25. Scanning electron micrographs of isolate CP.B1 (A) and CP.B2. (B). (A) Bar 2 μm. (B) Bar 750 nm.

Enrichment attempts in the *Sulfolobus* medium (Brock *et al.*, 1972) under chemolithotrophic and heterotrophic conditions and in the medium for CO-utilizing microorganisms were negative.

DNA isolated from the three novel isolates and successive analysis of the amplified 16S rRNA gene revealed a distant phylogenetic relationship of isolate CP.B1 to *Thermoanaerobacter tengcongensis* (Xue *et al.*, 2001), of CP.B2 to *Sulfurihydrogenibium azorense* (Aguiar *et al.*, 2004), and of CP.B3 to

Thermococcus waiotapuensis (Gonzalez *et al.*, 1999) (Table 11). All isolates grew under temperature and pH conditions as found in Champagne Pool (Table 12).

Table 12. Growth temperature and pH ranges for microbial strains isolated from Champagne Pool. Values in brackets are the optima.

Isolate	Energy metabolism	T [° C]	pH
CP.B1	Sulfur reduction	45-80 (65)	5.5 (N. D. ^a)
CP.B2	Hydrogen oxidation	45-75 (70)	4.8-5.8 (5.4)
CP.B3	Sulfur reduction	70-85 (N. D.)	4.5-8.0 (7.0-7.5)

^a N.D., not determined.

4.4.5 Growth experiments using Champagne Pool water

Growth of *B. caldovenax* cells could not be detected when inoculated into untreated or sterile-filtered Champagne Pool water. However, when the spring water was purged with N₂ or CO₂, or autoclaved prior to inoculation, microbial growth was observed. These results suggest that a volatile component inhibiting microbial life might have been removed from Champagne Pool water during the sparging or autoclaving process.

4.4.6 Stability of arsenic compounds

Calculation of the distribution of arsenic species revealed the predominance of As(OH)₃ (As³⁺, arsenite) under the chemophysical conditions (T = 75.2° C; pH = 5.5; Eh = -40 mV, Hirner *et al.*, 1998) present in Champagne Pool spring water (Figure 26). In less reducing conditions at Eh values of approximately above 100 mV, which might be found at the hot spring-atmosphere interface, where atmospheric oxygen dissolves into the top water layer of Champagne Pool, the pentavalent arsenic compound H₂AsO₄⁻ (As⁵⁺, arsenate) appears to be more dominant. Although oxygen solubility at the hot spring temperature is relatively low (oxygen saturation concentration is around 3 mg per liter at 75.2° C and 400 m altitude; <http://www.pointfour.com/cgi/pfscalc.cgi>), traces of oxygen have been

reported for the upper water layer of Champagne Pool (Giggenbach *et al.*, 1994; Jones *et al.*, 2001).

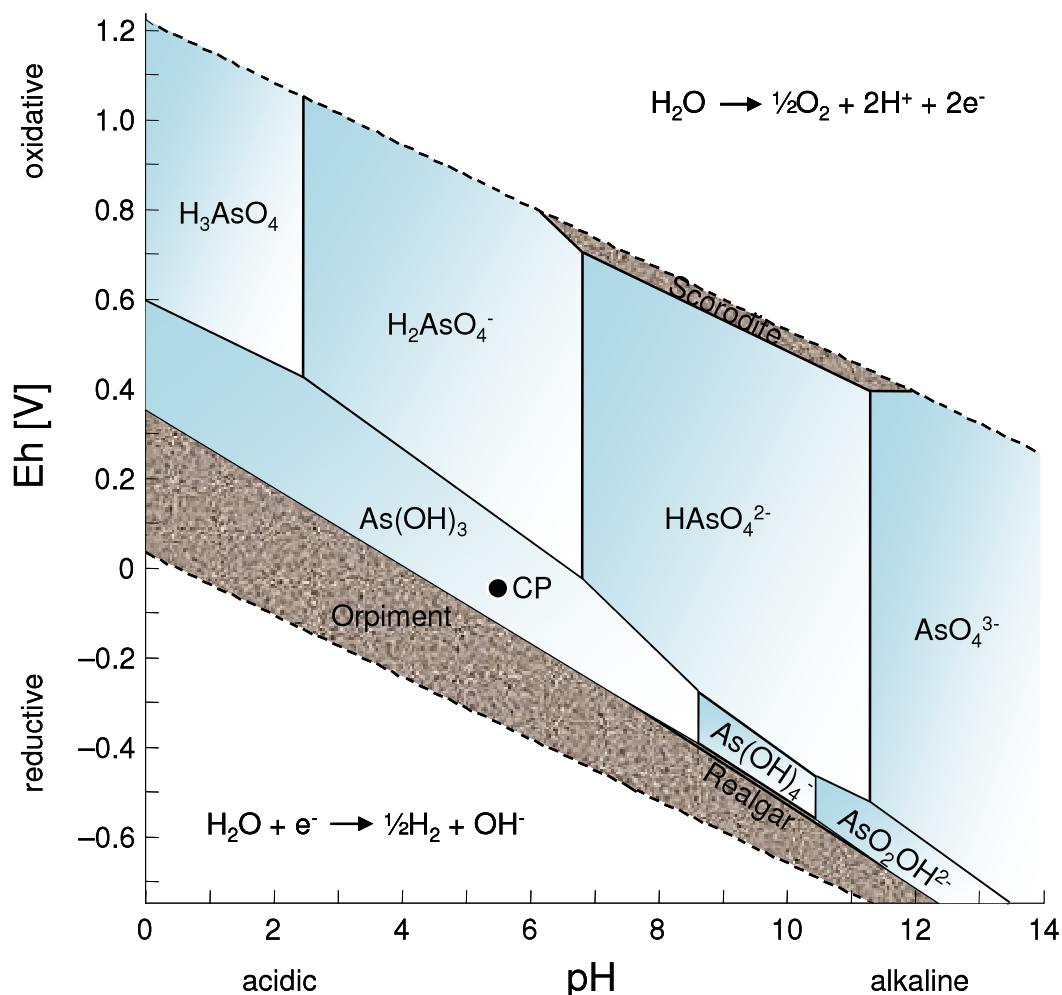


Figure 26. Eh-pH diagram displays predominance fields of arsenic species in spring water of Champagne Pool at a temperature of 75.2° C and a pressure of 101.3 kPa. Dotted lines indicate the stability area of water, where the upper dotted line represents the oxidation line of water and the lower dotted line the reduction line of water, respectively. Stability areas of aqueous arsenic species are displayed in blue-white and of the solid minerals orpiment (As_2S_3), realgar (As_4S_4), and scorodite ($\text{FeAsO}_4 \cdot 2\text{H}_2\text{O}$) in grey, respectively. The black circle indicates pH and Eh values found in Champagne Pool water (CP).

4.5 Discussion

Both archaeal (Figure 23) and bacterial representatives (Figure 24) but no Nanoarchaea were detected in the terrestrial hot spring Champagne Pool. While

culture-independent methods indicate the abundance of strains phylogenetically related to species of the genera *Sulfurihydrogenibium*, *Nevskia*, *Paracoccus*, *Sulfolobus* and *Thermophilum*, pure cultures were isolated from Champagne Pool distantly related to *Sulfurihydrogenibium azorense* (Aguiar *et al.*, 2004), *Thermoanaerobacter tengcongensis* (Xue *et al.*, 2001), and *Thermococcus waiotapuensis* (Gonzalez *et al.*, 1999). Those findings (Table 11) are in agreement with the physiochemical properties of Champagne Pool. Dissolved gases in the spring water contain CO₂, H₂, and O₂ in the shallow areas (Giggenbach *et al.*, 1994; Jones *et al.*, 2001) providing chemolithotrophic conditions for hydrogen-oxidizing microorganisms such as *Sulfurihydrogenibium* species. Available sulfur compounds in Champagne Pool are essential for growth of sulfur-oxidizing (*Sulfolobus* species), sulfur-reducing (*Thermoanaerobacter* and *Thermophilum*), and sulfur-dependent (*Thermococcus* species) microorganisms. The detection of the novel isolates CP.B2 and CP.B3 are in good accordance with results by Richard Pancost (personal communication), where the structural differences of biomembrane lipids on samples from Champagne Pool were investigated (Figure 27). The abundance of archaeol (Figure 27 A), an archaeal biomarker, and non-isoprenoidal ether lipids (Figure 27 B) characteristic for *Aquificales*, *Ammonifex*, and *Thermodesulfobacterium* strains were detected.

Other than *Nevskia* and *Paracoccus*, all detected microbial representatives are thermophilic. However, the low sequence similarities of approximately 91% between the DNA fragment c and *Nevskia ramosa*, and 90% among the cloned bacterial 16S rRNA genes and *Paracoccus thiocyanatus* may indicate that the sequences represent organisms phenotypically different from *Nevskia* and *Paracoccus* strains able to grow under thermophilic conditions. The detection of a *Thermophilum* signature is in agreement with previous reports based on electron microscopy examinations (Jones *et al.*, 2001) and PCR studies (Ellis *et al.*, 2005). However, in microscopic examinations of Champagne Pool water and sediment samples only filamentous, coccoid, and rod structures were present, while “golf club”- and “lobe”-shaped morphologies, distinct characteristics for members of the genera *Thermophilum* and *Sulfolobus*, respectively, could not be observed.

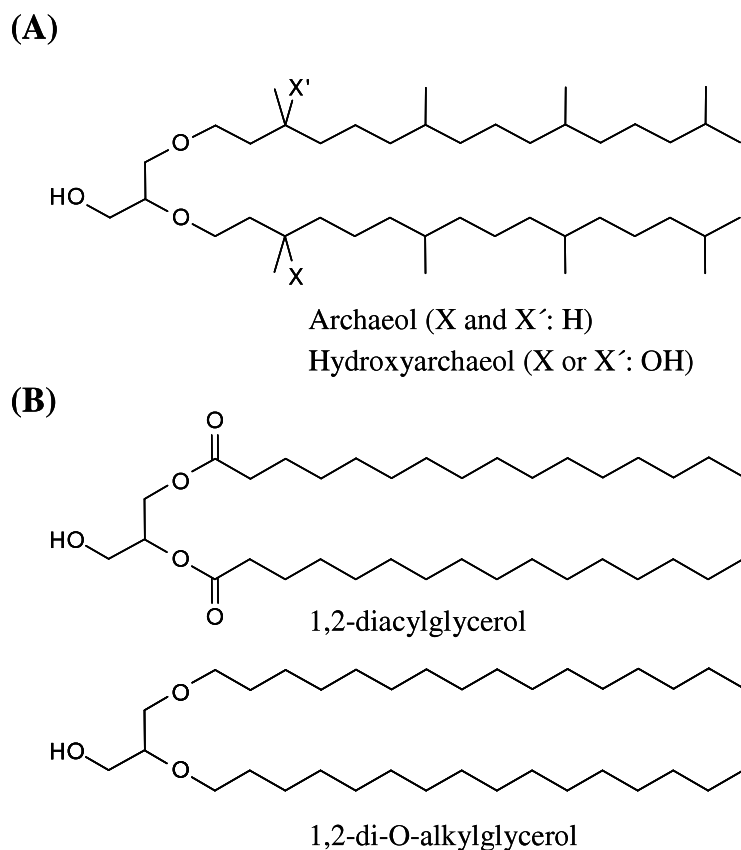


Figure 27. Structures of microbial membrane lipids found in samples obtained from Champagne Pool. (A) Archaeole, (B) bacterial diester and diether lipid structures.

DGGE profiles, nucleic acid yields, cell counts, and ATP measurements indicate low diversity and biomass in Champagne Pool. ATP determinations (Table 10) showed differences between sediment and water samples, with 6x (suspension) and 4x (glass slides) more ATP in the sediment, suggesting an accumulation of biomass within the sediment. However, the highest values obtained for glass slides incubated in Champagne Pool (8,900 RLU) were much lower than reported for other hot springs (>180,000 RLU) in New Zealand (Niederberger, 2005). Those findings are consistent with relatively low cell numbers of $5.6 \pm 0.5 \times 10^6$ cells per ml determined for Champagne Pool water samples by DAPI staining.

This evidence raises the question: what is the limiting factor for microbial diversity and biomass in Champagne Pool besides the thermal conditions in the spring? There may be several factors responsible. Geothermal systems of New Zealand are known to contain high concentrations of metalloids (Hirner *et al.*,

1998). Arsenic ions and compounds are found in Champagne Pool water to a concentration up to 5.6 mg per liter (Giggenbach *et al.*, 1994). Arsenic toxicity is mediated by arsenite reacting with thiol functional groups in enzymes thus inhibiting their activities and by arsenate through substitution of phosphate (Stolz & Oremland, 1999). It has also been shown that trivalent species of arsenic, predominately found in anaerobic environments such as Champagne Pool (Figure 26), were highly inhibitory to methanogenic microorganisms (Sierra-Alvarez *et al.*, 2004). Therefore, only metalloid ion-tolerant or metalloid ion-resistant microorganisms might survive in Champagne Pool. In the present study, culture experiments with *B. caldotenax* in medium supplemented with Champagne Pool water suggest that the spring water might contain volatile compounds toxic to some microorganisms. Possible candidates might be H_2S and toxic volatile methyl and hydride derivatives of arsenic and antimony, such as AsH_3 (arsine), CH_3AsH_2 (monomethylarsine), $(\text{CH}_3)_2\text{AsH}$ (dimethylarsine), $(\text{CH}_3)_3\text{As}$ (trimethylarsine), SbH_3 (stibine), CH_3SbH_2 (monomethylstibine), $(\text{CH}_3)_2\text{SbH}$ (dimethylstibine), and $(\text{CH}_3)_3\text{Sb}$ (trimethylstibine). In Champagne Pool geothermal water concentrations of 4.95 ppm AsH_3 , 1.90 ppb CH_3AsH_2 , 0.10 ppb $(\text{CH}_3)_2\text{AsH}$, 5 ppb SbH_3 , and 0.05 ppb CH_3SbH_2 have been detected (Hirner *et al.*, 1998). Previously published investigations (Jones *et al.*, 1999; Mountain *et al.*, 2003; Phoenix *et al.*, 2005) also considered that microbial cells in Champagne Pool may be subject to biomineralization and bioimmobilisation by rapid silicification and deposition in the sinter.

Champagne Pool seems to be an extreme environment for life forms in terms of its thermal and unique chemical properties. In this study, low microbial diversity and biomass in Champagne Pool and the isolation of three novel strains species was accomplished. The characterization and description of the novel isolates may bring deeper insights into the ecology of the thermal spring.

4.6 Acknowledgements

Research funding was provided by the New Zealand Foundation of Research, Science & Technology (Contract Number C05X0303: Extremophilic Microorganisms for Metal Sequestration from Aqueous Solutions). Special thanks

are due to Richard Fulton for permission to collect samples from Champagne Pool and Helen M. Turner who helped taking SEM micrographs.

Chapter 5: *Venenivibrio stagnispumantis*

***Venenivibrio stagnispumantis* gen. nov., sp. nov., a thermophilic hydrogen-oxidizing bacterium isolated from Champagne Pool, Waiotapu, New Zealand**

(A condensed version of this chapter has been accepted for publication in
International Journal of Systematic and Evolutionary Microbiology)

5.1 Abstract

A novel thermophilic, hydrogen-oxidizing bacterium, designated strain CP.B2^T, was isolated from a terrestrial hot spring in Waiotapu, New Zealand. Cells were motile, slightly rod-shaped, non-spore-forming, and Gram-negative. Isolate CP.B2^T was an obligate chemolithotroph growing by utilizing H₂ as electron donor and O₂ as corresponding electron acceptor. Elemental sulfur (S⁰) or thiosulfate (S₂O₃²⁻) was essential for growth. Microbial growth occurred under microaerophilic conditions in the O₂ range of 1% to 10.0% (v/v) O₂ (optimum 4% to 8% (v/v) O₂), between 45° C and 75° C (optimum 70° C), and at pH values 4.8 to 5.8 (optimum pH 5.4). The G+C content was 29.3 mol%. 16S rRNA gene sequence similarity demonstrated strain CP.B2^T to belong to the order *Aquificales*, with a close phylogenetic relationship to *Sulfurihydrogenibium azorense* (94% sequence identity). However, genotypic and metabolic characteristics differentiated the novel isolate from previously described genera of the *Aquificales*. CP.B2^T therefore represents a novel genus and a new species, for which the name *Venenivibrio stagnispumantis* gen. nov., sp. nov. is proposed. The type strain is CP.B2^T (=JCM 14244^T = DSM 18763^T).

5.2 Introduction

The Taupo Volcanic Zone in New Zealand is the terrestrial extension of the Tonga-Kermadec subduction system (Hedenquist, 1986a) exhibiting geothermal activities such as fumaroles, steaming grounds, mud pools, geysers and hot springs. Within the Taupo Volcanic Zone Champagne Pool is the largest hot spring. It is around 65 m in diameter and is located in a 900 year old hydrothermal

eruption crater (Lloyd, 1959). The name Champagne Pool derives from the constant flow of CO₂ visible as gas bubbles buffering the spring water at a pH value of around pH 5.5. Champagne Pool discharges siliceous geothermal fluid at approximately 75° C, rich in arsenic and antimony (Jones *et al.*, 2001). Although, a few studies (Ellis *et al.*, 2005; Jones *et al.*, 2001; Mountain *et al.*, 2003; Phoenix *et al.*, 2005) have recently described microbial activity in Champagne Pool, the successful isolation of a microorganism has not yet been reported.

Previous investigations (Chapter 4) applying culture-independent approaches, such as Denaturing Gradient Gel Electrophoresis (DGGE) analysis and construction of clone libraries based on the bacterial small-subunit ribosomal nucleic acid (16S rRNA) gene, indicated that hydrogen-oxidizing members of the *Aquificales* order were some of the few dominant microorganisms present in Champagne Pool. These findings are in good agreement with results of phylogenetic studies on five geothermal springs above 70° C in Yellowstone National Park, USA showing hydrogen-metabolizing organisms to dominate these hot spring communities. 77% of all obtained archaeal and bacterial 16S rRNA genes were assigned to species of the order *Aquificales* (Spear *et al.*, 2005). Skirnisdottir and colleagues (2000) reported that 68% of all obtained bacterial 16S rRNA genes obtained from a sulfide-rich hot spring in south-western Iceland belonged to the order *Aquificales*.

The order *Aquificales* comprise currently the genera *Aquifex* (Huber *et al.*, 1992), *Hydrogenivirga* (Nakagawa *et al.*, 2004), *Hydrogenobacter* (Kawasumi *et al.*, 1984), *Hydrogenobaculum* (Stöhr *et al.*, 2001b), and *Thermocrinis* (Huber *et al.*, 1998) of the *Aquificaceae* family; the genera *Hydrogenothermus* (Stöhr *et al.*, 2001b), *Persephonella* (Götz *et al.*, 2002b), *Sulfurihydrogenibium* (Takai *et al.*, 2003a) of the *Hydrogenothermaceae* family, and the genera *Balnearium* (Takai *et al.*, 2003c), *Desulfurobacterium* (L'Haridon *et al.*, 1998), and *Thermovibrio* (Huber *et al.*, 2002a) of the *Desulfurobacteriaceae* family (Euzeby, 1997). Representatives are thermophilic to hyperthermophilic bacteria commonly colonizing geothermally heated environments. Most *Aquificales* have in common the ability to use the Knallgas reaction ($2 \text{ H}_2 + \text{O}_2 \rightarrow 2 \text{ H}_2\text{O}$) to yield energy for biosynthesis, therefore using H₂ as electron donor and O₂ as electron acceptor. On

account of their chemolithotrophic metabolism these organisms are regarded as primary producers of bacterial biomass within high temperature ecosystems (Huber & Eder, 2001).

Although members of the order *Aquificales* are regarded as representing the earliest branching lineage within the phylogenetic domain *Bacteria* based on 16 rRNA gene sequences (Figure 1) (Burggraf *et al.*, 1992; Reysenbach *et al.*, 1994), signature protein sequences (e.g. heat shock protein 60 and 70, alanine-tRNA synthetase, CTP synthase, inorganic pyrophosphatase, and RNA polymerase subunit) support a later divergence of the order and a phylogenetic placing between the δ -/ ϵ -*Proteobacteria* and the *Chlamydiae* groups (Griffiths & Gupta, 2004).

In the present study, the novel thermophilic bacterium CP.B2^T isolated from Champagne Pool is characterized and it is shown that it differs from previously described strains of the order *Aquificales*. *Venenivibrio stagnispumantis* gen. nov., sp. nov. is the proposed name.

5.3 Materials and Methods

5.3.1 Collection of samples

Geothermal fluid (30 cm below spring water surface) and sediment (10 cm below water surface) were sampled in September 2005 at the north-east side of Champagne Pool, Waiotapu (Figure 4, Figure 16) located in the Taupo Volcanic Zone in New Zealand. The samples were collected in sterile 2-liter glass bottles (Schott) carefully avoiding trapping any air. Within two hours samples were transferred into enrichment medium.

5.3.2 Enrichment and isolation

Enrichments were performed in a modified version of MSH medium (4.4.4 Enrichment). The pH value of the medium was adjusted to 5.5. Aliquots of 40 ml and 8 ml were autoclaved under a CO₂ atmosphere in 160 ml serum bottles and 30

ml test tubes, respectively. After inoculation using a 5% inoculum, the initial gas phase was exchanged with 79% H₂/ 16% CO₂/ 5% O₂ at 170 kPa. Enrichment cultures were incubated at 70° C.

The enrichment contained only cells having a slightly curved, rod-shaped morphology. To ensure purity, dilution series were continued over eight 10-fold steps. Cells from the highest dilution step were subsequently inoculated in modified MSH medium solidified by 0.6% (w/v) gel rite gellan gum and 0.06% (w/v) MgSO₄.7H₂O. Individual colonies isolated from the solidified medium were used as inocula for new dilution series. This process was repeated at least twice. The first pure culture was designated as strain CP.B2^T.

5.3.3 Culture conditions

The novel isolate was routinely cultivated in modified MSH medium as described. Microbial growth was determined by measuring changes in turbidity at 450 nm and by direct cell counts using a Thoma counting chamber (depth, 0.02 mm).

The influence of pH on growth was determined at 70° C in the range of 4.5 to 6.5 using 10 mM MES, PIPES, MOPS, and HEPES. The pH value of the medium was checked at the incubation temperature prior to the inoculation and after the growth experiments. NaCl and O₂ requirement and tolerance were determined at 70° C and pH 5.5 in the range of 0% to 2% (w/v) NaCl and 0% to 20% (v/v) O₂, respectively.

The ability of CP.B2^T to metabolize different substrates was investigated using a basal MSH medium without Na₂S₂O₃.5H₂O and with only 4.00 g of MgSO₄.7H₂O to provide a sulfur source for assimilation. The basal medium was supplemented with either 80% (v/v) H₂, 10 mM Na₂S₂O₃, or 1% (w/v) S⁰ as electron donor and either 10 mM NaNO₂, 10 mM NaNO₃, 10 mM Na₂SO₃, 10 mM Na₂SO₄, 5 mM Na₂SeO₃, 5 mM Na₂SeO₄, 5 mM NaAsO₂, 5 mM Na₂HAsO₄, or O₂ as complementary electron acceptor. Further experiments were performed using 1 mM and 5 mM Na₂HAsO₄ and NaAsO₂ as electron acceptor and donor, respectively. As carbon source either casamino acids, sodium pyruvate, starch,

trypticase peptone, yeast extract (final concentration 0.2% (w/v)), or CO₂ were provided (Appendix F: Table 26).

In toxicity experiments, the novel bacterium was tested for tolerance to elevated arsenic and antimony ion levels. Modified MSH medium supplemented with defined concentrations of Na₂HAsO₄·7H₂O, NaAsO₂, and KSbOC₄H₄O₆·0.5H₂O was inoculated using a 2.5% inoculum of a fresh grown culture. The MIC was defined as the absence of growth of the species in 30 ml test tubes after 7 days.

Spectrophotometric determination of H₂S (Cline, 1969; Gilboa-Garber, 1971) after 24 h and 48 h growth was performed. A 100 µl aliquot of cell suspension was transferred to 500 µl 4% (w/v) zinc acetate solution (per liter: 40.0 g of Zn(C₂H₃O₂)₂·2H₂O and 20.0 ml acetic acid glacial) and then 100 µl 0.4% (w/v) N,N-dimethyl-p-phenylenediamine dichloride solution (per liter: 4.0 g of N,N-dimethyl-p-phenylenediamine dichloride and 400 ml H₂SO₄) and 100 µl 2% (w/v) ammonium iron sulfate solution (per liter: 20.0 g of NH₄Fe(SO₄)₂·12H₂O) were added. After incubation in the dark for 25 min, the absorbance of the sample at 670 nm was spectrophotometrically determined. Sulfide is initially fixed with zinc solution and reacts with N,N-dimethyl-p-phenylenediamine to colorless leucomethylene blue, which then in the presence of Fe³⁺ is oxidized to methylene blue. Methylene blue shows maximum absorbance at 670 nm.

5.3.4 Light and electron microscopy

Cells were routinely examined under a phase-contrast microscope (Olympus BH-2) equipped with a digital camera (Nikon Coolpix 4500). Gram-staining was carried out using standard methods (Hucker & Conn, 1927) with *Escherichia coli* cells (strain JM109) as a control. Cells were heat-fixed onto a microscope glass slide and then flooded with filtered crystal violet solution (per liter: 20.0 g of crystal violet, 200 ml 95% ethanol, 8.0 g of ammonium oxalate) for 30 s. Then the glass slide was rinsed gently with running water and covered with fresh iodine solution (per liter: 3.3 g of iodine crystals, 6.6 g of potassium iodine) for 30 s. The sample was rinsed with 96% ethanol until run-off became clear but not for more than 10 s to ensure Gram-positive cells were not decolorized. Ethanol is used to

remove the crystal violet-iodine complex from Gram-negative cells by dissolving lipids incorporated into the outer membrane, whereas the multi-layered peptidoglycan of Gram-positive cells is dehydrated by ethanol and the violet stain is retained due to closure of the pores as the cells shrink. Thus, Gram-positive cells appear violet. To further differentiate Gram-positive and Gram-negative cells samples were counterstained with the dye carbol fuchsin (per liter: 1.0 g of basic fuchsin, 5.0 g of phenol, 10 ml of 90% ethanol) staining Gram-negative cells red.

For scanning electron microscopy (SEM), cells were captured onto a 0.22 μm filter by filtration and fixed using 2.5% glutaraldehyde. The filter was exposed to four changes of 0.1 M sodium cacodylate buffer, rinsed in water and dehydrated in increasing concentrations of ethanol, 50%, 75%, and 90%, respectively, then four changes of absolute ethanol. The filter was critical point dried, sputtered with platinum, and viewed using a Hitachi S-4100 field emission SEM.

5.3.5 DNA isolation and base composition

Genomic DNA of CP.B2^T was isolated using a modification of the CTAB method described previously (Dempster *et al.*, 1999). A 40 ml bacterial suspension was harvested by centrifugation at 1,850 \times g (JouanCR4.11) for 10 min. The cell pellet was resuspended in 1 ml of CTAB buffer (100 mM Tris-HCl, 1.4 M NaCl, 20 mM EDTA, 2% (w/v) cetyltrimethylammoniumbromide (CTAB), 1% (w/v) polyvinylpyrrolidone (PVP) (360,000; pH 8.0) and freshly prepared 0.4% (w/v) 2-mercaptoethanol. The mixture was incubated at 100° C for 20 min followed by extractions with an equal volume of phenol and then with chloroform-isoamyl alcohol (24:1 by volume). Nucleic acids were precipitated with an equal volume of isopropanol and 0.1 volume of 3 M sodium acetate (pH 5.5) at -20° C overnight, then washed twice in 70% ethanol and air-dried.

The G+C content of the DNA was determined by the Identification Service of the German Collection of Microorganisms (Deutsche Sammlung von Mikroorganismen und Zellkulturen, Braunschweig, Germany) according to the method of Mesbah (1989).

5.3.6 PCR amplification and sequencing

PCR amplification of the 16S rRNA gene sequence between the corresponding *E. coli* position 9 and 1522 was performed using a forward primer 5'- AGA GTT TGA TCC TGG CTC AG -3' and a reverse primer 5'- AAG GAG GTG ATC CAR CCG CA -3' (Johnson, 1994). PCR mixtures consisted of PCR buffer (10 mM Tris-HCl, 50 mM KCl, pH 8.3), 1.5 mM MgCl₂, 0.2 mM dNTP (dATP, dCTP, dGTP, dTTP), 1.0 µM of each amplification primer, 5.0% (w/v) dimethyl sulfoxide (DMSO) and 1.0 unit of *Taq* polymerase (Roche). The following PCR conditions were applied: an initial denaturation step at 94° C for 210 s, two cycles annealing at 50° C for 30 s, extension at 72° C for 120 s and denaturation at 94° C for 30 s, followed by 31 cycles applying an annealing temperature of 48° C for 120 s. The final extension step was 300 s.

PCR products purified by agarose gel electrophoresis were used in cloning experiments applying the pGEM-T Easy vector system (Promega) as recommended by the manufacturer (4.3.3 PCR amplification of 16S rRNA gene and gene cloning experiments). DNA sequencing of the cloned inserts was undertaken by the Waikato DNA Sequencing Facility based at the University of Waikato in Hamilton, New Zealand using the MegaBACE capillary analysis system (Amersham Biosciences). Sequences of the inserts were obtained by using primer set M13pUC forward 5'- CCC AGT CAC GAC GTT GTA AAA CG -3' and M13pUC reverse 5'- AGC GGA TAA CAA TTT CAC ACA GG -3'. Sequences were checked by the Chimera Detection computer program (Cole *et al.*, 2003) of the Ribosomal Database Project II to identify the presence of possible chimeric artefacts (<http://rdp8.cme.msu.edu/cgis/chimera.cgi>).

PCR experiments were carried out targeting the DNA polymerase I (PolA) gene distinctive of species from the *Aquificales* order using forward primer 5'- ASA YCC WAA TWT VCA RAA YAT HC -3' and reverse primer 5'- CCC GTN CCY TGW ATN GGR TAR TT -3' (Griffiths & Gupta, 2006). DNA isolated from *Sulfurihydrogenibium azorense*, a member of the *Aquificales* order, acted as a control.

To determine, if *ars* genes were present in CP.B2^T and contribute to arsenic resistance, a nested PCR approach was employed to amplify *arsA*, *arsB*, and *arsC*, according to Ford and colleagues (2005). Conditions for PCR reactions using outer primers following PCR using inner primers (Table 13) were an initial denaturation step at 94° C for 300 s, 30 cycles annealing at 50° C for 60 s, extension at 72° C for 60 s, and denaturation at 94° C for 60 s, followed by a final extension step for 600 s.

Table 13. Target and sequences of oligonucleotide primers used in PCR studies. Abbreviations: OF, outer forward primer; OR, outer reverse primer; IF, inner forward primer; IR, inner reverse primer.

Primer	Target	Oligonucleotide primer sequence (5' → 3') ^a
<i>arsA</i> OF	ATPase	TATTTCTGCGCCACGGCGAT
<i>arsA</i> OR	ATPase	GAAGGCGAATGGTGTGAC
<i>arsA</i> IF	ATPase	CTGCTGGTCAGTACCGAT
<i>arsA</i> IR	ATPase	GATATGGTCAAACGTCAG
<i>arsB</i> OF	Arsenite efflux pump	CCGGTGGTGTGGAATATTGT
<i>arsB</i> OR	Arsenite efflux pump	ACTCCGTGAATCCCAGTT
<i>arsB</i> IF	Arsenite efflux pump	GTTGCTGGATGAGTCAGGCT
<i>arsB</i> IR	Arsenite efflux pump	GTATCGGAAATACCGGC
<i>arsC</i> OF	Arsenate reductase	CTGATATGAGCAACATCACTATTT
<i>arsC</i> OR	Arsenate reductase	ATTCAGCCGTTTTCTGCTTCA
<i>arsC</i> IF	Arsenate reductase	ATCATAACCCAGCCTGC
<i>arsC</i> IR	Arsenate reductase	CTGCGCATCCTGTAGGATARC

^a Primer sequence according to Ford *et al.*, 2005.

Randomly amplified polymorphic DNA (RAPD) testing was undertaken on DNA extracted from the CP.B2^T isolate and *S. azurensis* to determine the similarity using primer OPR13 5'- GGA CGA CAA G -3' (Williams *et al.*, 1990). After an initial denaturation step at 94° C for 90 s, 42 cycles of annealing at 36° C for 30 s, extension at 72° C for 120 s and denaturation at 94° C for 30 s, and a final extension step for 240 s were applied.

5.3.7 Phylogenetic analyses

The computer algorithm Basic Local Alignment Search Tool (BLAST) (Altschul *et al.*, 1997) was used to search the sequence database of the National Center for Biotechnology Information (NCBI, <http://www.ncbi.nlm.nih.gov>) for 16S rRNA gene sequence similarities. Phylogenetic analysis and alignment of 16S rRNA gene sequences was performed using the ARB software package (Ludwig *et al.*, 2004). The phylogenetic position of the sequences were determined using the PHYLIP package with analysis of sequences undertaken using DNADIST, DNAML, DNAPARS, FITCH, NEIGHBOR, and SEQBOOT programs (Felsenstein, 1993).

5.4 Results

5.4.1 Isolation

To enrich for hydrogen-oxidizing thermophilic microorganisms, 40 ml modified MSH medium was inoculated with 2 ml Champagne pool spring water and a gas atmosphere of 79% H₂/ 16% CO₂/ 5% O₂ pressurized to 170 kPa. After two days incubation at 70° C without agitation the medium became turbid due to microbial growth. Serial dilution series on solidified medium led to the isolation of CP.B2^T. The purity of the novel isolate was routinely checked by microscopy and sequence analysis of the 16S rRNA gene.

5.4.2 Morphology

Cells of isolate CP.B2^T appeared to have a slightly curved, rod-shaped morphology (Figure 28 b–d), with a mean length of $1.30 \pm 0.26 \mu\text{m}$ and a mean width of $0.37 \pm 0.04 \mu\text{m}$. The cells were motile and stained Gram-negative. Sporulation could not be observed during growth, in 6 months-old cultures, or at temperatures above the maximum growth temperature. The bacterial cells occurred predominate singly or in pairs. Large cell aggregates were formed in the late-stationary growth phase, macroscopically visible as whitish flocks (Figure 28 a).

5.4.3 Physiological characteristics

Strain CP.B2^T was able to grow between 45° C and 75° C with an optimum of around 70° C, whereas growth below 40° C and above 80° C was not observed even after one-week incubation. The pH range for growth was 4.8 to 5.8 with an optimum around 5.4. CP.B2^T grew without NaCl and NaCl concentration up to 0.8% (w/v) with an optimum of 0.4% (w/v) NaCl. Growth occurred only under microaerophilic conditions in the O₂ range of 1% to 10.0% (v/v) with an optimum of approximately 4% to 8% (v/v) O₂.

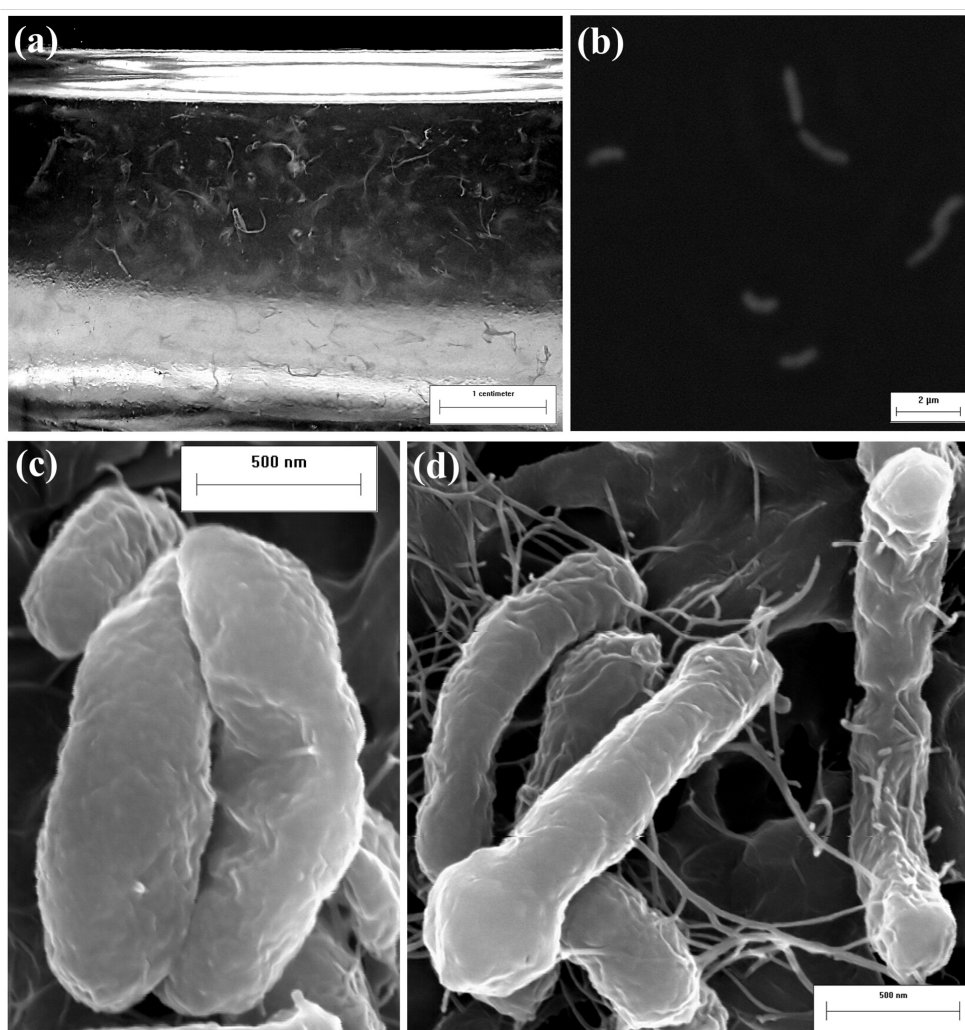


Figure 28. Macroscopic (a), phase-contrast, (b) and scanning electron (c-d) micrographs of isolate CP.B2^T. (a) Large cell aggregates were formed after two days incubation in serum bottles. Bar 1 cm. (b) Cells predominately occurred as single cells or in pairs. Bar 2 μm. (c-d) Electron micrographs showing vibrio (c) and biofilm-like (d) structures. Bars 500 nm.

5.4.4 Metabolic characteristics

Isolate CP.B2^T grew chemolithotrophically under microaerobic conditions utilizing H₂, sulfur compounds, and CO₂ as sole carbon source up to maximum concentration of 10⁹ cells per ml (Figure 29), with a doubling time of 230 min (Figure 30). H₂ could not be replaced by other electron donors such as S⁰ and S₂O₃²⁻ under anaerobic (either 100% N₂ supplemented with organic substrates or 80% N₂/ 20% CO₂) or microaerobic (either 94% N₂/ 6% O₂ with organic carbon sources or 79% N₂/ 16% CO₂/ 5% O₂) conditions as energy source. However, growth of CP.B2^T was dependent on either S⁰ or S₂O₃²⁻ in the medium. Reduction of the sulfur compounds could not be detected in significant quantities (< 9 µM sulfide in comparison to > 4 mM sulfide obtained for CP.B1 cultures) indicating that S⁰ and S₂O₃²⁻ were not involved in dissimilative metabolism. The strain was not capable of using any of the nine tested electron acceptors in sulfur-limited basal MSH medium providing around 16 mM SO₄²⁻ for assimilation. None of the tested organic compounds was utilized (Appendix F: Table 26). In all growth experiments, *S. azorensis* cultures were used as control to verify that all solutions and methods were working correctly.

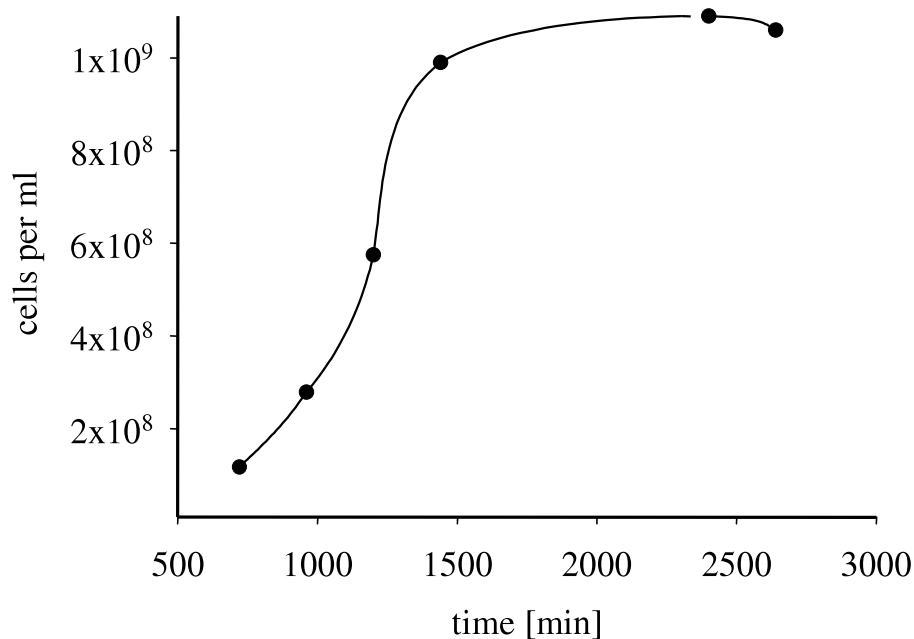


Figure 29. Growth curve observed for CP.B2^T cells.

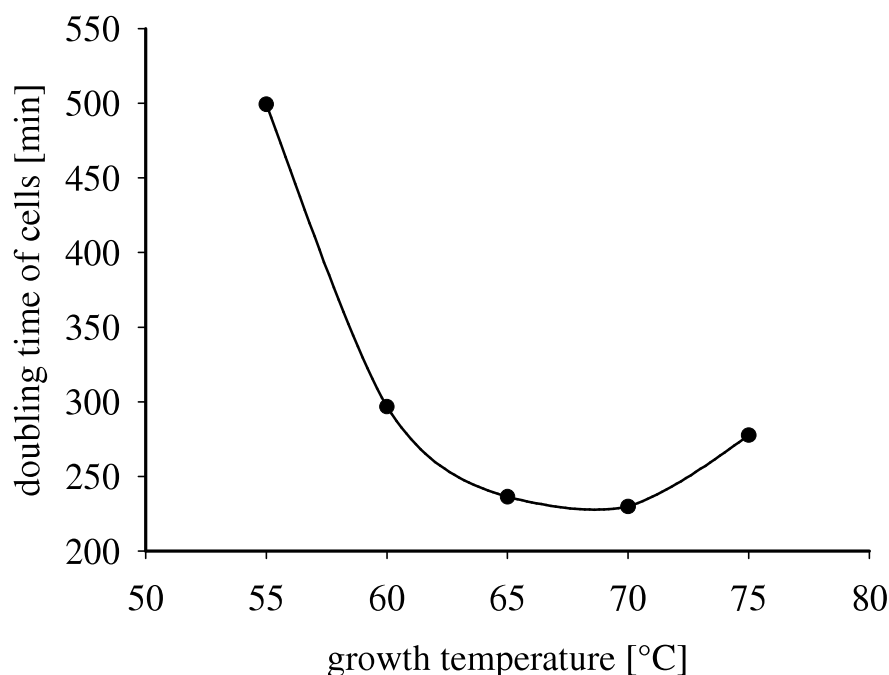


Figure 30. Effect of temperature on the growth of CP.B2^T cells. Doubling times were calculated from the slopes of the corresponding growth curves after 21 hours incubation. Microbial growth at 45° C and 50° C was only observed after one week.

5.4.5 Arsenic and antimony ion susceptibility tests

The novel strain was tested for tolerance to elevated arsenic and antimony ion levels. The isolate displayed growth in the presence of up to 8 mM NaAsO₂ and 15 mM KSbOC₄H₄O₆·0.5H₂O, respectively, and in the presence of more than 20 mM Na₂HAsO₄·7H₂O. However, growth was not observed when NaAsO₂ and Na₂HAsO₄ were provided as the sole electron donor and acceptor pair.

Amplification of the genes *arsA* and *arsB* were positive for the isolates CP.B2^T and CP.B3, whereas no amplification in CP.B2^T and non-specific amplification in CP.B3 occurred using the *arsC* primers (Figure 31). None of the studied *ars* genes could be detected in CP.B1 by PCR. The result obtained for CP.B1 either indicates that genes confer arsenic resistance, which have different sequences from those *ars* genes, which have been described to date, or that another mechanisms as described in Chapter 1 might be responsible for arsenic resistance and tolerance. However, in initial arsenic ion susceptibility assays no growth was

observed for CP.B1 cells in the presence of 500 μM NaAsO_2 and $\text{Na}_2\text{HAsO}_4 \cdot 7\text{H}_2\text{O}$ reflecting that the absence of an efflux system might be responsible for the observed sensitivity to arsenic species.

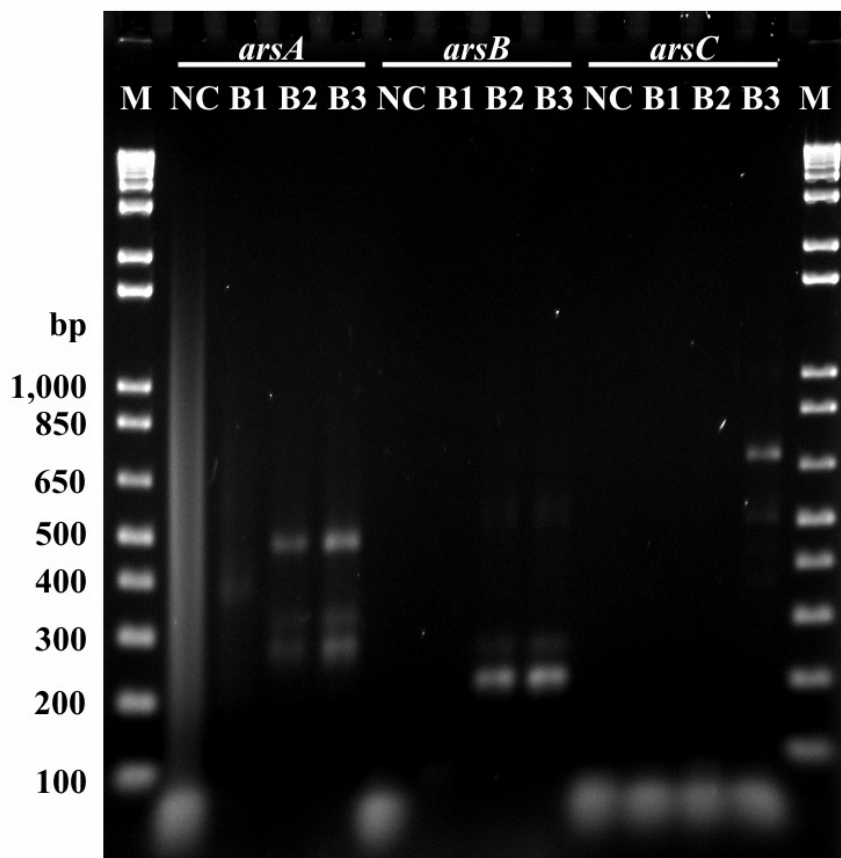
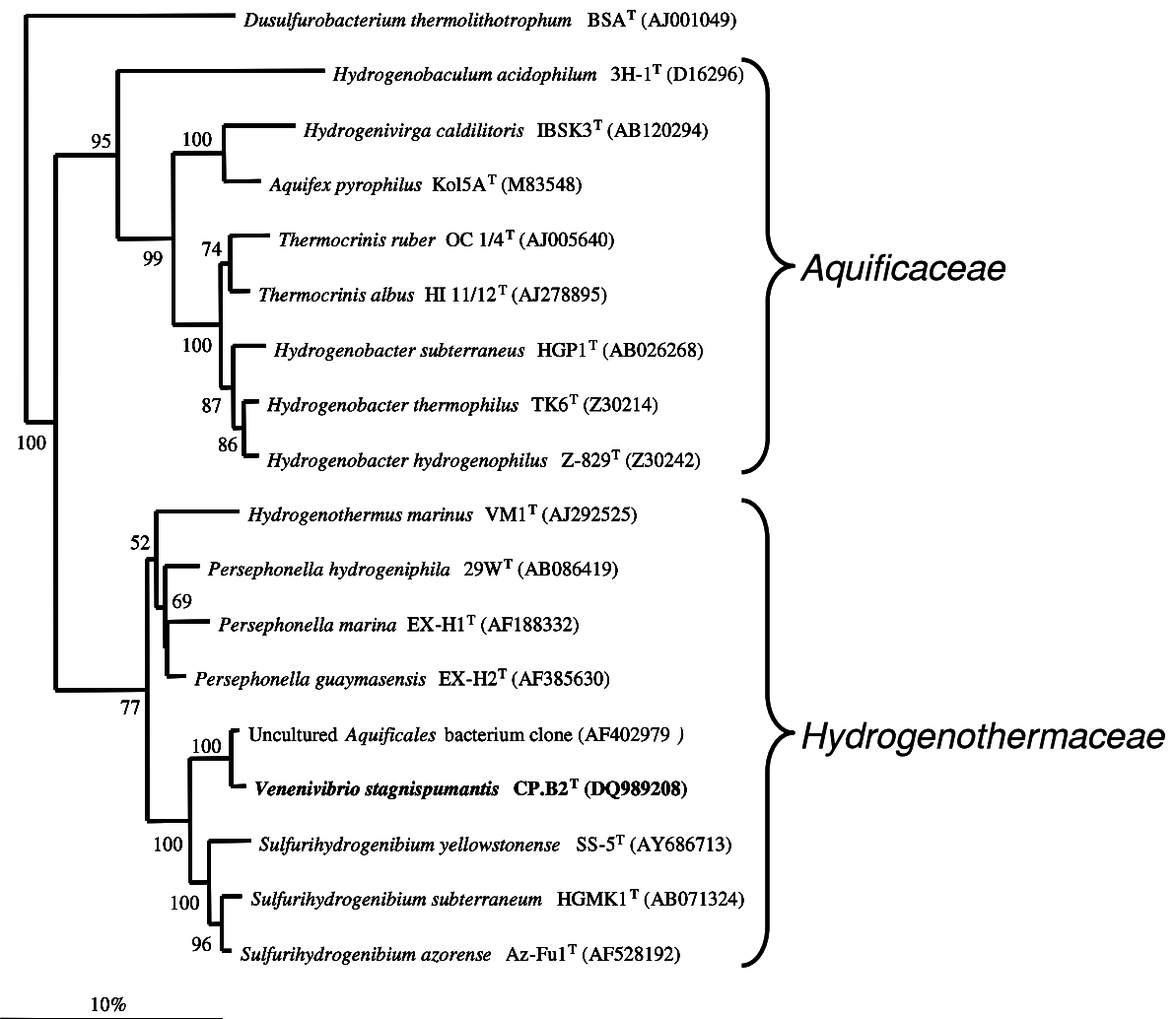


Figure 31. Image of ethidium bromide-stained 1.75% agarose gels displaying *ars* gene fragments from CP.B1, CP.B2^T and CP.B3. Abbreviations: M, 1 Kb Plus DNA ladder (Invitrogen); NC, negative control; B1, CP.B1; B2, CP.B2; and B3, CP.B3. Expected amplicon sizes were 300 bp (*arsA*), 259 bp (*arsB*), and 341 (*arsC*).

5.4.6 Genotypic characteristics

The G+C content of DNA isolated from strain CP.B2^T was 29.3 mol%. The amplified 16S rRNA gene sequence for CP.B2^T consisting of 1506 bases had a G+C content of 57.5 mol%.



Phylogenetic analysis based on 16S rRNA gene sequence indicates that CP.B2^T is closely related to previously described species of the order *Aquificales* (Figure 32). This evidence was supported by amplification of the DNA polymerase I (PolA) gene distinctive of members of the *Aquificales* by PCR (Figure 33 A). Within the order *Aquificales*, CP.B2^T displayed the greatest 16S rRNA gene

sequence similarity (94%) with *S. azorensis* (Aguiar *et al.*, 2004). However, RAPD profiles generated for both of the related strains were able to differentiate among the species (Figure 33 B). The results presented indicate that CP.B2^T represents a novel genus within the *Aquificales* order.

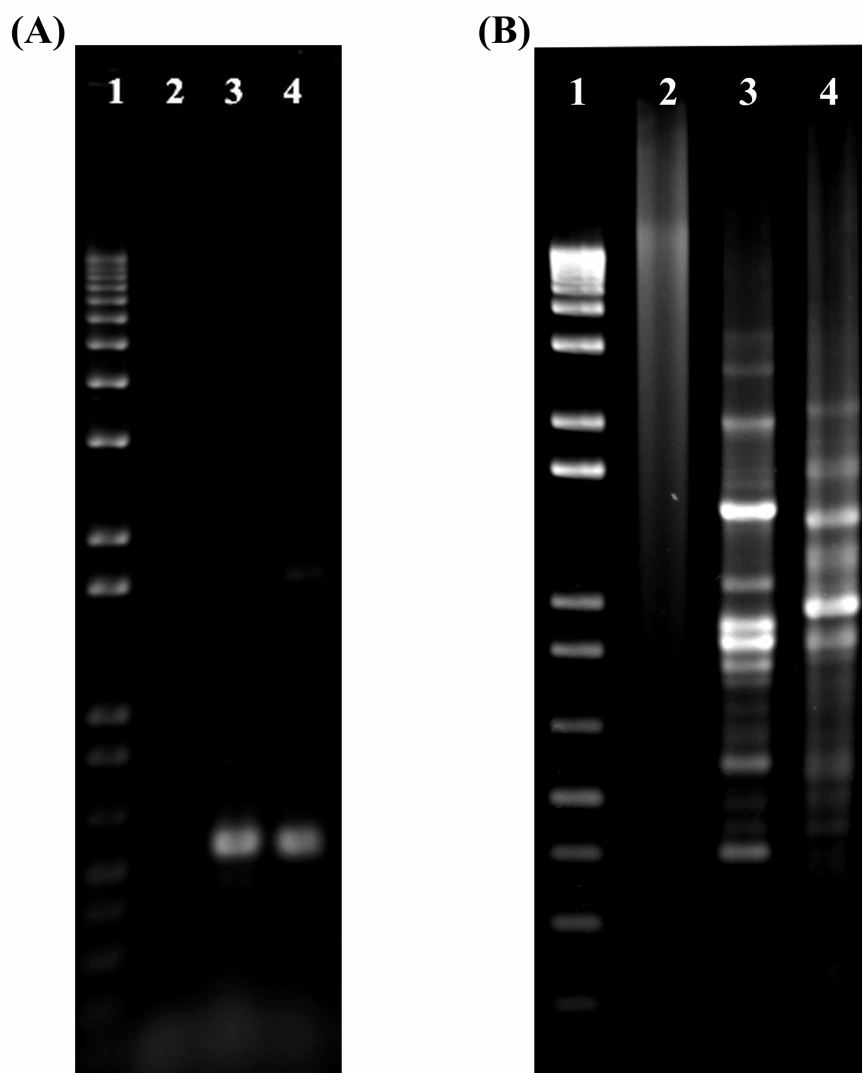


Figure 33. Image of ethidium bromide-stained 1.5% agarose gels. (A) displays the 500 bp gene fragment of *polA* amplified from CP.B2^T and *S. azorensis*. Lanes: 1, 1 Kb Plus DNA ladder (Invitrogen); 2, negative control; 3, CP.B2^T; 4, *S. azorensis* as positive control. (B) RAPD profiles generated from genomic DNA of CP.B2^T and *S. azorensis* cells using primer OPR13. Lanes: 1, 1 Kb Plus DNA ladder; 2, negative control; 3, CP.B2^T; 4, *S. azorensis*.

5.5 Discussion and proposal of a novel genus

A novel thermophilic bacterium was isolated from the geothermal Champagne Pool in Waiotapu, New Zealand. The new isolate CP.B2^T grew chemolithotrophically under microaerophilic conditions with H₂ as electron donor and O₂ as electron acceptor. Sulfur compounds, such as S⁰ or S₂O₃²⁻, were required for growth. Because of its 16S rRNA gene sequence and the molecular signature of the DNA polymerase I, the isolate belongs to the *Aquificales* order.

Phylogenetic analysis based on 16S rRNA gene sequences (Figure 32) indicates that it is closely related to the genus *Sulfurihydrogenibium*. However, the new isolate differs markedly in genotypic and metabolic properties from members of the genus *Sulfurihydrogenibium* and other genera of the order *Aquificales*. Although the physiological properties of the novel isolate largely resemble those of the genus *Sulfurihydrogenibium* (Table 14), the pH range is slightly limited and the optimal pH value is lower. This might be explained due to adaptation to its environment. Champagne Pool spring water is buffered by a constant flow of CO₂ keeping the pH value stable at around pH 5.5.

The low G+C content distinguishes it from previously described species of the genera *Sulfurihydrogenibium*, *Persephonella*, and *Hydrogenothermus*. This is the lowest G+C content reported for a species belonging to the *Aquificales* order. Strain CP.B2^T grew chemolithotrophically under microaerobic conditions utilizing H₂ as electron donor, O₂ as electron acceptor, and CO₂ as carbon source. Growth was dependent on S⁰ or S₂O₃²⁻, but no growth occurred when the sulfur compounds replaced H₂ as potential electron donor or O₂ as potential electron acceptor. *Sulfurihydrogenibium* species (Aguiar *et al.*, 2004; Nakagawa *et al.*, 2005; Takai *et al.*, 2003b), *Persephonella marina* and *P. guaymasensis* (Götz *et al.*, 2002a) are able to use sulfur compounds either as electron donors or acceptors. The hydrogen-oxidizing bacterium *H. marinus* requires elemental sulfur for growth for biosynthesis of sulfur-containing compounds (Stöhr *et al.*, 2001a), but like CP.B2^T cannot use it as potential electron donor. However, *H. marinus* can be clearly separated from CP.B2^T. As the name indicates, *H. marinus* is of marine origin, therefore adapted to higher NaCl concentrations (Table 14).

The novel isolate displayed tolerance to relatively high concentrations of arsenic and antimony compounds. CP.B2 cells grew in the presence of up to 8 mM NaAsO₂, 15 mM KSbOC₄H₄O₆.0.5H₂O and more than 20 mM Na₂HAsO₄.7H₂O. Those concentrations are considerably higher compared to levels found in Champagne Pool spring water but lower compared to levels found in the sediment (Jones *et al.*, 2001): 5.3 ppm (70 µM) As and 3.5 ppb (29 nM) Sb in the pool water and 16,700 ppm (223 mM) As and 15,600 ppm Sb (128 mM) in the orange sediment. PCR studies revealed the presence of *arsA* and *arsB* genes in CP.B2^T (Figure 31) suggesting arsenic resistance was determined by an energy-dependent efflux system mediated by an ATPase.

The occurrence of the novel isolate might not be limited to Champagne Pool in Waiotapu. A 16S rRNA gene sequence identity of 98% was obtained between CP.B2^T and a 16S rRNA gene clone (AF402979) amplified from an environmental DNA sample. The DNA sample was extracted from a hot spring in Rotorua, New Zealand (Sunna & Bergquist, 2003). Rotorua and Waiotapu are both located in the geothermally active Taupo Volcanic Zone indicating that CP.B2^T and close relatives might be distributed within this zone. Water samples obtained from a hot spring on Fountain Flat (N 44° 33.671, W 110° 49.989) in Yellowstone National Park, USA, featuring similar chemophysical properties (75 °C, pH 6.2) as Champagne Pool were used for enrichment experiments in modified MSH medium. The enrichment cultures had different morphological characteristics compared to CP.B2^T cells indicating that CP.B2^T was not present. However, it cannot be ruled out that the novel isolate might be abundant outside New Zealand.

Taken together, the results indicate that CP.B2^T represents a novel genus within the *Aquificales* order, for which the name *Venenivibrio stagnispumantis* gen. nov., sp. nov. is proposed.

Table 14. Comparison of properties of *Venenivibrio stagnispumantis* gen. nov., sp. nov. CP.B2^T with the related species *Sulfurihydrogenibium yellowstonense* (Nakagawa *et al.*, 2005), *S. azorense* (Aguiar *et al.*, 2004), *S. subterraneum* (Takai *et al.*, 2003b), *Persephonella guaymasensis* (Götz *et al.*, 2002a), and *Hydrogenothermus marinus* (Stöhr *et al.*, 2001a). In brackets are the optimal growth conditions.

Strain	<i>Venenivibrio stagnispumantis</i>	<i>Sulfurihydrogenibium yellowstonense</i>	<i>Sulfurihydrogenibium azorense</i>	<i>Sulfurihydrogenibium subterraneum</i>	<i>Persephonella guaymasensis</i>	<i>Hydrogenothermus marinus</i>
Source	Terrestrial hot spring	Terrestrial hot spring	Terrestrial hot spring	Subsurface gold mine	Hydrothermal vent	Hydrothermal area
T [° C]	45-75 (70)	55-78 (70)	50-73 (68)	40-70 (65)	60-80 (75)	45-80 (65)
pH	4.80-5.8 (5.4)	6.0-8.0 (7.5)	5.5-7.0 (6.0)	6.4-8.8 (7.5)	4.7-7.5 (6.0)	5.0-7.0
NaCl [% (w/v)]	0.0-0.8 (0.4)	0.0-0.6 (0.0)	0.0-0.25 (0.1)	0.0-4.8 (0.5)	1.0-4.5 (2.5)	0.5-6.0 (2-3)
Electron donor	H ₂	S ⁰ , S ₂ O ₃ ²⁻	H ₂ , S ⁰ , S ₂ O ₃ ²⁻ , SO ₃ ²⁻ , Fe ²⁺ , AsO ₃ ³⁻	H ₂ , S ⁰ , S ₂ O ₃ ²⁻	H ₂ , S ⁰ , S ₂ O ₃ ²⁻	H ₂
Electron acceptor	O ₂ (up to 10%),	O ₂ (up to 18%)	O ₂ (up to 9%), S ⁰ , SO ₃ ²⁻ , Fe ³⁺ , SeO ₄ ²⁻ , AsO ₄ ³⁻	O ₂ , NO ³⁻ , Fe ³⁺ , SeO ₃ ²⁻ , SeO ₄ ²⁻ , AsO ₄ ³⁻	O ₂ (up to 11%), NO ₃ ⁻	O ₂ (up to 8%)
G+C content [mol%]	29.3	32	33.6	31.3	37.4	43

5.5.1 Description of the genus *Venenivibrio* gen. nov.

Venenivibrio (Ve.ne.ni.vi'bri.o. L. neut. n. venenum, poison; N.L. masc. n. vibrio, that which vibrates; N.L. masc. n. Venenivibrio, the vibrio of poison).

Cells are slightly curved rods, motile and stain Gram-negative. No sporulation. Microaerophilic. Thermophilic. Strictly chemolithotrophic. Able to utilize molecular hydrogen as electron donor and oxygen as electron acceptor. Either elemental sulfur or thiosulfate is essential growth requirements. NaCl is not required for growth. G+C content of genomic DNA is around 29 mol%. On the basis of 16S rRNA gene sequence analysis the genus *Venenivibrio* is closely related to the genus *Sulfurihydrogenibium*. Species of the genus *Venenivibrio* occur in terrestrial geothermally heated freshwater systems.

The type species is *Venenivibrio stagnispumantis*.

5.5.2 Description of the species *Venenivibrio stagnispumantis* sp. nov.

Venenivibrio stagnispumantis (stag.ni.spu.man'tis. L. neut. n. stagnum, pool, L. pres. gen. part. spumantis of the bubbling one, N.L. stagnispumantis from the bubbling pool, referring to Champagne Pool).

Exhibits the following properties in addition to those described for the genus. Strain was isolated from the terrestrial hot spring, Champagne Pool, in Waiotapu, New Zealand. Slightly curved rods with a mean length of $1.30 \pm 0.26 \mu\text{m}$ and a mean width of $0.37 \pm 0.04 \mu\text{m}$. Temperature range for growth is 45° C to 75° C with an optimum of 70° C. pH range is 4.8 to 5.8 with an optimum of 5.4. Sodium chloride concentration range is 0% (w/v) to 0.8% (w/v) and is not required for growth, optimum growth occurs at 0.4% (w/v). Tolerates oxygen in the range of 1% to 10% (v/v) and is essential for growth. The base composition of genomic DNA is 29.3 G+C mol%. The 16S rRNA gene exhibits 94% similarity to the sequence from *S. azorense*.

The type strain is CP.B2^T and has been deposited in the Japan Collection of

Microorganisms (JCM) and the German Collection of Microorganisms (DSM) under accession numbers JCM 14244^T and DSM 18763^T, respectively.

5.6 Acknowledgements

Research funding was provided by the New Zealand Foundation of Research, Science & Technology (Contract Number C05X0303: Extremophilic Microorganisms for Metal Sequestration from Aqueous Solutions). Special thanks to Richard Fulton for permission to take spring water and sediment samples from Champagne Pool, to Helen M. Turner for the electron microscopy preparation, to Anna-Louise Reysenbach for providing samples of *S. azorensis* and to Craig Cary for spring water samples obtained from Yellowstone National Park (Permit issued by the National Park Service with support from the National Geographic Society). The help of Hans G. Trüper with naming the novel isolate is greatly appreciated.

Chapter 6: General discussion

Results of this study sought to provide insights into how thermophilic bacteria interact with metal and metalloid ions and to characterize microbial communities in a terrestrial hot spring rich in arsenic ions and compounds.

Initial cadmium ion susceptibility experiments determining minimal inhibition concentrations (MIC) for 46 thermophilic bacterial and archaeal representatives of to the genera *Aneurinibacillus*, *Anoxybacillus*, *Bacillus*, *Brevibacillus*, *Geobacillus*, and *Thermus* revealed relatively high MIC values for members of the genus *Geobacillus* and two different patterns of growth responses depending on the *Geobacillus* strain (Chapter 2). An increasing concentration of Cd^{2+} resulted either in a decrease of the maximum optical density (e.g. *G. thermocatenulatus*) or alternatively, in a delay of the onset of growth (e.g. *G. stearothermophilus*). *G. stearothermophilus* and *G. thermocatenulatus* displaying the same MIC value of 600 μM Cd^{2+} , but having different growth responses in the presence of Cd^{2+} , showed similar results in subsequent surface complexation models (SCMs) experiments. However, the variations in model parameters were too small to relate the different growth pattern observed at elevated concentrations of Cd^{2+} to different biosorption behaviors.

Experimental data from electrophoretic mobility, acid-base titration, and cadmium ion adsorption experiments obtained for the thermophilic bacteria *G. stearothermophilus* and *G. thermocatenulatus* were used to quantify the concentrations and deprotonation constants of binding sites and to determine the thermodynamic stability constants for the metal ion-bacteria complexes (Chapter 3). The developed SCMs incorporating the Donnan electrostatic model, which considers the cell wall as an ion-penetrable volume, whereas other electrostatic models only account for ion-impenetrable planar surfaces, predicted successfully proton and cadmium ion biosorption for *G. stearothermophilus* and *G. thermocatenulatus* as a function of pH and different bacteria-to-metal ion concentration ratios, which is a prerequisite for potential bioremediation

applications. In comparison to recently reported SCMs parameters obtained for mesophilic bacteria (Borrok *et al.*, 2004a; Borrok & Fein, 2005; Daughney & Fein, 1998; Daughney *et al.*, 2001; Yee & Fein, 2001), the results indicate different binding capacities for cadmium ions for both studied thermophilic *Geobacillus* strains. The developed SCMs implied cation complexation reactions dominantly occurring at one type of functional group with a deprotonation constants pK value of approximately 3.8. Consequently, it has been demonstrated that discrete one-binding site models could fully interpret the analytical data, which were in contrast to multi-binding models obtained for mesophilic species that have been studied to date.

Microbial biosorption influences the distribution and availability of metal ions in some natural and anthropogenic environments and might have potential to be utilized in waste management of metal- and metalloid-polluted water and soil. A better understanding of metal mobilization and demobilization in thermal settings must rely on more studies of metal ion surface complexation by bacterial and archaeal thermophiles in order to extend the knowledge that is solely based on SCMs obtained from mesophilic bacteria. It would be interesting to investigate if more thermophilic bacterial strains than the two studied *Geobacillus* strains differ from the generalized multi-site adsorption model which was proposed for mesophilic bacteria (Borrok *et al.*, 2005; Yee & Fein, 2001). Microorganisms which predominantly complex metal or metalloid ions at one binding site would be favored in potential bioremediation applications since for adsorption and desorption reactions less acid and base might be used, and therefore the process would be more time- and cost-effective. For large-scale applications microorganisms, which act as biosorbent, should permit simple cultivation in inexpensive available medium compounds, e.g. industrial waste products such as yeast, a by-product from fermentation processes.

Surveys of Champagne Pool, one of New Zealand's largest terrestrial hot springs exhibiting high concentrations of arsenic ions and compounds, have been mainly restricted to geological and geochemical descriptions as previously microbial culturing experiments failed. By a combination of first molecular analyses followed by culturing experiments, novel bacterial and archaeal species were

successfully isolated from Champagne Pool (Chapter 4). Low biomass concentration was indicated by relatively low recovered ATP and DNA yields and relatively low cell numbers ($5.6 \pm 0.5 \times 10^6$ cells per ml) obtained for Champagne Pool compared to other terrestrial hot springs in New Zealand. In toxicity assays using Champagne Pool water samples inoculated with *Bacillus caldotenax*, bacterial growth was only observed when the spring water was purged with N₂ or CO₂, or autoclaved prior to inoculation. These results suggest that a volatile component might be present within the hot spring inhibiting microbial growth. Toxic volatile methyl and hydride derivatives of arsenic and antimony (Hirner *et al.*, 1998) and H₂S have been previously reported for Champagne Pool.

Denaturing gradient gel electrophoresis (DGGE) and 16S rRNA gene clone library analyses revealed few dominant species, which were related to members of the genera *Nevskia*, *Paracoccus*, *Sulfurihydrogenibium*, *Sulfolobus*, and *Thermofilum*, and indicated *Sulfurihydrogenibium*-like populations to be highly abundant in Champagne Pool. These findings are in good agreement with previous reports which indicate the dominance of hydrogen-oxidizing bacteria in geothermal ecosystems in USA and Iceland (Skirnisdottir *et al.*, 2000; Spear *et al.*, 2005). Future work might involve further constructions of archaeal and bacterial 16S rRNA gene-based clone libraries of DNA obtained from Champagne Pool water, which could be compared to previous molecular results. This approach would establish if there are changes in microbial community structure, e.g. due to seasonal variability (this is unlikely, given the constancy of the pool environment, but cannot comprehensively be ruled out until further data is obtained) or contamination of the sampling site with material that was not originally from the pool (Champagne Pool has a large surface; and as a major tourist attraction, it is visited by many tourists). If 16S rRNA gene sequences distantly related to *Nevskia* and *Paracoccus* are still present in the terrestrial hot spring, appropriate media could be chosen to enrich these microorganisms.

From results of molecular analyses, media were selected to enrich hydrogen-oxidizing and sulfur-dependent microorganisms. Three novel species were isolated and analysis of the amplified 16S rRNA gene showed a close phylogenetic relationship of isolate CP.B1 to *Thermoanaerobacter*, of CP.B2 to

Sulfurihydrogenibium, and of CP.B3 to *Thermococcus*. Isolate CP.B2 represents a novel genus within the *Aquificales* order, for which the name *Venenivibrio stagnispumantis* gen. nov., sp. nov. is proposed (Chapter 5). The novel isolate displayed tolerance to relatively high concentrations of arsenic and antimony compounds, but growth was not observed when As^{3+} and As^{5+} were provided as the sole electron donor and acceptor pair. *V. stagnispumantis* grew in the presence of up to 8 mM As^{3+} , 15 mM Sb^{3+} , and more than 20 mM As^{5+} , which was considerably higher compared to concentrations found within the water column of the thermal spring Champagne Pool. Arsenic resistance was mediated by a two-component energy-dependent efflux system (ArsA and ArsB).

If time had permitted, Fluorescent *In Situ* Hybridization (FISH) or quantitative Polymerase Chain Reaction (qPCR) experiments would have been conducted in order to detect and enumerate particular phylogenetic groups within Champagne Pool. Fluorescently labelled oligonucleotide probes specific for *V. stagnispumantis* could support the molecular results, which suggest that this isolate is one of the more dominant species in the spring. Additionally it could be used to screen other geothermally active areas for the presence of *V. stagnispumantis* cells. The advantage of the FISH technique over other quantitative methods is the visualization of a specific target, which permits prediction of its spatial distribution, e.g. planktonic or sediment-associated. However, FISH experiment might be troublesome since sediment samples obtained from Champagne Pool cause strong background fluorescence. The qPCR technique allows faster procedure times than the FISH method and has been widely used to enumerate gene and transcript numbers within environmental samples. The reliability of this method is sensitive to biases during DNA extraction and PCR amplification, which may result in gene and transcript number variability. It has been also reported that quantification of low-copy genes was less accurate resulting in a higher portion of false-positive signals (Smith *et al.*, 2006), which might provide only semi-quantitative results for Champagne Pool, where it is expected the bacterium *V. stagnispumantis* dominates the microbial community. Therefore, less abundant microorganisms might be overrepresented in pPCR analysis.

Experiments are currently underway to characterize further isolate CP.B1 phenotypically and phylogenetically. Due to the absence of ‘classical’ *ars* genes in CP.B1, further studies might address changes at the transcriptome level (e.g. by differential display PCR) or the proteome level (e.g. by 2-dimensional difference electrophoresis) when CP.B1 cells are exposed to arsenic ions to determine the mode of resistance mechanisms.

References

- Aguiar, P., Beveridge, T. J. & Reysenbach, A. L. (2004).** *Sulfurihydrogenibium azorense*, sp. nov., a thermophilic hydrogen-oxidizing microaerophile from terrestrial hot springs in the Azores. *International Journal of Systematic and Evolutionary Microbiology* **54**, 33-39.
- Ahmad, S. A., Sayed, S. U., Barua, S., Khan, M. H., Jalil, A., Hadi, S. A. & Talukder, H. K. (2001).** Arsenic in drinking water and pregnancy outcomes. *Environmental Health Perspectives* **109**, 629-631.
- Allison, J. D., Brown, D. S. & Novo-Gradac, K. J. (1991).** MINTEQA2/PRODEFA2, A geochemical assessment model for environmental systems: Version 3.0 User's Manual, pp. EPA/600/603-691/021, p.106. Athens, Georgia: Environmental Research Laboratory, Office of Research and Development, U.S. Environmental Protection Agency.
- Altschul, S. F., Madden, T. L., Schaffer, A. A., Zhang, J., Zhang, Z., Miller, W. & Lipman, D. J. (1997).** Gapped BLAST and PSI-BLAST: a new generation of protein database search programs. *Nucleic Acids Research* **25**, 3389-3402.
- Ash, C., Farrow, J. A. E., Wallbanks, S. & Collins, M. D. (1991).** Phylogenetic heterogeneity of the genus *Bacillus* revealed by comparative analysis of small-subunit-ribosomal RNA sequences. *Letters in Applied Microbiology* **13**, 202-206.
- Ballatori, N. (2002).** Transport of toxic metals by molecular mimicry. *Environmental Health Perspectives* **110**, 689-694.
- Benson, A. A. & Cooney, R. A. (1988).** Antimony metabolites in marine algae. In *Organometallic Compounds in the Environment Principles and Reactions*, pp. 135-137. Edited by P. J. Craig & F. Glockling. Harlow: Longmans.
- Beveridge, T. J. (1989).** Role of cellular design in bacterial metal accumulation

and mineralization. *Annual Review of Microbiology* **43**, 147-171.

Beveridge, T. J. (1990). Mechanism of Gram variability in select bacteria. *Journal of Bacteriology* **172**, 1609-1620.

Birnboim, H. C. & Doly, J. (1979). A rapid alkaline extraction procedure for screening recombinant plasmid DNA. *Nucleic Acids Research* **7**, 1513-1523.

Bissen, M. & Frimmel, F. H. (2003). Arsenic – a Review. Part I: Occurrence, Toxicity, Speciation, Mobility. *Acta Hydrochimica et Hydrobiologica* **31**, 9–18.

Borrok, D., Fein, J. B. & Kulpa, C. F. (2004a). Proton and Cd adsorption onto natural bacterial consortia: testing universal adsorption behavior. *Geochimica et Cosmochimica Acta* **68**, 3231-3238.

Borrok, D., Fein, J. B., Tischler, M., O'Loughlin, E., Meyer, H., Liss, M. & Kemner, K. M. (2004b). The effect of acidic solutions and growth conditions on the adsorptive properties of bacterial surfaces. *Chemical Geology* **209**, 107-119.

Borrok, D., Turner, B. F. & Fein, A. B. (2005). A universal surface complexation framework for modeling proton binding onto bacterial surfaces in geologic settings. *American Journal of Science* **305**, 826-853.

Borrok, D. M. & Fein, J. B. (2005). The impact of ionic strength on the adsorption of protons, Pb, Cd, and Sr onto the surfaces of Gram negative bacteria: testing non-electrostatic, diffuse, and triple-layer models. *Journal of Colloid and Interface Science* **286**, 110-126.

Boyanov, M. I., Kelly, S. D., Kemner, K. M., Bunker, B. A., Fein, J. B. & Fowle, D. A. (2003). Adsorption of cadmium to *Bacillus subtilis* bacterial cell walls: A pH-dependent X-ray absorption fine structure spectroscopy study. *Geochimica et Cosmochimica Acta* **67**, 3299-3311.

Brock, T. D., Brock, K. M., Belly, R. T. & Weiss, R. L. (1972). *Sulfolobus* -

New genus of sulfur-oxidizing bacteria living at low pH and high-temperature. *Archiv für Mikrobiologie* **84**, 54-68.

Brock, T. D. (1986). Introduction: An overview of the thermophiles. In *Thermophiles: General, molecular and applied microbiology*, pp. 1-16. Edited by T. D. Brock. New York: Wiley & Sons.

Bruins, M. R., Kapil, S. & Oehme, F. W. (2000). Microbial resistance to metals in the environment. *Ecotoxicology and Environmental Safety* **45**, 198-207.

Bruins, M. R., Kapil, S. & Oehme, F. W. (2003). Characterization of a small plasmid (pMBCP) from bovine *Pseudomonas pickettii* that confers cadmium resistance. *Ecotoxicology and Environmental Safety* **54**, 241-248.

Burggraf, S., Olsen, G. J., Stetter, K. O. & Woese, C. R. (1992). A phylogenetic analysis of *Aquifex pyrophilus*. *Systematic and Applied Microbiology* **15**, 352 - 356.

Burnett, P.-G. G., Heinrich, H., Peak, P., Bremer, P. J., McQuillan, A. J. & Daughney, C. J. (2006). The effect of pH and ionic strength on proton adsorption by the thermophilic bacterium *Anoxybacillus flavithermus*. *Geochimica et Cosmochimica Acta* **70**, 1914-1927.

Chang, I. S., Groh, J. L., Ramsey, M. M., Ballard, J. D. & Krumholz, L. R. (2004). Differential expression of *Desulfovibrio vulgaris* genes in response to Cu(II) and Hg(II) toxicity. *Applied and Environmental Microbiology* **70**, 1847–1851.

Chatellier, X. & Fortin, D. (2004). Adsorption of ferrous ions onto *Bacillus subtilis* cells. *Chemical Geology* **212**, 209-228.

Cheeseman, K. H. & Slater, T. F. (1993). An introduction to free radical biochemistry. *British Medical Bulletin* **49**, 481-493.

- Chen, X., Schauder, S., Potier, N., Van Dorsselaer, A., Pelczer, I., Bassler, B. L. & Hughson, F. M. (2002).** Structural identification of a bacterial quorum-sensing signal containing boron. *Nature* **415**, 545-549.
- Chien, A., Edgar, D. B. & Trela, J. M. (1976).** Deoxyribonucleic acid polymerase from the extreme thermophile *Thermus aquaticus*. *Journal of Bacteriology* **127**, 1550-1557.
- Claessens, J., Behrends, T. & Van Cappellen, P. (2004).** What do acid-base titrations of live bacteria tell us? A preliminary assessment. *Aquatic Sciences* **66**, 19-26.
- Cline, J. D. (1969).** Spectrophotometric determination of hydrogen sulfide in natural waters. *Limnology and Oceanography* **14**, 454-458.
- Cole, J. R., Chai, B., Marsh, T. L. & other authors (2003).** The Ribosomal Database Project (RDP-II): previewing a new autoaligner that allows regular updates and the new prokaryotic taxonomy. *Nucleic Acids Research* **31**, 442-443.
- Corliss, J. B., Dymond, J., Gordon, L. I. & other authors (1979).** Submarine thermal springs on the Galapagos Rift. *Science* **203**, 1073-1083.
- Croal, L. R., Gralnick, J. A., Malasarn, D. & Newman, D. K. (2004).** The genetics of geochemistry. *Annual Review of Genetics* **38**, 175-202.
- Crowley, J. D., Traynor, D. A. & Weatherburn, D. C. (2000).** Enzymes and proteins containing manganese: an overview. *Metal Ions in Biological Systems* **37**, 209-278.
- Daughney, C. J. & Fein, J. B. (1998).** The effect of ionic strength on the adsorption of H^+ , Cd^{2+} , Pb^{2+} , and Cu^{2+} by *Bacillus subtilis* and *Bacillus licheniformis*: A surface complexation model. *Journal of Colloid and Interface Science* **198**, 53-77.

- Daughney, C. J. & Fortin, D. (2001).** Mineral adsorption by bacteria. In *Encyclopaedia of Surface and Colloid Science*, pp. 3430-3446. Edited by A. T. Hubbard. New York: Marcell Dekker Inc.
- Daughney, C. J., Fowle, D. A. & Fortin, D. E. (2001).** The effect of growth phase on proton and metal adsorption by *Bacillus subtilis*. *Geochimica et Cosmochimica Acta* **65**, 1025-1035.
- de Ronde, C. E. J., Baker, E. T., Massoth, G. J., Lupton, J. E., Wright, I. C., Feely, R. A. & Greene, R. R. (2001).** Intra-oceanic subduction-related hydrothermal venting, Kermadec volcanic arc, New Zealand. *Earth and Planetary Science Letters* **193**, 359-369.
- de Ronde, C. E. J., Faure, K., Bray, C. J., Chappell, D. A. & Wright, I. C. (2003).** Hydrothermal fluids associated with seafloor mineralization at two southern Kermadec arc volcanoes, offshore New Zealand. *Mineralium Deposita* **38**, 217-233.
- Deckert, G., Warren, P. V., Gaasterland, T. & other authors (1998).** The complete genome of the hyperthermophilic bacterium *Aquifex aeolicus*. *Nature* **392**, 353-358.
- Degens, E. T. & Ross, D. A. (1969).** *Hot brines and recent heavy metal deposits in the Red Sea*. New York: Springer Verlag.
- Dempster, E. L., Pryor, K. V., Francis, D., Young, J. E. & Rogers, H. J. (1999).** Rapid DNA extraction from ferns for PCR-based analyses. *Biotechniques* **27**, 66-68.
- Donk, P. J. (1920).** A highly resistant thermophilic organism. *Journal of Bacteriology* **5**, 373-374.
- Duffus, J. H. (2002).** "Heavy metals" - A meaningless term? (IUPAC technical report). *Pure and Applied Chemistry* **74**, 793-807.

- Edwards, C. (1990).** Thermophiles. In *Microbiology of extreme environments*. Edited by C. Edwards. New York: McGraw-Hill.
- Ehrlich, L. E. (1995).** *Geomicrobiology*, 3 edn. New York: Marcel Dekker.
- Ellis, D. G., Bizzoco, R. L. W., Maezato, Y., Baggett, J. N. & Kelley, S. T. (2005).** Microscopic examination of acidic hot springs of Waiotapu, North Island, New Zealand. *New Zealand Journal of Marine and Freshwater Research* **39**, 1001-1011.
- Emerson, D. & Moyer, C. L. (2002).** Neutrophilic Fe-oxidizing bacteria are abundant at the Loihi Seamount hydrothermal vents and play a major role in Fe oxide deposition. *Applied and Environmental Microbiology* **68**, 3085-3093.
- Euzeby, J. P. (1997).** List of bacterial names with standing in nomenclature: A folder available on the Internet. *International Journal of Systematic Bacteriology* **47**, 590-592.
- Fein, J. B., Daughney, C. J., Yee, N. & Davis, T. A. (1997).** A chemical equilibrium model for metal adsorption onto bacterial surfaces. *Geochimica et Cosmochimica Acta* **61**, 3319-3328.
- Felsenstein, J. (1993).** PHYLIP (Phylogeny Inference Package) version 3.5c. Distributed by the author. Seattle, University of Washington, Department of Genetics.
- Ferris, M. J., Muyzer, G. & Ward, D. M. (1996).** Denaturing gradient gel electrophoresis profiles of 16S rRNA-defined populations inhabiting a hot spring microbial mat community. *Applied and Environmental Microbiology* **62**, 340-346.
- Ford, T., Jay, J., Patel, A., Kile, M., Prommasith, P., Galloway, T., Sanger, R., Smith, K. & Depledge, M. (2005).** Use of ecotoxicological tools to evaluate the health of New Bedford Harbor sediments: A microbial biomarker approach.

Environmental Health Perspectives **113**, 186-191.

Gadd, G. M. & Griffiths, A. J. (1978). Microorganisms and heavy metal toxicity. *Microbial Ecology* **4**, 303–317.

Gadd, G. M. (1988). Accumulation of metals by microorganisms and algae. In *Biotechnology - A Comprehensive Treatise in 8 Volumes*, pp. 401-433. Edited by H.-J. Rehm & G. Reed. Weinheim: VCH Publishers.

Gadd, G. M. (1990). Metal tolerance. In *Microbiology of extreme environments*, pp. 178-210. Edited by C. Edwards. New York: McGraw-Hill.

Gadd, G. M. (2000). Bioremedial potential of microbial mechanisms of metal mobilization and immobilization. *Current Opinion in Biotechnology* **11**, 271-279.

Gadd, G. M. (2004). Microbial influence on metal mobility and application for bioremediation. *Geoderma* **122**, 109-119.

Gage, J. D. & Tyler, P. A. (1991). *Deep-seabiology: A natural history of organisms at the deep-sea floor*. Cambridge: Cambridge University Press.

Giggenbach, W. F., Sheppard, D. S., Robinson, B. W., Stewart, M. K. & Lyon, G. L. (1994). Geochemical structure and position of the Waiotapu geothermal field, New Zealand. *Geothermics* **23**, 599-644.

Gihring, T. M. & Banfield, J. F. (2001). Arsenite oxidation and arsenate respiration by a new *Thermus* isolate. *FEMS Microbiology Letters* **204**, 335-340.

Gilboa-Garber, N. (1971). Direct spectrophotometric determination of inorganic sulfide in biological materials and in other complex mixtures. *Analytical Biochemistry* **43**, 129-133.

Golovacheva, R. S., Loginova, L. G., Salikhov, T. A., Kolesnikov, A. A. & Zaitseva, G. N. (1975). A new thermophilic species, *Bacillus thermocatenulatus*

nov. spec. *Mikrobiologiya* **44**, 265-268.

Gonzalez, J. M., Sheckells, D., Viebahn, M., Krupatkina, D., Borges, K. M. & Robb, F. T. (1999). *Thermococcus waiotapuensis* sp. nov., an extremely thermophilic archaeon isolated from a freshwater hot spring. *Archives of Microbiology* **172**, 95-101.

Götz, D., Banta, A., Beveridge, T. J., Rushdi, A. I., Simoneit, B. R. T. & Reysenbach, A. (2002a). *Persephonella marina* gen. nov., sp. nov. and *Persephonella guaymasensis* sp nov., two novel, thermophilic, hydrogen-oxidizing microaerophiles from deep-sea hydrothermal vents. *International Journal of Systematic and Evolutionary Microbiology* **52**, 1349-1359.

Götz, D., Banta, A., Beveridge, T. J., Rushdi, A. I., Simoneit, B. R. T. & Reysenbach, A. (2002b). *Persephonella marina* gen. nov., sp nov and *Persephonella guaymasensis* sp nov., two novel, thermophilic, hydrogen-oxidizing microaerophiles from deep-sea hydrothermal vents. *International Journal of Systematic and Evolutionary Microbiology* **52**, 1349-1359.

Griffiths, E. & Gupta, R. S. (2004). Signature sequences in diverse proteins provide evidence for the late divergence of the order *Aquificales*. *International Microbiology* **7**, 41-52.

Griffiths, E. & Gupta, R. S. (2006). Molecular signatures in protein sequences that are characteristics of the phylum *Aquificae*. *International Journal of Systematic and Evolutionary Microbiology* **56**, 99-107.

Haas, J. R. (2004). Effects of cultivation conditions on acid-base titration properties of *Shewanella putrefaciens*. *Chemical Geology* **209**, 67-81.

Hall, J. L. (2002). Cellular mechanisms for heavy metal detoxification and tolerance. *Journal of Experimental Botany* **53**, 1-11.

Handley, P. S., Hargreaves, J. & Harty, D. W. (1988). Ruthenium red staining

reveals surface fibrils and a layer external to the cell wall in *Streptococcus salivarius* HB and adhesion deficient mutants. *Journal of General Microbiology* **134**, 3165-3172.

Harden, V. P. & Harris, J. O. (1953). The isoelectric point of bacterial cells. *Journal of Bacteriology* **65**, 198-202.

Hedenquist, J. W. & Henley, R. W. (1985). Hydrothermal eruptions in the Waiotapu geothermal system, New Zealand: Their origin, associated breccias and relation to precious metal mineralization. *Economic Geology* **80**, 1640-1668.

Hedenquist, J. W. (1986a). Geothermal systems in the Taupo Volcanic Zone: Their characteristics and relation to volcanism and mineralisation. *Bulletin of the Royal Society of New Zealand* **23**, 134-168.

Hedenquist, J. W. (1986b). Waiotapu geothermal field. In *Guide to the active epithermal (geothermal) systems and precious metal deposits of New Zealand, Monograph Series on Mineral Deposits*, pp. 65-79. Edited by R. W. Henley, J. W. Hedenquist & P. J. Roberts. Berlin-Stuttgart: Gebrüder Borntraeger.

Hirner, A. V., Feldmann, J., Krupp, E., Grumping, R., Goguel, R. & Cullen, W. R. (1998). Metal(loid)organic compounds in geothermal gases and waters. *Organic Geochemistry* **29**, 1765-1778.

Huber, H., Diller, S., Horn, C. & Rachel, R. (2002a). *Thermovibrio ruber* gen. nov., sp nov., an extremely thermophilic, chemolithoautotrophic, nitrate-reducing bacterium that forms a deep branch within the phylum *Aquificae*. *International Journal of Systematic and Evolutionary Microbiology* **52**, 1859-1865.

Huber, H., Hohn, M. J., Rachel, R., Fuchs, T., Wimmer, V. C. & Stetter, K. O. (2002b). A new phylum of Archaea represented by a nanosized hyperthermophilic symbiont. *Nature* **417**, 63-67.

Huber, R., Wilharm, T., Huber, D. & other authors (1992). *Aquifex pyrophilus*

gen. nov., sp. nov. represents a novel group of marine hyperthermophilic hydrogen-oxidizing bacteria. *Systematic and Applied Microbiology* **15**, 340-351.

Huber, R., Eder, W., Heldwein, S., Wanner, G., Huber, H., Rachel, R. & Stetter, K. O. (1998). *Thermocrinis ruber* gen. nov., sp. nov., a pink-filament-forming hyperthermophilic bacterium isolated from Yellowstone National Park. *Applied and Environmental Microbiology* **64**, 3576-3583.

Huber, R. & Eder, W. (2001). *Aquificales*. In *The Prokaryotes: An Evolving Electronic Resource for the Microbiological Community*. Edited by M. Dworkin. New York, <http://link.springer-ny.com/link/service/books/10125/>: release 3.8, Springer-Verlag.

Hucker, G. J. & Conn, H. J. (1927). Further studies on the methods of Gram staining. *New York state Agricultural Experiment Station Technical Bulletin No 128*.

Hudson, J. A. (1986). The taxonomy and ecology of the genus *Thermus*. Thermophile Research Unit, University of Waikato, Hamilton, New Zealand. PhD thesis.

Islam, F. S., Pederick, R. L., Gault, A. G., Adams, L. K., Polya, D. A., Charnock, J. M. & Lloyd, J. R. (2005). Interactions between the Fe(III)-reducing bacterium *Geobacter sulfurreducens* and arsenate, and capture of the metalloid by biogenic Fe(II). *Applied and Environmental Microbiology* **71**, 8642-8648.

Jeanthon, C. (2000). Molecular ecology of hydrothermal vent microbial communities. *Antonie van Leeuwenhoek* **77**, 117-133.

Jenkins, R. O., Forster, S. N. & Craig, P. J. (2002). Formation of methylantimony species by an aerobic prokaryote: *Flavobacterium* sp. *Archives of Microbiology* **178**, 274-278.

- Johnson, J. L. (1994).** Similarity analysis of rRNAs. In *Methods for general and molecular bacteriology*, pp. 683-700. Edited by P. Gerhardt, R. G. E. Murray, W. A. Wood & N. R. Krieg. Washington, D.C: American Society for Microbiology.
- Jones, B., Renaut, R. W. & Rosen, M. R. (1999).** Actively growing siliceous oncoids in the Waiotapu geothermal area, North Island, New Zealand. *Journal of the Geological Society* **156**, 89-103.
- Jones, B., Renaut, R. W. & Rosen, M. R. (2001).** Biogenicity of gold- and silver-bearing siliceous sinters forming in hot (75 degrees C) anaerobic spring-waters of Champagne Pool, Waiotapu, North Island, New Zealand. *Journal of the Geological Society* **158**, 895-911.
- Karl, D. M. (1995).** Ecology of free-hydrothermal vent microbial communities. In *The microbiology of deep-sea hydrothermal vents*, pp. 35-124. Edited by D. M. Karl. Boca Raton: CRC Press.
- Kashefi, K. & Lovley, D. R. (2003).** Extending the upper temperature limit for life. *Science* **301**, 934.
- Kawasumi, T., Igarashi, Y., Kodama, T. & Minoda, Y. (1984).** *Hydrogenobacter thermophilus* gen. nov., sp. nov. an extremely thermophilic, aerobic, hydrogen-oxidizing bacterium. *International Journal of Systematic Bacteriology* **34**, 5-10.
- Kelly, R. M. & Adams, M. W. W. (1994).** Metabolism In hyperthermophilic microorganisms. *Antonie van Leeuwenhoek* **66**, 247-270.
- Kisker, C., Schindelin, H. & Rees, D. C. (1997).** Molybdenum-cofactor-containing enzymes: structure and mechanism. *Annual Review of Biochemistry* **66**, 233-267.
- Knauer, K., Ahner, B., Xue, H. B. & Sigg, L. (1998).** Metal and phytochelatin content in phytoplankton from freshwater lakes with different metal

concentrations. *Environmental Toxicology and Chemistry* **17**, 2444-2452.

Kobayashi, M. & Shimizu, S. (1999). Cobalt proteins. *European Journal of Biochemistry* **261**, 1-9.

Köhler, M. & Völsgen, F. (1997). *Geomikrobiologie: Grundlagen und Anwendung*. Weinheim: Wiley-VCH.

Konings, W. N., Albers, S. V., Koning, S. & Driessen, A. J. M. (2002). The cell membrane plays a crucial role in survival of bacteria and archaea in extreme environments. *Antonie van Leeuwenhoek* **81**, 61-72.

Kroll, R. G. & Booth, I. R. (1983). The relationship between intracellular pH, the pH gradient and potassium transport in *Escherichia coli*. *Biochemical Journal* **216**, 709-716.

L'Haridon, S., Cilia, V., Messner, P., Raguenes, G., Gambacorta, A., Sleytr, U. B., Prieur, D. & Jeanthon, C. (1998). *Desulfurobacterium thermolithotrophum* gen. nov., sp. nov., a novel autotrophic, sulphur-reducing bacterium isolated from a deep-sea hydrothermal vent. *International Journal Of Systematic Bacteriology* **48**, 701-711.

Lane, D. J. (1991). 16S/23S rRNA sequencing. In *Nucleic acid techniques in bacterial systematics*, pp. 115–175. Edited by E. Stackebrandt & M. Goodfellow. New York, N.Y.: John Willy and Sons.

Lane, T. W. & Morel, F. M. M. (2000). A biological function for cadmium in marine diatoms. *Proceedings of the National Academy of Sciences of the United States of America* **97**, 4627-4631.

Langworthy, T. A. & Pond, J. L. (1986). Membranes and lipids of thermophiles. In *Thermophiles: General, molecular and applied microbiology*. Edited by T. D. Brock. New York: John Wiley & Sons.

- Levitus, S. & Boyer, T. (1994).** World Ocean Atlas, vol. 4: Temperature. Washington, D. C.: U.S. Department of Commerce.
- Li, X. Z., Nikaido, H. & Williams, K. E. (1997).** Silver-resistant mutants of *Escherichia coli* display active efflux of Ag⁺ and are deficient in porins. *Journal of Bacteriology* **179**, 6127-6132.
- Lindsay, W. L. (1979).** *Chemical equilibria in soils*. New York: John Wiley & Sons.
- Llanos, J., Capasso, C., Parisi, E., Prieur, D. & Jeanthon, C. (2000).** Susceptibility to heavy metals and cadmium accumulation in aerobic and anaerobic thermophilic microorganisms isolated from deep-sea hydrothermal vents. *Current Microbiology* **41**, 201-205.
- Lloyd, E. F. (1959).** The hot springs and hydrothermal eruptions of Waiotapu. *New Zealand Journal of Geology and Geophysics* **2**, 141-176.
- Lovley, D. R. (1993).** Dissimilatory metal reduction. *Annual Review of Microbiology* **47**, 263-290.
- Ludwig, W., Strunk, O., Westram, R. & other authors (2004).** ARB: a software environment for sequence data. *Nucleic Acids Research* **32**, 1363-1371.
- Madigan, M. T., Martinko, J. M. & Parker, J. (2000).** Brock: Biology of Microorganisms. Upper Saddle River, NJ: Prentice Hall.
- Malik, A. & Jaiswal, R. (2000).** Metal resistance in *Pseudomonas* strains isolated from soil treated with industrial wastewater. *World Journal of Microbiology and Biotechnology* **16**, 177-182.
- Malouin, F., Chamberland, S., Brochu, N. & Parr Jr, T. R. (1991).** Influence of growth media on *Escherichia coli* cell composition and ceftazidime susceptibility. *Antimicrobial Agents and Chemotherapy* **35**, 477-483.

- Marmur, J. (1961).** A procedure for the isolation of deoxyribonucleic acid from microorganisms. *Journal of Molecular Biology* **3**, 208-218.
- Martin, W. (1999).** Mosaic bacterial chromosomes: a challenge on route to a tree of genomes. *Bioessays* **21**, 99-104.
- Matin, A. (1990).** Keeping a neutral cytoplasm; the bioenergetics of obligate acidophiles. *FEMS Microbiology Review* **75**, 307-318.
- McSwain, B. S., Irvine, R. L., Hausner, M. & Wilderer, P. A. (2005).** Composition and distribution of extracellular polymeric substances in aerobic flocs and granular sludge. *Applied and Environmental Microbiology* **71**, 1051-1057.
- Mendoza-Cozatl, D., Loza-Tavera, H., Hernandez-Navarro, A. & Moreno-Sanchez, R. (2005).** Sulfur assimilation and glutathione metabolism under cadmium stress in yeast, protists and plants. *FEMS Microbiology Review* **29**, 653-671.
- Mesbah, M., Premachandran, U. & Whitman, W. (1989).** Precise measurement of the G+C content of deoxyribonucleic acid by high performance liquid chromatography. *International Journal of Systematic Bacteriology* **39**, 159-167.
- Morita, R. Y. (1975).** Psychrophilic bacteria. *Bacteriological Reviews* **39**, 144-167.
- Mountain, B. W., Benning, L. G. & Boerema, J. A. (2003).** Experimental studies on New Zealand hot spring sinters: rates of growth and textural development. *Canadian Journal of Earth Sciences* **40**, 1643-1667.
- Mulks, M. H., Souza, K. A. & Boylen, C. W. (1980).** Effect of restrictive temperature on cell wall synthesis in a temperature-sensitive mutant of *Bacillus stearothermophilus*. *Journal of Bacteriology* **144**, 413-421.

Muyzer, G., Dewaal, E. C. & Uitterlinden, A. G. (1993). Profiling of complex microbial-populations by denaturing gradient gel-electrophoresis analysis of polymerase chain reaction-amplified genes-coding for 16S ribosomal-RNA. *Applied and Environmental Microbiology* **59**, 695-700.

Nakagawa, S., Nakamura, S., Inagaki, F., Takai, K., Shirai, N. & Sako, Y. (2004). *Hydrogenivirga caldilitoris* gen. nov., sp nov., a novel extremely thermophilic, hydrogen- and sulfur-oxidizing bacterium from a coastal hydrothermal field. *International Journal of Systematic and Evolutionary Microbiology* **54**, 2079-2084.

Nakagawa, S., Shtaih, Z., Banta, A., Beveridge, T. J., Sako, Y. & Reysenbach, A. L. (2005). *Sulfurihydrogenibium yellowstonense* sp. nov., an extremely thermophilic, facultatively heterotrophic, sulfur-oxidizing bacterium from Yellowstone National Park, and emended descriptions of the genus *Sulfurihydrogenibium*, *Sulfurihydrogenibium subterraneum* and *Sulfurihydrogenibium azureum*. *International Journal of Systematic and Evolutionary Microbiology* **55**, 2263-2268.

Nazina, T. N., Tourova, T. P., Poltarau, A. B. & other authors (2001). Taxonomic study of aerobic thermophilic bacilli: descriptions of *Geobacillus subterraneus* gen. nov., sp. nov. and *Geobacillus uzoniensis* sp. nov. from petroleum reservoirs and transfer of *Bacillus stearothermophilus*, *Bacillus thermocatenulatus*, *Bacillus thermoleovorans*, *Bacillus kaustophilus*, *Bacillus thermoglucosidasius* and *Bacillus thermodenitrificans* to *Geobacillus* as the new combinations *G. stearothermophilus*, *G. thermocatenulatus*, *G. thermoleovorans*, *G. kaustophilus*, *G. thermoglucosidasius* and *G. thermodenitrificans*. *International Journal of Systematic and Evolutionary Microbiology* **51**, 433-446.

Niederberger, T. D. (2005). The microbial ecology and colonisation of surfaces in selected hot springs - a molecular- and culture-based approach. Thermophile Research Unit, University of Waikato, Hamilton, New Zealand. PhD thesis.

- Niederberger, T. D., Gotz, D. K., McDonald, I. R., Ronimus, R. S. & Morgan, H. W. (2006).** *Ignisphaera aggregans* gen. nov., sp. nov., a novel hyperthermophilic crenarchaeote isolated from hot springs in Rotorua and Tokaanu, New Zealand. *International Journal of Systematic and Evolutionary Microbiology* **56**, 965-971.
- Nies, D. H. (1999).** Microbial heavy-metal resistance. *Applied Microbiology and Biotechnology* **51**, 730-750.
- Nies, D. H. (2003).** Efflux-mediated heavy metal resistance in prokaryotes. *FEMS Microbiology Review* **27**, 313-339.
- Oger, C., Mahillon, J. & Petit, F. (2003).** Distribution and diversity of a cadmium resistance (CadA) determinant and occurrence of IS257 insertion sequences in staphylococcal bacteria isolated from a contaminated estuary (Seine, France). *FEMS Microbiology Ecology* **43**, 173-183.
- Palmiter, R. D. (1998).** The elusive function of metallothioneins. *Proceedings of the National Academy of Sciences of the United States of America* **95**, 8428-8430.
- Pask-Hughes, R. A. & Williams, R. A. D. (1978).** Cell envelope components of strains belonging to the genus *Thermus*. *Journal of General Microbiology* **107**, 65-72.
- Paulsen, I. T. & Saier, M. H. (1997).** A novel family of ubiquitous heavy metal ion transport proteins. *Journal of Membrane Biology* **156**, 99-103.
- Phoenix, V. R., Renaut, R. W., Jones, B. & Ferris, F. G. (2005).** Bacterial S-layer preservation and rare arsenic-antimony-sulphide bioimmobilization in siliceous sediments from Champagne Pool hot spring, Waiotapu, New Zealand. *Journal of the Geological Society* **162**, 323-331.
- Pope, J. G., Brown, K. L. & McConchie, D. M. (2005).** Gold concentrations in springs at Waiotapu, New Zealand: Implications for precious metal deposition in

geothermal systems. *Economic Geology* **100**, 677-687.

Porter, K. G. & Feig, Y. S. (1980). The use of DAPI for identifying and counting aquatic microflora. *Limnology and Oceanography* **25**, 943-948.

Price, R. C., Gamble, J. A., Smith, I. E. M., Stewart, R. B., Eggins, S. & Wnight, I. C. (2005). An integrated model for the temporal evolution of andesites and rhyolites and crustal development in New Zealand's North Island. *Journal of Volcanology and Geothermal Research* **140**, 1-24.

Rawlings, D. E. (2002). Heavy metal mining using microbes. *Annual Review of Microbiology* **56**, 65-91.

Reysenbach, A. L., Wickham, G. S. & Pace, N. R. (1994). Phylogenetic analysis of the hyperthermophilic pink filament community in Octopus Spring, Yellowstone National Park. *Applied and Environmental Microbiology* **60**, 2113–2119.

Reysenbach, A. L. & Gotz, D. (2001). Methods for the study of hydrothermal vent microbes. In *Methods in Microbiology*, Vol 30, pp. 639-656.

Robinson, N. J., Whitehall, S. K. & Cavet, J. S. (2001). Microbial metallothioneins. *Annual Review of Biochemistry* **44**, 183-213.

Ronimus, R. (1993). Investigation into the control of genome topology in the archaeal isolate AN1. Thermophile Research Unit, University of Waikato, Hamilton, New Zealand. PhD thesis.

Rosen, B. P. (1996). Bacterial resistance to heavy metals and metalloids. *Journal of Biological Inorganic Chemistry* **1**, 273-277.

Saier, M. H. (2000). A functional-phylogenetic classification system for transmembrane solute transporters. *Microbiology and Molecular Biology Reviews* **64**, 354-411.

- Schär-Zammaretti, P., Dillmann, M. L., D'Amico, N., Affolter, M. & Ubbink, J. (2005).** Influence of fermentation medium composition on physicochemical surface properties of *Lactobacillus acidophilus*. *Applied and Environmental Microbiology* **71**, 8165-8173.
- Scheffers, D. J. & Pinho, M. G. (2005).** Bacterial cell wall synthesis: New insights from localization studies. *Microbiology and Molecular Biology Reviews* **69**, 585-607.
- Schleifer, K. H. & Kandler, O. (1972).** Peptidoglycan types of bacterial cell walls and their taxonomic implications. *Bacteriological Reviews* **36**, 407-477.
- Schultze-Lam, S., Thompson, J. B. & Beveridge, T. J. (1993).** Metal ion immobilization by bacterial surfaces in freshwater environments. *Water Pollution Research Journal of Canada* **28**, 51-81.
- Shumate, S. E. & Strandberg, G. W. (1985).** Accumulation of metals by microbial cells. In *Comprehensive Biotechnology*, pp. 235-247. Edited by M. Moo-Young, C. N. Robinson & J. A. Howell. New York: Pergamon Press.
- Sierra-Alvarez, R., Cortinas, I., Yenal, U. & Field, J. A. (2004).** Methanogenic inhibition by arsenic compounds. *Applied and Environmental Microbiology* **70**, 5688-5691.
- Silver, S. & Phung, L. T. (1996).** Bacterial heavy metal resistance: New surprises. *Annual Review of Microbiology* **50**, 753-789.
- Singh, S., Kayastha, A. M., Asthana, R. K., Srivastava, P. K. & Singh, S. P. (2001).** Response of *Rhizobium leguminosarum* to nickel stress. *World Journal of Microbiology and Biotechnology* **17**, 667-672.
- Skinner, F. A. (1968).** The limits of microbial existence. *Proceedings of the Royal Society of London Series B* **171**, 77-89.

- Skirnisdottir, S., Hreggvidsson, G. O., Hjorleifsdottir, S., Marteinson, V. T., Petursdottir, S. K., Holst, O. & Kristjansson, J. K. (2000).** Influence of sulfide and temperature on species composition and community structure of hot spring microbial mats. *Applied and Environmental Microbiology* **66**, 2835-2841.
- Smith, C. J., Nedwell, D. B., Dong, L. F. & Osborn, A. M. (2006).** Evaluation of quantitative polymerase chain reaction-based approaches for determining gene copy and gene transcript numbers in environmental samples. *Environmental Microbiology* **8**, 804-815.
- Smith, R. L. & Maguire, M. E. (1998).** Microbial magnesium transport: unusual transporters searching for identity. *Molecular Microbiology* **28**, 217-226.
- Sonnenfeld, E. M., Beveridge, T. J. & Doyle, R. J. (1985a).** Discontinuity of charge on cell wall poles of *Bacillus subtilis*. *Canadian Journal of Microbiology* **31**, 875-877.
- Sonnenfeld, E. M., Beveridge, T. J., Koch, A. L. & Doyle, R. J. (1985b).** Asymmetric distribution of charge on the cell wall of *Bacillus subtilis*. *Journal of Bacteriology* **163**, 1167-1171.
- Spada, S., Pembroke, J. T. & Wall, J. G. (2002).** Isolation of a novel *Thermus thermophilus* metal efflux protein that improves *Escherichia coli* growth under stress conditions. *Extremophiles* **6**, 301-308.
- Spear, J. R., Walker, J. J. & Pace, N. R. (2005).** Hydrogen and primary production: Inference of biogeochemistry from phylogeny in a geothermal ecosystem. In *Geothermal biology and geochemistry in Yellowstone National Park*, pp. 113-127. Edited by W. P. Inskeep & T. R. McDermott: Thermal Biology Institute, Montana State University.
- Stetter, K. O. (1986).** Diversity of extremely thermophilic archaeobacteria. In *Thermophiles: General, molecular and applied microbiology*, pp. 39-74. Edited

by T. D. Brock. New York: Wiley & Sons.

Stetter, K. O. (1996). Hyperthermophilic prokaryotes. *FEMS Microbiology Review* **18**, 149-158.

Stöhr, R., Waberski, A., Volker, H., Tindall, B. J. & Thomm, M. (2001a). *Hydrogenothermus marinus* gen. nov., sp. nov., a novel thermophilic hydrogen-oxidizing bacterium, recognition of *Calderobacterium hydrogenophilum* as a member of the genus *Hydrogenobacter* and proposal of the reclassification of *Hydrogenobacter acidophilus* as *Hydrogenobaculum acidophilum* gen. nov., comb. nov., in the phylum 'Hydrogenobacter/Aquifex'. *International Journal of Systematic and Evolutionary Microbiology* **51**, 1853-1862.

Stöhr, R., Waberski, A., Volker, H., Tindall, B. J. & Thomm, M. (2001b). *Hydrogenothermus marinus* gen. nov., sp. nov., a novel thermophilic hydrogen-oxidizing bacterium, recognition of *Calderobacterium hydrogenophilum* as a member of the genus *Hydrogenobacter* and proposal of the reclassification of *Hydrogenobacter acidophilus* as *Hydrogenobaculum acidophilum* gen. nov., comb. nov., in the phylum 'Hydrogenobacter/Aquifex'. *International Journal of Systematic and Evolutionary Microbiology* **51**, 1853-1862.

Stolz, J. E., Basu, P., Santini, J. M. & Oremland, R. S. (2006). Arsenic and selenium in microbial metabolism. *Annual Review of Microbiology* **60**, 107-130.

Stolz, J. F. & Oremland, R. S. (1999). Bacterial respiration of arsenic and selenium. *FEMS Microbiology Review* **23**, 615-627.

Straub, K. L., Benz, M. & Schink, B. (2001). Iron metabolism in anoxic environments at near neutral pH. *FEMS Microbiology Ecology* **34**, 181-186.

Sundaram, T. K. (1986). Physiology and growth of thermophilic bacteria. In *Thermophiles: General, molecular and applied microbiology*. Edited by T. D. Brock. New York: John Wiley & Sons.

- Sunna, A. & Bergquist, P. (2003).** A gene encoding a novel extremely thermostable 1,4-beta-xylanase isolated directly from an environmental DNA sample. *Extremophiles* **7**, 63-70.
- Suzuki, M. T. & Giovannoni, S. J. (1996).** Bias caused by template annealing in the amplification of mixtures of 16S rRNA genes by PCR. *Applied and Environmental Microbiology* **62**, 625-630.
- Svetlichny, V. A., Sokolova, T. G., Zavarzin, G. A., Gerhardt, M. & Ringpfeil, T. (1991).** *Carboxydothemus hydrogenoformans* gen. nov., sp. nov., a CO₂-utilizing thermophilic anaerobic bacterium from hydrothermal environments of Kunashir Island. *Systematics and Applied Microbiology* **14**, 254-260.
- Takai, K., Kobayashi, H., Nealson, K. H. & Horikoshi, K. (2003a).** *Sulfurihydrogenibium subterraneum* gen. nov., sp. nov., from a subsurface hot aquifer. *International Journal of Systematic and Evolutionary Microbiology* **53**, 823-827.
- Takai, K., Kobayashi, H., Nealson, K. H. & Horikoshi, K. (2003b).** *Sulfurihydrogenibium subterraneum* gen. nov., sp. nov., from a subsurface hot aquifer. *International Journal of Systematic and Evolutionary Microbiology* **53**, 823-827.
- Takai, K., Nakagawa, S., Sako, Y. & Horikoshi, K. (2003c).** *Balnearium lithotrophicum* gen. nov., sp. nov., a novel thermophilic, strictly anaerobic, hydrogen-oxidizing chemolithoautotroph isolated from a black smoker chimney in the Suiyo Seamount hydrothermal system. *International Journal of Systematic and Evolutionary Microbiology* **53**, 1947-1954.
- Tansey, M. R. & Brock, T. D. (1972).** The upper temperature limit for eukaryotic organisms. *Proceedings of the National Academy of Sciences of the United States of America* **69**, 2426-2428.
- Tivey, M. K. (1998).** How to build a black smoker chimney: The formation of

mineral deposits at mid-ocean ridges. In *Oceanus*, pp. 22-26.

Udo, E. E., Jacob, L. E. & Mathew, B. (2000). A cadmium resistance plasmid, pXU5, in *Staphylococcus aureus*, strain ATCC25923. *FEMS Microbiology Letters* **189**, 79-80.

Unz, R. F. & Shuttleworth, K. L. (1996). Microbial mobilization and immobilization of heavy metals. *Current Opinion in Biotechnology* **7**, 307-310.

van der Wal, A., Minor, M., Norde, W., Zehnder, A. J. B. & Lyklema, J. (1997). Electrokinetic potential of bacterial cells. *Langmuir* **13**, 165-171.

Vecchio, A., Finoli, C., Di Simine, D. & Andreoni, V. (1998). Heavy metal biosorption by bacterial cells. *Fresenius Journal of Analytical Chemistry* **361**, 338-342.

Vig, K., Megharaj, M., Sethunathan, N. & Naidu, R. (2003). Bioavailability and toxicity of cadmium to microorganisms and their activities in soil: a review. *Advances in Environmental Research* **8**, 121-135.

Volesky, B. & Holan, Z. R. (1995). Biosorption of heavy metals. *Biotechnology Progress* **11**, 235-250.

von Wintzingerode, F., Gobel, U. B. & Stackebrandt, E. (1997). Determination of microbial diversity in environmental samples: pitfalls of PCR-based rRNA analysis. *FEMS Microbiology Review* **21**, 213-229.

Watt, R. K. & Ludden, P. W. (1999). Nickel-binding proteins. *Cellular and Molecular Life Sciences* **56**, 604-625.

Westall, J. C. (1982). FITEQL: A computer program for determination of chemical equilibrium constants from experimental data: Version 2.0: Department of Chemistry, Oregon State University.

- Wetzel, R. G. & Likens, G. E. (2000).** *Limnological Analysis*. New York: Springer-Verlag.
- WHO (2004).** *Guidelines for drinking-water quality: Volume 1 - Recommendations*, 3 edn. Geneva: World Health Organization.
- Wightman, P. G., Fein, J. B., Wesolowski, D. J., Phelps, T. J., Benezeth, P. & Palmer, D. A. (2001).** Measurement of bacterial surface protonation constants for two species at elevated temperatures. *Geochimica et Cosmochimica Acta* **65**, 3657-3669.
- Williams, J. G., Kubelik, A. R., Livak, K. J., Rafalsk, J. A. & Tingly, S. V. (1990).** DNA polymorphisms amplified by arbitrary primers are useful as genetic markers. *Nucleic Acids Research* **18**, 6531-6535.
- Woese, C. R., Kandler, O. & Wheelis, M. L. (1990).** Towards a natural system of organisms: proposal for the domains Archaea, Bacteria, and Eucarya. *Proceedings of the National Academy of Sciences of the United States of America* **87**, 4576-4579.
- Xue, Y. F., Xu, Y., Liu, Y., Ma, Y. H. & Zhou, P. J. (2001).** *Thermoanaerobacter tengcongensis* sp. nov., a novel anaerobic, saccharolytic, thermophilic bacterium isolated from a hot spring in Tengcong, China. *International Journal of Systematic and Evolutionary Microbiology* **51**, 1335-1341.
- Yee, N. & Fein, J. (2001).** Cd adsorption onto bacterial surfaces: A universal adsorption edge? *Geochimica et Cosmochimica Acta* **65**, 2037-2042.
- Yee, N., Fowle, D. A. & Ferris, F. G. (2004).** A Donnan potential model for metal sorption onto *Bacillus subtilis*. *Geochimica et Cosmochimica Acta* **68**, 3657-3664.
- Yilmaz, E. I. (2003).** Metal tolerance and biosorption capacity of *Bacillus*

circulans strain EB1. *Research in Microbiology* **154**, 409-415.

Zeigler, D. R. (2001). *Bacillus Genetic Stock Center, Catalog of Strains*, 7 edn.

Zheng, Z. W., Fang, W., Lee, H. Y. & Yang, Z. Y. (2005). Responses of *Azorhizobium caulinodans* to cadmium stress. *FEMS Microbiology Ecology* **54**, 455-461.

Zinoni, F., Birkmann, A., Stadtman, T. C. & Bock, A. (1986). Nucleotide sequence and expression of the selenocysteine-containing polypeptide of formate dehydrogenase (formate-hydrogen-lyase-linked) from *Escherichia coli*. *Proceedings of the National Academy of Sciences of the United States of America* **83**, 4650-4654.

Zobrist, J., Dowdle, P. R., Davis, J. A. & Oremland, R. S. (2000). Mobilization of arsenite by dissimilatory reduction of adsorbed arsenate. *Environmental Science and Technology* **34**, 4747-4753.

Appendix A: Growth curves

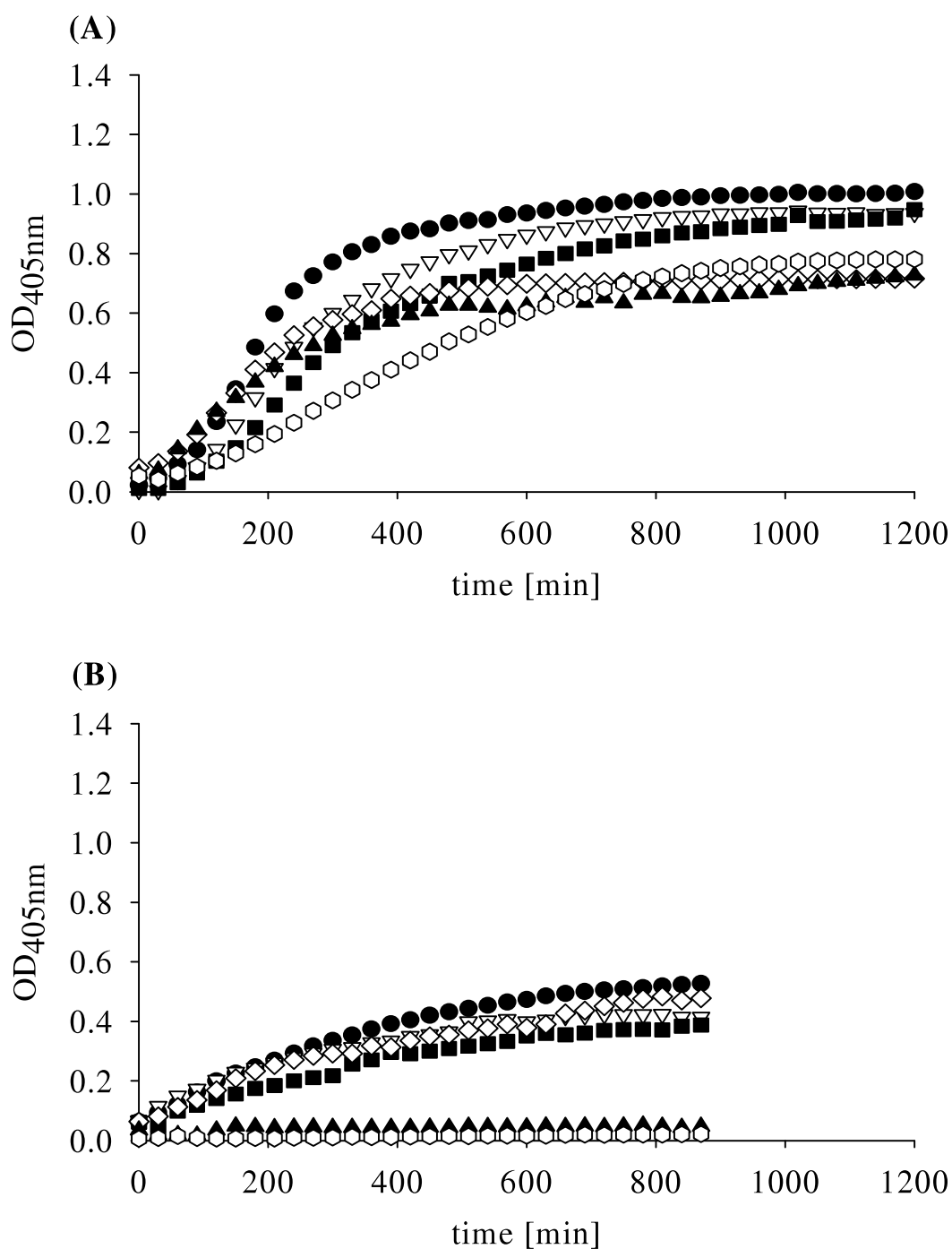


Figure 34. Microbial growth monitored spectrophotometrically at 405 nm as a function of concentration of Cd²⁺ (black circles: 0 μM, white triangles: 100 μM, black squares: 200 μM, white diamonds: 400 μM, black triangles: 600 μM, white hexagons: 800 μM). (A) Growth curves for *B. mycoides* (DSM 299) and (B) growth curves for *G. thermocatenulatus* (DSM 730). For clarity, only every second data point is shown.

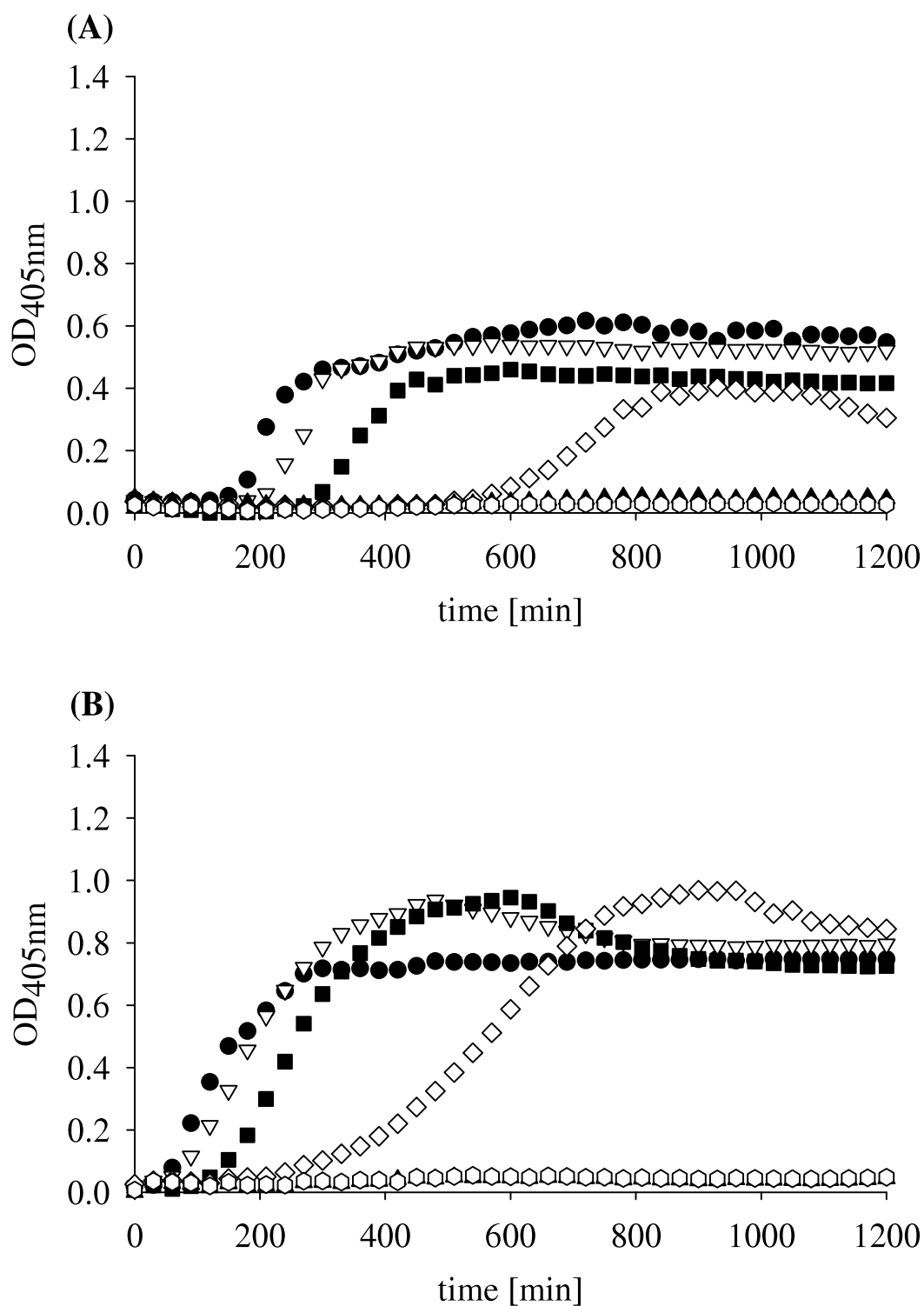


Figure 35. Microbial growth monitored spectrophotometrically at 405 nm as a function of concentration of Cd²⁺ (black circles: 0 μM, white triangles: 100 μM, black squares: 200 μM, white diamonds: 400 μM, black triangles: 600 μM, white hexagons: 800 μM). (A) Growth curves for *G. thermoglucosidasius* (DSM 2543) and (B) growth curves for TOK13.A4. For clarity, only every second data point is shown.

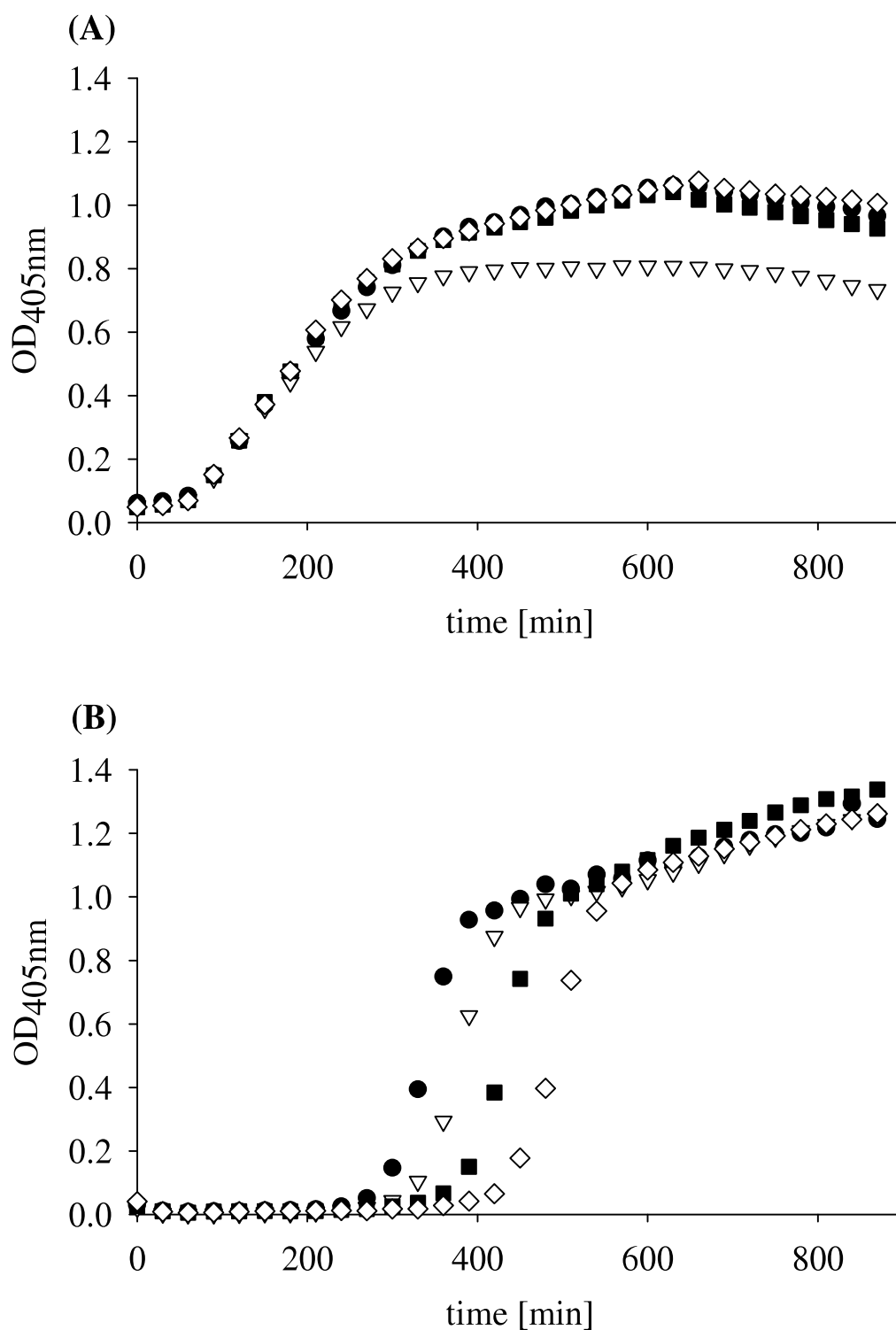


Figure 36. Microbial growth monitored spectrophotometrically at 405 nm as a function of concentration of As⁵⁺ (black circles: 0 μM, white triangles: 2 μM, black squares: 4 μM, white diamonds: 8 μM). (A) Growth curves for *G. thermoleovorans* (DSM 5366) and (B) growth curves for *G. stearothermophilus* (DSM 6790). For clarity, only every second data point is shown.

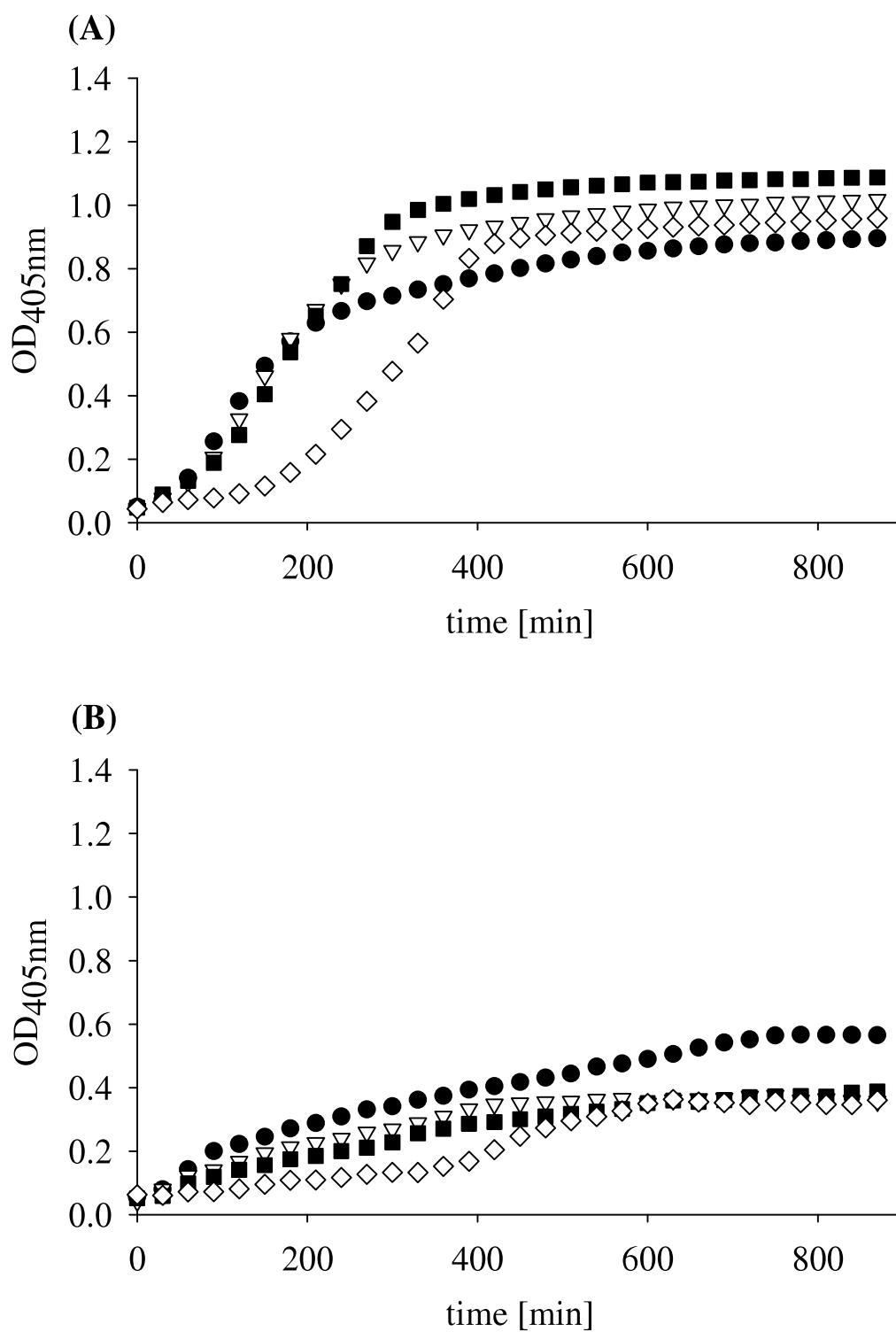


Figure 37. Microbial growth monitored spectrophotometrically at 405 nm as a function of concentration of As⁵⁺ (black circles: 0 μM, white triangles: 2 μM, black squares: 4 μM, white diamonds: 8 μM). (A) Growth curves for *B. mycoides* (DSM 299) and (B) growth curves for *G. thermocatenulatus* (DSM 730). For clarity, only every second data point is shown.

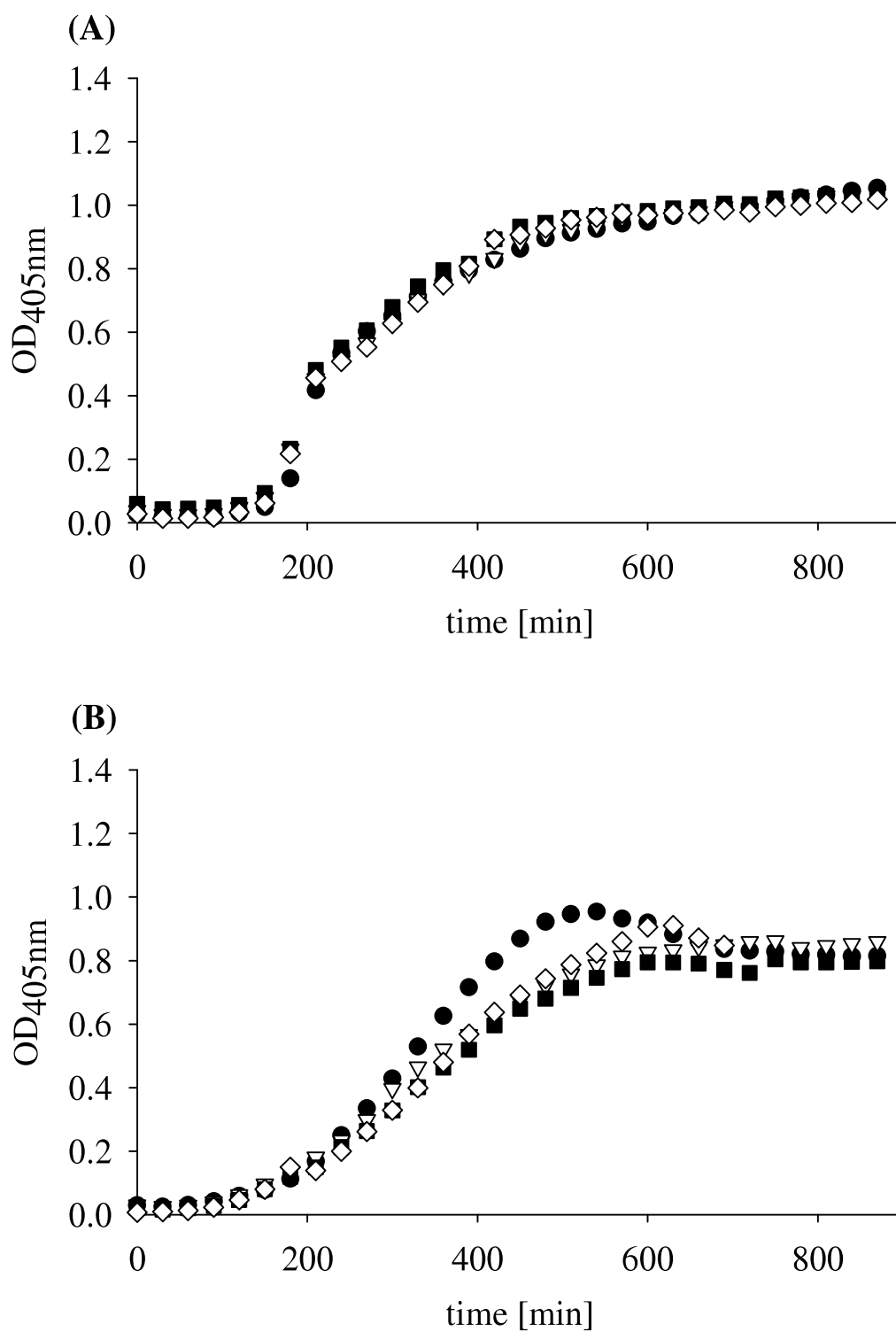


Figure 38. Microbial growth monitored spectrophotometrically at 405 nm as a function of concentration of As⁵⁺ (black circles: 0 μM, white triangles: 2 μM, black squares: 4 μM, white diamonds: 8 μM). (A) Growth curves for *G. thermoglucosidasius* (DSM 2543) and (B) growth curves for TOK13.A4. For clarity, only every second data point is shown.

Appendix B: One-site and two-site models

Table 15. One-site SCMs calculated for each individual dataset obtained from Cd^{2+} adsorption experiments using *G. thermocatenulatus* cells (DSM 730).

Dataset	$\text{p}K_1$	$\text{p}K_2$	$\text{p}K_3$	$V(Y)$
Set 1, subset A	1.608	-	-	0.077
Set 1, subset A	-	1.712	-	1.074
Set 1, subset A	-	-	2.123	1.193
Set 1, subset B	1.523	-	-	0.111
Set 1, subset B	-	1.506	-	2.876
Set 1, subset B	-	-	1.948	3.221
Set 1, subset C	1.295	-	-	0.235
Set 1, subset C	-	1.017	-	7.803
Set 1, subset C	-	-	1.438	1.127
Set 2, subset A	1.564	-	-	0.166
Set 2, subset A	-	1.352	-	1.218
Set 2, subset A	-	-	1.761	1.278
Set 2, subset B	1.221	-	-	1.855
Set 2, subset B	-	0.737	-	5.999
Set 2, subset B	-	-	1.168	7.575
Set 2, subset C	1.227	-	-	0.698
Set 2, subset C	-	0.756	-	3.183
Set 2, subset C	-	-	1.316	9.612
Set 3, subset A	1.154	-	-	0.996
Set 3, subset A	-	0.632	-	2.045
Set 3, subset A	-	-	1.025	2.141
Set 3, subset B	0.984	-	-	3.872
Set 3, subset B	-	0.408	-	6.548
Set 3, subset B	-	-	0.807	7.662
Set 3, subset C	1.137	-	-	1.569
Set 3, subset C	-	0.618	-	4.901
Set 3, subset C	-	-	1.056	6.982

Table 15. Continued.

Dataset	pK_1	pK_2	pK_3	$V(Y)$
Set 1	1.342	-	-	0.458
Set 1	-	1.091	-	4.114
Set 1	-	-	1.525	5.302
Set 2	1.231	-	-	1.076
Set 2	-	0.750	-	3.533
Set 2	-	-	1.237	6.261
Set 3	1.071	-	-	2.409
Set 3	-	0.520	-	4.778
Set 3	-	-	0.932	5.916
Set 1, 2 and 3	1.185	-	-	1.807
Set 1, 2 and 3	-	0.672	-	4.776
Set 1, 2 and 3	-	-	1.122	6.682

Table 16. One-site SCMs calculated for each individual dataset obtained from Cd^{2+} adsorption experiments using *G. stearotheophilus* cells (DSM 6790).

Dataset	pK_1	pK_2	pK_3	$V(Y)$
Set 1, subset A	2.458	-	-	0.742
Set 1, subset A	-	2.852	-	8.138
Set 1, subset A	-	-	2.904	8.457
Set 1, subset B	2.262	-	-	1.516
Set 1, subset B	-	2.367	-	17.930
Set 1, subset B	-	-	2.416	18.660
Set 1, subset C	2.280	-	-	0.949
Set 1, subset C	-	3.174	-	10.920
Set 1, subset C	-	-	3.302	14.830
Set 2, subset A	1.933	-	-	6.157
Set 2, subset A	-	1.544	-	9.526
Set 2, subset A	-	-	1.590	9.554
Set 2, subset B	2.221	-	-	2.112
Set 2, subset B	-	2.017	-	10.060
Set 2, subset B	-	-	2.067	10.270
Set 2, subset C	2.327	-	-	1.102
Set 2, subset C	-	2.573	-	14.010
Set 2, subset C	-	-	2.636	14.980
Set 3, subset A	2.120	-	-	3.357
Set 3, subset A	-	1.828	-	7.344
Set 3, subset A	-	-	1.876	7.387
Set 3, subset B	1.992	-	-	5.270
Set 3, subset B	-	1.664	-	11.260
Set 3, subset B	-	-	1.713	11.530
Set 3, subset C	2.234	-	-	2.278
Set 3, subset C	-	2.197	-	14.210
Set 3, subset C	-	-	2.250	14.820

Table 16. Continued.

Dataset	pK_1	pK_2	pK_3	$V(Y)$
Set 1	2.467	-	-	1.892
Set 1	-	2.883	-	18.190
Set 1	-	-	2.951	20.080
Set 2	2.278	-	-	6.973
Set 2	-	1.991	-	18.350
Set 2	-	-	2.038	18.720
Set 3	2.199	-	-	5.735
Set 3	-	1.909	-	13.180
Set 3	-	-	1.959	13.490
Set 1, 2 and 3	2.303	-	-	5.905
Set 1, 2 and 3	-	2.065	-	20.090
Set 1, 2 and 3	-	-	2.104	20.510

Table 17. Two-site SCMs generated for each individual dataset obtained from Cd^{2+} adsorption experiments using *G. thermocatenulatus* cells (DSM 730).

Dataset	$\text{p}K_1$	$\text{p}K_2$	$\text{p}K_3$	$V(Y)$
Set 1, subset A	N. C. ^a	N. C.	-	
Set 1, subset A	N. C.	-	N. C.	
Set 1, subset A	-	N. C.	N. C.	
Set 1, subset B	N. C.	N. C.	-	
Set 1, subset B	N. C.	-	N. C.	
Set 1, subset B	-	N. C.	N. C.	
Set 1, subset C	N. C.	N. C.	-	
Set 1, subset C	N. C.	-	N. C.	
Set 1, subset C	-	N. C.	N. C.	
Set 2, subset A	N. C.	N. C.	-	
Set 2, subset A	N. C.	-	N. C.	
Set 2, subset A	-	N. C.	N. C.	
Set 2, subset B	N. C.	N. C.	-	
Set 2, subset B	N. C.	-	N. C.	
Set 2, subset B	-	N. C.	N. C.	
Set 2, subset C	N. C.	N. C.	-	
Set 2, subset C	N. C.	-	N. C.	
Set 2, subset C	-	N. C.	N. C.	
Set 3, subset A	N. C.	N. C.	-	
Set 3, subset A	N. C.	-	N. C.	
Set 3, subset A	-	N. C.	N. C.	
Set 3, subset B	N. C.	N. C.	-	
Set 3, subset B	N. C.	-	N. C.	
Set 3, subset B	-	N. C.	N. C.	
Set 3, subset C	N. C.	N. C.	-	
Set 3, subset C	N. C.	-	N. C.	
Set 3, subset C	-	N. C.	N. C.	

Table 17. Continued.

Dataset	pK_1	pK_2	pK_3	$V(Y)$
Set 1	N. C.	N. C.	-	
Set 1	N. C.	-	N. C.	
Set 1	-	N. C.	N. C.	
Set 2	N. C.	N. C.	-	
Set 2	N. C.	-	N. C.	
Set 2	-	N. C.	N. C.	
Set 3	N. C.	N. C.	-	
Set 3	N. C.	-	N. C.	
Set 3	-	N. C.	N. C.	
Set 1, 2 and 3	N. C.	N. C.	-	
Set 1, 2 and 3	N. C.	-	N. C.	
Set 1, 2 and 3	-	N. C.	N. C.	

^a N. C., data which does not converge.

Table 18. Two-site SCMs generated for each individual dataset obtained from Cd^{2+} adsorption experiments using *G. stearotheophilus* cells (DSM 6790).

Dataset	pK_1	pK_2	pK_3	$V(Y)$
Set 1, subset A	N. C. ^a	N. C.	-	
Set 1, subset A	N. C.	-	N. C.	
Set 1, subset A	-	N. C.	N. C.	
Set 1, subset B	N. C.	N. C.	-	
Set 1, subset B	N. C.	-	N. C.	
Set 1, subset B	-	N. C.	N. C.	
Set 1, subset C	2.373	4.284	-	0.501
Set 1, subset C	2.348	-	4.535	0.557
Set 1, subset C	-	N. C.	N. C.	
Set 2, subset A	N. C.	N. C.	-	
Set 2, subset A	N. C.	-	N. C.	
Set 2, subset A	-	N. C.	N. C.	
Set 2, subset B	N. C.	N. C.	-	
Set 2, subset B	N. C.	-	N. C.	
Set 2, subset B	-	N. C.	N. C.	
Set 2, subset C	2.337	4.573	-	1.202
Set 2, subset C	2.337	-	4.604	1.200
Set 2, subset C	-	N. C.	N. C.	
Set 3, subset A	N. C.	N. C.	-	
Set 3, subset A	N. C.	-	N. C.	
Set 3, subset A	-	N. C.	N. C.	
Set 3, subset B	N. C.	N. C.	-	
Set 3, subset B	N. C.	-	N. C.	
Set 3, subset B	-	N. C.	N. C.	
Set 3, subset C	N. C.	N. C.	-	
Set 3, subset C	N. C.	-	N. C.	
Set 3, subset C	-	N. C.	N. C.	

Table 18. Continued.

Dataset	pK_1	pK_2	pK_3	$V(Y)$
Set 1	2.460	5.205	-	1.953
Set 1	2.464	-	5.060	1.958
Set 1	-	N. C.	N. C.	
Set 2	N. C.	N. C.	-	
Set 2	N. C.	-	N. C.	
Set 2	-	N. C.	N. C.	
Set 3	N. C.	N. C.	-	
Set 3	N. C.	-	N. C.	
Set 3	-	N. C.	N. C.	
Set 1, 2 and 3	N. C.	N. C.	-	
Set 1, 2 and 3	N. C.	-	N. C.	
Set 1, 2 and 3	-	N. C.	N. C.	

^a N. C., data which does not converge.

Appendix C: Surface complexation model data

Table 19. Dataset 1 obtained from titration experiments using *G. thermocatenulatus* cells (24.70 g wet cells). Proton concentration (H^+) in mol per liter.

Added H^+	pH	Dilution factor	Added H^+	pH	Dilution factor
-6.72E-04	4.03	0.985	-1.88E-03	7.58	0.959
-7.38E-04	4.14	0.983	-1.89E-03	7.72	0.959
-8.02E-04	4.26	0.982	-1.91E-03	7.86	0.958
-8.56E-04	4.29	0.981	-1.93E-03	8.01	0.958
-9.74E-04	4.50	0.979	-1.94E-03	8.09	0.958
-1.04E-03	4.63	0.977	-1.95E-03	8.21	0.958
-1.08E-03	4.73	0.976	-1.95E-03	8.27	0.957
-1.13E-03	4.84	0.975	-1.96E-03	8.37	0.957
-1.18E-03	4.94	0.974	-1.97E-03	8.47	0.957
-1.23E-03	5.05	0.973	-1.98E-03	8.60	0.957
-1.29E-03	5.18	0.972	-2.00E-03	8.73	0.956
-1.33E-03	5.27	0.971	-2.01E-03	8.87	0.956
-1.37E-03	5.38	0.970	-2.03E-03	9.00	0.956
-1.42E-03	5.49	0.969	-2.04E-03	9.12	0.955
-1.47E-03	5.62	0.968	-2.06E-03	9.25	0.955
-1.51E-03	5.75	0.967	-2.09E-03	9.37	0.955
-1.55E-03	5.87	0.966	-2.11E-03	9.49	0.954
-1.59E-03	6.00	0.965	-2.14E-03	9.60	0.953
-1.61E-03	6.09	0.965	-2.18E-03	9.72	0.953
-1.65E-03	6.21	0.964	-2.22E-03	9.83	0.952
-1.68E-03	6.35	0.964	-2.27E-03	9.92	0.951
-1.70E-03	6.43	0.963	-2.33E-03	10.04	0.950
-1.72E-03	6.55	0.963	-7.04E-04	4.10	0.940
-1.73E-03	6.58	0.962	-7.22E-04	4.13	0.939
-1.73E-03	6.59	0.962	-7.81E-04	4.23	0.938
-1.77E-03	6.82	0.961	-8.42E-04	4.35	0.937
-1.80E-03	6.98	0.961	-9.01E-04	4.47	0.936
-1.81E-03	7.03	0.961	-9.51E-04	4.57	0.935
-1.81E-03	7.05	0.961	-1.00E-03	4.68	0.934
-1.83E-03	7.25	0.960	-1.06E-03	4.80	0.933
-1.85E-03	7.37	0.960	-1.11E-03	4.91	0.932
-1.86E-03	7.42	0.960	-1.16E-03	5.03	0.931

Table 19. Continued.

Added H ⁺	pH	Dilution factor	Added H ⁺	pH	Dilution factor
-1.21E-03	5.14	0.930	-1.91E-03	8.62	0.915
-1.26E-03	5.26	0.929	-1.92E-03	8.75	0.915
-1.30E-03	5.38	0.928	-1.93E-03	8.88	0.914
-1.35E-03	5.50	0.927	-1.95E-03	9.01	0.914
-1.39E-03	5.62	0.926	-1.97E-03	9.13	0.914
-1.43E-03	5.64	0.925	-1.99E-03	9.25	0.913
-1.55E-03	6.02	0.922	-2.01E-03	9.37	0.913
-1.59E-03	6.17	0.922	-2.04E-03	9.49	0.912
-1.61E-03	6.27	0.921	-2.07E-03	9.60	0.912
-1.62E-03	6.31	0.921	-2.11E-03	9.72	0.911
-1.63E-03	6.36	0.921	-2.15E-03	9.82	0.910
-1.65E-03	6.43	0.921	-2.20E-03	9.92	0.910
-1.67E-03	6.57	0.920	-2.26E-03	10.03	0.909
-1.68E-03	6.64	0.920			
-1.70E-03	6.75	0.919			
-1.71E-03	6.82	0.919			
-1.73E-03	6.97	0.919			
-1.74E-03	7.00	0.919			
-1.74E-03	7.02	0.919			
-1.76E-03	7.17	0.918			
-1.77E-03	7.28	0.918			
-1.79E-03	7.41	0.918			
-1.80E-03	7.58	0.917			
-1.81E-03	7.62	0.917			
-1.81E-03	7.65	0.917			
-1.83E-03	7.81	0.917			
-1.85E-03	7.95	0.916			
-1.86E-03	8.10	0.916			
-1.87E-03	8.20	0.916			
-1.88E-03	8.34	0.916			
-1.89E-03	8.43	0.915			
-1.90E-03	8.55	0.915			

Table 20. Dataset 2 obtained from titration experiments using *G. thermocatenulatus* cells (24.70 g wet cells). Proton concentration (H^+) in mol per liter.

Added H^+	pH	Dilution factor	Added H^+	pH	Dilution factor
-5.72E-04	4.04	0.963	-1.86E-03	7.65	0.936
-6.39E-04	4.14	0.961	-1.88E-03	7.80	0.936
-7.06E-04	4.25	0.960	-1.89E-03	7.89	0.935
-7.70E-04	4.36	0.959	-1.90E-03	8.04	0.935
-8.34E-04	4.46	0.958	-1.91E-03	8.11	0.935
-8.97E-04	4.57	0.956	-1.92E-03	8.18	0.935
-9.58E-04	4.68	0.955	-1.92E-03	8.22	0.935
-1.02E-03	4.78	0.954	-1.94E-03	8.40	0.934
-1.08E-03	4.87	0.953	-1.94E-03	8.42	0.934
-1.15E-03	5.00	0.951	-1.96E-03	8.63	0.934
-1.21E-03	5.10	0.950	-1.98E-03	8.74	0.933
-1.27E-03	5.22	0.949	-1.99E-03	8.88	0.933
-1.32E-03	5.33	0.947	-2.01E-03	9.00	0.933
-1.38E-03	5.45	0.946	-2.03E-03	9.12	0.932
-1.42E-03	5.56	0.945	-2.05E-03	9.24	0.932
-1.47E-03	5.68	0.944	-2.08E-03	9.36	0.931
-1.51E-03	5.81	0.943	-2.10E-03	9.48	0.931
-1.54E-03	5.91	0.943	-2.14E-03	9.58	0.930
-1.58E-03	6.02	0.942	-2.18E-03	9.69	0.930
-1.61E-03	6.16	0.941	-2.22E-03	9.80	0.929
-1.64E-03	6.26	0.941	-2.27E-03	9.90	0.928
-1.66E-03	6.35	0.940	-2.33E-03	10.00	0.927
-1.69E-03	6.49	0.940	-6.17E-04	4.12	0.915
-1.71E-03	6.60	0.939	-6.82E-04	4.23	0.914
-1.73E-03	6.74	0.939	-7.42E-04	4.33	0.913
-1.75E-03	6.85	0.938	-8.04E-04	4.44	0.912
-1.77E-03	7.00	0.938	-8.66E-04	4.54	0.910
-1.78E-03	7.08	0.938	-9.27E-04	4.65	0.909
-1.80E-03	7.18	0.937	-9.85E-04	4.76	0.908
-1.81E-03	7.29	0.937	-1.04E-03	4.86	0.907
-1.82E-03	7.38	0.937	-1.10E-03	4.97	0.906
-1.84E-03	7.52	0.936	-1.16E-03	5.09	0.905

Table 20. Continued.

Added H ⁺	pH	Dilution factor	Added H ⁺	pH	Dilution factor
-1.21E-03	5.19	0.904	-1.88E-03	8.71	0.890
-1.26E-03	5.26	0.902	-1.90E-03	8.84	0.889
-1.34E-03	5.45	0.901	-1.92E-03	8.96	0.889
-1.39E-03	5.57	0.900	-1.94E-03	9.08	0.889
-1.43E-03	5.69	0.899	-1.96E-03	9.20	0.888
-1.47E-03	5.81	0.898	-1.99E-03	9.31	0.888
-1.50E-03	5.93	0.898	-2.02E-03	9.43	0.887
-1.53E-03	6.05	0.897	-2.05E-03	9.54	0.887
-1.56E-03	6.17	0.897	-2.09E-03	9.64	0.886
-1.58E-03	6.27	0.896	-2.14E-03	9.75	0.885
-1.61E-03	6.41	0.896	-2.19E-03	9.85	0.884
-1.63E-03	6.56	0.895	-2.25E-03	9.95	0.883
-1.64E-03	6.61	0.895	-2.31E-03	10.04	0.882
-1.65E-03	6.68	0.895			
-1.66E-03	6.73	0.894			
-1.68E-03	6.89	0.894			
-1.69E-03	6.95	0.894			
-1.70E-03	7.00	0.894			
-1.71E-03	7.06	0.893			
-1.72E-03	7.21	0.893			
-1.73E-03	7.29	0.893			
-1.74E-03	7.35	0.893			
-1.76E-03	7.51	0.892			
-1.77E-03	7.63	0.892			
-1.79E-03	7.77	0.892			
-1.80E-03	7.89	0.892			
-1.81E-03	8.02	0.891			
-1.82E-03	8.12	0.891			
-1.83E-03	8.22	0.891			
-1.84E-03	8.33	0.891			
-1.86E-03	8.45	0.890			
-1.87E-03	8.59	0.890			

Table 21. Dataset 3 obtained from titration experiments using *G. thermocatenulatus* cells (24.70 g wet cells). Proton concentration (H^+) in mol per liter.

Added H^+	pH	Dilution factor	Added H^+	pH	Dilution factor
-6.95E-04	4.01	0.970	-1.78E-03	7.40	0.947
-7.50E-04	4.11	0.968	-1.83E-03	7.80	0.946
-8.12E-04	4.22	0.967	-1.85E-03	7.97	0.945
-8.67E-04	4.33	0.966	-1.85E-03	8.00	0.945
-9.24E-04	4.45	0.965	-1.86E-03	8.01	0.945
-9.80E-04	4.56	0.964	-1.88E-03	8.28	0.945
-1.04E-03	4.68	0.963	-1.89E-03	8.37	0.944
-1.09E-03	4.79	0.962	-1.89E-03	8.38	0.944
-1.14E-03	4.90	0.961	-1.90E-03	8.40	0.944
-1.19E-03	5.02	0.959	-1.92E-03	8.62	0.944
-1.24E-03	5.13	0.958	-1.93E-03	8.72	0.943
-1.29E-03	5.25	0.957	-1.94E-03	8.73	0.943
-1.34E-03	5.38	0.956	-1.94E-03	8.74	0.943
-1.38E-03	5.47	0.955	-1.96E-03	8.94	0.943
-1.42E-03	5.58	0.955	-1.98E-03	9.03	0.942
-1.45E-03	5.69	0.954	-1.98E-03	9.05	0.942
-1.47E-03	5.75	0.953	-1.99E-03	9.07	0.942
-1.50E-03	5.86	0.953	-2.02E-03	9.24	0.942
-1.52E-03	5.95	0.952	-2.04E-03	9.34	0.941
-1.56E-03	6.08	0.952	-2.05E-03	9.36	0.941
-1.59E-03	6.24	0.951	-2.10E-03	9.53	0.940
-1.60E-03	6.27	0.951	-2.14E-03	9.65	0.939
-1.60E-03	6.30	0.951	-2.18E-03	9.74	0.939
-1.64E-03	6.50	0.950	-2.23E-03	9.84	0.938
-1.66E-03	6.62	0.949	-2.29E-03	9.94	0.937
-1.68E-03	6.74	0.949	-2.36E-03	10.03	0.935
-1.70E-03	6.87	0.949	-6.35E-04	4.03	0.917
-1.71E-03	6.96	0.948	-6.97E-04	4.14	0.916
-1.73E-03	7.06	0.948	-7.58E-04	4.26	0.915
-1.74E-03	7.16	0.948	-8.14E-04	4.36	0.914
-1.76E-03	7.31	0.947	-8.72E-04	4.47	0.913
-1.77E-03	7.38	0.947	-9.29E-04	4.58	0.912

Table 21. Continued.

Added H ⁺	pH	Dilution factor	Added H ⁺	pH	Dilution factor
-9.85E-04	4.69	0.911	-1.77E-03	8.12	0.895
-1.04E-03	4.80	0.910	-1.79E-03	8.27	0.894
-1.09E-03	4.89	0.909	-1.80E-03	8.39	0.894
-1.16E-03	5.02	0.907	-1.82E-03	8.53	0.894
-1.21E-03	5.14	0.906	-1.83E-03	8.65	0.894
-1.25E-03	5.25	0.905	-1.85E-03	8.78	0.893
-1.30E-03	5.36	0.904	-1.87E-03	8.91	0.893
-1.34E-03	5.48	0.904	-1.89E-03	9.03	0.892
-1.38E-03	5.61	0.903	-1.91E-03	9.15	0.892
-1.41E-03	5.73	0.902	-1.94E-03	9.26	0.891
-1.44E-03	5.84	0.902	-1.97E-03	9.38	0.891
-1.47E-03	5.95	0.901	-2.00E-03	9.48	0.890
-1.50E-03	6.08	0.900	-2.05E-03	9.60	0.889
-1.53E-03	6.25	0.900	-2.09E-03	9.70	0.889
-1.54E-03	6.28	0.900	-2.14E-03	9.80	0.888
-1.55E-03	6.33	0.899	-2.20E-03	9.90	0.887
-1.56E-03	6.38	0.899	-2.26E-03	9.99	0.886
-1.59E-03	6.57	0.899	-2.34E-03	10.08	0.884
-1.59E-03	6.59	0.899			
-1.60E-03	6.61	0.898			
-1.63E-03	6.86	0.898			
-1.64E-03	6.97	0.897			
-1.65E-03	7.02	0.897			
-1.67E-03	7.18	0.897			
-1.68E-03	7.22	0.897			
-1.69E-03	7.32	0.897			
-1.70E-03	7.42	0.896			
-1.72E-03	7.58	0.896			
-1.72E-03	7.63	0.896			
-1.73E-03	7.67	0.896			
-1.75E-03	7.85	0.895			
-1.76E-03	7.98	0.895			

Table 22. Dataset 1 obtained from titration experiments using *G. stearothermophilus* cells (12.96 g wet cells). Proton concentration (H^+) in mol per liter.

Added H^+	pH	Dilution factor	Added H^+	pH	Dilution factor
-2.76E-04	4.01	0.896	-1.21E-03	7.53	0.877
-3.31E-04	4.12	0.895	-1.21E-03	7.56	0.877
-3.79E-04	4.22	0.894	-1.23E-03	7.70	0.877
-4.28E-04	4.34	0.893	-1.25E-03	7.84	0.877
-4.72E-04	4.46	0.892	-1.26E-03	8.00	0.876
-5.17E-04	4.58	0.891	-1.27E-03	8.08	0.876
-5.59E-04	4.70	0.890	-1.28E-03	8.21	0.876
-6.00E-04	4.83	0.890	-1.29E-03	8.30	0.876
-6.39E-04	4.94	0.889	-1.30E-03	8.39	0.876
-6.79E-04	5.07	0.888	-1.32E-03	8.55	0.875
-7.17E-04	5.19	0.887	-1.33E-03	8.69	0.875
-7.55E-04	5.31	0.887	-1.34E-03	8.82	0.875
-7.94E-04	5.42	0.886	-1.36E-03	8.94	0.874
-8.35E-04	5.53	0.885	-1.37E-03	9.07	0.874
-8.80E-04	5.68	0.884	-1.39E-03	9.19	0.874
-9.16E-04	5.83	0.883	-1.41E-03	9.32	0.873
-9.36E-04	5.89	0.883	-1.44E-03	9.43	0.873
-9.48E-04	5.93	0.883	-1.47E-03	9.55	0.872
-9.88E-04	6.09	0.882	-1.50E-03	9.66	0.872
-1.02E-03	6.24	0.881	-1.54E-03	9.77	0.871
-1.04E-03	6.32	0.881	-1.58E-03	9.87	0.871
-1.06E-03	6.45	0.881	-1.64E-03	9.97	0.870
-1.07E-03	6.50	0.880	-1.70E-03	10.07	0.869
-1.09E-03	6.60	0.880	-2.50E-04	4.08	0.856
-1.10E-03	6.66	0.880	-3.08E-04	4.21	0.855
-1.12E-03	6.81	0.879	-3.53E-04	4.31	0.855
-1.13E-03	6.89	0.879	-4.02E-04	4.44	0.854
-1.15E-03	6.98	0.879	-4.44E-04	4.55	0.853
-1.16E-03	7.14	0.878	-4.87E-04	4.67	0.852
-1.17E-03	7.16	0.878	-5.30E-04	4.80	0.851
-1.17E-03	7.17	0.878	-5.70E-04	4.91	0.851
-1.19E-03	7.42	0.878	-6.11E-04	5.04	0.850

Table 22. Continued.

Added H ⁺	pH	Dilution factor	Added H ⁺	pH	Dilution factor
-6.51E-04	5.16	0.849	-1.24E-03	8.57	0.838
-6.91E-04	5.28	0.848	-1.25E-03	8.71	0.838
-7.31E-04	5.40	0.848	-1.27E-03	8.83	0.837
-7.71E-04	5.53	0.847	-1.29E-03	8.96	0.837
-8.09E-04	5.60	0.846	-1.30E-03	9.08	0.837
-8.66E-04	5.80	0.845	-1.33E-03	9.20	0.836
-9.01E-04	5.96	0.844	-1.35E-03	9.32	0.836
-9.18E-04	6.03	0.844	-1.38E-03	9.44	0.835
-9.43E-04	6.15	0.844	-1.41E-03	9.55	0.835
-9.59E-04	6.22	0.843	-1.45E-03	9.66	0.834
-9.85E-04	6.38	0.843	-1.49E-03	9.75	0.834
-9.96E-04	6.42	0.843	-1.54E-03	9.87	0.833
-1.00E-03	6.46	0.843	-1.60E-03	9.97	0.832
-1.01E-03	6.49	0.842	-1.66E-03	10.06	0.831
-1.02E-03	6.60	0.842			
-1.03E-03	6.65	0.842			
-1.05E-03	6.76	0.842			
-1.06E-03	6.82	0.842			
-1.07E-03	6.96	0.841			
-1.08E-03	7.01	0.841			
-1.09E-03	7.06	0.841			
-1.11E-03	7.26	0.841			
-1.12E-03	7.37	0.840			
-1.13E-03	7.43	0.840			
-1.14E-03	7.59	0.840			
-1.16E-03	7.73	0.839			
-1.17E-03	7.89	0.839			
-1.18E-03	7.97	0.839			
-1.19E-03	8.08	0.839			
-1.20E-03	8.19	0.839			
-1.22E-03	8.31	0.838			
-1.23E-03	8.44	0.838			

Table 23. Dataset 2 obtained from titration experiments using *G. stearotheophilus* cells (12.96 g wet cells). Proton concentration (H^+) in mol per liter.

Added H^+	pH	Dilution factor	Added H^+	pH	Dilution factor
-3.72E-04	4.09	0.987	-1.29E-03	7.39	0.967
-4.25E-04	4.20	0.986	-1.32E-03	7.60	0.967
-4.76E-04	4.32	0.985	-1.33E-03	7.72	0.966
-5.24E-04	4.44	0.984	-1.34E-03	7.78	0.966
-5.68E-04	4.55	0.983	-1.35E-03	7.83	0.966
-6.15E-04	4.67	0.982	-1.36E-03	8.00	0.966
-6.57E-04	4.78	0.981	-1.37E-03	8.03	0.966
-7.02E-04	4.90	0.980	-1.37E-03	8.04	0.966
-7.45E-04	5.02	0.979	-1.39E-03	8.30	0.965
-7.88E-04	5.13	0.978	-1.40E-03	8.40	0.965
-8.31E-04	5.25	0.977	-1.41E-03	8.41	0.965
-8.74E-04	5.38	0.977	-1.41E-03	8.42	0.965
-9.14E-04	5.50	0.976	-1.45E-03	8.88	0.964
-9.53E-04	5.62	0.975	-1.47E-03	8.98	0.963
-9.89E-04	5.73	0.974	-1.47E-03	8.99	0.963
-1.03E-03	5.85	0.973	-1.48E-03	9.00	0.963
-1.05E-03	5.97	0.973	-1.51E-03	9.21	0.963
-1.07E-03	6.03	0.972	-1.53E-03	9.29	0.962
-1.09E-03	6.13	0.972	-1.53E-03	9.30	0.962
-1.11E-03	6.18	0.971	-1.59E-03	9.53	0.961
-1.12E-03	6.24	0.971	-1.63E-03	9.64	0.960
-1.13E-03	6.30	0.971	-1.67E-03	9.73	0.959
-1.16E-03	6.48	0.970	-1.69E-03	9.77	0.959
-1.17E-03	6.50	0.970	-1.75E-03	9.88	0.958
-1.17E-03	6.51	0.970	-1.81E-03	9.98	0.957
-1.21E-03	6.77	0.969	-1.87E-03	10.08	0.956
-1.23E-03	6.93	0.969	-3.01E-04	4.02	0.944
-1.24E-03	6.98	0.969	-3.58E-04	4.14	0.943
-1.25E-03	7.00	0.968	-4.10E-04	4.26	0.942
-1.26E-03	7.11	0.968	-4.59E-04	4.37	0.941
-1.27E-03	7.27	0.968	-5.07E-04	4.49	0.940
-1.29E-03	7.34	0.967	-5.54E-04	4.61	0.940

Table 23. Continued.

Added H ⁺	pH	Dilution factor	Added H ⁺	pH	Dilution factor
-5.98E-04	4.72	0.939	-1.33E-03	8.33	0.923
-6.43E-04	4.84	0.938	-1.34E-03	8.44	0.923
-6.87E-04	4.96	0.937	-1.35E-03	8.45	0.923
-7.30E-04	5.07	0.936	-1.38E-03	8.72	0.922
-7.73E-04	5.19	0.935	-1.39E-03	8.81	0.922
-8.15E-04	5.31	0.934	-1.41E-03	8.96	0.922
-8.56E-04	5.44	0.933	-1.43E-03	9.04	0.921
-8.91E-04	5.55	0.933	-1.45E-03	9.19	0.921
-9.26E-04	5.62	0.932	-1.48E-03	9.29	0.920
-9.38E-04	5.66	0.932	-1.51E-03	9.41	0.920
-9.73E-04	5.81	0.931	-1.55E-03	9.51	0.919
-9.97E-04	5.91	0.930	-1.59E-03	9.62	0.918
-1.02E-03	6.04	0.930	-1.64E-03	9.72	0.917
-1.05E-03	6.15	0.929	-1.69E-03	9.82	0.916
-1.07E-03	6.29	0.929	-1.75E-03	9.92	0.915
-1.09E-03	6.40	0.928	-1.81E-03	10.01	0.914
-1.12E-03	6.55	0.928			
-1.13E-03	6.65	0.927			
-1.16E-03	6.80	0.927			
-1.17E-03	6.88	0.927			
-1.18E-03	6.95	0.927			
-1.20E-03	7.13	0.926			
-1.20E-03	7.15	0.926			
-1.21E-03	7.16	0.926			
-1.24E-03	7.48	0.925			
-1.26E-03	7.65	0.925			
-1.26E-03	7.69	0.925			
-1.27E-03	7.70	0.925			
-1.29E-03	7.97	0.924			
-1.30E-03	8.07	0.924			
-1.31E-03	8.08	0.924			
-1.31E-03	8.14	0.924			

Table 24. Data obtained from Cd^{2+} adsorption experiments using *G. thermocatenulatus* cells (19.71 g wet cells).

Dataset	Initial Cd^{2+} [mol/l]	Adsorbed Cd^{2+} [mol/l]	Final pH	Dilution factor
Set 1, subset A	4.19E-05	3.86E-05	5.55	0.796
Set 1, subset A	4.19E-05	3.92E-05	6.04	0.796
Set 1, subset A	4.19E-05	3.93E-05	6.23	0.796
Set 1, subset A	4.19E-05	3.94E-05	6.37	0.796
Set 1, subset A	4.19E-05	3.93E-05	6.51	0.796
Set 1, subset A	4.19E-05	3.93E-05	6.57	0.796
Set 1, subset A	4.19E-05	3.93E-05	6.72	0.796
Set 1, subset A	4.19E-05	3.94E-05	6.94	0.796
Set 1, subset A	4.19E-05	3.95E-05	7.15	0.796
Set 1, subset A	4.19E-05	3.94E-05	7.33	0.795
Set 1, subset B	4.42E-05	3.72E-05	5.42	0.462
Set 1, subset B	4.42E-05	3.96E-05	6.33	0.462
Set 1, subset B	4.42E-05	3.96E-05	6.08	0.462
Set 1, subset B	4.42E-05	4.00E-05	6.63	0.462
Set 1, subset B	4.42E-05	4.03E-05	6.89	0.462
Set 1, subset B	4.42E-05	4.04E-05	6.96	0.462
Set 1, subset B	4.42E-05	4.05E-05	7.00	0.462
Set 1, subset B	4.42E-05	4.05E-05	7.03	0.461
Set 1, subset B	4.42E-05	4.06E-05	7.40	0.461
Set 1, subset B	4.42E-05	4.03E-05	7.57	0.461
Set 1, subset C	4.32E-05	1.56E-05	4.45	0.233
Set 1, subset C	4.32E-05	2.98E-05	5.30	0.233
Set 1, subset C	4.32E-05	3.22E-05	5.58	0.233
Set 1, subset C	4.32E-05	3.48E-05	6.08	0.233
Set 1, subset C	4.32E-05	3.57E-05	6.33	0.233
Set 1, subset C	4.32E-05	3.67E-05	6.66	0.233
Set 1, subset C	4.32E-05	3.64E-05	6.71	0.233
Set 1, subset C	4.32E-05	3.72E-05	7.04	0.233
Set 1, subset C	4.32E-05	3.80E-05	7.34	0.233
Set 1, subset C	4.31E-05	3.79E-05	7.35	0.233

Table 24. Continued.

Dataset	Initial Cd ²⁺ [mol/l]	Adsorbed Cd ²⁺ [mol/l]	Final pH	Dilution factor
Set 2, subset A	3.99E-05	3.49E-05	5.06	0.886
Set 2, subset A	3.99E-05	3.64E-05	5.41	0.886
Set 2, subset A	3.99E-05	3.66E-05	5.61	0.886
Set 2, subset A	3.99E-05	3.68E-05	5.71	0.886
Set 2, subset A	3.99E-05	3.68E-05	5.79	0.886
Set 2, subset A	3.99E-05	3.71E-05	5.93	0.886
Set 2, subset A	3.99E-05	3.72E-05	6.04	0.886
Set 2, subset A	3.99E-05	3.72E-05	6.26	0.886
Set 2, subset A	3.99E-05	3.73E-05	6.35	0.886
Set 2, subset A	3.98E-05	3.72E-05	6.50	0.886
Set 2, subset A	3.98E-05	3.73E-05	6.66	0.886
Set 2, subset A	3.98E-05	3.73E-05	6.81	0.886
Set 2, subset B	4.35E-05	1.15E-05	3.99	0.386
Set 2, subset B	4.35E-05	1.73E-05	4.23	0.385
Set 2, subset B	4.35E-05	1.98E-05	4.35	0.385
Set 2, subset B	4.35E-05	2.48E-05	4.59	0.385
Set 2, subset B	4.35E-05	2.71E-05	4.70	0.385
Set 2, subset B	4.35E-05	2.93E-05	4.84	0.385
Set 2, subset B	4.35E-05	3.21E-05	5.06	0.385
Set 2, subset B	4.35E-05	3.38E-05	5.24	0.385
Set 2, subset B	4.35E-05	3.55E-05	5.43	0.385
Set 2, subset B	4.35E-05	3.67E-05	5.76	0.385
Set 2, subset B	4.35E-05	3.79E-05	6.06	0.385
Set 2, subset B	4.35E-05	3.84E-05	6.25	0.385
Set 2, subset C	4.34E-05	3.10E-06	3.72	0.176
Set 2, subset C	4.34E-05	4.23E-06	3.85	0.176
Set 2, subset C	4.34E-05	4.54E-06	3.93	0.176
Set 2, subset C	4.34E-05	5.86E-06	4.00	0.176
Set 2, subset C	4.34E-05	7.26E-06	4.13	0.176
Set 2, subset C	4.34E-05	8.56E-06	4.21	0.176
Set 2, subset C	4.34E-05	1.30E-05	4.47	0.176
Set 2, subset C	4.34E-05	1.94E-05	4.80	0.176
Set 2, subset C	4.34E-05	2.19E-05	4.96	0.176
Set 2, subset C	4.34E-05	2.34E-05	5.10	0.176
Set 2, subset C	4.34E-05	3.08E-05	5.80	0.176
Set 2, subset C	4.34E-05	3.21E-05	6.06	0.176

Table 24. Continued.

Dataset	Initial Cd ²⁺ [mol/l]	Adsorbed Cd ²⁺ [mol/l]	Final pH	Dilution factor
Set 3, subset A	4.21E-05	2.37E-05	4.09	0.999
Set 3, subset A	4.21E-05	2.88E-05	4.29	0.999
Set 3, subset A	4.21E-05	3.29E-05	4.53	0.999
Set 3, subset A	4.21E-05	3.54E-05	4.76	0.999
Set 3, subset A	4.21E-05	3.67E-05	4.95	0.999
Set 3, subset A	4.21E-05	3.73E-05	5.09	0.999
Set 3, subset A	4.21E-05	3.85E-05	5.49	0.999
Set 3, subset A	4.20E-05	3.90E-05	5.62	0.999
Set 3, subset A	4.20E-05	3.92E-05	5.92	0.999
Set 3, subset A	4.20E-05	3.94E-05	6.32	0.999
Set 3, subset A	4.20E-05	3.96E-05	6.55	0.999
Set 3, subset A	4.20E-05	3.96E-05	6.85	0.999
Set 3, subset B	4.44E-05	5.76E-06	3.44	0.444
Set 3, subset B	4.44E-05	6.57E-06	3.48	0.444
Set 3, subset B	4.44E-05	7.20E-06	3.59	0.444
Set 3, subset B	4.44E-05	9.45E-06	3.73	0.444
Set 3, subset B	4.44E-05	1.24E-05	3.88	0.444
Set 3, subset B	4.44E-05	1.42E-05	3.97	0.444
Set 3, subset B	4.44E-05	2.00E-05	4.25	0.444
Set 3, subset B	4.44E-05	3.14E-05	4.82	0.444
Set 3, subset B	4.44E-05	3.53E-05	5.10	0.444
Set 3, subset B	4.44E-05	3.84E-05	5.56	0.444
Set 3, subset B	4.44E-05	3.96E-05	5.99	0.444
Set 3, subset B	4.44E-05	4.06E-05	6.48	0.444
Set 3, subset C	4.35E-05	1.68E-06	3.27	0.223
Set 3, subset C	4.35E-05	1.85E-06	3.32	0.223
Set 3, subset C	4.35E-05	2.20E-06	3.40	0.223
Set 3, subset C	4.35E-05	2.85E-06	3.48	0.223
Set 3, subset C	4.35E-05	3.61E-06	3.58	0.223
Set 3, subset C	4.35E-05	4.66E-06	3.75	0.223
Set 3, subset C	4.35E-05	6.32E-06	3.88	0.223
Set 3, subset C	4.35E-05	1.08E-05	4.18	0.223
Set 3, subset C	4.35E-05	1.66E-05	4.49	0.223
Set 3, subset C	4.35E-05	3.00E-05	5.34	0.223
Set 3, subset C	4.35E-05	3.55E-05	6.20	0.223
Set 3, subset C	4.35E-05	3.65E-05	6.62	0.223

Table 25. Data obtained from Cd^{2+} adsorption experiments using *G. stearotheophilus* cells (10.56 g wet cells).

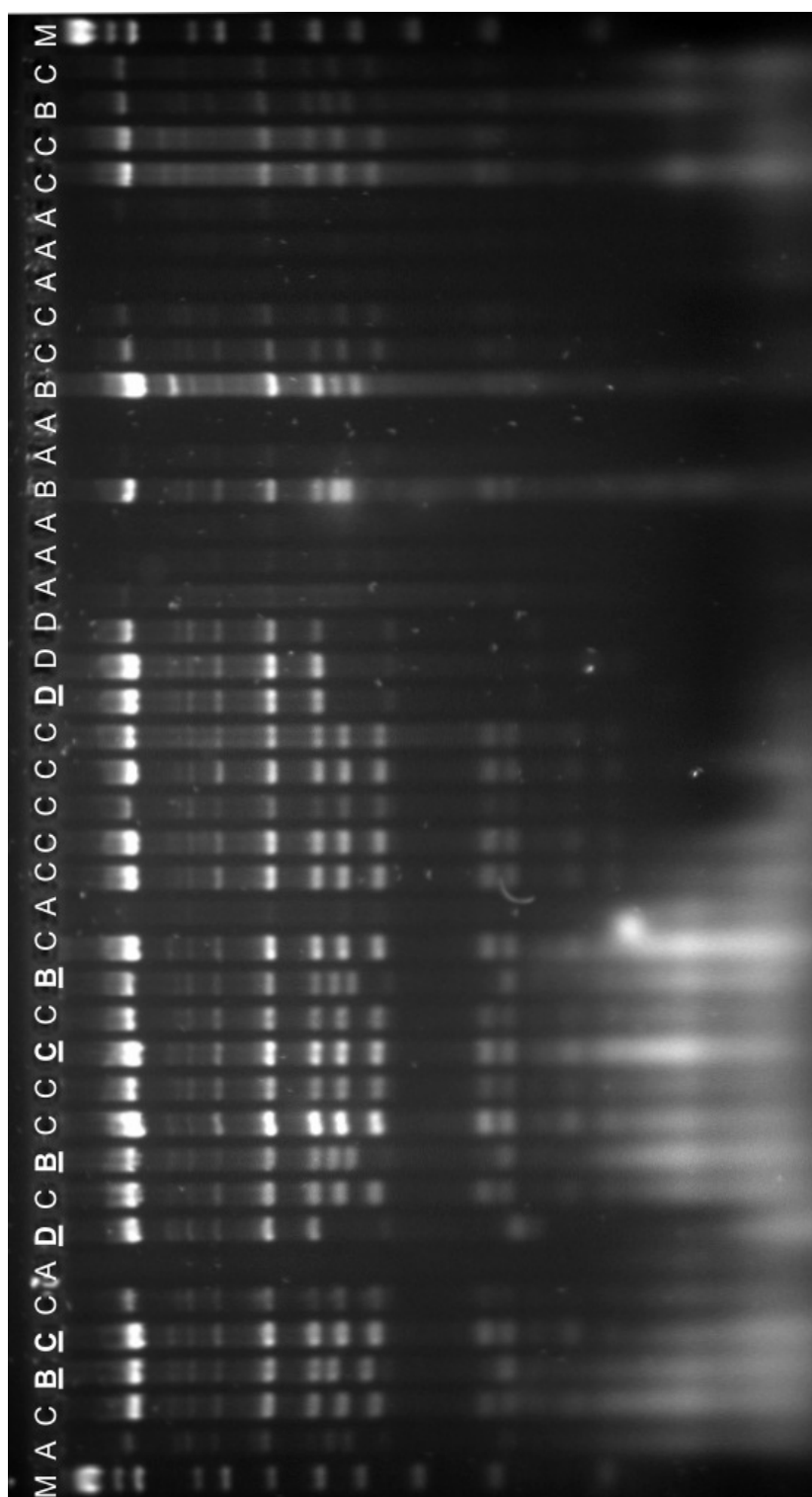
Dataset	Initial Cd^{2+} [mol/l]	Adsorbed Cd^{2+} [mol/l]	Final pH	Dilution factor
Set 1, subset A	4.31E-05	3.43E-05	5.79	0.608
Set 1, subset A	4.31E-05	3.49E-05	6.04	0.608
Set 1, subset A	4.31E-05	3.49E-05	6.24	0.608
Set 1, subset A	4.31E-05	3.52E-05	6.35	0.608
Set 1, subset A	4.31E-05	3.53E-05	6.54	0.608
Set 1, subset A	4.31E-05	3.49E-05	6.69	0.608
Set 1, subset A	4.31E-05	3.52E-05	6.88	0.608
Set 1, subset A	4.31E-05	3.57E-05	7.19	0.608
Set 1, subset A	4.31E-05	3.54E-05	7.35	0.608
Set 1, subset B	4.41E-05	5.85E-06	4.13	0.346
Set 1, subset B	4.41E-05	1.59E-05	4.83	0.346
Set 1, subset B	4.41E-05	2.47E-05	5.40	0.346
Set 1, subset B	4.41E-05	2.75E-05	5.69	0.346
Set 1, subset B	4.41E-05	3.02E-05	6.02	0.346
Set 1, subset B	4.41E-05	3.19E-05	6.25	0.346
Set 1, subset B	4.41E-05	3.29E-05	6.45	0.346
Set 1, subset B	4.41E-05	3.39E-05	6.76	0.346
Set 1, subset B	4.41E-05	3.51E-05	6.88	0.346
Set 1, subset B	4.41E-05	3.54E-05	7.12	0.346
Set 1, subset B	4.41E-05	3.62E-05	7.86	0.346
Set 1, subset C	4.33E-05	6.23E-06	4.59	0.199
Set 1, subset C	4.33E-05	1.95E-05	5.89	0.199
Set 1, subset C	4.33E-05	2.48E-05	6.56	0.199
Set 1, subset C	4.33E-05	2.48E-05	6.55	0.199
Set 1, subset C	4.33E-05	2.63E-05	6.79	0.199
Set 1, subset C	4.33E-05	2.79E-05	6.94	0.199
Set 1, subset C	4.33E-05	2.93E-05	7.16	0.199
Set 1, subset C	4.33E-05	3.22E-05	7.59	0.199
Set 1, subset C	4.33E-05	3.19E-05	7.59	0.199
Set 1, subset C	4.33E-05	3.30E-05	7.75	0.199

Table 25. Continued.

Dataset	Initial Cd ²⁺ [mol/l]	Adsorbed Cd ²⁺ [mol/l]	Final pH	Dilution factor
Set 2, subset A	4.13E-05	1.59E-05	4.28	0.999
Set 2, subset A	4.13E-05	2.63E-05	4.49	0.999
Set 2, subset A	4.13E-05	2.90E-05	4.63	0.999
Set 2, subset A	4.13E-05	3.11E-05	4.96	0.999
Set 2, subset A	4.13E-05	3.36E-05	5.30	0.999
Set 2, subset A	4.13E-05	3.42E-05	5.46	0.999
Set 2, subset A	4.13E-05	3.44E-05	5.64	0.999
Set 2, subset A	4.13E-05	3.41E-05	5.73	0.999
Set 2, subset A	4.13E-05	3.41E-05	5.94	0.999
Set 2, subset A	4.13E-05	3.36E-05	6.00	0.999
Set 2, subset A	4.13E-05	3.41E-05	6.17	0.999
Set 2, subset A	4.13E-05	3.34E-05	6.31	0.999
Set 2, subset B	4.00E-05	4.81E-06	3.95	0.511
Set 2, subset B	4.00E-05	9.89E-06	4.38	0.511
Set 2, subset B	3.99E-05	1.71E-05	4.76	0.511
Set 2, subset B	3.99E-05	2.02E-05	4.90	0.511
Set 2, subset B	3.99E-05	2.43E-05	5.18	0.511
Set 2, subset B	3.99E-05	2.48E-05	5.27	0.511
Set 2, subset B	3.99E-05	2.76E-05	5.47	0.511
Set 2, subset B	3.99E-05	2.95E-05	5.76	0.511
Set 2, subset B	3.99E-05	3.09E-05	6.04	0.511
Set 2, subset B	3.99E-05	3.22E-05	6.25	0.511
Set 2, subset B	3.99E-05	3.22E-05	6.61	0.511
Set 2, subset C	3.98E-05	1.37E-06	3.65	0.255
Set 2, subset C	3.98E-05	2.59E-06	3.99	0.255
Set 2, subset C	3.98E-05	3.50E-06	4.14	0.255
Set 2, subset C	3.98E-05	2.60E-06	4.05	0.255
Set 2, subset C	3.98E-05	1.10E-05	4.89	0.255
Set 2, subset C	3.98E-05	1.46E-05	5.16	0.255
Set 2, subset C	3.98E-05	1.93E-05	5.55	0.255
Set 2, subset C	3.98E-05	2.21E-05	5.97	0.255
Set 2, subset C	3.98E-05	2.39E-05	6.12	0.255
Set 2, subset C	3.98E-05	2.72E-05	6.56	0.255
Set 2, subset C	3.98E-05	2.73E-05	6.61	0.255
Set 2, subset C	3.98E-05	2.73E-05	6.72	0.255

Table 25. Continued.

Dataset	Initial Cd ²⁺ [mol/l]	Adsorbed Cd ²⁺ [mol/l]	Final pH	Dilution factor
Set 3, subset A	4.16E-05	2.44E-05	4.62	0.946
Set 3, subset A	4.16E-05	3.02E-05	4.89	0.946
Set 3, subset A	4.16E-05	3.26E-05	5.05	0.946
Set 3, subset A	4.16E-05	3.37E-05	5.20	0.946
Set 3, subset A	4.16E-05	3.48E-05	5.37	0.946
Set 3, subset A	4.16E-05	3.56E-05	5.42	0.946
Set 3, subset A	4.16E-05	3.48E-05	5.61	0.946
Set 3, subset A	4.16E-05	3.42E-05	5.79	0.946
Set 3, subset A	4.16E-05	3.40E-05	5.92	0.946
Set 3, subset A	4.16E-05	3.42E-05	6.05	0.946
Set 3, subset A	4.16E-05	3.47E-05	6.19	0.946
Set 3, subset A	4.16E-05	3.38E-05	6.48	0.946
Set 3, subset B	4.55E-05	2.98E-06	3.65	0.477
Set 3, subset B	4.55E-05	4.84E-06	3.80	0.477
Set 3, subset B	4.55E-05	6.02E-06	3.88	0.477
Set 3, subset B	4.55E-05	6.19E-06	3.97	0.477
Set 3, subset B	4.55E-05	8.23E-06	4.11	0.477
Set 3, subset B	4.55E-05	9.20E-06	4.20	0.477
Set 3, subset B	4.55E-05	1.30E-05	4.38	0.477
Set 3, subset B	4.55E-05	1.48E-05	4.50	0.477
Set 3, subset B	4.55E-05	1.78E-05	4.63	0.477
Set 3, subset B	4.55E-05	2.54E-05	5.01	0.477
Set 3, subset B	4.55E-05	2.84E-05	5.35	0.477
Set 3, subset B	4.55E-05	3.17E-05	5.53	0.477
Set 3, subset C	4.14E-05	2.52E-06	3.76	0.272
Set 3, subset C	4.14E-05	2.75E-06	3.91	0.272
Set 3, subset C	4.14E-05	2.29E-06	3.83	0.272
Set 3, subset C	4.14E-05	5.40E-06	4.22	0.272
Set 3, subset C	4.14E-05	5.98E-06	4.34	0.272
Set 3, subset C	4.14E-05	9.50E-06	4.63	0.272
Set 3, subset C	4.14E-05	1.54E-05	5.03	0.272
Set 3, subset C	4.14E-05	1.62E-05	5.11	0.272
Set 3, subset C	4.14E-05	2.19E-05	5.52	0.272
Set 3, subset C	4.14E-05	2.42E-05	5.92	0.272
Set 3, subset C	4.14E-05	2.82E-05	6.39	0.272
Set 3, subset C	4.14E-05	2.81E-05	6.44	0.272



164

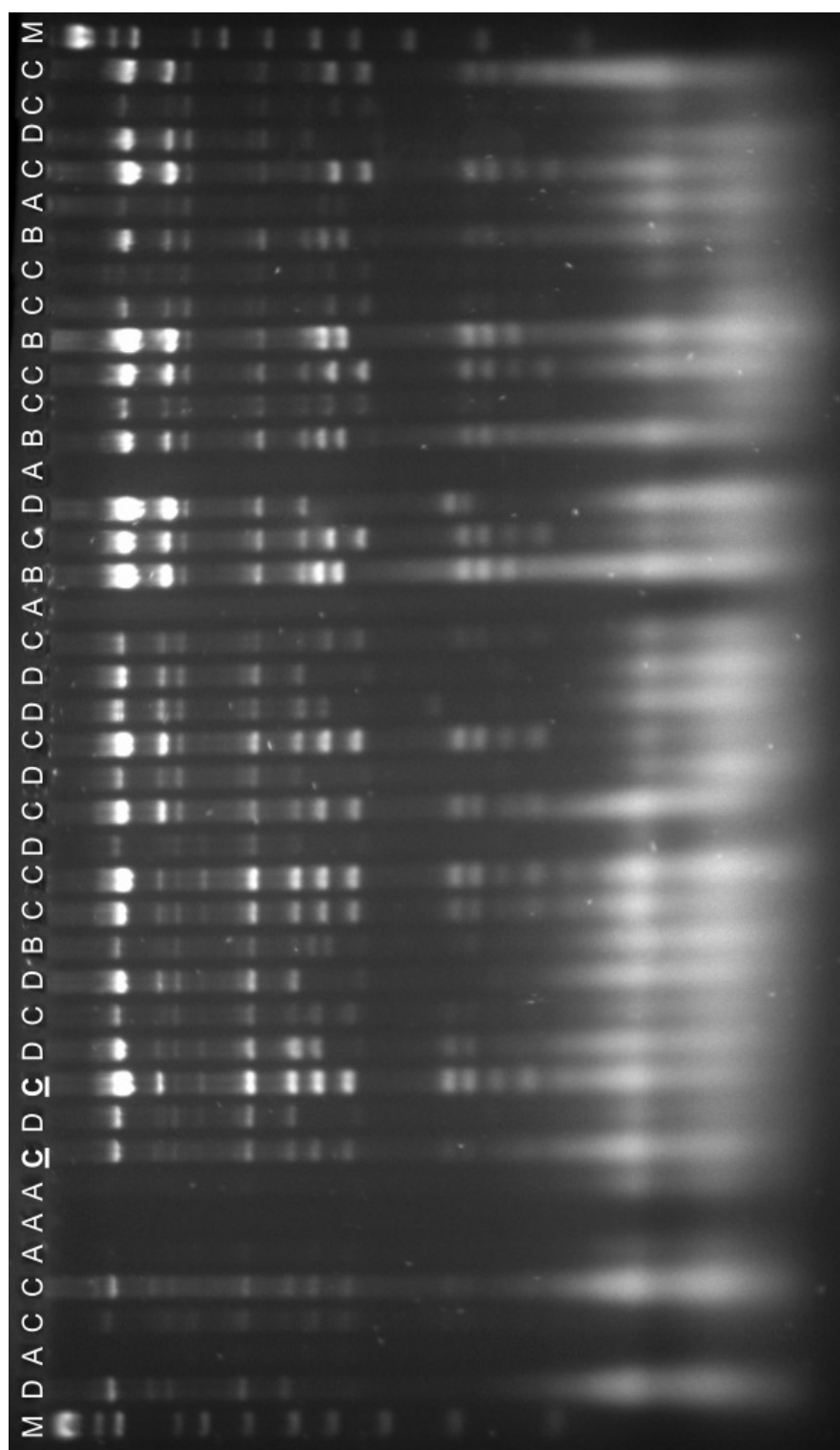


Figure 39. RFPL profiles of bacterial 16S rRNA genes. Continued on next page.

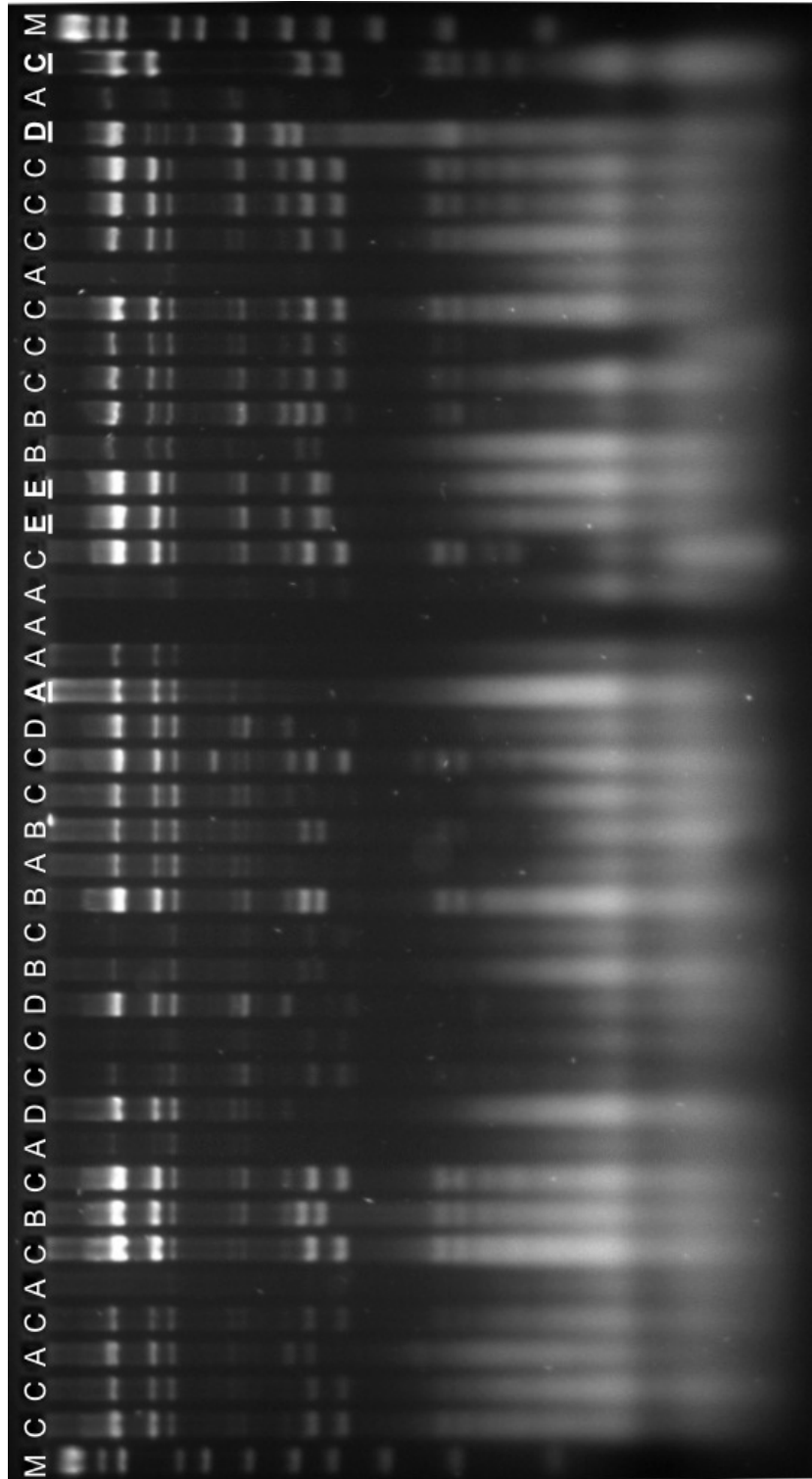


Figure 39. Restriction fragment length polymorphism (RFLP) profiles of bacterial 16S rRNA genes obtained from samples of Champagne Pool after enzymatic digestions with *EcoR* I, *Rsa* I, and *Bam*H I. M, 1 Kb Plus DNA ladder (Invitrogen); A, no sample or vector without insert; B, OTU Bac03; C, OTU Bac04; D, OTU Bac12; E, OTU Bac86. Bold and underlined letters indicate samples that have been subject to further sequence analyses.

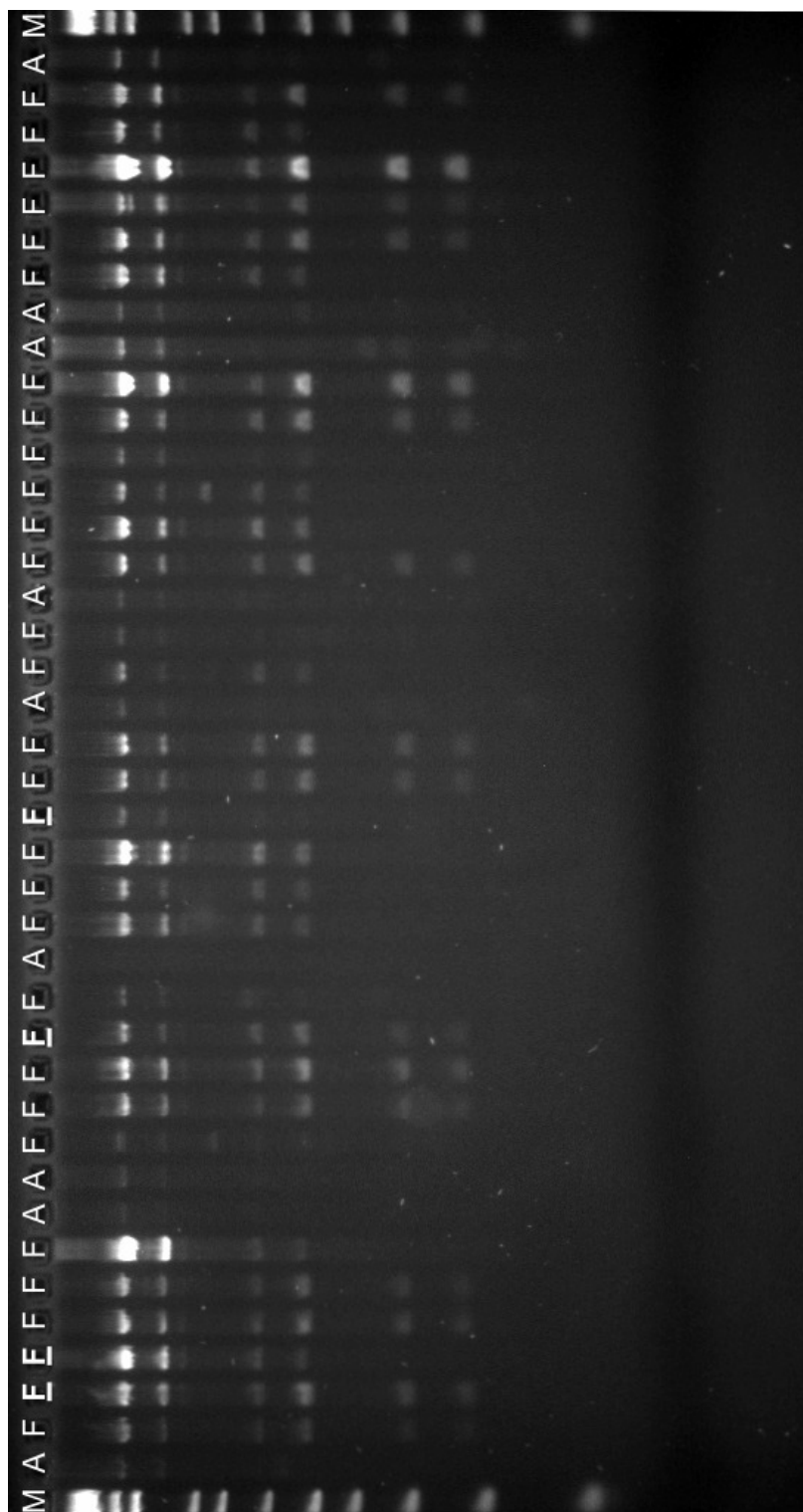


Figure 40. RFPL profiles of archaeal 16S rRNA genes. Continued on next page.

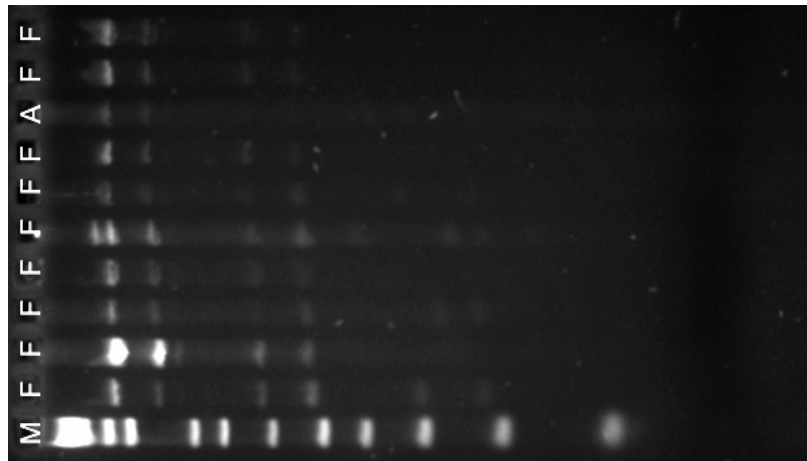


Figure 40. Restriction fragment length polymorphism (RFLP) profiles of archaeal 16S rRNA genes obtained from samples of Champagne Pool after enzymatic digestions with *EcoR* I, *Rsa* I, and *BamH* I. M, 1 Kb Plus DNA ladder (Invitrogen); A, no sample or vector without insert; F, OTU Arc03. Bold and underlined letters indicate samples that have been subject to further sequence analyses.

Appendix E: Nucleotide sequences and alignments

Nucleotide sequences of 16S rRNA gene fragments amplified from DNA extracted from samples obtained from Champagne Pool in GenBank format. Single letter code: a, adenosine; c, cytidine; g, guanosine; t, thymidine.

LOCUS **DQ989208** 1506 bp DNA linear BCT 01-NOV-2006

DEFINITION Venenivibrio stagnispumantis strain CP.B2 16S ribosomal RNA gene, complete sequence.

ACCESSION DQ989208

VERSION DQ989208.1 GI:116518485

FEATURES Location/Qualifiers

source 1..1506

 /organism="Venenivibrio stagnispumantis"

 /mol type="genomic DNA"

 /strain="CP.B2"

 /db xref="taxon:407998"

 /note="type strain of Venenivibrio stagnispumantis"

rRNA 1..1506

 /product="16S ribosomal RNA"

ORIGIN

```

1 agagtttgat cctggctcag cgcgaacggt ggccggcgtgc ctaacacatg caagtcgtgg
61 ggcagcaggc cttaccttcg ggtaaggtgc tggcgaccgg caaacgggtg agtaacacgt
121 agcttaccta cccataggtt ggggataact gcccgaaagg gcagctaata cccaataatg
181 agaaaactcc aaagccgcaa ggcgcctatg gatggggctg cgtcccacga gcttgttggt
241 gaggtaatgg ctcaccaagg ctacgacggg tagccgtctt gagaggatga ccggccacag
301 tgggactgag acacggcccg caccctacg gggggcagca gtggggaata ttgggcaatg
361 gccgaaaggc tgaccagca acgccgcgtg gtggatgaag cccttcgggg tgtaaacacc
421 ttttctgggg gaagattatg acggtacccc aggaataagg gacggctaac tacgtgccag
481 cagccgcggt aatacgtagg tcccgaacgt tgcgcgaaat tactgggctt aaagggtccg
541 tagcggctct gtaagtggta ggtgaaagcc cacgggttaa ccgtggaatt gccttccaaa
601 ctgccggact tgaggtggaa gaggtcggcg gaattcccg tgtacgtgta aatgcgtaga
661 tatcgggagg aacaccagta gcgaagcggc gactgggaca ttcttgacgc tgagggacga
721 aagctaggga gcaaaccgga ttagataccc gggtagtcct agccgtaaac gatggatgct
781 tgatgtgacc tgggatacca ggtcgtgtcg taagctaacg cggttaagcat ccgcctggg
841 gagtacggcc gcaaggttga aactcaaagg aattgacggg gaccgcaca accggtggag
901 cgtctggttt aattcgatgc taaccgaaa acctcaccag ggtttgacat ccggtgtgtc

```

```

961 gtatccgaaa gggtagctagc ctatgatttc tcataggtgc gccggacagg tgggtgcatgg
1021 tcgtcgtcag ctcggtcgtg gagatgttgg gtttaagtccc gcaacgagcg caacccttgc
1081 cctgtgttac cagcgggtta tgccggggac tcacagggga ctgccggcga taagtcggag
1141 gaaggagggg atgacgtcag atcagtatgc cctttatgcc ctgggttaca caggcgctac
1201 agtggcaggg acaatgggat gcaatgcagc aatgcggagc taaccccaaa aaccctgtcg
1261 tgggtgcgat tgggggttgc aactcacccc catgaaggcg gaatcggtag taatggcgaa
1321 tcagcaatgt cgccgtgaat acgttcccgg gtcttgtaca caccgcccgt cacgccatgg
1381 gagtcgggtt catcggaagt ccccgagcta accgcaagga ggcaggggcc gatgatgggc
1441 ccgatgactg gggcgaaagtc gtaacaaggt agccctaggg gaacctgcgg ctggatcacc
1501 tcctta

```

//

```

LOCUS      EF101533      330 bp  DNA linear  ENV 10-DEC-2006
DEFINITION Uncultured archaeon isolate DGGE fragment a 16S ribosomal
            RNA gene, partial sequence.
ACCESSION  EF101533
VERSION    EF101533.1 GI:118723383
FEATURES   Location/Qualifiers
            source      1..330
                        /organism="uncultured archaeon"
                        /mol_type="genomic DNA"
                        /isolate="DGGE fragment a"
                        /isolation_source="geothermal hot spring water"
                        /db_xref="taxon:115547"
                        /environmental sample
                        /country="New Zealand: Waiotapu, Champagne Pool"
            rRNA        <1..>330
                        /product="16S ribosomal RNA"

```

ORIGIN

```

1  aggatgtgca tgccgtcgcc ggctcgtgct cgtaggtgtc ctgttaagtc aggcaacgag
61  cgagaccccc acctcctagt tgcgtactcc aggcgcttcc gggagccgtg ggcactctag
121 ggaggactgc cggcgataag cgggaggaag gtgggggcta cggcaggttc agtatgcccc
181 gaaaatcccc gggctacacg cgagtctgca agtggcgggg aacagcggga ttcctgacct
241 cgaaagaggg gaggtaatct cccgtaaac cgcctcatt aggaatcgag ggtctgacaa
301 ctgcacctcg ttaaactag aaatccctag

```

//

LOCUS **EF101534** 411 bp DNA linear ENV 10-DEC-2006
 DEFINITION Uncultured archaeon isolate DGGE fragment b 16S ribosomal RNA gene, partial sequence.
 ACCESSION EF101534
 VERSION EF101534.1 GI:118723384
 FEATURES Location/Qualifiers
 source 1..411
 /organism="uncultured archaeon"
 /mol type="genomic DNA"
 /isolate="**DGGE fragment b**"
 /isolation source="geothermal hot spring water"
 /db xref="taxon:115547"
 /environmental sample
 /country="New Zealand: Waiotapu, Champagne Pool"
 rRNA <1..>411
 /product="16S ribosomal RNA"

ORIGIN

```

1 ctgcggtca attggagtca acgcctggaa tcttaccggg ggagaccgca gtatgacggc
61 cagcttacga ccttgccctga ctgcgcggaga ggaggtgcat ggccgtcgcc agctcgtggt
121 gtgaaatgtc ctgttaagtc aggcaacgag cgagaccccc actcctagtt ggtattacgg
181 tctccggacc gtgaccacac taggaggact gccgccgtaa ggcggaggaa ggagggggcc
241 acggcaggtc agcatgcccc gaaactcccg ggccgcacgc gggttacaat ggcagggaca
301 acgggaagct acctcgaaag ggggagccaa tcctaaacc tgccgcagtt gggatcgagg
361 gctgaaaccc gccctcgtga acgaggatcc ctataaccgc gggtaacaa c

```

//

LOCUS **EF101535** 146 bp DNA linear ENV 10-DEC-2006
 DEFINITION Uncultured bacterium isolate DGGE fragment c 16S ribosomal RNA gene, partial sequence.
 ACCESSION EF101535
 VERSION EF101535.1 GI:118723385
 FEATURES Location/Qualifiers
 source 1..146
 /organism="uncultured bacterium"

```

/mol type="genomic DNA"
/isolate="DGGE fragment c"
/isolation source="geothermal hot spring water"
/db xref="taxon:77133"
/environmental sample
/country="New Zealand: Waiotapu, Champagne Pool"

rRNA      <1..>146
          /product="16S ribosomal RNA"

ORIGIN
      1 ccagcaatac tgcgtgtttg atgaaggcct tcgggttgta aagcacttta acttggaag
      61 aaaatgcttc cctacctacg tgaagccttg actgtaccag acagcaataa gcaccggcta
      121 aactgtgcc agcagccgcg gtaata

//

LOCUS      EF101536      64 bp   DNA linear   ENV 10-DEC-2006
DEFINITION Uncultured bacterium isolate DGGE fragment d 16S ribosomal
            RNA gene, partial sequence.
ACCESSION  EF101536
VERSION    EF101536.1 GI:118723386
FEATURES   Location/Qualifiers
            source          1..64
                                /organism="uncultured bacterium"
                                /mol type="genomic DNA"
                                /isolate="DGGE fragment d"
                                /isolation source="geothermal hot spring water"
                                /db xref="taxon:77133"
                                /environmental sample
                                /country="New Zealand: Waiotapu, Champagne Pool"

rRNA      <1..>64
          /product="16S ribosomal RNA"

ORIGIN
      1 ccagcgacgc tgcgtggtgg atgaaggcct tcgggttgta accccttttc tgggggacga
      61 tcct

//

```

LOCUS **EF101537** 699 bp DNA linear ENV 10-DEC-2006
DEFINITION Uncultured archaeon 16S ribosomal RNA gene, partial sequence.
ACCESSION EF101537
VERSION EF101537.1 GI:118723387
FEATURES Location/Qualifiers
 source 1..699
 /organism="uncultured archaeon"
 /mol_type="genomic DNA"
 /isolation_source="geothermal hot spring water"
 /db_xref="taxon:115547"
 /clone="OTU **Arc03**"
 /environmental_sample
 /country="New Zealand: Waiotapu, Champagne Pool"
 rRNA <1..>699
 /product="16S ribosomal RNA"

ORIGIN

```

1  ccaggcccta cgggtggcgca ccaggcgcg c aacgtcccca atgcgcgcaa gcgtgagggc
61  gctaccccgga gtgcctcctt ttggaggctt ttctccggct ctaaaaaggc ggaggaataa
121  gcgggggggca agtctggtgt cagccgccgc ggtaacacca gctccgcgag tggtcgggac
181  gtttactggg cctaaagcgc ctgtagccgg ctactaagt tgctccttaa agccccgggc
241  tcaaccggg gactgggagc aatactagt agctagggg cgggagaggc caggggtact
301  cccggaggag gggcgaaatc cgtagatcct gggaggacca ccagtggcgg aggcgcctgg
361  ctagaacgcg cccgacggtg agaggcgaaa gccggggcag caaacaggat tagataccct
421  ggtagtcccg gctgtaaacg atgcgggcta ggtgtcacgt gggcttagag ctacagtgg
481  gccgcaagga agccgttaag ccgcgccct ggggagtacg gtcgcaagac tgaaacttaa
541  aggaattggc gggggagcac cacaaggggt ggaacctgcg gctcaattgg agtcaacgcc
601  tggaatctta ccgggggaga ccgcagtatg acggccaggc ttacgacctt gcctgactcg
661  cggagaggag gtgcatggcc gtcgccagct cgtgttgtg

```

//

LOCUS **EF101538** 1426 bp DNA linear ENV 10-DEC-2006
DEFINITION Uncultured bacterium 16S ribosomal RNA gene, partial sequence.
ACCESSION EF101538
VERSION EF101538.1 GI:118723388
FEATURES Location/Qualifiers
 source 1..1426

```

/organism="uncultured bacterium"
/mol type="genomic DNA"
/isolation source="geothermal hot spring water"
/db xref="taxon:77133"
/clone="OTU Bac03"
/environmental sample
/country="New Zealand: Waiotapu, Champagne Pool"

rRNA      <1..>1426
           /product="16S ribosomal RNA"

```

ORIGIN

```

1  ggcggcagtg cttaacacat gcaagtcgag cgggcgcttc gggcgtcagc ggcggaacggg
61  ttagtaacgc gtgggaacgt gccctttgct ctggaatagc cctgggaaac tgggggtaat
121 accggatgtg ccctgagggg gaaagattta tcggcaaggg atcggcccgc gtctgattag
181 gtagttggtg aggtaacggc tcaccaagcc gacgatcggg agtggtttga gaggatgatc
241 agcaacactg ggactgagac acggcccaga ctctacggg aggcagcagt ggggaatctt
301 agacaatggg cgcaagcctg atctagccat gccgcgtggg tgatgaaggc cttagggtcg
361 taaagccctt tcgccgggga agataatgac ggtacccggg aaagaaaccc cggctaactc
421 cgtgccagca gccgcggtaa tacggagggg gttagcgttg ttcggaatga ctgggcgtaa
481 agcgcgcgta ggcggtatcat caagtcgggg gtgaaatccc ggggctcaac cccggaatgg
541 ccttcgagac tgggtgtctt gagttcgaga gaggtgagtg gaattccgag tgtagaggtg
601 aaattcgtag atattcggag gaacaccagt ggcgaaggcg gctactggc tcgacactga
661 cgctgaggtg cgaaagcgtg gggagcaaac aggattagat accctggtag tccacgcccg
721 taaacgatga atgccagacg tcgggggggt tgctcttcgg tgtcacacct aacggattaa
781 gcattccgcc ctggggagta cggtcgcaag attaaactca aaggaattga cgggggccccg
841 acaacggtgg agcatgtggt ttaattcgaa gcaacgcgca gaaccttacc aaccttgac
901 atgcctgac cggcctggag aaggcttttc ccgcaaggga cagggtggaca ggtgctgcat
961 ggctgtcgtc agctcgtgtc gtgagatggt cggttaagtc cggcaacgag cgcaaccac
1021 acccttggtt gccagcacgt aatggtgggc actttagggg aactgccgt gataagcggg
1081 aggaaggtgt ggatgacgtc aagtcctcat ggcccttacg ggttgggcta cacacgtgct
1141 acaatggtgg tgacagaggg ttcattcccta aaagccatct cagttcggat tgtcgtctgc
1201 aactcgacgg catgaagtcg gaatcgctag taatcgcgca tcagctcggc gcggtgaata
1261 cgttcccggg ccttgtagac accgcccgtc acaccatggg agttgggttg acccgaaggt
1321 ggtgcgccga ccgtaaggg gggcagccaa ccacggtcag ttcagcgact ggggtgaagt
1381 cgtaacaagg tagccgtagg ggaacctgcg gctggatcac ctctt

```

//

LOCUS	EF101539	715 bp	DNA linear	ENV 10-DEC-2006
DEFINITION	Uncultured bacterium 16S ribosomal RNA gene, partial sequence.			
ACCESSION	EF101539			

VERSION EF101539.1 GI:118723389
FEATURES Location/Qualifiers
 source 1..715
 /organism="uncultured bacterium"
 /mol_type="genomic DNA"
 /isolation_source="geothermal hot spring water"
 /db_xref="taxon:77133"
 /clone="OTU **Bac04**"
 /environmental_sample
 /country="New Zealand: Waiotapu, Champagne Pool"
 rRNA <1..>715
 /product="16S ribosomal RNA"

ORIGIN

```

1 agagtttgat cctggctcag cgcgaacggt ggcggcgtgc ctaacacatg caagtcgtgg
61 ggcagcaggc cttaccttcg ggtaaggtgc tggcgaccgg caaacgggtg agtaacacgt
121 agcttaccta cccataggtt ggggataact gcccgaagg gcagctaata cccaataatg
181 aggaaactcc aaagccgcaa ggcgcctatg gatggggctg cgtcccatca gcttggtggt
241 gaggtaatgg ctaccaagg ctacgacggg tagccggtct gagaggatga ccggccacag
301 tgggactgag acacggcccg caccctacg gggggcagca gtggggaata ttgggcaatg
361 gccgaaggc tgaccagca acgcccgtg gtgatgaag cccttcgggg tgtaaacacc
421 ttttctgggg gaagataatg acggtacccc aggaataagg gacggctaac tacgtgccag
481 cagccgcggt aatacgtagg tcccgaacgt tgcgcgaaat tactgggcgt aaagggtccg
541 taggcggtct ggtaagtgga aggtgaaagc ccacggctta accgtggaat tgccttccaa
601 actgccggac ttgaggatgg aagaggtcgg cggaattccc ggttgtagcg gttgaaatgc
661 gtagatatcg ggaggaacac cagtagcgaa ggcggcgact gggacattcc tgacg

```

//

LOCUS **EF101540** 536 bp DNA linear ENV 10-DEC-2006
DEFINITION Uncultured bacterium 16S ribosomal RNA gene, partial sequence.
ACCESSION EF101540
VERSION EF101540.1 GI:118723390
FEATURES Location/Qualifiers
 source 1..536
 /organism="uncultured bacterium"
 /mol_type="genomic DNA"
 /isolation_source="geothermal hot spring water"


```

/db xref="taxon:77133"
/clone="OTU Bac12"
/environmental sample
/country="New Zealand: Waiotapu, Champagne Pool"
rRNA <1..>536
/product="16S ribosomal RNA"

```

ORIGIN

```

1 gaaagggcac tagcctatga tttctcatag gtgcgccgga cagtgggtgca tggctcgtcgt
61 cagctcgtgt cgtgagatgt tgggttaagt cccgcaacga gcgcaaccct tgccctgtgt
121 taccagcggg ttatgccggg gactcacagg ggactgccgg cgataagtcg gaggaaggag
181 gggatgacgt cagatcagta tgccctttat gccctgggct acacaggcgc tacagtggca
241 gggacaatgg gatgcaatgc agcaatgcgg agctaacccc aaacctgtc gtggtgcgga
301 ttgggggttg caactacccc ccatgaaggc ggaatcggtg gtaatggcga atcagcaatg
361 tcgccgtgaa tacgttcccg ggtcttgtag acaccgcccg tcacgccatg ggagtcgggt
421 tcacggaag tccccgagct aaccgcaagg aggcaggggc cgatgatggg cccgatgact
481 ggggcgaagt cgtaacaagg tagccctagg ggaacctgcg gctggatcac ctccct

```

//

```

LOCUS      EF101541      962 bp   DNA linear   BCT 10-DEC-2006
DEFINITION Archaeon CP.B3 16S ribosomal RNA gene, partial sequence.
ACCESSION  EF101541
VERSION    EF101541.1   GI:118723391
FEATURES   Location/Qualifiers
    source   1..962
             /organism="archaeon CP.B3"
             /mol_type="genomic DNA"
             /strain="CP.B3"
             /isolation_source="geothermal hot spring water"
             /db_xref="taxon:413980"
             /country="New Zealand: Waiotapu, Champagne Pool"
rRNA <1..>962
/product="16S ribosomal RNA"

```

ORIGIN

```

1 cgcaatgcgg gaaacgcgac ggggggaccc cagtgccgtg gcaatgccac ggcttttccg
61 gagtgtaagg agctccggga ataagggtcg ggcaaggccg gtggcagccg ccgcggtaat
121 accggcggcc cgagtgggtg ccactattat tgggcctaaa gcgtccgtag ccggggccgt

```

```

181 aagtcacctg cgaaatctca cggctcaacc gtggggctcg ctggggatac tgcgggcctt
241 gggaccggga gaggcggagg gtacctctgg ggtaggggtg aaatcctata atcccagggg
301 gaccgccagt ggcgaaggcg ctccgctgga acgggtccga cggtgaggga cgaagccag
361 gggagcaaac cggattagat acccgggtag tcctggctgt aaaggatgcg ggctaggtgt
421 cgggtgagct tcgggctcgc ccggtgccgg agggaagccg ttaagccgc cgcctgggga
481 gtacggccgc aaggctgaaa cttaaaggaa ttggcggggg agcaccacaa ggggtggagc
541 gtgcggttta attggattca acgccgggaa cctcaccggg ggcgacggca ggatgaaggc
601 caggctgaag gtcttgccgg acacgccgag aggaggtgca tggccgcggt cagctcgtag
661 cgtgaggcgt ccacttaagt gtggtaacga gcgagaccgg tgccccagtg tgccagtcct
721 ccccgtggg gaggaggcac tctgggggga ccgccggcga taagccggag gaaggagcgg
781 ggcacggtag gtcagtatgc ccgaaaccc ccgggctaca cgcgcgtac aatgggcggg
841 acaatgggat ccgaccccg aaggggaagg aaatccccta aaccgcccc cagttcggat
901 tgcgggctgc aactcgccg catgaagctg gaatccctag taccgcgggt catcatcgcg
961 cg

```

//

LOCUS	EF101542	1310 bp	DNA linear	BCT 10-DEC-2006
DEFINITION	Bacterium CP.B1 16S ribosomal RNA gene, partial sequence.			
ACCESSION	EF101542			
VERSION	EF101542.1 GI:118723392			
FEATURES	Location/Qualifiers			
source	1..1310			
	/organism="bacterium CP.B1"			
	/mol type="genomic DNA"			
	/strain="CP.B1"			
	/isolation source="geothermal hot spring water"			
	/db xref="taxon:413981"			
	/country="New Zealand: Waiotapu, Champagne Pool"			
rRNA	<1..>1310			
	/product="16S ribosomal RNA"			

ORIGIN

```

1 cggcggacgg gtgagtaacg cgtgagcaac ctacccttga gacagggata accctgggaa
61 accggggcta atacctgata tacttcatca gggcatcctg atggaggaaa gggcgggaag
121 ccgctcaaga tgggctcgcg tcccacagc tagttggtga ggtaacggct caccaaggct
181 acgacgggta gccggcctga gagggtggtc ggccacactg ggactgagac acggcccaga
241 ctccctacggg aggcagcagt ggggaatctt ccgcaatggg cgaaagcctg acggagcgac
301 gccgcgtgag cgaagaaggc cttcgggtcg taaagctcga tagtgtggga agaaggtatg
361 acggtaccac acgaaagccc cggctaacta cgtgccagca gccgcggtaa gacgtagggg

```

Appendix E: Nucleotide sequences and alignments

```

421 cgagcgttgt ccggagttac tgggcgtaaa gggcgcgtag cggtttagca agtcaggtgt
481 aaaaggccac ggctcaaccg tggatatgca tctgaaactg ctgagctaga gggcaggaga
541 ggggagtgga attcccgtg tagcgtgaa atgcgtagat atcgggagga ataccagtgg
601 cgaaagcgac tcctggactg gccctgacgc tgaggcgga aagcgtgggg agcaaacagg
661 attagatacc ctggtagtcc acgctgtaaa cgatgggtgc taggtgtggg gagcggaagc
721 tttccgtgcc gtaggaaacc caataagcac cccgcctggg agtacggccg caaggtgaa
781 actcaaagga attgacgggg gcccgacaa gcggtggagc atgtggttta attcgaagca
841 acgcaagaa cttaccagg gcttgacatg caggtagtag cgagccgaaa ggtgagcgac
901 cctctcttat gggagggagc ctgcacaggt ggtgcatggt tgcgtcagc tcgtgtcgtg
961 agatgttggg ttaagtcccg caacgagcgc aaccctgcc tctagtggc agcgggtaaa
1021 gccgggcact ctagaggagc tgccgtcgat aagacggagg aaggtgggga tgacgtcaaa
1081 tcatcatgcc ctatatgcc tgggccacac acgtgctaca atggccggtg cagagggaag
1141 cgaagccgcg agccggagcg aatcccaagc cggctctcagt tcggattgca ggctgcaact
1201 cgctgcatg aaggcggaat cgctagtaat cgcggatcag catgcccggt gaatgcgttc
1261 ccgggccttg tacacaccgc ccgtcacacc acgagagtct gcaacaccgc

```

//

Alignments of archaeal sequences of 16S rRNA gene fragments obtained from Champagne Pool and closest relatives. Abbreviations: Thf.pend, *Thermofilum pendens*; Sulf.acid, *Sulfolobus acidocaldarius*; Sulfo.toko, *Sulfolobus tokodaii*; Thc.waio, *Thermococcus waiotapuensis*. Positions without nucleotide variability are indicated in bold.

	1	11	21	31	41	51	61	71	80
DGGE a
Thf.pend	GACTCCGTT	GATCTGCCGG	ACCCGACCGC	TATCGGGGTG	GGGCTAAGCC	ATGGAAGTCT	AGGAGCCTCG	GCTCCGGCGG	
DGGE b
Sulf.acid	.ATTCCGTT	GATCTGCCGG	ACCCGACCGC	TATCGGGGTA	GGGATAAGCC	ATGGGAGTCT	TACACTCTAG	AGTGTGGCGG	
OTU Arc03
Sulf.toko	AATTCCGTT	GATCTGCCGG	ACCCGACCGC	TATCGGGGTA	GCACTAAGCC	ATGGGAGTCG	TACACCCAG	GGTGTGGCGG	
CP.B3
Thc.waio
	81	91	101	111	121	131	141	151	160
DGGE a
Thf.pend	ACGGCTCAGT	AGCACGTGGC	TAACCTACCC	TCGGGAGGGG	GATAACCCCG	GGAAACTGGG	GATAAACCCC	CAAGGCGCGG	
DGGE b
Sulf.acid	ACGGCTGAGT	AACACGTGGC	TAACCTACCC	TCGGGACGGG	GATAACCCCG	GGAAACTGGG	GATAATCCCC	GAAGGGAAGG	
OTU Arc03
Sulf.toko	ACGGCTGAGT	AACACGTGGC	TAACCTACCC	TCGGGAGGGG	GATAACCCCG	GGAAACTGGG	GATAATCCCC	CAAGGGGAGG	
CP.B3
Thc.waio	..GGCTCAGT	AACACGTGGG	TAACCTACCC	TCGGGAGGGG	GATAACCCCG	GGAAACTGGG	GCTAATCCCC	CAAGGTCTGA	

	161	171	181	191	201	211	221	231	240
DGGE a
Thf.pend	ACAC CTGGAA	TGGGTCCGCG	CTG AAAGATG	CGCCCGAGGA	TGGGGCTGCG	CCCTATCAGG	TAGTTGGCGG	GGTAACGGCC	
DGGE b
Sulf.acid	AGTC CTGGAA	TGGTTCCTTC	CCT AAAGTTC	CGCCCGAGGA	TGGGGCTACG	GCCCATCAGG	CTGTCGGTGG	GGTAAAGGCC	
OTU Arc03
Sulf.toko	AGTC CTGGAA	CGGTTCCTCC	CTT AAAGTTC	CGCCCGAGGA	TGGGGCTGCG	GCCCATCAGG	CTGTTGGCGG	GGTAACGGCC	
CP.B3
Thc.waio	GGTAC CTGGAA	GGTCCTCGGG	CCG AAAGTCT	CGCCCGAGGA	TGGGCCGGCG	GCCGATTAGG	TAGTTGGTGG	GGTAACGGCC	
	241	251	261	271	281	291	301	311	320
DGGE a
Thf.pend	CGCCA AGCCG	ATAACGGGTG	GGGGCCGTGA	GAGCGGAGCC	CGAGATGGGA	GACAAGCCCA	GGCTAACCAG	GGGCGAAACT	
DGGE b
Sulf.acid	CACCGA ACCT	ATAACGGGTA	GGGGCCGTGG	AAGCGGAGCC	CCAGTTGGGA	GACAAGCCCA	GGCTAACCAG	GCGCGAAACG	
OTU Arc03CCA	GGCTAACCAG	GCGCGCAACG	
Sulf.toko	CGCCAA ACCT	ATAACGGGTA	GGGGCCGTGG	GAGCGGAGCC	CCAGTTGGGA	GACAAGCCCA	GGCTAACCAG	GCGGGAAACG	
CP.B3
Thc.waio	CACCA AGCCT	AAGATCGGTA	CGGGCCATGA	GAGTGGAGCC	GGAGATGGAA	GACAAGTCCA	GGCTAAGCAG	GCGCGAAACC	
	321	331	341	351	361	371	381	391	400
DGGE a
Thf.pend	TCCGCAATGC	GGGAA ACCGT	GACGGAGTCA	CCCCGAGTAC	CAAGGGTGGC	TTTTGCCCCG	TCTAAAAAGC	CGGGGAATAA	
DGGE b
Sulf.acid	TCCCCAATGC	GCGAA AGCGT	GAGGGCGCTA	CCCCGAGTTC	CGCAGGAGGC	TTTTCCCCGC	TCTAAAAAGG	CGGGGAATAA	
OTU Arc03	TCCCCAATGC	GCGCA AGCGT	GAGGGCGCTA	CCCCGAGTTC	CTTTGGAGGC	TTTTCTCCGG	TCTAAAAAGG	CGGAGAATAA	
Sulf.toko	TCCCCAATGC	GCGAA AGCGT	GAGGGCGCTA	CCCCGAGTCC	CGTAGGGGGC	TTTTCCCCGC	TCTACAAAGG	CGGGGAATAA	
CP.B3CGCAAT	GCGGG AAACG	CGACGGGGGG	ACCC AGTGT	GAATCACGGC	TTTTCCGGAG	TGTAAGGAGC	TCCGGAATAA	
Thc.waio	TCCGCAATGC	GGGAA ACCGC	GACGGGGGGA	CCCC AGTGT	GAATCACGGC	TTTTCCGGAG	TGTAAGGAGC	TCCGGAATAA	

	401	411	421	431	441	451	461	471	480
DGGE a
Thf.pend	GCGGGGGGAA	GCTGTGGCCG	CCGCGGTAAT	ACCACCCGCG	AGTGGTCGGG	ACGTTTATTG	GGCCTAAAGC	GTCCGTAGCC	
DGGE b
Sulf.acid	GCGGGGGGAA	GTTGTGGCCG	CCGCGGTAAT	ACCATCCGCG	AGTGGTCGGG	GTGATTACTG	GGCCTAAAGC	GCCTGTAGCC	
OTU Arc03	GCGGGGGGAA	GTTGTGGCCG	CCGCGGTAAC	ACCATCCGCG	AGTGGTCGGG	ACGTTTACTG	GGCCTAAAGC	GCCTGTAGCC	
Sulf.toko	GCGGGGGGAA	GTTGTGGCCG	CCGCGGTAAC	ACCATCCGCG	AGTGGTCGGG	ACGCTTACTG	GGCCTAAAGC	GCCTGTAGCC	
CP.B3	GGGCTGGGAA	GGCGTGGCCG	CCGCGGTAAT	ACCGGGCCCG	AGTGGTGGCC	ACTATTATTG	GGCCTAAAGC	GTCCGTAGCC	
Thc.waio	G.GCTGGGAA	GCGGTGGCAG	CCGCGGTAAT	ACCGGGCCCG	AGTGGTGGCC	ACTATTATTG	GGCCTAAAGC	GTCCGTAGCC	
	481	491	501	511	521	531	541	551	560
DGGE a
Thf.pend	GGCCCGGTAA	GTCCCTCCTT	AAAGCCACAG	GCTCAACCGT	GGGGCGGAGG	GATACTGCCG	GGCTAGGGGG	CGGAGAGGCC	
DGGE b
Sulf.acid	GGCCACCAAA	GTCGCCCCTT	AAAGTCCCCG	GCTCAACCGG	GGATGGGGGC	GATACTGGTG	GGCTAGGGGG	CGGAGAGGCCG	
OTU Arc03	GGCTCACTAA	GTTGCTCCTT	AAAGCCCCGG	GCTCAACCGG	GGGTGGGAGC	AATACTAGTG	AGCTAGGGGG	CGGAGAGGCC	
Sulf.toko	GGCCCACTAA	GTCGCCCCTT	AAAGACCCGG	GCTCAACCGG	GGATGGGGGC	GATACTGGTG	GGCTAGGGGG	CGGAGAGGCT	
CP.B3	GGGCCCGTAA	GTCCCTGGCG	AAATCTCACG	GCTCAACCGT	GGGCGCTGGG	GATACTGCCG	GCCTTGGGAC	CGGAGAGGCCG	
Thc.waio	GGGCCCGTAA	GTCTCTGACG	AAATCTCACG	GCTCAACCGT	GGGCGCTGGG	GATACTGCCG	GCCTTGGGAC	CGGAGAGGCCG	
	561	571	581	591	601	611	621	631	640
DGGE a
Thf.pend	GGGGGTACTC	CTGGGGTAGG	GGCGAAATCC	TATAATCCCA	GGAGGACCAC	CAGTGGCGAA	GGCGCCCGGC	TAGCACGCGC	
DGGE b
Sulf.acid	GGGGGTACTC	CCGGAGTAGG	GGCGAAATCC	TTAGATACCG	GGAGGACCAC	CAGTGGCGGA	AGCGCCCCGC	TAGAACGCGC	
OTU Arc03	AGGGGTACTC	CCGGAGGAGG	GGCGAAATCC	GTAGATCCTG	GGAGGACCAC	CAGTGGCGGA	GGCGCCTGGC	TAGAACGCGC	
Sulf.toko	AGGGGTACTC	CCAGAGGAGG	GGCGAAATCC	GTAGATCCTG	GGAGGACCAC	CAGTGGCGGA	GGCGCCTAGC	TAGAACGCGC	
CP.B3	GAGGGTACCC	CTGGGGTAGG	GGTGAAATCC	TATAATCCCA	GGGGGACC GC	CAGTGGCGAA	GGCGCTCCGC	TGGAACGGGT	
Thc.waio	GATGGTACCC	CTGGGGTAAG	GGTGAAATCC	TATAATCCCA	GGGGGACC GC	CAGTGGCGAA	GGCGCTCCGC	TGGAACGGGT	

	641	651	661	671	681	691	701	711	720
DGGE a
Thf.pend	CGACGGTGAG	GGACGAAAGC	TGGGGGAGCA	AAGGGGATTA	GATACCCCGG	TAGTCCCAGC	TGTAAACGAT	GCGGGCTAGG	
DGGE b
Sulf.acid	CGACGGTGAG	AGGCGAAAGC	CGGGGCAGCA	AACGGGATTA	GATACCCCGG	TAGTCCCAGC	TGTAAACGAT	GCGGGCTAGG	
OTU Arc03	CGACGGTGAG	AGGCGAAAGC	CGGGGCAGCA	AACAGGATTA	GATACCCCTGG	TAGTCCCAGC	TGTAAACGAT	GCGGGCTAGG	
Sulf.toko	CGACGGTGAG	AGGCGAAAGC	CGGGGCAGCA	AATGGGATTA	GATACCCAG	TAGTCCCAGC	TGTAAACGAT	GCGGGCTAGG	
CP.B3	CGACGGTGAG	GGACGAAGGC	CAGGGGAGCA	AAACGGATTA	GATACCCGGG	TAGTCCTGGC	TGTAAAGGAT	GCGGGCTAGG	
Thc.waio	CGACGGTGAG	GGACGAAGGC	CAGGGGAGCA	AAACGGATTA	GATACCCGGG	TAGTCCTGGC	TGTAAAGGAC	GCGGGCTAGG	
	721	731	741	751	761	771	781	791	800
DGGE a
Thf.pend	TGTTGGGGCT	TCGAGCCCGT	CCAGTGCCGT	AGGAAGCCGT	TAAGCCCGCC	GCCTGGGGAG	TACGGCCGCA	AGGCTGAAAC	
DGGE b
Sulf.acid	TGTCGAGGCT	TAGAGCCTAC	TCGGTGCCGC	AGGAAGCCGT	TAAGCCCGCC	GCCTGGGGAG	TACGGTCGCA	AGACTGAAAC	
OTU Arc03	TGTCACGGCT	TAGAGCTCAC	GTGGTGCCGC	AGGAAGCCGT	TAAGCCCGCC	GCCTGGGGAG	TACGGTCGCA	AGACTGAAAC	
Sulf.toko	TGTCAGGGCT	TAGAGCTCAC	CTGGTGCCGC	AGGAAGCCGT	TAAGCCCGCC	GCCTGGGGAG	TACGGTCGCA	AGACTGAAAC	
CP.B3	TGTCGGAGCT	TCGGGCTCGC	CCGGTGCCGG	AGGAAGCCGT	TAAGCCCGCC	GCCTGGGGAG	TACGGCCGCA	AGGCTGAAAC	
Thc.waio	TGTCGGAGCT	TCGGGCTCGC	CCGGTGCCGG	AGGAAGCCGT	TAAGCCCGCC	GCCTGGGGAG	TACGGCCGCA	AGGCTGAAAC	
	801	811	821	831	841	851	861	871	880
DGGE a
Thf.pend	TTAAAGGAAT	TGGCGGGGGA	GCACCACAAG	GGGTGAAGCT	TGCGGTTTAA	TTGGAGTCAA	CGCCGGAAC	CTTACCGGGG	
DGGE bC	TGCGGCTCAA	TTGGAGTCAA	CGCCTGGAAT	CTTACCGGGG	
Sulf.acid	TTAAAGGAAT	TGGCGGGGGA	GCACCACAAG	GGGTGGAACC	TGCGGCTCAA	TTGGAGTCAA	CGCCTGGAAT	CTTACCGGGG	
OTU Arc03	TTAAAGGAAT	TGGCGGGGGA	GCACCACAAG	GGGTGGAACC	TGCGGCTCAA	TTGGAGTCAA	CGCCTGGAAT	CTTACCGGGG	
Sulf.toko	TTAAAGGAAT	TGGCGGGGGA	GCACCACAAG	GGGTGGAACC	TGCGGCTCAA	TTGGAGTCAA	CGCCTGGAAT	CTTACCGGGG	
CP.B3	TTAAAGGAAT	TGGCGGGGGA	GCACCACAAG	GGGTGGAGCG	TGCGGTTTAA	TTGGATTCAA	CGCCGGGAAC	CTCACC GG G	
Thc.waio	TTAAAGGAAT	TGGCGGGGGA	GCACCACAAG	GGGTGGAGCG	TGCGGTTTAA	TTGGATTCAA	CGCCGGGAAC	CTCACC GG G	

	881	891	901	911	921	931	941	951	960
DGGE a	AGG	ATGTGCATGC	CGTCGCCGGC	TCGTGCTCGT
Thf.pend	GCGACAGCAG	GATGAAGGCC	AGCTGCGACC	TTGCCAGACG	AGCTGAGAGG	AGGTGCATGG	CGTCGCCGGC	TCGTGCCGTG	
DGGE b	GAGACCGCAG	TATGACGGCC	AGCTACGACC	TTGCCTGACT	CGCGGAGAGG	AGGTGCATGG	CGTCGCCAGC	TCGTGTTGTG	
Sulf.acid	GAGACCGCAG	TATGACGGCC	AGCTACGACC	TTGCCTGACT	CGCGGAGAGG	AGGTGCATGG	CGTCGCCAGC	TCGTGTTGTG	
OTU Arc03	GAGACCGCAG	TATGACGGCC	AGCTTCGACC	TTGCCTGACT	CGCGGAGAGG	AGGTGCATGG	CGTCGCCAGC	TCGTGTTGTG	
Sulf.toko	GAGACCGCAG	GATGACGGCC	AGCTACGACC	TTGCCTGACT	CGCGGAGAGG	AGGTGCATGG	CGTCGCCAGC	TCGTGTTGTG	
CP.B3	GCGACGGCAG	GATGAAGGCC	AGCTGAGGTC	TTGCCGGACA	CGCCGAGAGG	AGGTGCATGG	CGCCGTCAGC	TCGTACCGTG	
Thc.waio	GCGACGGCAG	GATGAAGGCC	AGCTGAGGTC	TTGCCGGACA	CGCCGAGAGG	AGGTGCATGG	CGCCGTCAGC	TCGTACCGTG	
	961	971	981	991	1001	1011	1021	1031	1040
DGGE a	AGGTGTCCTG	TTAAGTCAGG	CAACGAGCGA	GACCCCCACC	CCTAGTTGCT	ACCCAGGGCT	TCGAGCCGGC	ACTCTAGGAG	
Thf.pend	AGGTGTCCTG	TTAAGTCAGG	GAACGAGCGA	GACCCCCGCC	CCTAGTTGCT	ACCCAGCCCT	TCGGGCTGGC	ACTCTAGGGG	
DGGE b	AAATGTCCTG	TTAAGTCAGG	CAACGAGCGA	GACCCCCACT	CCTAGTTGGT	ATTACGGTCT	CCGACCGTGC	ACACTAGGAG	
Sulf.acid	AAATGTCCGG	TTAAGTCCGG	CAACGAGCGA	GACCCCCACC	CCTAGTTGGT	ATTCTGGACT	CCGTCCAGAC	ACACTAGGGG	
OTU Arc03	
Sulf.toko	AAATGTCCTG	TTAAGTCAGG	CAACGAGCGA	GACCCCCACC	CCTAGTTGGT	ATCCCCATCT	CCGATGGGGC	ACACTAGGGG	
CP.B3	AGGCGTCCAC	TTAAGTGTGG	TAACGAGCGA	GACCCGTGCC	CCCAGTTGCC	AGTCCTCCCG	CTGGGAGGAC	ACTCTGGGGG	
Thc.waio	AGGCGTCCAC	TTAAGTGTGG	TAACGAGCGA	GACCCGTGCC	CCCAGTTGCC	AGTCTTCCCG	TTGGGAGGAC	ACTCTGGGGG	
	1041	1051	1061	1071	1081	1091	1101	1111	1120
DGGE a	GACTGCCGGC	GTAAGCCGAG	GAAGGTGGGG	GCTACGGCAG	GTCAGTATGC	CCCGAAATCC	CCGGGCTACA	CGCGAGCTGC	
Thf.pend	GACTGCCGGC	GTAAGCCGAG	GAAGGTGGGG	GCTACGGCAG	GTCAGTATGC	CCCGAAACCC	CCGGGCTACA	CGCGAGCTGC	
DGGE b	GACTGCCGCC	GTAAGGCGAG	GAAGGAGGGG	GCCACGGCAG	GTCAGCATGC	CCCGAAACTC	CCGGGCCGCA	CGCGGGTTAC	
Sulf.acid	GACTGCCGGC	GTAAGCCGAG	GAAGGAGGGG	GCCACGGCAG	GTCAGCATGC	CCCGAAACTC	CCGGGCCGCA	CGCGGGTTAC	
OTU Arc03	
Sulf.toko	GACTGCCGCC	GTAAGGCGAG	GAAGGAGGGG	GCCACGGCAG	GTCAGCATGC	CCCGAAACCC	CCGGGCCGCA	CGCGGGTTAC	
CP.B3	GACCGCCGGC	GTAAGCCGAG	GAAGGAGCGG	GCGACGGTAG	GTCAGTATGC	CCCGAAACCC	CCGGGCTACA	CGCGCGCTAC	
Thc.waio	GACCGCCGGC	GTAAGCCGAG	GAAGGAGCGG	GCGACGGTAG	GTCAGTATGC	CCCGAAACCC	CCGGGCTACA	CGCGCGCTAC	

	1121	1131	1141	1151	1161	1171	1181	1191	1200
DGGE a	AATGGCGGGG	ACAGCGGGAT	CCGACCCCGA	AAGAGGGAGG	TAATCCCTAA	ACCCGCCTCA	TTAGGAATCG	AGGGTTGAAA	
Thf.pend	AATGGCGGGG	ACAGCGGGTT	CCGACCCCGA	AAGGGGGAGG	TAATCCCTAA	ACCCGCCTCA	GTAGGAATCG	AGGGCTGCAA	
DGGE b	AATGGCAGGG	ACAACGGGAA	GCTACCTCGA	AAGGGGGAGC	CAATCCCTAA	ACCTGCCGCA	GTGGGATCG	AGGGCTGAAA	
Sulf.acid	AATGGCAGGG	ACAACGGGAT	GCTACCTCGA	AAGGGGGAGC	CAATCCCTAA	ACCTGCCGCA	GTGGGATCG	AGGGCTGAAA	
OTU Arc03	
Sulf.toko	AATGGCAGGG	ACAGCGGGAT	GCGACCCCGA	AAGGGGGAGC	CAATCCCCAA	ACCTGCCGCA	GTGGGATCG	AGGGCTGAAA	
CP.B3	AATGGGCGGG	ACAATGGGAT	CCGACCCCGA	AAGGGGAAGG	AAATCCCTAA	ACCGCCCCCA	GTTCGGATTG	CGGGCTGCAA	
Thc.waio	AATGGGCGGG	ACAATGGGAT	CCGACCCCGA	AAGGGGAAGG	GAATCCCTAA	ACCGCCCCCA	GTTCGGATTG	CGGGCTGCAA	
	1201	1211	1221	1231	1241	1251	1261	1271	1280
DGGE a	CTCGCCCTCG	TTAACGTAGA	TCCCTA....	
Thf.pend	CTCGCCCTCG	TGAACGTGGA	TCCCTATAAC	CGCGGTCACA	ACGCGCGGTG	AATACGTCCC	TGCTCCTTGC	ACACACCGCC	
DGGE b	CCCGCCCTCG	TGAACGAGGA	TCCCTATAAC	CGCGGTCAAA	AC.....	
Sulf.acid	CCCGCCCTCG	TGAACGAGGA	TCCCTATAAC	CGCGGTCAAA	ACCGCGGTG	AATACGTCCC	TGCTCCTTGC	ACACACCGCC	
OTU Arc03	
Sulf.toko	CCCGCCCTCG	TGAACGAGGA	TCCCTATAAC	CGCGGTCAAA	ACCGCGGTG	AATACGTCCC	TGCTCCTTGC	ACACACCGCC	
CP.B3	CTCGCCCGCA	TGAAGCTGGA	TCCCTATAAC	CGCGGTCATA	TCGCGCG...	
Thc.waio	CTCGCCCGCA	TGAAGCTGGA	TCCCTATAAC	CGCGGTCATA	TCGCGCGGCG	AATACGTCCC	TGCTCCTTGC	ACACACCGCC	
	1281	1291	1301	1311	1321	1331	1341	1351	1360
DGGE a	
Thf.pend	CGTCGCTCCA	CCCAGAGGAG	GCCTAGGTGA	GGCCTCCTGC	GCGTGGGAGG	TCGAACCTGG	GCCTCCCAAG	GGGGGAGAAT	
DGGE b	
Sulf.acid	CGTCGCTCCA	CCCAGAGGAG	AAAGGGGTGA	GGTCCCTTGC	ATGTGGGGGA	TCGAACCTCT	TTCCCGCGAG	GGGGGAGAAT	
OTU Arc03	
Sulf.toko	CGTCGCTCCA	CCCAGAGAGAG	GAAGGGGTGA	GGTCCCCTGC	ATGTGGGGGA	TCGAACCTCT	TCCTCTCGAG	GGGGGAGAAT	
CP.B3	
Thc.waio	CGTCACTCCA	CCCAGAGCGGG	GTCCGGGTGA	GGCTTGCTCT	TTAGGCCGGG	TCGAGCCCGG	GCTCCGTGAG	GGGGGAGAAT	

	1361	1371	1381	1391	1401
DGGE a
Thf.pend	CGTAACAAGG	TGCCGTAGGG	AACCTCGGCC	GGATCACCTC	CTTTC
DGGE b
Sulf.acid	CGTAACAAGG	TAC
OTU Arc03
Sulf.toko	CGTAACAAGG	TACCGTAGGG	AACCTCGGCT	GGATCACCTC	A....
CP.B3
Thc.waio	CGTAACAAGG	TACCGTA

Alignments of bacterial sequences of 16S rRNA gene fragments obtained from Champagne Pool and closest relatives. Abbreviations: Nev.ramo, *Nevskia ramosa*; Sfh.azor, *Sulfurihydrogenibium azorense*; Pac.thio, *Paracoccus thiocyanatus*; Tha.teng, *Thermoanaerobacter tengcongensis*.

	1	11	21	31	41	51	61	71	80
DGGE c
Nev.ramoGCTAACACA	TGCAAGTCGA	ACGAGCTAGT	GGCGGACGGG	
DGGE d
OTU Bac04	...AGAGTTT	GATCCTGGCT	CAGCGCGAAC	GTTGGCGGCG	TGCTAACACA	TGCAAGTCGT	GGGGTTTACC	GGCAAACGGG	
OTU Bac12
Sfh.azorCGCGAAC	GTTGGCGGCG	TGCTAACACA	TGCAAGTCGT	GGGGTTTACC	GGCAAACGGG	
CP.B2	...AGAGTTT	GATCCTGGCT	CAGCGCGAAC	GTTGGCGGCG	TGCTAACACA	TGCAAGTCGT	GGGGTTTACC	GGCAAACGGG	
OTU Bac03GGCGGCA	GGCTAACACA	TGCAAGTCGA	GCGGTTTAGC	GGCGGACGGG	
Pac.thio	GGCTAACACA	TGCAAGTCGA	GCGGTTTAGC	GGCGGACGGG	
CP.B1C	GGCGGACGGG	
Tha.teng	ATTAGAGTTT	GATCCTGGCT	CAGGACGAAC	GCTGGCGGCG	TGCTAACACA	TGCAAGTCGA	GCGGTTTAGC	GGCGGACGGG	
	81	91	101	111	121	131	141	151	160
DGGE c
Nev.ramo	TGAGGAATAC	GTAGGGATCT	GCCTTTAAGT	GGGGGATAAC	CCGGGGAAAC	CCGGATTAAAT	ACCGCATGAT	GCAACAAGG	
DGGE d
OTU Bac04	TGAGTAACAC	GTAGCTACCT	ACCCATAGGT	TGGGGATAAC	TGCCCCGAAAG	GGCAGCTAAT	ACCCAATAAT	GAAACAAGG	
OTU Bac12
Sfh.azor	TGAGTAACGC	GTAGCTACCT	ACCCATAGGT	TGGGGATAAC	CATCCGAAAG	GGTGGCTAAT	ACCCAATAAT	GAGACAAGT	
CP.B2	TGAGTAACAC	GTAGCTACCT	ACCCATAGGT	TGGGGATAAC	TGCCCCGAAAG	GGCAGCTAAT	ACCCAATAAT	AAAACAAGG	
OTU Bac03	TTAGTAACGC	GTGGGAACGT	GCCCTTTGCT	CTGGAATAGC	CCTGGGAAAC	TGGGGGTAAT	ACCGGATGTG	TGAGGAAAGT	
Pac.thio	TGAGTAACGC	GTGGGAACGT	GCCCTTTGCT	ACGGAATAGT	CCTGGGAAAC	TGGGGGTAAT	ACCGTATACG	TATTGAAAGT	
CP.B1	TGAGTAACGC	GTGAGCACCT	ACCCTTGAGA	CAGGGATAAC	CCTGGGAAAC	CGGGGCTAAT	ACCTGATATA	GCATGAAAGG	
Tha.teng	TGAGTAACGC	GTGAGCACCT	ACCCTTGAGA	CAGGGATAAC	CCTGGGAAAC	CGGGGCTAAT	ACCTGATATA	GCATGAAAGC	

	161	171	181	191	201	211	221	231	240
DGGE c
Nev.ramo	CAT CG CTTTT	A AG GAACCTA	CGT CGG ATTA	GCT AGTTGGT	GAGTAATGGC	TCACCAAGGC	GACGATCCGT	AATGGTCTGA	
DGGE d
OTU Bac04	CAG CG CCTAT	GATGGGGCTG	CGT CCC ATCA	GCTT GTTGGT	GAGTAATGGC	TCACCAAGGC	TACGACGGGT	AGCGGTCTGA	
OTU Bac12
Sfh.azor	TTG CG CCTAT	GATGGGGCTG	CGT CCC ATCA	GCT AGTTGGT	GAGTAATGGC	TCACCAAGGC	TACGACGGGT	AACGGTCTGA	
CP.B2	CAG CG CCTAT	GATGGGGCTG	CGT CCC ATCA	GCTT GTTGGT	GAGTAATGGC	TCACCAAGGC	TACGACGGGT	AGCGGTCTGA	
OTU Bac03	TTT CG GCAAG	GATCGGCCCCG	CGT CTG ATTA	GGT AGTTGGT	GAGTAACGGC	TCACCAAGCC	GACGATCCGT	AGTGGTTTGA	
Pac.thio	TTT CG GCGAA	GATCGGCCCCG	CGT TGG ATTA	GGT AGTTGGT	GGGTAATGGC	TCACCAAGCC	GACGATCCAT	AGTGGTTTGA	
CP.B1	GGC CG CTCAA	GATGGGCTCG	CGT CCC ATCA	GCT AGTTGGT	GAGTAACGGC	TCACCAAGGC	TACGACGGGT	AGCGGCCTGA	
Tha.teng	GAC CG CCCAA	GATGGGCTCG	CGT CCC ATCA	GCT AGTTGGT	GAGTAACGGC	TCACCAAGGC	GACGACGGGT	AGCGGCCTGA	
	241	251	261	271	281	291	301	311	320
DGGE c
Nev.ramo	GAGGATGATC	AGTC AC ACCG	GA ACTGAGAC	ACGGTCCGGA	CTCCTACGGG	AGGCAGCAGT	GGGGAATATT	GGACAATGGG	
DGGE d
OTU Bac04	GAGGATGACC	GGCC AC AGTG	GG ACTGAGAC	ACGGCCCGCA	CCCCTACGGG	GGGCAGCAGT	GGGGAATATT	GGGCAATGGC	
OTU Bac12
Sfh.azor	GAGGATGATC	GGTC AC AGCG	GG ACTGAGAC	ACGGCCCGCA	CCCCTACGGG	GGGCAGCAGT	GGGGAATATT	GGGCAATGGC	
CP.B2	GAGGATGACC	GGCC AC AGTG	GG ACTGAGAC	ACGGCCCGCA	CCCCTACGGG	GGGCAGCAGT	GGGGAATATT	GGGCAATGGC	
OTU Bac03	GAGGATGATC	AGCA AC ACTG	GG ACTGAGAC	ACGGCCCAGA	CTCCTACGGG	AGGCAGCAGT	GGGGAATCTT	AGACAATGGG	
Pac.thio	GAGGATGATC	AGCC AC ACTG	GG ACTGAGAC	ACGGCCCAGA	CTCCTACGGG	AGGCAGCAGT	GGGGAATCTT	AGACAATGGG	
CP.B1	GAGGGTGGTC	GGCC AC ACTG	GG ACTGAGAC	ACGGCCCAGA	CTCCTACGGG	AGGCAGCAGT	GGGGAATCTT	CCGCAATGGG	
Tha.teng	GAGGGTGGTC	GGCC AC ACTG	GG ACTGAGAC	ACGGCCCAGA	CTCCTACGGG	AGGCAGCAGT	GGGGAATCTT	CCGCAATGGG	

	321	331	341	351	361	371	381	391	400
DGGE cCCAGCAAT	ACTGCGTGTT	TGATGAAGGC	CTTCGGGTTG	TAAAGACTTT	ACTTGGAAG	AACCTGACTG	
Nev.ramo	CGAAAGCCTG	ATCCAGCAAT	ACCGCGTGTG	TGAAGAAGGC	CTTCGGGTTG	TAAAGACTTT	AGTTGGAAG	ATAATGACGG	
DGGE dCCAGCGAC	GCTGCGTGGT	GGATGAAGGC	CTTCGGGTTG	TAACCCCTTT	TTGGGGGACG	ATCCT.....	
OTU Bac04	CGAAAGGCTG	ACCCAGCAAC	GCCGCGTGGT	GGATGAAGCC	CTTCGGGGTG	TAAACCCCTTT	TTGGGGGAAG	ATAATGACGG	
OTU Bac12	
Sfh.azor	CGAAAGGCTG	ACCCAGCAAC	GCCGCGTGGT	GGATGAAGCC	CTTCGGGGTG	TAAACCCCTTT	TTGGGGGAAG	ATAATGACGG	
CP.B2	CGAAAGGCTG	ACCCAGCAAC	GCCGCGTGGT	GGATGAAGCC	CTTCGGGGTG	TAAACCCCTTT	TTGGGGGAAG	ATTATGACGG	
OTU Bac03	CGCAAGCCTG	ATCTAGCCAT	GCCGCGTGGG	TGATGAAGGC	CTTAGGGTCG	TAAAGCCTTT	CCCGGGGAAG	ATAATGACGG	
Pac.thio	GGCAACCCTG	ATCTAGCCAT	GCCGCGTGAG	TGATGAAGGC	CCTAGGGTTG	TAAAGTCTTT	CGCTGGGAAG	ATAATGACGG	
CP.B1	CGAAAGCCTG	ACGGAGCGAC	GCCGCGTGAG	CGAAGAAGGC	CTTCGGGTCG	TAAAGTCGAT	ATGTGGGAAG	AAGGTGACGG	
Tha.teng	CGAAAGCCTG	ACGGAGCGAC	GCCGCGTGAG	CGAAGAAGGC	CTTCGGGTCG	TAAAGTCGAT	ATGTGGGAAG	AAGGTGACGG	
	401	411	421	431	441	451	461	471	480
DGGE c	TACCAACAGA	ATGCACCGGC	TAACACTGTG	CCAGCAGCCG	CGGTAATA..	
Nev.ramo	TACCGACAGA	ATGCACCGGC	TAACTCTGTG	CCAGCAGCCG	CGGTAATACA	GAGGGGCTAG	CGTTAATCGG	TTTACTGGGC	
DGGE d	
OTU Bac04	TACCCAGGA	ATGGGACGGC	TAACTACGTG	CCAGCAGCCG	CGGTAATACG	TAGGTCCGAA	CGTTGCGCGA	ATTACTGGGC	
OTU Bac12	
Sfh.azor	TACCCAGGA	ATGGGACGGC	TAACTACGTG	CCAGCAGCCG	CGGTAATACG	TAGGTCCGAA	CGTTGCGCGA	ATTACTGGGC	
CP.B2	TACCCAGGA	ATGGGACGGC	TAACTACGTG	CCAGCAGCCG	CGGTAATACG	TAGGTCCGAA	CGTTGCGCGA	ATTACTGGGC	
OTU Bac03	TACCCGGTAA	AGACCCCGGC	TAACTCCGTG	CCAGCAGCCG	CGGTAATACG	GAGGGGTTAG	CGTTGTTCCG	ATGACTGGGC	
Pac.thio	TACCAGCAGA	AGGCCCCGGC	TAACTCCGTG	CCAGCAGCCG	CGGTAATACG	GAGGGGCTAG	CGTTGTTCCG	ATTACTGGGC	
CP.B1	TACCACACGA	AAGCCCCGGC	TAACTACGTG	CCAGCAGCCG	CGGTAAGACG	TAGGGGCGAG	CGTTGTCCGG	ATTACTGGGC	
Tha.teng	TACCACACGA	AAGCCCCGGC	TAACTACGTG	CCAGCAGCCG	CGGTAAGACG	TAGGGGCGAG	CGTTGTCCGG	ATTACTGGGC	

	481	491	501	511	521	531	541	551	560
DGGE c
Nev.ramo	GTAAAGCGTG	CGTAGCGGTT	TGATA AAGTGA	TTGT GAAAGC	CCCGGGCTCA	ACCTGGGAAT	TGCGGTCGAT	ACTGTCAGAC	
DGGE d
OTU Bac04	GTAAAGGGTC	CGTAGCGGTC	TGGTA AAGTGA	AGGT GAAAGC	CCACGGCTTA	ACCGTGGAAT	TGCCTTCCAA	ACTGCCGGAC	
OTU Bac12
Sfh.azor	GTAAAGGGTC	CGTAGCGGTC	TGGTA AAGTGA	AGGT GAAATC	CTACGGCTCA	ACCGTAGAAT	TGCCTTCCAA	ACTGCTGGAC	
CP.B2	GTAAAGGGTC	CGTAGCGGTC	TGGTA AAGTGT	AGGT GAAAGC	CCACGGGTTA	ACCGTGGAAT	TGCCTTCCAA	ACTGCCGGAC	
OTU Bac03	GTAAAGCGCG	CGTAGCGGAT	CATCA AAGTGG	GGGT GAAATC	CCGGGGCTCA	ACCCCGGAAT	GGCCTTCGAG	ACTGGTGGTC	
Pac.thio	GTAAAGCGCA	CGTAGCGGAC	CTGA AAGTGG	GGGT GAAATC	CCGGGGCTCA	ACCTCGGAAC	TGCCTTCAA	ACTACGGGTC	
CP.B1	GTAAAGGGCG	CGTAGCGGTT	TAGCA AAGTAG	GTGT AAAAGG	CCACGGCTCA	ACCGTGGAATA	TGCATCTGAA	ACTGCTGAGC	
Tha.teng	GTAAAGGGCG	CGTAGCGGTT	TAGCA AAGTAG	GTGT AAAAGG	CCACGGCTCA	ACCGTGGAATA	TGCACCTGAA	ACTGCTAGGC	
	561	571	581	591	601	611	621	631	640
DGGE c
Nev.ramo	TCGAAACGGT	AGAGGGAGGC	GGAACTCCAG	GTGTACGGTG	AAATGCGTAG	ATATCTGGAA	GAACACCGAT	GGCGAAGCAA	
DGGE d
OTU Bac04	TTGAGATGGA	AGAGGTCGGC	GGAATTCCCG	GTGTACGGTG	AAATGCGTAG	ATATCGGGAG	GAACACCAGT	AGCGAAGCGG	
OTU Bac12
Sfh.azor	TTGAGCAGGG	AGAGGTCGGC	GGAATTCCCG	GTGTACGGTG	AAATGCGTAG	ATATCGGGAG	GAACACCAGT	GGCGAAGCGG	
CP.B2	TTGAGGTGGA	AGAGGTCGGC	GGAATTCCCG	GTGTACGGTG	AAATGCGTAG	ATATCGGGAG	GAACACCAGT	AGCGAAGCGG	
OTU Bac03	TTGAGTCGAG	AGAGGTGAGT	GGAATTCCGA	GTGTAAGGTG	AAATTTCGTAG	ATATTTCGGAG	GAACACCAGT	GGCGAAGCGG	
Pac.thio	TGGAGTCGAG	AGAGGTGAGT	GGAATTCCGA	GTGTAAGGTG	AAATTTCGTAG	ATATTTCGGAG	GAACACCAGT	GGCGAAGCGG	
CP.B1	TAGAGGCAGG	AGAGGGGAGT	GGAATTCCCG	GTGTACGGTG	AAATGCGTAG	ATATCGGGAG	GAATACCAGT	GGCGAAACGA	
Tha.teng	TAGAGGCAGG	AGAGGGGAGT	GGAATTCCCG	GTGTACGGTG	AAATGCGTAG	ATATCGGGAG	GAATACCAGT	GGCGAAGCGA	

	641	651	661	671	681	691	701	711	720
DGGE c
Nev.ramo	CCCTGGGCCT	GTTTTGACGC	TGAGGCACGA	AAGCGTGGTA	GCAAACAGGA	TTAGATACCC	TGGTAGTCCA	CGCCGTAAAC	
DGGE d
OTU Bac04	CACTGGGACA	TTCCTGACG
OTU Bac12
Sfh.azor	CACTGGAACT	GTCCTTGACGC	TGAGGGACGA	AAGCTAGGGA	GCAAACCGGA	TTAGATACCC	GGGTAGTCCT	AGCCGTAAAC	
CP.B2	CACTGGGACA	TTCCTGACGC	TGAGGGACGA	AAGCTAGGGA	GCAAACCGGA	TTAGATACCC	GGGTAGTCCT	AGCCGTAAAC	
OTU Bac03	TACTGGCTCG	ACACTTGACGC	TGAGGTGCGA	AAGCGTGGGA	GCAAACAGGA	TTAGATACCC	TGGTAGTCCA	CGCCGTAAAC	
Pac.thio	TACTGGCTCG	ATACTTGACGC	TGAGGTGCGA	AAGCGTGGGA	GCAAACAGGA	TTAGATACCC	TGGTAGTCCA	CGCCGTAAAC	
CP.B1	TCCTGGACTG	GCCCTTGACGC	TGAGGCGCGA	AAGCGTGGGA	GCAAACAGGA	TTAGATACCC	TGGTAGTCCA	CGCTGTAAAC	
Tha.teng	TCCTGGACTG	GCCCTTGACGC	TGAGGCGCGA	GAGCGTGGGA	GCGAACAGGA	TTAGATACCC	TGGTAGTCCA	CGCTGTAAAC	
	721	731	741	751	761	771	781	791	800
DGGE c
Nev.ramo	ATGAGAACTT	GACGTTGGTT	TAAATCGGTG	TCGTAGCTAA	CGCGATAAGT	TCTCCGCTG	GAGTACGGCC	GCAAGGTAA	
DGGE d
OTU Bac04
OTU Bac12
Sfh.azor	ATGGATGCTA	GATGTTGGCCT	AAAGGCTGTG	CCGCAGCTAA	CGCGTTAAGC	ATCCCGCCTG	GAGTACGGCC	GCAAGGTAA	
CP.B2	ATGGATGCTT	GATGTTGACCT	AAAGGTCGTG	TCGTAGCTAA	CGCGTTAAGC	ATCCCGCCTG	GAGTACGGCC	GCAAGGTAA	
OTU Bac03	ATGAATGCCA	GACGTCGGGG	TGCTTCGGTG	TCACACCTAA	CGGATTAAGC	ATTCCGCTG	GAGTACGGTC	GCAAGATTAA	
Pac.thio	ATGAATGCCA	GTCGTCGGGC	AGGTTCGGTG	ACACACCTAA	CGGATTAAGC	ATTCCGCTG	GAGTACGGTC	GCAAGATTAA	
CP.B1	ATGGGTGCTA	GGTTGGGGGA	GATTTCCGTG	CCGTAGGAAA	CCCAATAAGC	ACCCCGCCTG	GAGTACGGCC	GCAAGGCTAA	
Tha.teng	ATGGGTGCTA	GGTTGGGGGA	GATTTCCGTG	CCGTAGGAAA	CCCAATAAGC	ACCCCGCCTG	GAGTACGGCC	GCAAGGCTAA	

	801	811	821	831	841	851	861	871	880
DGGE c
Nev.ramo	ACTCAAAGGA	ATTGACGGGG	GCCCGACAAC	GGTGGAGTAT	GTGGTTTAAT	TCGATGCAAC	GCGAAGAACC	TTACCTGGTC	
DGGE d
OTU Bac04
OTU Bac12
Sfh.azor	ACTCAAAGGA	ATTGACGGGG	ACCCGACAAC	GGTGGAGCGT	CTGGTTTAAT	TCGATGCTAA	CCGAAAACC	TTACCAGGGT	
CP.B2	ACTCAAAGGA	ATTGACGGGG	ACCCGACAAC	GGTGGAGCGT	CTGGTTTAAT	TCGATGCTAA	CCGAAAACC	TCACCAGGGT	
OTU Bac03	ACTCAAAGGA	ATTGACGGGG	GCCCGACAAC	GGTGGAGCAT	GTGGTTTAAT	TCGAAGCAAC	GCGCAGAACC	TTACCAACCC	
Pac.thio	ACTCAAAGGA	ATTGACGGGG	GCCCGACAAC	GGTGGAGCAT	GTGGTTTAAT	TCGAAGCAAC	GCGCAGAACC	TTACCAACCC	
CP.B1	ACTCAAAGGA	ATTGACGGGG	GCCCGACAAC	GGTGGAGCAT	GTGGTTTAAT	TCGAAGCAAC	GCGAAGAACC	TTACCAGGGC	
Tha.teng	ACTCAAAGGA	ATTGACGGGG	GCCCGACAAC	GGTGGAGCAT	GTGGTTTAAT	TCGAAGCAAC	GCGAAGAACC	TTACCAGGGC	
	881	891	901	911	921	931	941	951	960
DGGE c
Nev.ramo	TTGACATGTC	AAGGAGTCTG	CAGAGATCGG	ATGTGCCTTC	GGGAACCTGA	ACACAGGTGC	TGCATGGCTG	TCGTCAGCTC	
DGGE d
OTU Bac04
OTU Bac12GAAAGGCA	CTAGCGATTT	CTCGTGCGCC	GGACAG-TGG	TGCATGGTCG	TCGTCAGCTC	
Sfh.azor	TTGACATGGG	TGTGTCGGGT	ATGAAAGACC	CTAGGGATTA	TTCCCGCGCC	GCACAGGTGG	TGCATGGTCG	TCGTCAGCTC	
CP.B2	TTGACATCGG	TGTGTCGTAT	CCGAAAGGTA	CTAGCGATTT	CTCGTGCGCC	GGACAGGTGG	TGCATGGTCG	TCGTCAGCTC	
OTU Bac03	TTGACATCGC	CTGACCGGCC	TGGAGAAAGT	CTTTCCCGCA	AGGGACAGGT	GGACAGGTGC	TGCATGGCTG	TCGTCAGCTC	
Pac.thio	TTGACATCGC	AGGACCGCCC	GAGAGATGGG	TTTTCTCGTA	AGAGACCTGT	GGACAGGTGC	TGCATGGCTG	TCGTCAGCTC	
CP.B1	TTGACATGAG	GTAGTAGCAG	CCGAAAGTGG	CGACCTCTTA	TGGGGAGCCT	GCACAGGTGG	TGCATGGTTG	TCGTCAGCTC	
Tha.teng	TTGACATGAG	GTAGTAGCAG	CCGAAAGTGG	CGACCTCGAA	AGGGGAGCCT	GCACAGGTGG	TGCATGGTTG	TCGCCAGCTC	

	961	971	981	991	1001	1011	1021	1031	1040
DGGE c
Nev.ramo	GTGTCGTGAG	ATGTTGGGTT	AAGTCCCGCA	ACGAGCGCAA	CCCTTGCCCT	TAGTTGCCAT	CATTCAATTGG	GCACTCTAAG	
DGGE d
OTU Bac04
OTU Bac12	GTGTCGTGAG	ATGTTGGGTT	AAGTCCCGCA	ACGAGCGCAA	CCCTTGCCCT	GTGTTACCAG	CGGTTACCGG	GCACTCACAG	
Sfh.azor	GTGTCGTGAG	ATGTTGGGTT	AAGTCCCGCA	ACGAGCGCAA	CCCTTGCCCT	GTGTTACCAG	CGGTAACCGG	GTACTCACAG	
CP.B2	GTGTCGTGAG	ATGTTGGGTT	AAGTCCCGCA	ACGAGCGCAA	CCCTTGCCCT	GTGTTACCAG	CGGTTACCGG	GCACTCACAG	
OTU Bac03	GTGTCGTGAG	ATGTTGGGTT	AAGTCCCGCA	ACGAGCGCAA	CCCTTGCCCT	GTGTTACCAG	CGGTTACCGG	GCACTCACAG	
Pac.thio	GTGTCGTGAG	ATGTTGGGTT	AAGTCCCGCA	ACGAGCGCAA	CCCTTGCCCT	GTGTTACCAG	CGGTTACCGG	GCACTCACAG	
CP.B1	GTGTCGTGAG	ATGTTGGGTT	AAGTCCCGCA	ACGAGCGCAA	CCCTTGCCCT	GTGTTACCAG	CGGTTACCGG	GCACTCACAG	
Tha.teng	GTGTCGTGAG	ATGTTGGGTT	AAGTCCCGCA	ACGAGCGCAA	CCCTTGCCCT	GTGTTACCAG	CGGTTACCGG	GCACTCACAG	
	1041	1051	1061	1071	1081	1091	1101	1111	1120
DGGE c
Nev.ramo	GGGACGCCG	GTGAAAACCG	GAGGAAGGTG	GGGATGACGT	CAAGTCATCA	TGCCCCTTAT	GACCAGGGCT	ACACACGTAC	
DGGE d
OTU Bac04
OTU Bac12	GGGACTGCCG	GCGAAAGTCG	GAGGAAGGAG	GGGATGACGT	CAGATCAGTA	TGCCCTTTAT	GCCCTGGGCT	ACACAGGCGC	
Sfh.azor	GGGACTGCCG	GCGAAAGTCG	GAGGAAGGAG	GGGATGACGT	CAGATCAGTA	TGCCCTTTAT	GCCCTGGGCT	ACACAGGCGC	
CP.B2	GGGACTGCCG	GCGAAAGTCG	GAGGAAGGAG	GGGATGACGT	CAGATCAGTA	TGCCCTTTAT	GCCCTGGGCT	ACACAGGCGC	
OTU Bac03	GGAAC TGCCG	GTGAAAGCGG	GAGGAAGGTG	TGGATGACGT	CAAGTCCTCA	TGGCCCTTAC	GGGTTGGGCT	ACACACGTGC	
Pac.thio	GAAACTGCCG	ATGAAAGTCG	GAGGAAGGTG	TGGATGACGT	CAAGTCCTCA	TGGCCCTTAC	GGGTTGGGCT	ACACACGTGC	
CP.B1	GGGACTGCCG	TCGAAAGACG	GAGGAAGGTG	GGGATGACGT	CAAATCATCA	TGCCCTATAT	GCCCTGGGCC	ACACACGTGC	
Tha.teng	GGGACTGCCG	TCGAAAGACG	GAGGAAGGTG	GGGATGACGT	CAAATCATCA	TGCCCTATAT	GCCCTGGGCC	ACACACGTGC	

	1121	1131	1141	1151	1161	1171	1181	1191	1200
DGGE c
Nev.ramo	TACAATGGCG	GTACAGAGGG	TAATCCCAAG	CCGTCGTAGT	CCGGATTGAG	TCTGCAACTC	GACTCCATGA	AGTCGGAATC	
DGGE d
OTU Bac04
OTU Bac12	TACAGTGGAG	GGACAATGGG	AAACCCCAAC	CCTTCGTGGT	GCGGATTGGG	GTGCAACTC	ACCCCATGA	AGGC GGAATC	
Sfh.azor	TACAGTGGAG	GGACAATGGG	AAATCCCAAC	CCTTCGTGGT	GCGGATTGGG	GTGCAACTC	ACCCCATGA	AGGC GGAATC	
CP.B2	TACAGTGGAG	GGACAATGGG	AAACCCCAAC	CCTTCGTGGT	GCGGATTGGG	GTGCAACTC	ACCCCATGA	AGGC GGAATC	
OTU Bac03	TACAATGGGG	TGACAGAGGG	TCATCCCAAA	GCCTCTCAGT	TCGGATTGCG	TCTGCAACTC	GACGGCATGA	AGTCGGAATC	
Pac.thio	TACAATGGGG	TGACAGTGGG	TAATCCCAAA	GCCTCTCAGT	TCGGATTGGG	TCTGCAACTC	GACCCCATGA	AGTTGGAATC	
CP.B1	TACAATGGCG	GTACAGAGGG	AAATCCCAAG	CCGTCTCAGT	TCGGATTGAG	GCTGCAACTC	GCCTGCATGA	AGGC GGAATC	
Tha.teng	TACAATGGCG	GTACAGAGGG	AAATCCCAAG	CCGTCTCAGT	TCGGATTGAG	GCTGCAACTC	GCCTGCATGA	AGGC GGAATC	
	1201	1211	1221	1231	1241	1251	1261	1271	1280
DGGE c
Nev.ramo	GCTAGTAATC	GCGGATCAGC	TTGTGCGGTG	AATACGTTCC	CGAGCCTTGT	ACACACCGCC	CGTCACACCA	TGGGAGTTGG	
DGGE d
OTU Bac04
OTU Bac12	GGTAGTAATG	GCGAATCAGC	ATGTGCCGTG	AATACGTTCC	CGGGTCTTGT	ACACACCGCC	CGTCACGCCA	TGGGAGTCGG	
Sfh.azor	GGTAGTAATG	GCGAATCAGC	ATGTGCCGTG	AATACGTTCC	CGGGTCTTGT	ACACACCGCC	CGTCACGCCA	TGGGAGTCGG	
CP.B2	GGTAGTAATG	GCGAATCAGC	ATGTGCCGTG	AATACGTTCC	CGGGTCTTGT	ACACACCGCC	CGTCACGCCA	TGGGAGTCGG	
OTU Bac03	GCTAGTAATC	GCGCATCAGC	TCGGGCGGTG	AATACGTTCC	CGGGCCTTGT	ACACACCGCC	CGTCACACCA	TGGGAGTTGG	
Pac.thio	GCTAGTAATC	GCGGAACAGC	ATGCGCGGTG	AATACGTTCC	CGGGCCTTGT	ACACACCGCC	CGTCACACCA	TGGGAGTTGG	
CP.B1	GCTAGTAATC	GCGGATCAGC	ATGCCCGGTG	AATGCGTTCC	CGGGCCTTGT	ACACACCGCC	CGTCACACCA	CGAGAGTCTG	
Tha.teng	GCTAGTAATC	GCGGATCAGC	ATGCGCGGTG	AATGCGTTCC	CGGGCCTTGT	ACACACCGCC	CGTCACACCA	CGAGAGTCTG	

	1281	1291	1301	1311	1321	1331	1341	1351	1360
DGGE c
Nev.ramo	CTGC ACCAGA	AGCC.....
DGGE d
OTU Bac04
OTU Bac12	GTT CATCGGA	AGTCCCCGAG	A ACCGCAAGC	AGGGGCCGAT	GATGGGCCCG	AT GACTGGGG	C GAAGTCGTA	A CAAGGTAGC	
Sfh.azor	GTT CATCGGA	AGTCCCCGAG	A ACCGCAAGC	AGGGGCCGAT	GATGGGCCCTG	AT GACTGGGG	CG.....
CP.B2	GTT CATCGGA	AGTCCCCGAG	A ACCGCAAGC	AGGGGCCGAT	GATGGGCCCG	AT GACTGGGG	C GAAGTCGTA	A CAAGGTAGC	
OTU Bac03	GTT GACCGA	AGGTGGTGCG	G ACCGTAAGC	AGCCAACCAC	GGTCAGTTCA	GCG ACTGGGG	T GAAGTCGTA	A CAAGGTAGC	
Pac.thio	GTCT ACCGA	CGGCCGTGCG	A ACCGCAAGG	CAGCGGACCA	CGGTAGGCTC	AG.....
CP.B1	CAAC ACCG.
Tha.teng	CAAC ACCGA	AGCCGGTGGC	A ACCGAAAGG	AGCCGTCGAA	GGTGGGGCAG	AT GATTGGGG	T GAAGTCGTA	A CAAGGTAA.	
	1361	1371	1381	1391					
DGGE c					
Nev.ramo					
DGGE d					
OTU Bac04					
OTU Bac12	CCTAGGGGAA	CCTGCGGCTG	GATCACCTCC	TT.					
Sfh.azor					
CP.B2	CCTAGGGGAA	CCTGCGGCTG	GATCACCTCC	TTA					
OTU Bac03	CGTAGGGGAA	CCTGCGGCTG	GATCACCTCC	TT.					
Pac.thio					
CP.B1					
Tha.teng					

Appendix F: Culture experiments

Table 26. Effect of potential electron donors, electron acceptors, and carbon sources on growth of strain CP.B2^T. Cultures were transferred at least three times on the same e⁻ donor / e⁻ acceptor combination to ensure the growth was not due to substrate carry-over from the inoculum. Abbreviations: -, no growth at all; +, growth after first transfer in fresh medium; +++, growth after third transfer in fresh medium, ¹⁾ in presence of 8 mM S₂O₃²⁻, ²⁾ in presence of 1% S⁰. Negative controls are indicated in bold.

e ⁻ donor	e ⁻ acceptor	Carbon source	Gas phase 1.7 kPa	Growth
none	10 mM NaNO₂	CO₂	N₂/CO₂ (80%/20%)	-
none	10 mM NaNO₃	CO₂	N₂/CO₂ (80%/20%)	-
none	10 mM Na₂SO₃	CO₂	N₂/CO₂ (80%/20%)	-
none	10 mM Na₂SO₄	CO₂	N₂/CO₂ (80%/20%)	-
none	5 mM Na₂SeO₃	CO₂	N₂/CO₂ (80%/20%)	-
none	5 mM Na₂SeO₄	CO₂	N₂/CO₂ (80%/20%)	-
none	5 mM NaAsO₂	CO₂	N₂/CO₂ (80%/20%)	-
none	5 mM	CO₂	N₂/CO₂ (80%/20%)	-
H₂	none	CO₂	H₂/CO₂ (80%/20%)	-
H ₂	O ₂	CO ₂	H ₂ /CO ₂ /O ₂ (79%/15%/6%)	-
H ₂	O ₂	CO ₂	H ₂ /CO ₂ /O ₂ (79%/15%/6%)	¹⁾ +++
H ₂	O ₂	CO ₂	H ₂ /CO ₂ /O ₂ (79%/15%/6%)	²⁾ +++
H ₂	10 mM NaNO ₂	CO ₂	H ₂ /CO ₂ (80%/20%)	-
H ₂	10 mM NaNO ₃	CO ₂	H ₂ /CO ₂ (80%/20%)	-
H ₂	10 mM Na ₂ SO ₃	CO ₂	H ₂ /CO ₂ (80%/20%)	-
H ₂	10 mM Na ₂ SO ₄	CO ₂	H ₂ /CO ₂ (80%/20%)	-
H ₂	5 mM Na ₂ SeO ₃	CO ₂	H ₂ /CO ₂ (80%/20%)	-
H ₂	5 mM Na ₂ SeO ₄	CO ₂	H ₂ /CO ₂ (80%/20%)	-
H ₂	5 mM NaAsO ₂	CO ₂	H ₂ /CO ₂ (80%/20%)	-
H ₂	5 mM Na ₂ HAsO ₄	CO ₂	H ₂ /CO ₂ (80%/20%)	-
H ₂	10 mM NaNO ₂	CO ₂	H ₂ /CO ₂ /O ₂ (79%/15%/6%)	-
H ₂	10 mM NaNO ₃	CO ₂	H ₂ /CO ₂ /O ₂ (79%/15%/6%)	+
H ₂	10 mM Na ₂ SO ₃	CO ₂	H ₂ /CO ₂ /O ₂ (79%/15%/6%)	-
H ₂	10 mM Na ₂ SO ₄	CO ₂	H ₂ /CO ₂ /O ₂ (79%/15%/6%)	-
H ₂	5 mM Na ₂ SeO ₃	CO ₂	H ₂ /CO ₂ /O ₂ (79%/15%/6%)	-
H ₂	5 mM Na ₂ SeO ₄	CO ₂	H ₂ /CO ₂ /O ₂ (79%/15%/6%)	+
H ₂	5 mM NaAsO ₂	CO ₂	H ₂ /CO ₂ /O ₂ (79%/15%/6%)	-
H ₂	5 mM Na ₂ HAsO ₄	CO ₂	H ₂ /CO ₂ /O ₂ (79%/15%/6%)	+

Table 26. Continued.

e ⁻ donor	e ⁻ acceptor	Carbon source	Gas phase 1.7 kPa	Growth
H ₂	1 mM NaAsO ₂	CO ₂	H ₂ /CO ₂ /O ₂ (79%/15%/6%)	+
H ₂	1 mM Na ₂ HAsO ₄	CO ₂	H ₂ /CO ₂ /O ₂ (79%/15%/6%)	+
H ₂	10 mM NaNO ₂	0.2% casa-amino acids	H ₂ (100%)	-
H ₂	10 mM NaNO ₂	0.2% Na-pyruvate	H ₂ (100%)	-
H ₂	10 mM NaNO ₂	0.2% starch	H ₂ (100%)	-
H ₂	10 mM NaNO ₂	0.2% trypticase peptone	H ₂ (100%)	-
H ₂	10 mM NaNO ₂	0.2% yeast extract	H ₂ (100%)	-
H ₂	10 mM NaNO ₃	0.2% casa-amino acids	H ₂ (100%)	-
H ₂	10 mM NaNO ₃	0.2% Na-pyruvate	H ₂ (100%)	-
H ₂	10 mM NaNO ₃	0.2% starch	H ₂ (100%)	-
H ₂	10 mM NaNO ₃	0.2% trypticase peptone	H ₂ (100%)	-
H ₂	10 mM NaNO ₃	0.2% yeast extract	H ₂ (100%)	-
H ₂	10 mM Na ₂ SO ₃	0.2% casa-amino acids	H ₂ (100%)	-
H ₂	10 mM Na ₂ SO ₃	0.2% Na-pyruvate	H ₂ (100%)	-
H ₂	10 mM Na ₂ SO ₃	0.2% starch	H ₂ (100%)	-
H ₂	10 mM Na ₂ SO ₃	0.2% trypticase peptone	H ₂ (100%)	-
H ₂	10 mM Na ₂ SO ₃	0.2% yeast extract	H ₂ (100%)	-
H ₂	10 mM Na ₂ SO ₄	0.2% casa-amino acids	H ₂ (100%)	-
H ₂	10 mM Na ₂ SO ₄	0.2% Na-pyruvate	H ₂ (100%)	-
H ₂	10 mM Na ₂ SO ₄	0.2% starch	H ₂ (100%)	-
H ₂	10 mM Na ₂ SO ₄	0.2% trypticase peptone	H ₂ (100%)	-
H ₂	10 mM Na ₂ SO ₄	0.2% yeast extract	H ₂ (100%)	-
H ₂	5 mM Na ₂ SeO ₃	0.2% casa-amino acids	H ₂ (100%)	-
H ₂	5 mM Na ₂ SeO ₃	0.2% Na-pyruvate	H ₂ (100%)	-
H ₂	5 mM Na ₂ SeO ₃	0.2% starch	H ₂ (100%)	-
H ₂	5 mM Na ₂ SeO ₃	0.2% trypticase peptone	H ₂ (100%)	-
H ₂	5 mM Na ₂ SeO ₃	0.2% yeast extract	H ₂ (100%)	-
H ₂	5 mM Na ₂ SeO ₄	0.2% casa-amino acids	H ₂ (100%)	-
H ₂	5 mM Na ₂ SeO ₄	0.2% Na-pyruvate	H ₂ (100%)	-
H ₂	5 mM Na ₂ SeO ₄	0.2% starch	H ₂ (100%)	-
H ₂	5 mM Na ₂ SeO ₄	0.2% trypticase peptone	H ₂ (100%)	-
H ₂	5 mM Na ₂ SeO ₄	0.2% yeast extract	H ₂ (100%)	-
H ₂	5 mM NaAsO ₂	0.2% casa-amino acids	H ₂ (100%)	-
H ₂	5 mM NaAsO ₂	0.2% Na-pyruvate	H ₂ (100%)	+

Table 26. Continued.

e ⁻ donor	e ⁻ acceptor	Carbon source	Gas phase 1.7 kPa	Growth
H ₂	5 mM NaAsO ₂	0.2% starch	H ₂ (100%)	-
H ₂	5 mM NaAsO ₂	0.2% trypticase peptone	H ₂ (100%)	+
H ₂	5 mM NaAsO ₂	0.2% yeast extract	H ₂ (100%)	-
H ₂	5 mM Na ₂ HAsO ₄	0.2% casa-amino acids	H ₂ (100%)	-
H ₂	5 mM Na ₂ HAsO ₄	0.2% Na-pyruvate	H ₂ (100%)	+
H ₂	5 mM Na ₂ HAsO ₄	0.2% starch	H ₂ (100%)	-
H ₂	5 mM Na ₂ HAsO ₄	0.2% trypticase peptone	H ₂ (100%)	-
H ₂	5 mM Na ₂ HAsO ₄	0.2% yeast extract	H ₂ (100%)	-
H ₂	10 mM NaNO ₂	0.2% casa-amino acids	H ₂ /O ₂ (94%/6%)	-
H ₂	10 mM NaNO ₂	0.2% Na-pyruvate	H ₂ /O ₂ (94%/6%)	-
H ₂	10 mM NaNO ₂	0.2% starch	H ₂ /O ₂ (94%/6%)	-
H ₂	10 mM NaNO ₂	0.2% trypticase peptone	H ₂ /O ₂ (94%/6%)	-
H ₂	10 mM NaNO ₂	0.2% yeast extract	H ₂ /O ₂ (94%/6%)	-
H ₂	10 mM NaNO ₃	0.2% casa-amino acids	H ₂ /O ₂ (94%/6%)	-
H ₂	10 mM NaNO ₃	0.2% Na-pyruvate	H ₂ /O ₂ (94%/6%)	-
H ₂	10 mM NaNO ₃	0.2% starch	H ₂ /O ₂ (94%/6%)	-
H ₂	10 mM NaNO ₃	0.2% trypticase peptone	H ₂ /O ₂ (94%/6%)	-
H ₂	10 mM NaNO ₃	0.2% yeast extract	H ₂ /O ₂ (94%/6%)	-
H ₂	10 mM Na ₂ SO ₃	0.2% casa-amino acids	H ₂ /O ₂ (94%/6%)	-
H ₂	10 mM Na ₂ SO ₃	0.2% Na-pyruvate	H ₂ /O ₂ (94%/6%)	-
H ₂	10 mM Na ₂ SO ₃	0.2% starch	H ₂ /O ₂ (94%/6%)	-
H ₂	10 mM Na ₂ SO ₃	0.2% trypticase peptone	H ₂ /O ₂ (94%/6%)	-
H ₂	10 mM Na ₂ SO ₃	0.2% yeast extract	H ₂ /O ₂ (94%/6%)	-
H ₂	10 mM Na ₂ SO ₄	0.2% casa-amino acids	H ₂ /O ₂ (94%/6%)	-
H ₂	10 mM Na ₂ SO ₄	0.2% Na-pyruvate	H ₂ /O ₂ (94%/6%)	-
H ₂	10 mM Na ₂ SO ₄	0.2% starch	H ₂ /O ₂ (94%/6%)	-
H ₂	10 mM Na ₂ SO ₄	0.2% trypticase peptone	H ₂ /O ₂ (94%/6%)	-
H ₂	10 mM Na ₂ SO ₄	0.2% yeast extract	H ₂ /O ₂ (94%/6%)	-
H ₂	5 mM Na ₂ SeO ₃	0.2% casa-amino acids	H ₂ /O ₂ (94%/6%)	-
H ₂	5 mM Na ₂ SeO ₃	0.2% Na-pyruvate	H ₂ /O ₂ (94%/6%)	-
H ₂	5 mM Na ₂ SeO ₃	0.2% starch	H ₂ /O ₂ (94%/6%)	-
H ₂	5 mM Na ₂ SeO ₃	0.2% trypticase peptone	H ₂ /O ₂ (94%/6%)	-
H ₂	5 mM Na ₂ SeO ₃	0.2% yeast extract	H ₂ /O ₂ (94%/6%)	-
H ₂	5 mM Na ₂ SeO ₄	0.2% casa-amino acids	H ₂ /O ₂ (94%/6%)	-

Table 26. Continued.

e ⁻ donor	e ⁻ acceptor	Carbon source	Gas phase 1.7 kPa	Growth
H ₂	5 mM Na ₂ SeO ₄	0.2% Na-pyruvate	H ₂ /O ₂ (94%/6%)	-
H ₂	5 mM Na ₂ SeO ₄	0.2% starch	H ₂ /O ₂ (94%/6%)	-
H ₂	5 mM Na ₂ SeO ₄	0.2% trypticase peptone	H ₂ /O ₂ (94%/6%)	-
H ₂	5 mM Na ₂ SeO ₄	0.2% yeast extract	H ₂ /O ₂ (94%/6%)	-
H ₂	5 mM NaAsO ₂	0.2% casa-amino acids	H ₂ /O ₂ (94%/6%)	-
H ₂	5 mM NaAsO ₂	0.2% Na-pyruvate	H ₂ /O ₂ (94%/6%)	-
H ₂	5 mM NaAsO ₂	0.2% starch	H ₂ /O ₂ (94%/6%)	-
H ₂	5 mM NaAsO ₂	0.2% trypticase peptone	H ₂ /O ₂ (94%/6%)	-
H ₂	5 mM NaAsO ₂	0.2% yeast extract	H ₂ /O ₂ (94%/6%)	-
H ₂	5 mM Na ₂ HAsO ₄	0.2% casa-amino acids	H ₂ /O ₂ (94%/6%)	-
H ₂	5 mM Na ₂ HAsO ₄	0.2% Na-pyruvate	H ₂ /O ₂ (94%/6%)	-
H ₂	5 mM Na ₂ HAsO ₄	0.2% starch	H ₂ /O ₂ (94%/6%)	-
H ₂	5 mM Na ₂ HAsO ₄	0.2% trypticase peptone	H ₂ /O ₂ (94%/6%)	-
H ₂	5 mM Na ₂ HAsO ₄	0.2% yeast extract	H ₂ /O ₂ (94%/6%)	-
8 mM S₂O₃²⁻	none	CO₂	N₂/CO₂ (80%/20%)	-
8 mM S ₂ O ₃ ²⁻	10 mM NaNO ₂	CO ₂	N ₂ /CO ₂ (80%/20%)	-
8 mM S ₂ O ₃ ²⁻	10 mM NaNO ₃	CO ₂	N ₂ /CO ₂ (80%/20%)	-
8 mM S ₂ O ₃ ²⁻	10 mM Na ₂ SO ₃	CO ₂	N ₂ /CO ₂ (80%/20%)	-
8 mM S ₂ O ₃ ²⁻	10 mM Na ₂ SO ₄	CO ₂	N ₂ /CO ₂ (80%/20%)	-
8 mM S ₂ O ₃ ²⁻	5 mM Na ₂ SeO ₃	CO ₂	N ₂ /CO ₂ (80%/20%)	-
8 mM S ₂ O ₃ ²⁻	5 mM Na ₂ SeO ₄	CO ₂	N ₂ /CO ₂ (80%/20%)	-
8 mM S ₂ O ₃ ²⁻	5 mM NaAsO ₂	CO ₂	N ₂ /CO ₂ (80%/20%)	-
8 mM S ₂ O ₃ ²⁻	5 mM Na ₂ HAsO ₄	CO ₂	N ₂ /CO ₂ (80%/20%)	-
1% S⁰	none	CO₂	N₂/CO₂ (80%/20%)	-
1% S ⁰	10 mM NaNO ₂	CO ₂	N ₂ /CO ₂ (80%/20%)	-
1% S ⁰	10 mM NaNO ₃	CO ₂	N ₂ /CO ₂ (80%/20%)	-
1% S ⁰	10 mM Na ₂ SO ₃	CO ₂	N ₂ /CO ₂ (80%/20%)	-
1% S ⁰	10 mM Na ₂ SO ₄	CO ₂	N ₂ /CO ₂ (80%/20%)	-
1% S ⁰	5 mM Na ₂ SeO ₃	CO ₂	N ₂ /CO ₂ (80%/20%)	-
1% S ⁰	5 mM Na ₂ SeO ₄	CO ₂	N ₂ /CO ₂ (80%/20%)	-
1% S ⁰	5 mM NaAsO ₂	CO ₂	N ₂ /CO ₂ (80%/20%)	-
1% S ⁰	5 mM Na ₂ HAsO ₄	CO ₂	N ₂ /CO ₂ (80%/20%)	-

Table 26. Continued.

e ⁻ donor	e ⁻ acceptor	Carbon source	Gas phase 1.7 kPa	Growth
1 mM NaAsO ₂	1 mM Na ₂ HAsO ₄	CO ₂	N ₂ /CO ₂ (80%/20%)	+
none	none	0.2% casa-amino acids	N ₂ (100%)	¹⁾ -
none	none	0.2% Na-pyruvate	N ₂ (100%)	¹⁾ -
none	none	0.2% starch	N ₂ (100%)	¹⁾ -
none	none	0.2% trypticase peptone	N ₂ (100%)	¹⁾ +
none	none	0.2% yeast extract	N ₂ (100%)	¹⁾ +
organic	O ₂	0.2% casa-amino acids	N ₂ /O ₂ (94%/6%)	¹⁾ -
organic	O ₂	0.2% Na-pyruvate	N ₂ /O ₂ (94%/6%)	¹⁾ -
organic	O ₂	0.2% starch	N ₂ /O ₂ (94%/6%)	¹⁾ +
organic	O ₂	0.2% trypticase peptone	N ₂ /O ₂ (94%/6%)	¹⁾ +
organic	O ₂	0.2% yeast extract	N ₂ /O ₂ (94%/6%)	¹⁾ +
H ₂	O ₂	0.2% casa-amino acids	H ₂ /O ₂ (94%/6%)	¹⁾ -
H ₂	O ₂	0.2% Na-pyruvate	H ₂ /O ₂ (94%/6%)	¹⁾ -
H ₂	O ₂	0.2% starch	H ₂ /O ₂ (94%/6%)	¹⁾ -
H ₂	O ₂	0.2% trypticase peptone	H ₂ /O ₂ (94%/6%)	¹⁾ -
H ₂	O ₂	0.2% yeast extract	H ₂ /O ₂ (94%/6%)	¹⁾ -

Appendix G: NZAPLUME III research cruise

Introduction

It is estimated that more than 90% of the entire sea floor has an average temperature below 4° C (Levitus & Boyer, 1994). However, the discovery of hot brines in the Red Sea in the 1960s (Degens & Ross, 1969) and hydrothermal vents in the Pacific Ocean in the late 1970s (Corliss *et al.*, 1979) showed the existence of submarine geothermal areas within the cold oceanic environment, and in the case of hydrothermal vents, the presence of thermophilic microorganisms in these habitats (Jeamthong, 2000; Stetter, 1996). The temperature of vent water varies from around 23° C (Galapagos vents) to around 350° C (vents of the East Pacific Rise) and is typically rich in dissolved metal ions (Gage & Tyler, 1991). When discharged hot vent fluid mixes with colder seawater metal sulfides and oxides such as zinc sulfide, iron sulfide, copper-iron sulfide, manganese oxide, and iron oxide are precipitated out and form a turbid hydrothermal vent plume (Tivey, 1998). The plume rises (up to 200 m) until the precipitates are neutral buoyant and is distributed by currents. In response to chemophysical conditions different from terrestrial hot springs (e.g. steeper temperature gradient, higher hydrostatic pressure, higher NaCl concentration), free-living microorganisms associated with hydrothermal vents (Karl, 1995) may have evolved unique strategies to interact with metal ions.

The geothermally active Kermadec arc lies in a subduction zone where the Pacific plate slides beneath the Indo-Australian plate and runs for approximately 1,200 km from the North Island of New Zealand northeast towards Tonga. The research cruises NZAPLUME I and II (New Zealand and American plume mapping expedition) surveyed several active submarine volcanoes and hydrothermal plumes in this area (de Ronde *et al.*, 2001; de Ronde *et al.*, 2003). The primary aim of this study during the NZAPLUME III cruise along the Kermadec arc started on 23rd September until 17th October 2004 was to identify and isolate novel microorganisms from hydrothermal vent plumes using molecular biological and microbiological approaches. Secondary aims, conducted in collaboration with Sean Langley and Danielle Fortin (University of Ottawa, Canada) included identification of minerals

within the plume samples by X-ray diffraction analyses, and evaluation of particulates (both mineral and biological) using electron microscopy.

Material and Methods

Teflon-coated 10-liter Niskin bottles were used to obtain discrete water samples (Figure 41). Samples were then collected directly from Niskin bottles for further processing.



Figure 41. Stainless steel stand accommodating 19 Niskin bottles. During sampling, the unit is connected to the mother ship via a tow-cable several thousands of meters in length and provides information on conductivity (salinity), pressure (depth), and optical light scattering (turbidity). The optical light scattering sensor (nephelometer) detects relative low concentrations of metal sulfides and oxides precipitated when discharged vent fluids mix with cold seawater.

In culture experiments, artificial seawater medium was used supplemented with various substrates (Table 27) to enrich sulfur-oxidizing (SO), sulfur-reducing (SR), manganese-oxidizing (MO), manganese-reducing (MR), arsenite-oxidizing (AO), and iron-oxidizing (IO) microorganisms. The basal medium contained (per liter):

27.5 g of NaCl, 5.38 g of $\text{MgCl}_2 \cdot 6\text{H}_2\text{O}$, 6.78 g of $\text{MgSO}_4 \cdot 7\text{H}_2\text{O}$, 0.72 g of KCl, 0.2 g of NaHCO_3 , 1.4 g of $\text{CaCl}_2 \cdot 2\text{H}_2\text{O}$, 1.0 g of NH_4Cl , and 0.05 g of $\text{K}_2\text{HPO}_4 \cdot 3\text{H}_2\text{O}$ (Emerson & Moyer, 2002) and trace element solution adapted from Reysenbach and Gotz (2001) containing per liter medium: 15.0 mg of $\text{MgSO}_4 \cdot 7\text{H}_2\text{O}$, 2.5 mg of $\text{MnSO}_4 \cdot 2\text{H}_2\text{O}$, 5.0 mg of NaCl, 0.5 mg of $\text{FeSO}_4 \cdot 7\text{H}_2\text{O}$, 0.5 mg of CoCl_2 , 0.5 mg of $\text{CaCl}_2 \cdot 2\text{H}_2\text{O}$, 0.5 mg of ZnSO_4 , 0.5 mg of $\text{SrCl}_2 \cdot 6\text{H}_2\text{O}$, 0.05 mg of $\text{CuSO}_4 \cdot 5\text{H}_2\text{O}$, 0.05 mg of $\text{AlK}(\text{SO}_4)_2$, 0.05 mg of H_3BO_3 , and 0.05 mg of $\text{NaMoO}_4 \cdot 2\text{H}_2\text{O}$. Growth medium for iron-reducing microorganisms (IR) (Reysenbach & Gotz, 2001) consisted of (per liter): 2.52 g of NaHCO_3 , 20.0 g of NaCl, 0.5 g of $\text{MgSO}_4 \cdot 7\text{H}_2\text{O}$, 0.25 g of NH_4Cl , 0.05 g of $\text{CaCl}_2 \cdot 2\text{H}_2\text{O}$, 0.05 g of K_2HPO_4 , 7.0 mg of $\text{FeSO}_4 \cdot 7\text{H}_2\text{O}$, 1.0 mg of $\text{Na}_2\text{WO}_4 \cdot 7\text{H}_2\text{O}$, 1.0 mg of resazurin, 3.67 g of $\text{Fe}(\text{C}_6\text{H}_5\text{O}_7) \cdot x\text{H}_2\text{O}$ (Fe-citrate), and trace element solution as described above. Media inoculated with plume samples were incubated at least for five days at 50° C and at 75° C.

Table 27. Electron donors and acceptors pairs used in cultivation experiments. Abbreviations: SO, sulfur-oxidizing; SR, sulfur-reducing; MO, manganese-oxidizing; MR, manganese-reducing; AO, arsenite-oxidizing; IO, iron-oxidizing; IR, iron-reducing microorganisms.

Target	Electron donor	Electron acceptor
SO	10 mM NaSCN (S^0)	21% (v/v) O_2
SO	10 mM $\text{K}_2\text{S}_4\text{O}_6$ ($\text{S}^{2.5+}$; consists of S^{5+} and S^0)	21% (v/v) O_2
SR	10 mM Na-acetate	10 mM DMSO
MO	10 mM $\text{MnSO}_4 \cdot 4\text{H}_2\text{O}$ (Mn^{2+})	1-2% (v/v) O_2
MR	10 mM Na-acetate	10 mM MnO_2 (Mn^{4+})
AO	2 mM NaAsO_2 (As^{3+})	1-2% (v/v) O_2
IO	10 mM $\text{FeSO}_4 \cdot 7\text{H}_2\text{O}$ (Fe^{2+})	1-2% (v/v) O_2
IR	10 mM Na-acetate	15 mM Fe-citrate

Collected water samples were archived in 4% (v/v) formaldehyde for microbial DAPI enumeration. Water samples obtained with and without a plume signature (as background control) were captured on four different filter membranes (Table 28) for latter DNA extraction, X-ray diffraction, and scanning electron microscopy (SEM) analyses. Nucleic acid isolation was conducted according the CTAB method as described in Chapter 4 (4.3.2 DNA extraction). The mineralogy of the particulates

captured on the filters was assessed by X-ray diffraction at the Department of Earth Sciences, University of Ottawa in Canada, using a zero-background sample holder on a Philips X'Pert diffractometer, a monochromatic Cu K- α x-ray source operating at 45 kV and 40 mA, and a Kevex Si (Li) solid-state detector. All samples were run in a step-scan mode at 0.02° per second from 5° to 75° 2 θ . SEM and energy dispersive X-ray spectroscopy (EDS) were performed at the Department of Earth Science, Carleton University in Ottawa, Canada. Filter discs of dried plume samples were fixed to a sample slide using carbon tape and subsequently coated with a 20 nm thick layer of gold and palladium. The samples were imaged in a JEOL JSM-6400 scanning electron microscope operating at 20 kV. The instrument was coupled to a Link Analytical Pentafet X-ray detector, which collected spectra for 80 seconds (live count time).

Table 28. Processing of water samples for further analyses.

Volume	Pore size	Preservation	Analyses
240 ml	0.22 μ m	at -20° C	DNA extraction
120 ml	0.22 μ m	at -20° C	DNA extraction
3000 ml	0.45 μ m	at -20° C under N ₂ -atmosphere	X-ray diffraction
1000 ml	0.45 μ m	at 4° C in filtered water sample and 2% glutaraldehyde	SEM

Results and Discussion

In total, 59 samples from different vent sites and different water depths were collected (Table 29). Microbial growth was not observed in any of the used media at either temperature. There is no obvious reason why this was the case. It might be that 1) the growth media compositions were not appropriate for the microorganisms present within the hydrothermal plume samples; 2) the organisms did not survive transport from the vent; or possibly 3) there were no or at relatively low concentration thermophilic microorganisms present in the collected plume samples.

A similar result was obtained for DNA extractions performed on five filters, where DNA yield was not sufficient and attempts to amplify archaeal and bacterial 16S

rRNA genes by PCR (4.3.3 PCR amplification) remained negative.

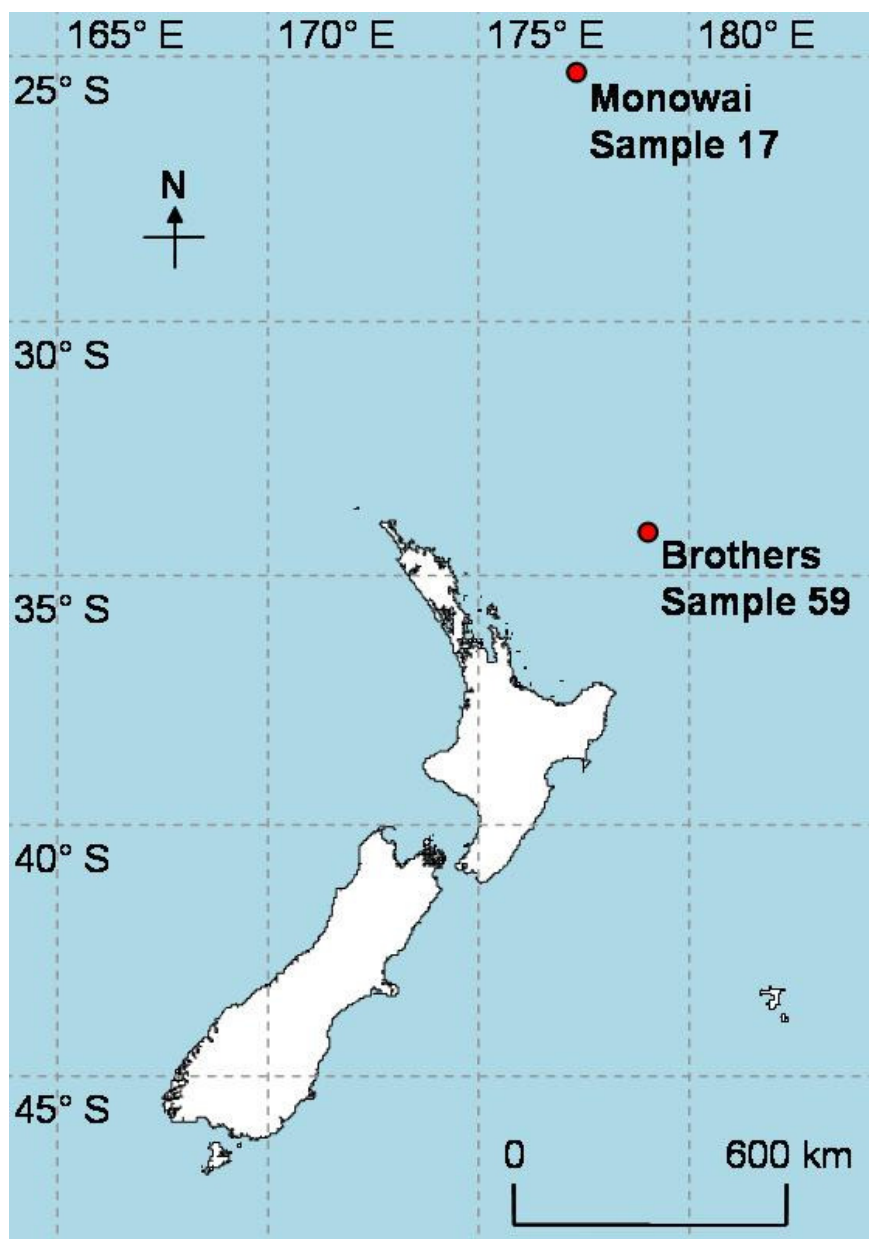


Figure 42. Relative position of the sample sites Monowai and Brothers Volcanoes (indicated by red circles) to the New Zealand mainland. Map was generated using the New Zealand Freshwater Fish Database Assistant software developed by I. G. Jowett (National Institute of Water & Atmospheric Research).

Figure 43 shows the X-ray diffraction pattern derived from a sample with a low nephelometer reading (0.009 nephelometry turbidity units, NTU) collected from Brothers Volcano (Sample 59, Figure 42, Table 29). The diffraction pattern included several sharp peaks, corresponding to peaks for the evaporite minerals halite (mineral form of NaCl), and sylvite (mineral form of KCl). The pattern was also dominated by

a large hump extending from approximately 5.5 to 3.0 Å. This feature is indicative of amorphous material. Although no exact identification could be made, the feature may represent amorphous silica or sulfur. Attempts were made to perform a longer, more-detailed scan on this region of the diffraction pattern, in hopes of extracting more useful data to permit a mineral identification, but no additional information could be gained.

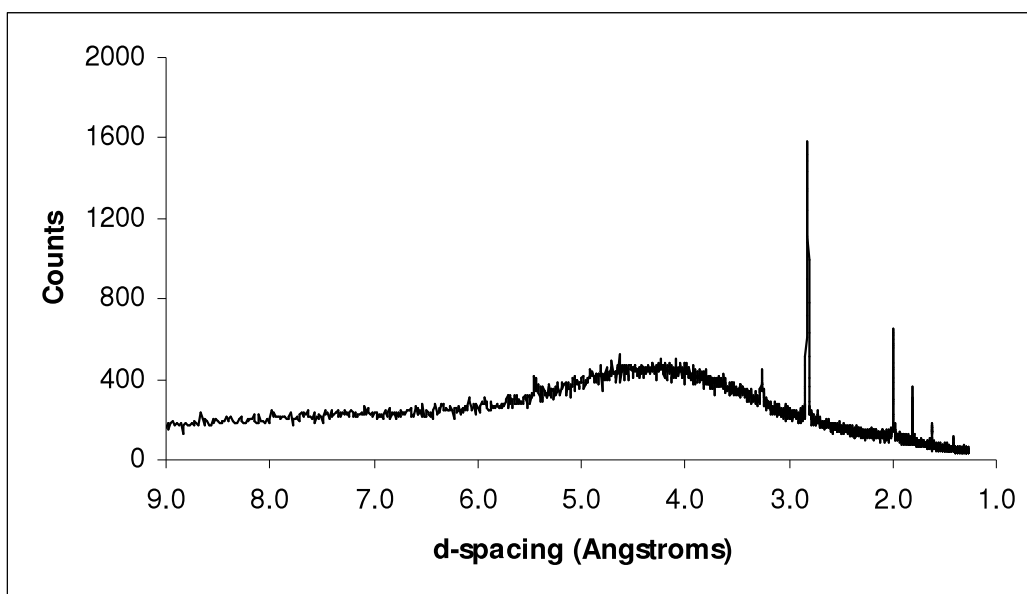


Figure 43. X-ray diffraction pattern obtained from the filtrate of the Brothers Volcano plume (Sample 59, NTU = 0.009). Peaks correspond to halite and sylvite. The broad hump is indicative of amorphous material, possibly silica or sulfur.

An X-ray diffraction pattern obtained from a sample with a much higher nephelometer reading (4.5 NTU) collected from Monowai Cone Volcano (Sample 17, Figure 42, Table 29) is depicted in Figure 44. Despite the higher nephelometry value, and the presence of visible rust-colored material on the filter, the pattern was virtually identical to that obtained from sample 59, again representing halite, sylvite, and unidentified amorphous material. The presence of rust-colored material in samples with high-nephelometry values suggested the presence of an iron oxide mineral, but the lack of corresponding peaks in the diffractograms would suggest that any iron oxide present was either amorphous or present in very small quantity with respect to the salt minerals. These results were consistent for all of the samples analyzed, regardless of plume source.

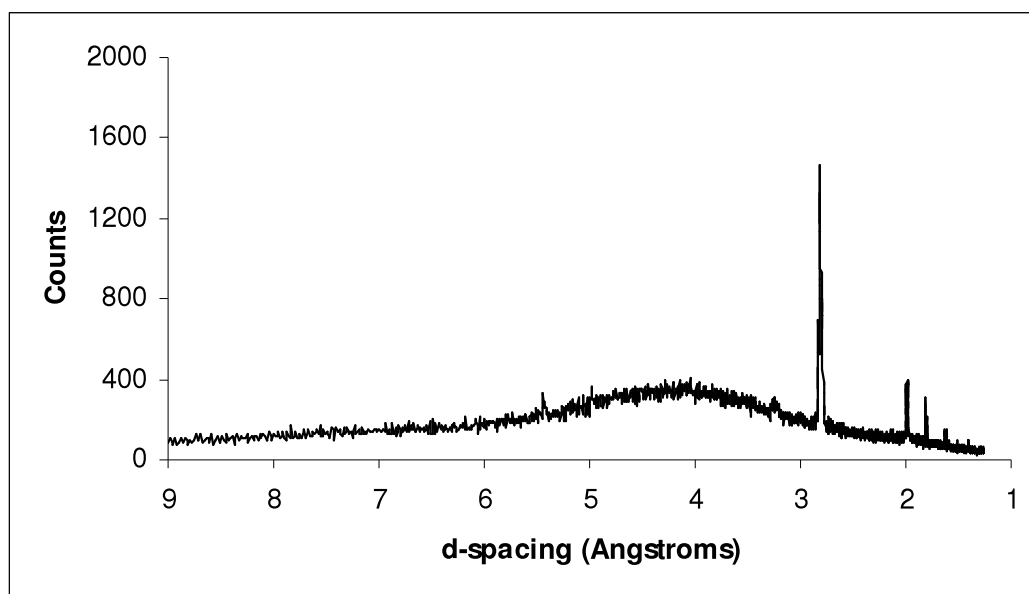


Figure 44. X-ray diffraction pattern for the sample 17 obtained from Monowai Volcano plume (NTU = 4.5). Peaks are representative for halite and sylvite. The broad hump is indicative of amorphous material, possibly silica or sulfur.

Scanning electron micrographs revealed that plume samples appeared nearly devoid of material other than occasional cubic crystals of halite (as determined by EDS). There was a general lack of identifiable organic matter in all samples, although diatom skeletons (Figure 45 A) and small spherical structures (Figure 45 B) were occasionally observed. In samples with high nephelometry values, the filters were nearly covered with similar cubic crystals ranging in size from less than one to several μm in length, and organic matter could not be distinguished (Figure 45 C and D). These results were essentially consistent for all of the samples analyzed, with the amount of halite observed increasing as the nephelometry values of the samples increased.

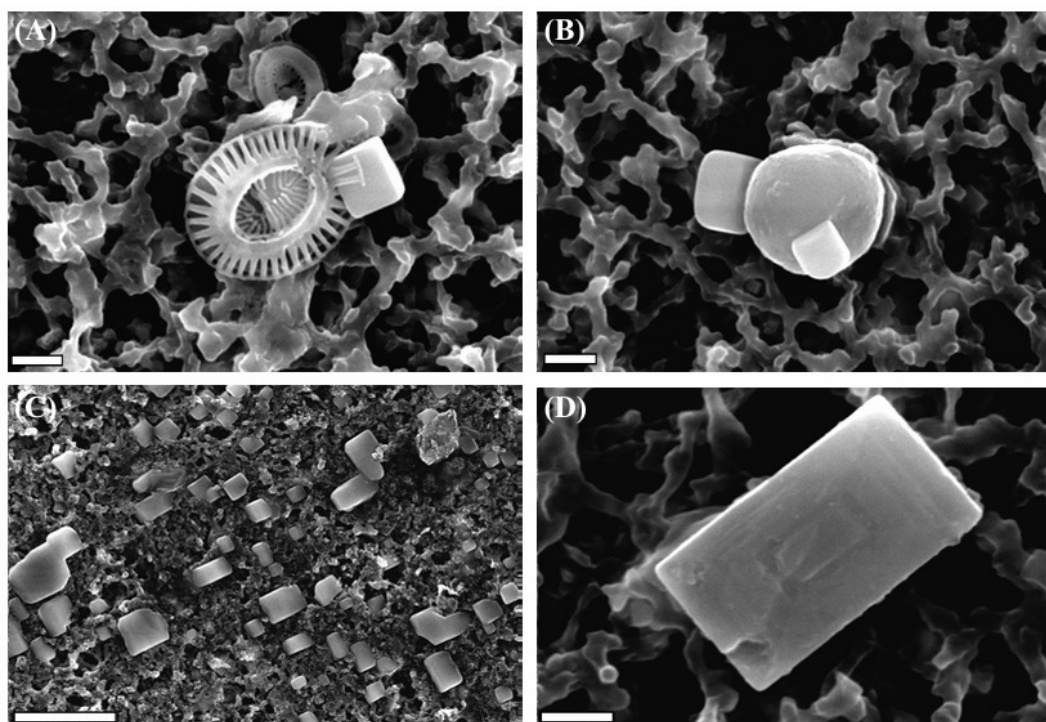


Figure 45. Scanning electron micrographs of plume samples showing (A) a diatom skeleton, and (B) a spherical structure (possibly a coccoid bacterium), both in close association with cubic crystals of halite. Bars 1 μm . (C) Abundance of halite crystals in samples 17, which displayed relatively high nephelometric turbidity units. Bar 10 μm . (D) Single crystals ranged in size from 1 to several μm in length. Bar 1 μm .

The lack of growth observed in the prepared media, together with the evidence from DNA extraction and SEM / EDS, suggest that the obtained plume samples did not contain a significant quantity of thermophilic microorganisms.

Table 29. Location of sample sites specified in geographic coordinates and water depths. For each sample the measured nephelometric turbidity unit (NTU) is given. Volcanoes “U” and “V” lying within Tonga’s Economic Exclusive Zone have not been designated to names yet.

Sample	Site	Latitude			Longitude			Depth [m]	NTU
1	Ritchie Ridge	39°	58.382	' S	178°	14.474	' E	848	0.015
2	Putoto	27°	53.385	' S	177°	35.782	' W	589	0.120
3	Gamble - Rakahore	27°	01.730	' S	177°	31.314	' W	750	0.006
4	Gamble - Rakahore	27°	01.730	' S	177°	31.314	' W	1499	0.006
5	Hinepuia	26°	24.054	' S	177°	15.383	' W	352	0.125
6	Hinepuia	26°	24.567	' S	177°	14.854	' W	340	0.358
7	Hinepuia	26°	25.071	' S	177°	14.122	' W	301	0.450
8	Hinepuia	26°	24.116	' S	177°	15.361	' W	400	0.009
9	Hinepuia	26°	24.183	' S	177°	15.319	' W	283	0.007
10	Hinepuia	26°	24.639	' S	177°	15.244	' W	21	0.061
11	Hinepuia	26°	24.448	' S	177°	15.183	' W	148	0.020
12	Hinepuia	26°	24.381	' S	177°	15.155	' W	250	0.028
13	Hinepuia	26°	24.331	' S	177°	15.131	' W	320	0.040
14	Hinepuia	26°	24.195	' S	177°	15.088	' W	363	0.325
15	Hinepuia	26°	23.916	' S	177°	15.032	' W	317	0.200
16	Monowai	25°	50.395	' S	177°	11.127	' W	642	0.022
17	Monowai	25°	53.422	' S	177°	11.101	' W	129	4.500
18	Monowai	25°	53.422	' S	177°	11.101	' W	80	0.057
19	Monowai	25°	48.018	' S	177°	9.474	' W	1050	0.120
20	Volcano "U"	25°	25.836	' S	177°	6.747	' W	644	0.028
21	Volcano "U"	25°	25.939	' S	177°	6.585	' W	499	0.030
22	North of Volcano "V"	25°	58.582	' S	177°	2.484	' W	797	0.012
23	"U" - Monowai	25°	36.164	' S	177°	6.264	' W	1392	0.028
24	Monowai	25°	46.392	' S	177°	10.090	' W	1038	0.100
25	Monowai	25°	46.842	' S	177°	9.772	' W	1101	0.200
26	Monowai	25°	48.402	' S	177°	9.976	' W	1053	0.280
27	Monowai	25°	46.441	' S	177°	9.990	' W	1117	0.280
28	Monowai	25°	53.428	' S	177°	11.089	' W	137	4.300
29	Monowai	25°	53.428	' S	177°	11.089	' W	55	0.042

Table 29. Continued.

Sample	Site	Latitude			Longitude			Depth [m]	NTU
30	Monowai	25°	53.509	' S	177°	11.098	' W	133	4.895
31	Monowai	25°	53.509	' S	177°	11.098	' W	164	0.123
32	Monowai	25°	47.738	' S	177°	10.245	' W	1328	0.259
33	Volcano "U"	25°	25.815	' S	177°	6.933	' W	550	0.032
34	Lau Havre gap	25°	07.472	' S	177°	27.053	' W	2000	0.017
35	Monowai - Hinepuia	25°	05.305	' S	177°	12.663	' W	1099	0.010
36	Hinepuia	26°	23.804	' S	177°	15.064	' W	345	0.330
37	Hinepuia - Rakahore	26°	38.181	' S	177°	13.676	' W	1002	0.009
38	Gamble	27°	12.528	' S	177°	25.999	' W	102	0.056
39	Gamble	27°	12.491	' S	177°	26.349	' W	303	0.045
40	Putoto - Gamble	27°	36.406	' S	177°	53.388	' W	2201	0.010
41	Putoto	27°	52.675	' S	177°	36.004	' W	608	0.022
42	North of Hinetapeka	28°	20.866	' S	177°	39.869	' W	749	0.009
43	Hinetapeka	28°	39.193	' S	177°	47.373	' W	182	0.031
44	Macauley	30°	12.417	' S	178°	26.750	' W	283	0.046
45	Wright	31°	51.001	' S	179°	11.258	' W	1094	0.045
46	Wrighty	31°	49.128	' S	179°	14.398	' W	795	0.009
47	Brothers	34°	53.069	' S	179°	4.431	' E	1288	0.100
48	Brothers	34°	53.069	' S	179°	4.431	' E	1360	0.132
49	Brothers	34°	53.069	' S	179°	4.431	' E	1176	0.170
50	Brothers	34°	50.196	' S	179°	3.359	' E	1483	0.038
51	Brothers	34°	53.089	' S	179°	4.077	' E	1271	0.249
52	Brothers	34°	51.817	' S	179°	3.746	' E	1205	0.110
53	Brothers	34°	52.004	' S	179°	3.370	' E	1301	0.260
54	Brothers	34°	52.004	' S	179°	3.370	' E	495	0.013
55	Brothers	34°	53.099	' S	179°	4.263	' E	1135	0.275
56	Brothers	34°	54.143	' S	179°	2.965	' E	1498	0.011
57	Brothers	34°	52.613	' S	179°	3.972	' E	1191	0.400
58	Brothers	34°	53.835	' S	179°	2.355	' E	1319	0.050
59	Brothers	34°	47.790	' S	179°	6.184	' E	1090	0.009

Appendix H: Publications

Journal articles and manuscripts

Hetzer, A., C. J. Daughney, and H. W. Morgan. 2006. Cadmium ion biosorption by the thermophilic bacteria *Geobacillus stearothermophilus* and *G. thermocatenulatus*. *Applied and Environment Microbiology*, 72:4020-4027.

Hetzer, A., H. W. Morgan, I. R. McDonald, and C. J. Daughney. 2007. Microbial life in Champagne Pool, a geothermal spring in Waiotapu, New Zealand. *Extremophiles*, 11:605-614.

Hetzer, A., I. R. McDonald, and H. W. Morgan. In press. *Venenivibrio stagnispumantis* gen. nov., sp. nov., a thermophilic hydrogen-oxidizing bacterium isolated from Champagne Pool, Waiotapu, New Zealand. *International Journal of Systematic and Evolutionary Microbiology*.

Conference proceedings

Hetzer, A., H. W. Morgan, R. Ronimus. 2004. Cadmium toxicity experiments using aerobic thermophilic bacteria. The 49th annual conference of the New Zealand Microbiological Society (NZMS) in Palmerston North, New Zealand.

Abstract text:

Cadmium is considered to be an important environmental pollutant that is toxic to many organisms. So far, only a few studies about heavy metal tolerance of thermophilic microorganisms have been described. The aim of our investigation is to isolate heavy metal tolerant microorganisms and gain a deeper insight into their detoxification strategies.

Thermophilic bacteria of the genera *Bacillus*, *Brevibacillus*, *Geobacillus*,

Anoxybacillus and *Thermus* are aerobic and have overlapping ranges of optimal pH values and temperatures for growth but differ in the composition of their cell walls. In cadmium toxicity experiments more than 50 species of the genus *Bacillus*, *Brevibacillus*, *Geobacillus*, *Anoxybacillus* and *Thermus* were tested in the presence of up to 3.2 mM cadmium.

Interestingly, two different patterns of response in the growth curves occurred: an increasing concentration of cadmium led either to a decreasing optical density at a given point of time or to a delay of the onset of positive growth phases. The bacteria that displayed the highest cadmium tolerance, 9 species of the tested genera, were selected for further cultivation experiments using two different media. The ability to tolerate cadmium depended on the selected medium. The results of this study will be presented.

Hetzer, A., R. Ronimus, C. J. Daughney, and H. W. Morgan. 2005. Cadmium biosorption onto two thermophilic bacteria. The 50th annual conference of the New Zealand Microbiological Society (NZMS) in Dunedin, New Zealand.

Abstract text:

Biosorption of metals is the action of forming compounds with metal ions by cell surfaces thereby lowering the effective concentration of the metal ions from a solution. The chemical composition of microbial cell walls and exopolysaccharides can vary considerably within a species displaying qualitative and quantitative varieties of proton-active functional groups that may act as ligands for metal ions.

Microbial biosorption influences the distribution and availability of metal ions in some natural systems and it is utilized in waste treatment of metal-polluted water and soil. Although it having been subject of many studies, as yet, there is still not a single report describing the metal adsorption by thermophilic bacteria that has been published. The aim of our investigation is to generate surface complexation models for two thermophilic bacteria that describe the interaction between the binding sites exposed on the cell surfaces and cadmium ions.

Thermophilic bacteria of the genera *Aneurinibacillus*, *Anoxybacillus*, *Bacillus*, *Brevibacillus* and *Geobacillus* were tested in initial cadmium toxicity experiments. The highest tolerance to cadmium, 400 – 3200 μM , was observed for the species belonging to the genus *Geobacillus*. *Geobacillus thermocatenulatus* and *Geobacillus stearothermophilus* were selected for further investigations. Acid-base titrations were conducted to determine the concentrations and deprotonation constants of binding sites onto the bacterial surfaces. Cadmium adsorption experiments were performed to determine the thermodynamic stability constants for the metal complexes. Based on the experimental data surface complexation models were developed.

The binding capacities for protons and cadmium ions were higher for *G. thermocatenulatus* than those for *G. stearothermophilus*. Cadmium adsorption increased with pH and biomass for both bacteria. The parameters for the surface complexation models will be presented in comparison to published data for mesophilic microorganisms.

Hetzer, A., C. J. Daughney, and H. W. Morgan. 2006. Cadmium ion biosorption onto the thermophilic bacteria *Geobacillus stearothermophilus* and *G. thermocatenulatus*. The 11th International Symposium on Microbial Ecology (ISME) in Vienna, Austria.

Abstract text:

Microbial biosorption influences the distribution and availability of metal ions in some natural and anthropogenic environments and it is utilized in waste management of metal-polluted water and soil. Although several previous investigations have applied surface complexation models (SCMs) to describe the extent of cation adsorption by mesophilic bacteria, not a single study was ever published about thermophilic microorganisms. We assume that mesophilic and thermophilic bacteria differ in cell wall composition and therefore may display different biosorption behaviors.

The aim of our study is to develop SCMs for the thermophilic Gram-positive bacteria *Geobacillus stearothermophilus* and *G. thermocatenulatus* characterizing the complexation between cadmium ions and chemically reactive functional groups within and onto the cell wall as a function of pH and biomass. Experimental data from electrophoretic mobility, potentiometric titration, and cadmium ion adsorption experiments were used quantifying the concentrations and deprotonation constants of binding sites and to determine the thermodynamic stability constants for the metal-bacteria complexes. In comparison to recent reported model parameters obtained for mesophilic bacteria, our results indicate the functional group, with a deprotonation constants pK value of approximately 3.8, to be more dominant in cation complexation reactions accounting for 66 and 80% of all titrable groups for *G. thermocatenulatus* and *G. stearothermophilus*, respectively. The experimental results show that the two thermophilic species studied in this investigation display binding capacities for protons and cadmium ions that are different from the mesophilic species that have been studied to date.

Hetzer, A., H. W. Morgan, I. R. McDonald, and C. J. Daughney. 2007. Survey of microbial life in a hydrothermal spring rich in arsenic compounds. The 9th International Conference on the Biogeochemistry of Trace Elements (ICOBTE) in Beijing, China.

Abstract text:

Champagne Pool, one of New Zealand's largest terrestrial hot springs and rich in metalloids such as arsenic and antimony compounds, has been subject to extensive geological and geochemistry descriptions. Only few microbiological studies recently described microbial activity based on culture-independent methods. In the current investigation, a combined approach of culture and culture-independent studies was applied to investigate microbial life in Champagne Pool. Culture-independent methods such as microscopy, DNA yield, and ATP content confirmed relatively low biomass in Champagne Pool compared to other terrestrial hot springs within New Zealand and low cell numbers of $5.6 \pm 0.5 \times 10^6$ cells per ml were determined. Denaturing Gradient Gel Electrophoresis (DGGE) and 16S rRNA (small-subunit

ribosomal nucleic acid) gene clone libraries analyses indicated low microbial diversity and the presence of *Sulfurihydrogenibium*, *Nevskia*, *Paracoccus*, *Sulfolobus* and *Thermofilum*-like populations in Champagne Pool. Three novel species were isolated and phylogenetic analysis of 16S rRNA gene sequences revealed relationships with members of the genera *Thermoanaerobacter*, *Sulfurihydrogenibium*, and *Thermococcus*. One of the isolate represents a novel genus and was able to grow in the presence of relatively high concentrations of arsenic and antimony compounds.

Hetzer, A., H. W. Morgan, I. R. McDonald, and C. J. Daughney. 2007. Microbial life in a hydrothermal spring rich in arsenic compounds. The 17th V. M. Goldschmidt conference in Cologne, Germany.

Abstract text:

The geothermal spring Champagne Pool in Waiotapu, New Zealand has an estimated volume of 50,000 m³ and discharges fluid at 75° C, which is oversaturated with arsenic and antimony compounds such as orpiment (As₂S₃) and stibnite (Sb₂S₃) that precipitate and form orange deposits. Although Champagne Pool is geochemically well characterized only few studies addressed its role as a potential habitat for microbial life. In the current investigation, a combined approach of first culture-independent studies followed by culturing experiments was applied to describe microbial density and diversity within Champagne Pool. ATP measurements and epifluorescence microscopy showed relatively low biomass in Champagne Pool compare to other terrestrial hot springs within New Zealand and relatively low cell numbers of $5.6 \pm 0.5 \times 10^6$ cells per ml. Denaturing Gradient Gel Electrophoresis and 16S rRNA gene clone libraries analyses indicated low microbial diversity and the abundance of hydrogen-oxidizing and sulfur-dependent populations, which were dominated by members belonging to the order *Aquificales*. On account of the results culture media were designed and two novel bacteria and a novel archaeon were successfully isolated. Experiments suggested that the observed relatively low biomass and biodiversity might be due to the presence of volatile components (H₂S,

methyl and hydride derivatives of arsenic and antimony) within the spring which are inhibiting microbial growth.

Hetzer, A., H. W. Morgan, I. R. McDonald, and C. J. Daughney. 2007. Champagne Pool: Cocktail of geothermal energy, arsenic compounds and microbial life. The 18th International Symposium on Environmental Biogeochemistry (ISEB) in Taupo, New Zealand.

Abstract text:

The terrestrial hot spring Champagne Pool in Waiotapu, New Zealand is approximately 65 m in diameter and discharges fluid at 75° C and pH 5.5, which is oversaturated with arsenic and antimony compounds such as orpiment (As₂S₃) and stibnite (Sb₂S₃) that precipitate and form orange deposits. Although Champagne Pool is geologically and geochemically well characterized only few studies investigated its role as potential habitat for microbial life forms using culture-independent methods. However, a successful isolation of microorganisms obtained from Champagne Pool has not been previously reported.

In the current investigation, a combined approach of first culture-independent studies following culturing experiments was applied to describe microbial density and diversity within Champagne Pool. Culture-independent methods consisting of adenosine 5'-triphosphate (ATP) measurements and epifluorescence microscopy indicated relatively low biomass in Champagne Pool compare to other terrestrial hot springs within New Zealand and relatively low cell numbers of $5.6 \pm 0.5 \times 10^6$ cells per ml. Denaturing Gradient Gel Electrophoresis and 16S rRNA gene clone libraries analyses indicated low microbial diversity and the abundance of *Sulfurihydrogenibium*, *Nevskia*, *Paracoccus*, *Sulfolobus* and *Thermofilum*-like populations which were dominated by members belonging to the order *Aquificales*, with a distant phylogenetic relationship to *Sulfurihydrogenibium*.

On account of the results culture media were selected and designed to target the enrichment of hydrogen-oxidizing and sulfur-dependent microorganisms. Two novel bacteria and a novel archaeon were successfully obtained having 16S rRNA gene sequences with similarities of around 98% between isolate CP.B1

Thermoanaerobacter tengcongensis, 94% between isolate CP.B2 and *Sulfurihydrogenibium azorense*, and 99% between CP.B3 and *Thermococcus waiotapuensis*, respectively. Isolate CP.B2 represents a novel genus within the *Aquificales* order, for which the name *Venenivibrio stagnispumantis* gen. nov., sp. nov. is proposed. *V. stagnispumantis* cells grew chemolithotrophically under microaerophilic conditions with H₂ as electron donor and O₂ as electron acceptor and displayed tolerance to relatively high concentrations of arsenic and antimony compounds (8 mM As³⁺, 15 mM Sb³⁺, and >20 mM As⁵⁺), but growth was not observed when As³⁺ and As⁵⁺ were provided as the sole electron donor and acceptor pair. Arsenic resistance was mediated by a two-component energy-dependent efflux system (ArsA and ArsB).

Cruise Report

C. J. Daughney and A. Hetzer. 2006. Microbial studies. In *Cruise report: NZAPLUME III New Zealand American Plume mapping Expedition. September 23 – October 17, 2004*, pp. 49-52. Edited by C. E. J. de Ronde. Institute of Geological & Nuclear Sciences, Lower Hutt, New Zealand.